FINITE ELEMENT MODELLING AND ANALYSIS OF THE HUMAN CERVICAL SPINE

NG HONG WAN

SCHOOL OF MECHANICAL AND AEROSPACE ENGINEERING

NANYANG TECHNOLOGICAL UNIVERSITY

2005

Finite Element Modelling and Analysis of the Human Cervical Spine

Ng Hong Wan

School of Mechanical and Aerospace Engineering

A thesis submitted to the Nanyang Technological University in fulfilment of the requirements for the degree of

Doctor of Philosophy

2005

Acknowledgements

I would like to express my sincere appreciate on to my supervisor, A/P Teo EC for his guidance and support during my studies. Without his guidance and direction, this research could not have been completed. I am grateful to Dr Tan SB (Director of Orthopaedic Department, Singapore General Hospital) for providing clinical insights and provision of cervical cadavers.

I would particularly like to express my deepest gratitude to my wife, who was instrumental in my pursuit of this research work. Her constant encouragement and motivation during difficult times helped me to complete this research. Finally, I dedicate this dissertation to my parents. There is no possible way to show them how grateful I am for their support.

Summary

Throughout the years, the biomechanics of the cervical spine after injuries, surgical techniques or degenerative disease has aroused the interest of many clinicians and researchers. An accurate assessment on the cervical spine biomechanical responses is very important clinically as the magnitude of these changes dictates the necessary treatment procedure (e.g., external implant devices or surgical intervention).

In this report, a non-linear three-dimensional multi-segmental finite element (FE) model of the intact cervical spine, including the associated ligamentous tissues was developed and validated in terms of the range of motions (ROMs), force/displacement responses, internal strains and disc pressure under a wide range of physiological loading conditions.

The model was subsequently used to investigate in detailed the qualitative understanding and assessment of the cervical spine under various situations (effects of material sensitivity, ligamentous injuries, laminectomy, laminotomy, facetectomy and disc degeneration). The influences of the degeneration and laminectomies on the immediate post-surgical period were also highlighted and discussed. With the experience and methodology used in the analyzing of the cervical spine, another study was taken to redefine the existing methodology of developing the cervical spinal FE model using CT scan data.

Finally, it was concluded that the various cervical conditions (ligamentous injuries, laminectomy, laminotomy, facetectomy and disc degeneration) investigated in this study influence both the internal and external biomechanical responses of the cervical spine. The nature and magnitudes of these changes depended on a number of factors

and loading vectors. The results obtained from the current study provide a basic understanding of the cervical instability and facilitate the development of the cervical spine surgical treatment guidelines and definitions. It is hoped that in future, the analysis of the cervical spinal stability using patient specific cervical spine model can become possible and will greatly enhance the prediction accuracy for the particular patient.

Table of Contents

List of Figures

List of Tables

Chapter 1. Introduction

1.1 Rationale for Studying the Cervical Spine

The human cervical spine is composed of seven bony vertebrae connected between the head and the torso. The head rests on top of the cervical column and the lower end of the cervical spine is connected to the thoracic spine. The unique cervical bony vertebral articulating joints, the associated ligamentous structures and intervertebral disc together provide the specific movements and mobility of the head-neck region. Any external load applied to the head will result in three-dimensional movements between the adjacent vertebrae and the force will be transmitted to the lower parts of the body via the medium of the intervertebral joints and posterior articular facets.

However, the exposed head-neck region also makes the cervical spine susceptible to traumatic injury, as the muscles are relatively passive during the episode. Any injurious loading condition (e.g., force applied to the head and/or spinal column) often results in excessive vertebral motion and encroachment of the spinal cord. The excessive vertebral motion resulting from trauma may also cause a reduction in the structural integrity of the passive constraints. Ligamentous injuries (passive) may render the vertebral joints unstable, which may make the patient susceptible to neurological injuries.

In addition, the human cervical spine degenerates with age (Young, 2000). Spondylosis or stenosis, due to degeneration of the joints, intervertebral discs, ligaments and connective tissue of the cervical vertebrae often affects the normal functionality of spine. Progression of the cervical spine degenerative disease (spondylosis) causes compression

in the form of myelopathy (spinal cord compression), radiculopathy (spinal nerve root compression) or both, as shown in Figure 1 and Figure 2. Currently, cervical spondylotic myelopathy (CSM) is the most common spinal cord disorder in older persons above 55 years old (Orr and Zdeblick, 1999; Schmidt et al., 2002; Young, 2000). Furthermore, in severe disc degeneration due to spondylosis, the progressive loss of water in the nucleus pulposus cause a loss in disc height and the associated relaxation of the annulus fibrosus may result in osteophyte formation. Degenerative changes also affect the facets joints and ligaments in the posterior column. These changes affect the normal functional capability of the cervical spinal column and result in abnormal range of motions (ROM) and increase of internal stress in the various spinal components.

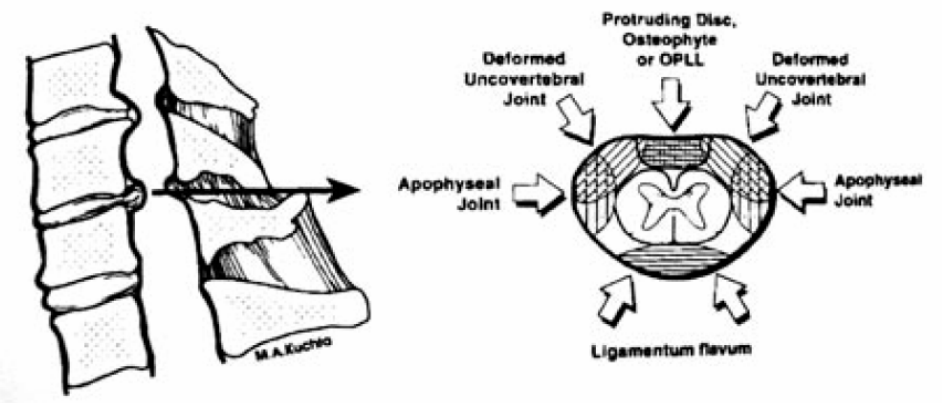

Figure 1: Pathologic anatomy of cervical spondylitic myelopathy (Law et al., 1995).

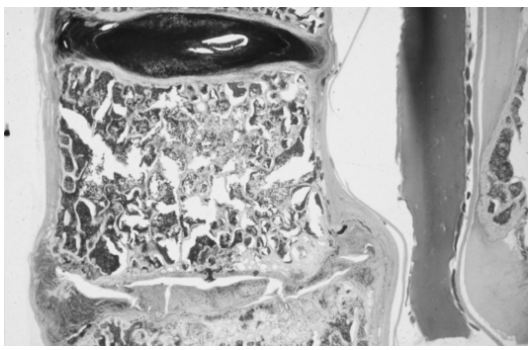

Figure 2: Illustration of the cervical myelopathy (spinal cord compression) (An and Simpson, 1994).

The social economic cost due to these spinal disorders and injuries was high. In year 2002, 516,000 patients in Singapore were diagnosed with neck pain or injuries in the last 6 months. 50,000 patients (10%) took medical leave (Tan, 2002). Most patients who experience spinal pains are usually managed with a combination of pain-relieving drugs and physical therapy. For acute disorders or traumatic injuries, surgery is the preferred treatment to decompress the neurological structures and, if necessary, to realign the cervical spine and to stabilize an unstable cervical spine segment. Different surgical options are available for the treatment of the various cervical spinal disorders and injuries that include the anterior approach, either anterior cervical discectomy with a fusion (ACDF) or corpectomy with strut grafting, or the posterior approach, either single/multi level facetectomy, laminotomy, laminectomy or a combination of these techniques (Epstein, 2002; Schmidt et al., 2002; White and Panjabi, 1990). In this overwhelming amount of surgical techniques, it has become quite a challenge for the surgeon to choose the best way to treat the patient. However, the lack of understanding on the biomechanics of the cervical spine limits the surgeon's ability to predict the outcomes of the various treatment plans and select the best treatment plans.

Various cervical conditions can also lead to the structural disruption of the motion segment or biomechanical changes, resulting in cervical spinal instability and increasing risk of neurological deficit. Therefore, an accurate assessment on the biomechanical responses is an important clinical parameter because the magnitude of these changes dictates the necessary treatment procedure (e.g., external implant devices or surgical intervention). The percentage increase in the range of motions (ROM) is important in determining the treatment technique that would most effectively reduce the abnormal ROM. Therefore, biomechanical research on the cervical spine is most useful if it can

provide clinically relevant information. However, there is no detailed study conducted in the past to investigate the influence of the cervical spinal injury, disc degeneration and surgical treatment techniques on the biomechanics of the cervical spine using the finite element (FE) method of analysis.

Accordingly, this project seeks to analyse the biomechanical responses of the intact, injured, degenerated and surgically altered cervical spine. These involved the development of the cervical multi-segmental FE models based on the embalmed cadaveric specimen. The hypothesis of the present research is: **ligamentous injuries, disc degeneration and various surgical treatments affect both the external and internal biomechanical parameters of the cervical spine.**

The work presented in this thesis investigated in detailed the qualitative understanding and assessment of the cervical spine under various situations. With the experience and methodology used in the analyzing of the cervical spine models, another study was taken to redefine the existing methodology of developing the cervical spinal FE model using CT scan data. In this way, it is hoped that in future, the analysing of the cervical spinal stability using patient specific cervical spine model can greatly enhance the accuracy and reliability of the prediction for the particular patient.

1.2 Research Aims

The objective of this research is to test the hypothesis described earlier using the FE method of analysis.

The scope of this research is to:

- develop a comprehensive FE model of the cervical spine that is capable of incorporating the following significant features
    - Creation of a multiple cervical functional spinal unit (FSU) for investigation on the influence of various treatments on the biomechanics of the cervical spine at the altered and unaltered levels.
    - Incorporation of geometric nonlinearity which considers large deformation and strain occurring in the cervical spine motion segments and defines appropriate methodology for the application of pure moments that support large deformation effects
    - Realistic simulation of the facet joint contacts as an interface problem, which allows rotation and sliding between the opposing surfaces.
    - Realistic simulation of the intervertebral disc annulus as a composite of annulus ground substance reinforced by annulus fibers.
    - Simulation of the nucleus pulposus as an incompressible fluid using three dimensional hydrostatic fluid elements
    - Accurate incorporation of unconvertebral joints
    - Incorporation of material nonlinearity
- Validate the nonlinear models against a wide range of *in vitro* studies
    - under compression, anterior shear, posterior shear, flexion, extension, lateral bending and axial rotation
- Perform biomechanical studies on the cervical spine model due to
    - Ligamentous injuries
    - Material sensitivity, including the effect of osteoporosis
    - Surgical procedures
    - Disc degeneration

- Define a protocol for the development of patient specific cervical spinal models for clinical studies.

1.3 Description of the Thesis

The report is divided into nine chapters and a brief description of each chapter is as follows: The values of cervical spine research, objectives of this study as well as its significance are discussed in Chapter 1. Chapter 2 presents a brief description on the anatomy and kinematics of the cervical spine. Chapter 3 deals with the literature review of previous experimental and FE models. Chapter 4 describes the development of the FE model of the cervical spine. Chapter 5 investigates the flexibility of the finite element model against a wide range of experimental data. This chapter also investigates the influence of ligaments on the cervical spine biomechanics. Chapter 6 explores the effect of various surgical techniques on the cervical spine biomechanical responses. In particular, the influence of these surgical techniques on the adjacent altered and unaltered levels. The influence of material variations, geometry and loading setups are investigated as well. Chapter 7 studies the consequence of disc degeneration. Chapter 8 presents the methodology for the development of a patient specific cervical spine FE model. Conclusions drawn from the analysis of the cervical spine models under various conditions are summarised in Chapter 9. As a major proportion of this work was concerned with the formulation of a mathematical model of suitable complexity, the model may offer a wider range of future investigations into the roles of the surrounding tissues and bony structures of the human cervical motion segment. Some contributions, suggestions and recommendations for future work are finally covered.

It is hoped that the work presented in this thesis will be judged to have fulfilled the objectives and scopes described earlier clearly and concisely whilst demonstrating that the intelligent use of the structural model (Finite Element Method) can be usefully employed in the biomechanical analysis of cervical spine structures under various conditions. Eleven papers related to the objective and scope of this study have been either accepted or published in reputable journals and conferences (Refer Related Publications).

Chapter 2. Anatomy and Kinematics of the Cervical Spine

2.1 Introduction

The human body is constantly compelled to struggle for a state of structural and functional equilibrium, in which the skeletal system has a large role to play in maintaining body balance. The skeletal system consists of bones of various sizes and functions, which provides the body framework, shape and articulations. Biomechanically, the skeletal system may be considered as an arrangement of levers that is moved by muscles or external forces. The type, range, and power of movement are governed by the nature of the joints between the moving parts, the lengths of the bony levers, the size and arrangement of the muscles acting on the levers, and the weight of the load to be moved.

Each part of the spine allows girdle-like support for all vertebrae, it serves as points of attachment for muscles and tendons, and the long bones serve as levers to make movement and locomotion possible. It also surrounds and provides protection for the internal organs and provides movement when acted upon by the muscles.

The skeleton is further classified into axial and appendicular parts (Figure 3). The axial skeleton is made up of the backbone or vertebral column, the breastbone or sternum, twelve pairs of ribs, and the skull. The axial skeleton provides a framework that supports and protects organ systems in the dorsal and ventral body cavities. As for the appendicular skeleton, it consists of the body's upper and lower limbs.

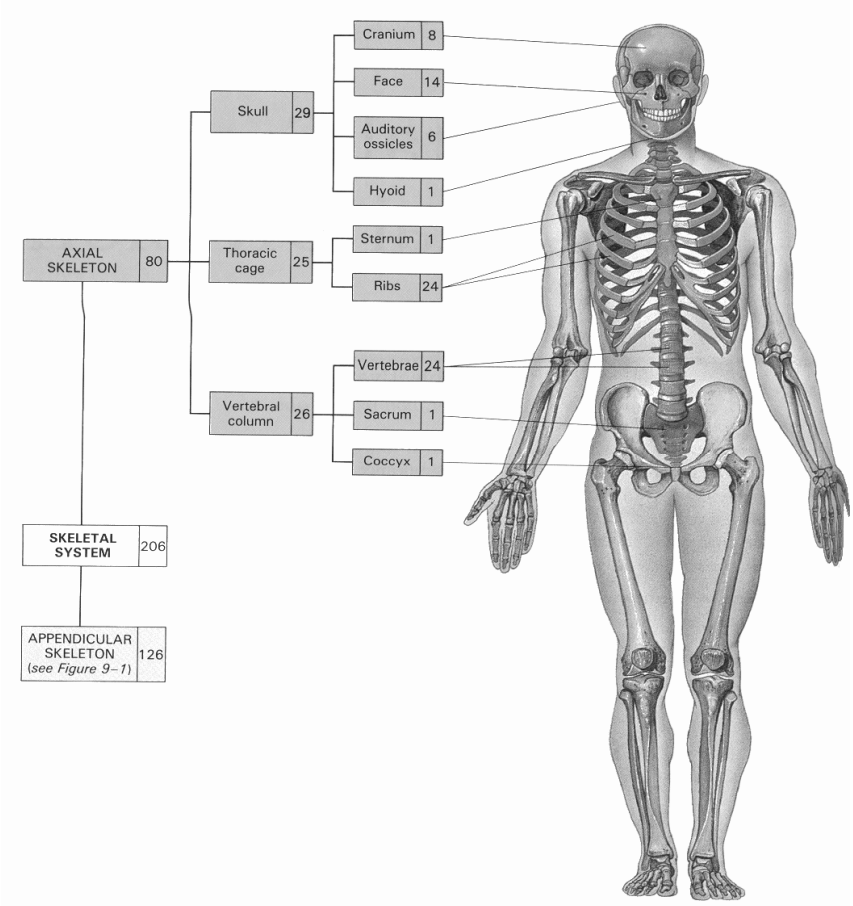

Figure 3: Divisions of the skeletal system (Martini and Ober, 2001).

2.2 The Spinal Column

The spinal or vertebral column is the central pillar of the body, which serves to protect the spinal cord and support the weight of the head and trunk, and as a point of attachment for the ribs, ligaments, muscles and other soft tissues structures of the back. It is a flexible structure made up of 33 irregular bones called vertebrae. Most of these units are connected together by ligaments and fibro cartilaginous discs called intervertebral discs (IVDs) to form a flexible curved support for the body.

The spinal column is divided into five common classifications according to the site and characteristics. The spinal column (Figure 4) consists of twenty-four separate bony vertebrae, together with five fused vertebrae of the sacrum and usually four fused

vertebrae of the coccyx. The spinal column has three principal functions: it supports the human in the upright posture; it allows movement and it protects the spinal cord (Oliver and Middleditch, 1991).

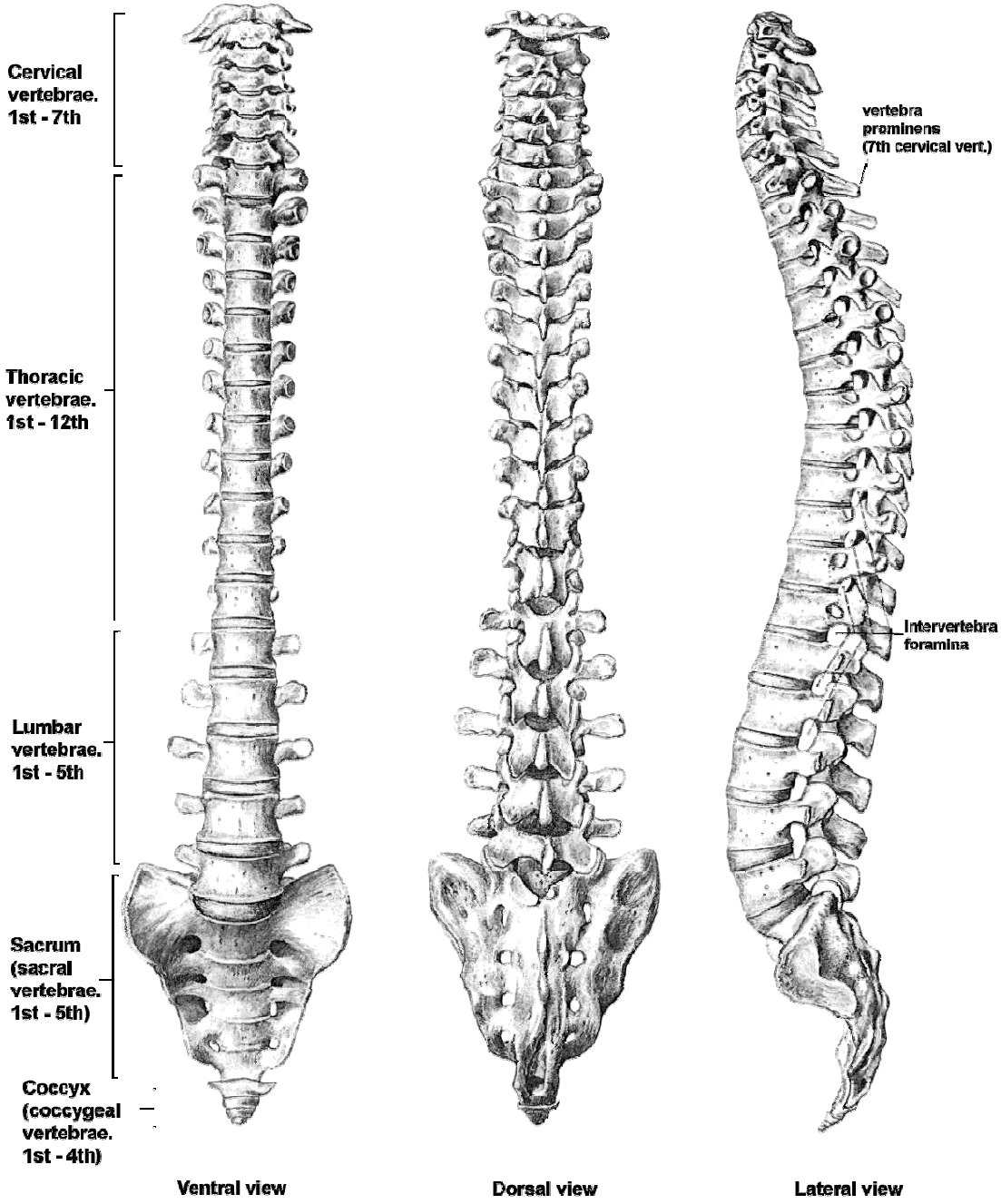

Figure 4: The spinal column showing the four spinal region (Sobotta et al., 1997).

In general, all the vertebrae from the four spinal regions possess common physical features. However, a closer study on each group of the vertebra of the respective spinal region above indicates special features that distinguish one vertebra from another. This is because various situations impose various tasks upon the vertebrae, which, in consequence, exhibit structural modifications to meet them. Moreover, the weight borne by the individual vertebrae increases progressively as the spine connected in series is descended; vertebral bodies, in consequence, become more massive as they proceed from the cervical to the lumbar region.

Each region classified in Figure 4 exhibits certain flexibility for human movement. Generally, the movement between individual vertebrae takes place (i) at the disc and (ii) at the joints or articulations formed between the articular processes (superior and inferior articular processes) of the over- and underlying vertebral arches.

However, as the aim of this project was to analyse the biomechanical responses of the cervical spine after various conditions, and the anatomy of the cervical spine has been documented qualitatively and quantitatively in various textbooks and published papers, this thesis does not merit the full description on the anatomy of the cervical spine (Martini and Ober, 2001; Nissan and Gilad, 1984; Oliver and Middleditch, 1991; Tan et al., 2002; Tan et al., 2004). However, the anatomical relationships of the bony cervical vertebrae, ligaments, intervertebral discs and cervical articulations are briefly described in the following sections as a foundation for a clearer understanding of the structural elements involved in the cervical spinal instability caused by various situations (trauma, disease or surgery).

2.2.1 General Cervical Vertebrae Characteristics

In the head-neck region, the cervical spine supports the head and allows a wide range of head motion. The cervical spine has seven vertebrae (Figure 5): the atlas (C1), the axis (C2) and C3-C7. C1 and C2 are different in structure compared to C3-C7 and they are uniquely modified to permit articulating movements of the head and neck.

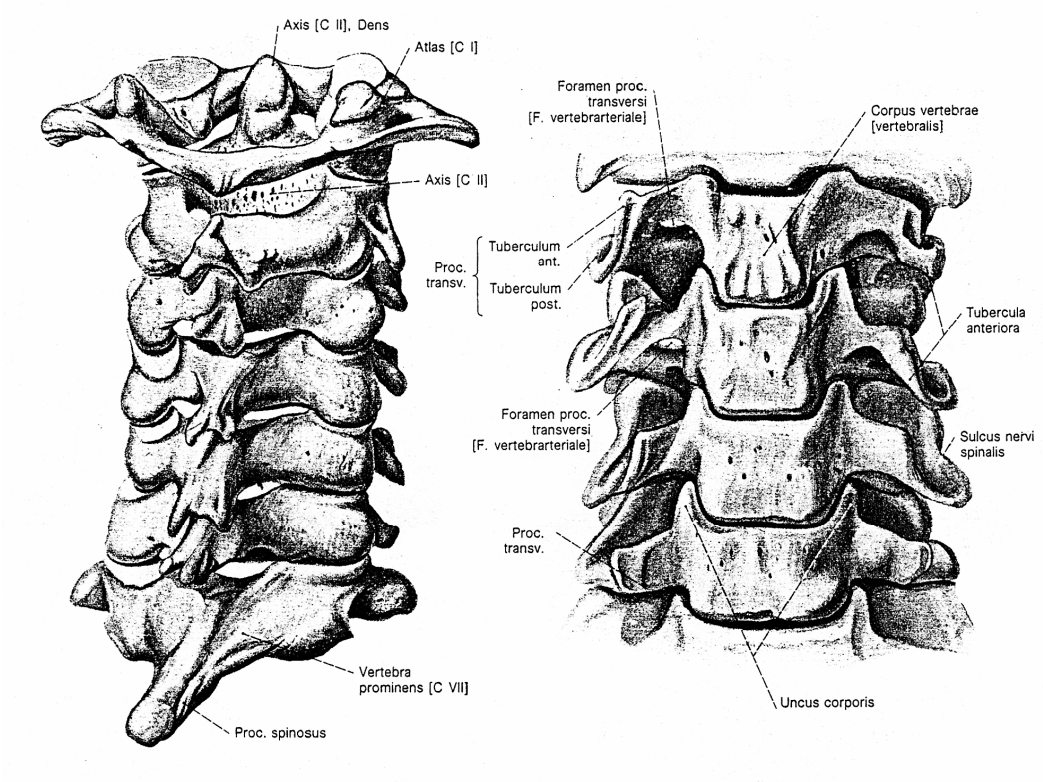

Figure 5: The seven cervical vertebrae (C1-C7) (Sobotta et al., 1997).

2.2.1.1 The Upper Cervical Spinal Vertebrae

The upper cervical spine is made up of two vertebrae, the atlas (C1) and the axis (C2). The atlas (C1) articulates superiorly with the occiput and inferiorly with the axis (C2). The atlas (Figure 6) differs from all other vertebrae in that it does not have a body, but consists of two lateral masses, which are joined together by an anterior and posterior arch (Oliver and Middleditch, 1991). The axis has a vertical pillar of bone or dens

projecting upwards from the superior surface of the body of the vertebral body (Figure 7) and it provides a pivot around which the atlas and the head rotate (Oliver and Middleditch, 1991).

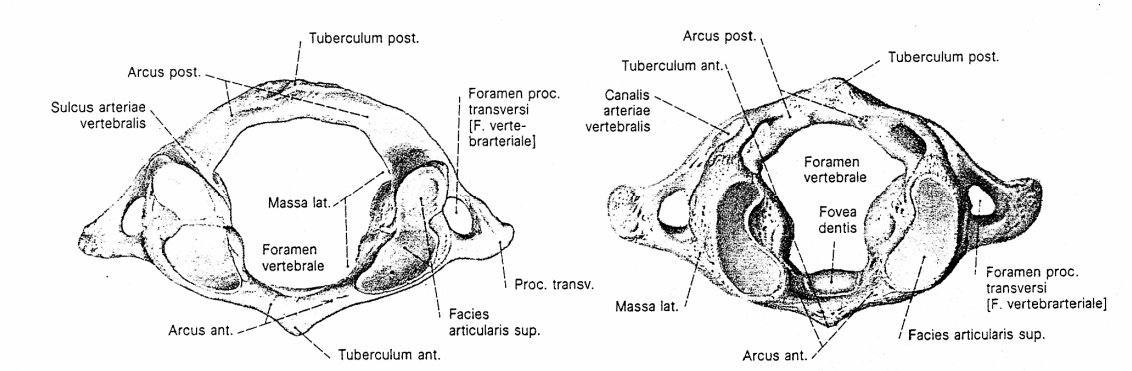

Figure 6: First cervical vertebra (C1) (Sobotta et al., 1997).

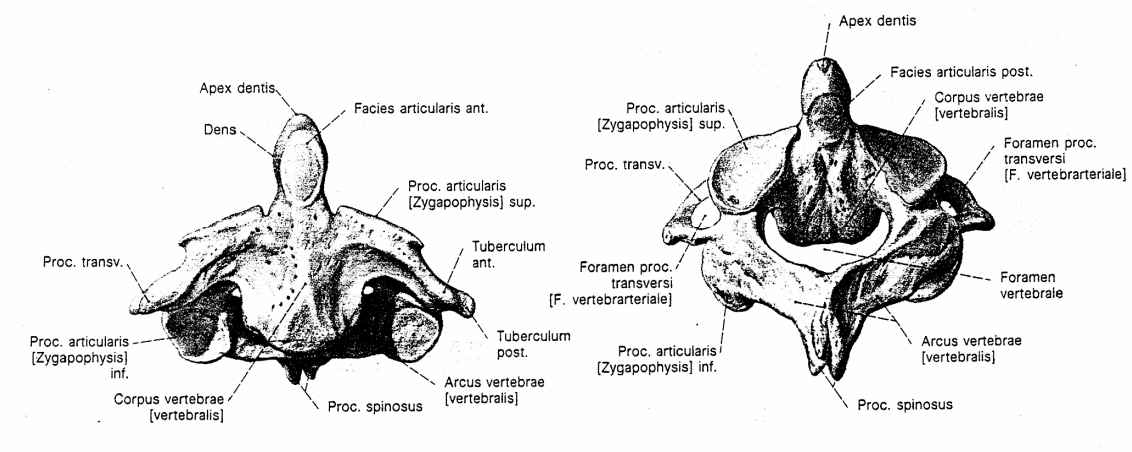

Figure 7: Second cervical vertebra (C2) (Sobotta et al., 1997).

2.2.1.2 The Lower Cervical Spinal Vertebrae

A typical vertebra in the lower cervical spine (Figure 8) has an elliptical vertebral body and a body posterior arch. The posterior arch can be divided into the pedicles, the lamina, the spinous process, the transverse process and the superior and inferior articulating facet joints. The spinal cord is protected and surrounded by the posterior elements (Oliver and Middleditch, 1991).

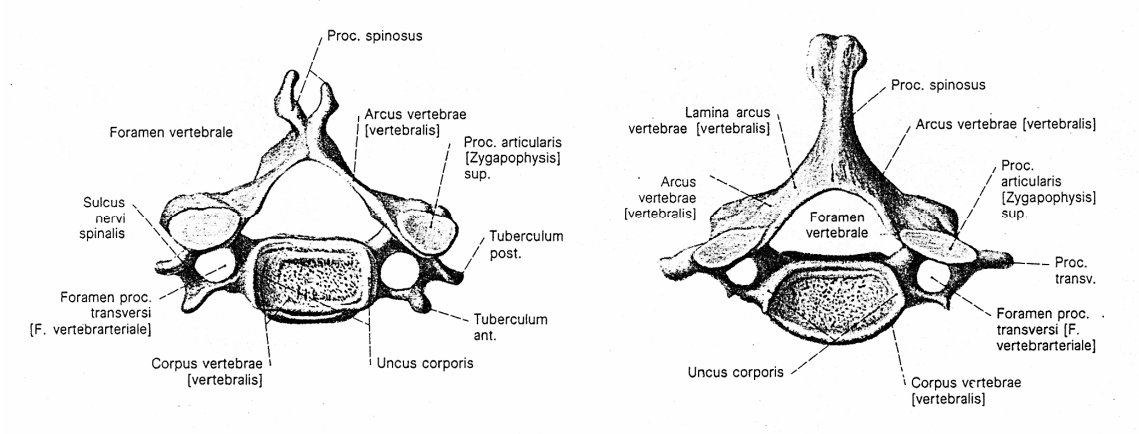

Figure 8: A typical vertebra of the lower cervical spine (C3 to C7)(Sobotta et al., 1997).

Typically, the bony vertebrae (C1-C7) are composite in nature. Physically, it is a honeycomb block of interconnecting trabecular bone, the cancellous bone, surrounded by a thin shell of harder compact/cortical bone.

The vertebral body of C2-C7 is roughly elliptical but varies in size and shape. It has a posterior surface, which forms part of the vertebral foramen and canal. The superior and inferior surfaces are nearly flat and are rough for the attachment of the discs, except at the periphery where the site of the ring is smooth. The vertebral body has a stiff outer shell, the cortical bone and a porous inner marrow, the trabecular bone. Recently, Panjabi et al., 2001a documented the cortical bone and endplate thicknesses of the lower cervical spine (C3 to C7) quantitatively.

2.2.2 The Intervertebral Discs

The space between two vertebrae from C2 to C7 is occupied by the IVD (Figure 9), except for the atlas and axis (1st and 2nd cervical vertebrae). The IVD consists of the nucleus pulposus and its limiting membrane, the annulus fibrosus and the vertebral end plate. It acts as a joint to allow angular motion and vertical displacement between two

vertebral bodies. The three basic components of the disc are the annulus fibrosus, the nucleus pulposus and the vertebral end plate (Oliver and Middleditch, 1991).

Pooni et al., 1986 showed that the cervical discs tended to have an elliptical cross-sectional shape. In the same year, Gilad and Nissan, 1986 using x-rays photographs, quantitatively measured the anterior and posterior disc height of 157 normal, healthy men. They showed that the anterior cervical disc height was larger than the posterior disc height. Recently, Mercer and Bogduk, 1999 determined the anatomy of the cervical spine qualitatively through micro-section studies. They showed that the three-dimensional architecture of the cervical annulus fibrosus is more like a crescentic anterior interosseous ligament than a ring of fibers surrounding the nucleus pulposus. These dimensions and anatomy descriptions reported in the literatures were used in the current study to define the intervertebral disc.

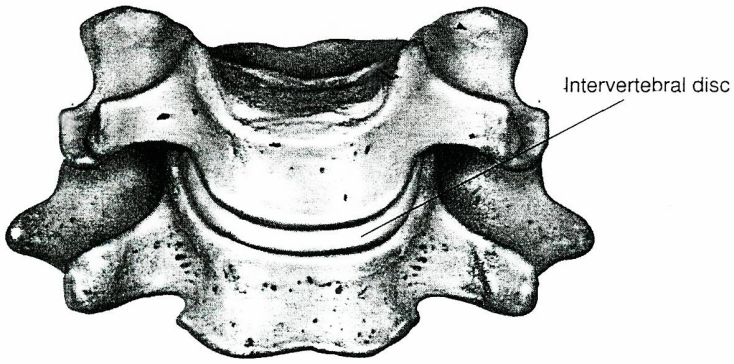

Figure 9: The intervertebral disc (Clark et al., 1998).

2.2.3 The Cervical Articulation Joints

The cervical articulation joints can be divided into two main parts: the upper and lower cervical articulation joints. The lower cervical articulation joints contains the posterior articulating facets and unconvertebral joints (Oliver and Middleditch, 1991).

2.2.3.1 The Lower Cervical Spine Articulation Joints (C2-C7)

2.2.3.1.1 Posterior Facets Joints

The articulating surface (Figure 10) of each superior and inferior articular process is covered with a 1 to 2 mm thick layer of hyaline cartilage. The hyaline-lined portion of a superior and inferior articular process is known as the articular facet. The junction between the superior and inferior articular facets on one side of two adjacent vertebrae is known as a facet joint. Direction and range of movement at these joints is determined by the orientation of the articular facets (Cramer and Darby, 1995). To facilitate and improve the development of the detailed finite element models, Panjabi et al., 1993 conducted a study to provide quantitative three-dimensional surface anatomy of the articular facets for the entire human vertebral column based on a study of 276 vertebrae. Recently, Yoganandan et al., 2003 determined the difference of the cervical level or gender dependency on the facet joint morphology in the human cervical spine. Geometric properties of the facet joint width, cartilage thickness, and cartilage gap were extracted from the anatomic sections from occiput to T1 levels using cryomicrotomy techniques. These posterior articular surface dimensions reported in the literatures were used in the comparison against the dimensions of the current FE model.

Figure 10: Sagittal frozen anatomic section of the human cervical spine showing the facet joint (Yoganandan et al., 2001).

2.2.3.1.2 Unconvertebral Joints

The uncinate processes (Figure 11) project upwards from the superior, lateral border of the vertebral bodies of C3 - C6 and correspond with reciprocally shaped cavities on the lower border of the vertebra above. The joints allow for a large degree of movement between the vertebral bodies and through the intervertebral disc, particularly in axial rotation (Yoganandan et al., 2001). The joints enable the disc to accommodate the coupling of lateral bending and axial rotation that is governed by the facet joints. Furthermore, for the purposes of mathematical modelling, Kumaresan et al., 1997a have documented the three-dimensional geometries of the luschka joints quantitatively, using cryomicrotomy. These anatomy descriptions and dimensions were used in the current study to define the unconvertebral joints.

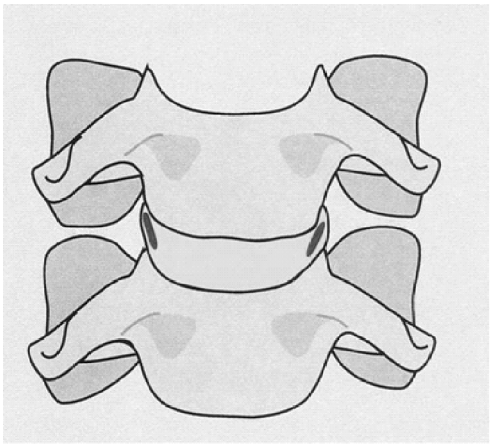

Figure 11: Schematic of the bilateral unconvertebral joints (Yoganandan et al., 2001).

2.2.4 The Ligaments

Ligaments are uniaxial in nature and designed to carry loads primarily in the direction in which their fibers run. The movements of the individual ligament's attachment points to the vertebrae provide tensile resistance to motion by developing tension in the ligament when stretched. The spinal ligaments have two important functions: they act to give strength and stability to the complex articulation of the spine; and act to protect

the spine and its contents against excessive movements. They readily resist tensile forces but buckle when subjected to compression. When a spinal functional unit (to be described later) is subjected to complex force and moment vectors, the individual ligaments provide tensile resistance to external loads by developing tension. The ligaments of the cervical spine region can be divided into the upper (Figure 12) and lower (Figure 13) cervical ligaments (Oliver and Middleditch, 1991).

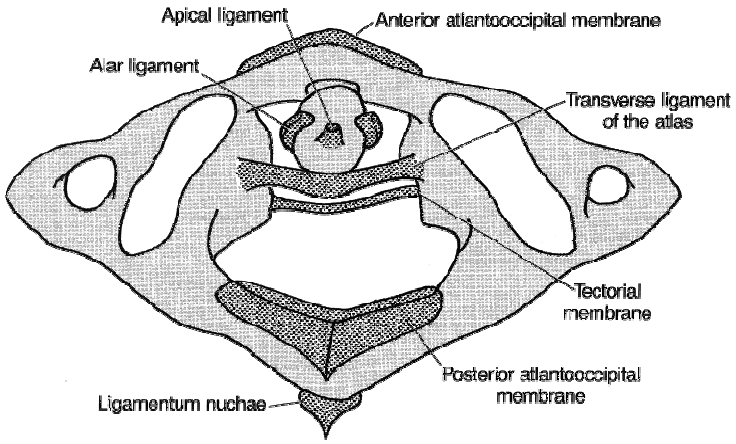

Figure 12: Ligaments of the upper cervical spine (Oliver and Middleditch, 1991).

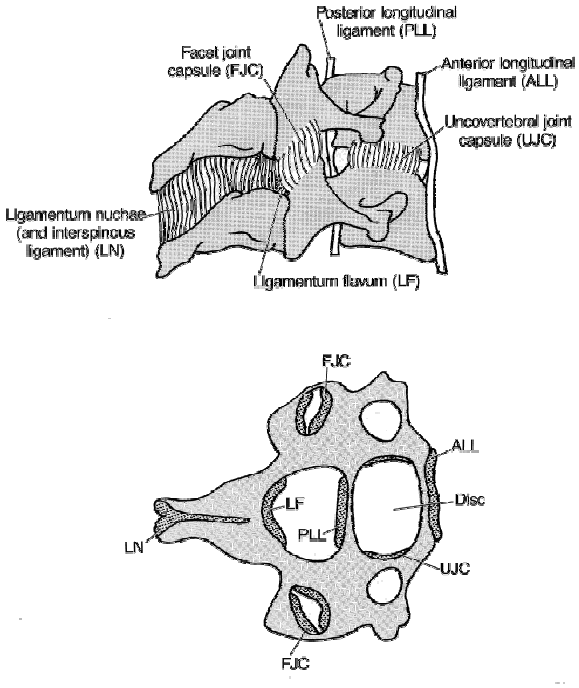

Figure 13: Ligaments of the lower cervical spine (Oliver and Middleditch, 1991).

2.3 Kinematics of the Functional Spinal Unit

A cervical functional spinal unit (FSU) or spinal motion segment (SMS) (Figure 14) is the smallest segment of the spine, which exhibits similar biomechanical characteristics to the entire spine (White and Panjabi, 1990). The FSU or SMS is composed of two adjacent bony vertebrae (connected by intervertebral disc) and the connecting ligamentous tissue. The behaviour of a spinal motion segment is dependent upon, among other things, the physical properties of its components, such as the intervertebral disc, ligaments, and articulating facets.

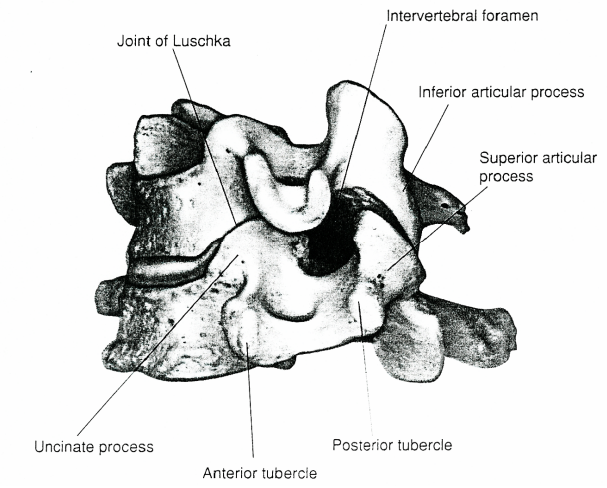

Figure 14: A cervical motion segment (Clark et al., 1998).

In general, a body may move in any six degrees of freedom. The motion is mainly caused by a combination of translation along any direction and rotation about any axis in space. Clinically, rotation of the spine or a vertebra in the sagittal plane is called flexion or extension. Rotation in the coronal plane is defined as lateral bending, and axial rotation is used to define the angular motion in the transverse plane. Linear translations are called antero-posterior displacement, lateral displacement and axial compression/distraction in the transverse, coronal and sagittal planes of the spine or the

vertebra, respectively. Generally, FSU rotation can be defined by the coordinate system (Figure 15) described by White and Panjabi, 1990. The sagittal plane is the yz plane; the frontal plane is the xy plane; the horizontal place is the xz plane. Movements are described in relation to the origin of the coordinate system. The origin is the zero point. ±z translation is anterior-posterior shear; ±y translation is tension-compression and ±x translation is left-right shear. The convention for rotations is determined by imagining oneself at the origin of the coordinate system looking in the positive direction of the axis. Clockwise rotations are positive while anti-clockwise rotations are negative. ±x rotation is flexion-extension, ±y rotation is axial rotation, and ±z rotation is axial rotation.

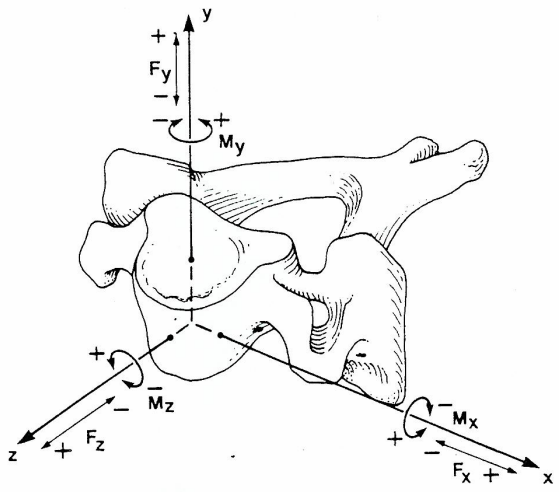

Figure 15: A multiplanar coordinate system with its origin at the centre of the vertebral body (White and Panjabi, 1990).

Load displacement or rotational motion curve is often used as a measure of physical properties of the spinal column and is nonlinear, which differs from other man-made structures (such as a steel spring, which is linear, i.e., the ratio of the load applied and the displacement produced is constant) (Panjabi, 2003). The motion is characterised by two phases (Figure 16). During the initial phase (neutral zone), the spinal column or FSU easily deforms at small loads. The second phase (elastic zone) involves

exponentially increasing motion resistance as the load increases. The combination of these two phases yields the non-linear characteristic of the FSU's load displacement curve. The range of motions (ROM) of the FSU is defined as the combination of the neutral and elastic zones (Panjabi, 2003).

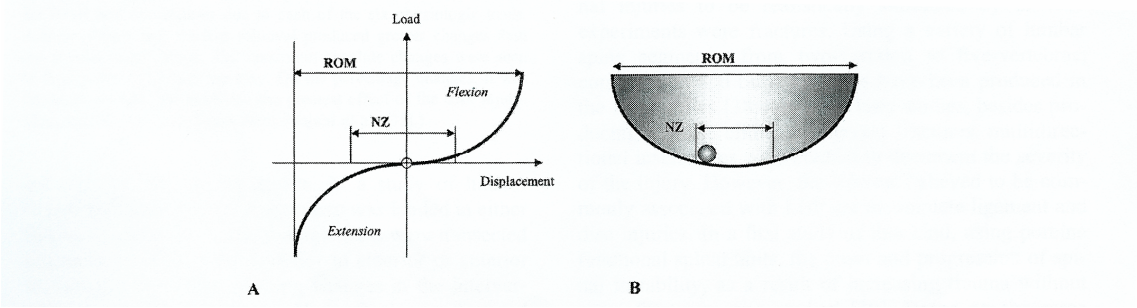

Figure 16: Load displacement curve. A) Spine segment subjected to flexion and extension loads exhibit a nonlinear load displacement curve. B) A ball in a bowl is a graphic analogue of the load displacement curve (Panjabi, 2003).

2.3.1 Spinal Instability

The pattern and amount of motion under an external load are dependent on the stiffness of the segment. Any alternation of the stiffness due to degeneration, trauma or surgery will also alter the pattern and amount of motion under the same external load actions. The motion of a normal spinal motion segment can be established by observing the deformation produced by a given force system. Any deviation from this normal range may then be considered as a sign of instability of the segment.

Spinal instability has been classified as a condition in which abnormal motions at the segmental levels are observed in response to the physiological loads (White and Panjabi, 1990). Damage to the spinal cord or nerve roots, injury and pain are sometimes included with clinical definitions of instability. Such definitions, although clinically relevant, are found to be in contrast with the definition of instability of a system in the

engineering sense. In the latter definition, the loss of stability of a conservative system occurs at a critical load, in a limit form or a bifurcation at which the second variation of the total potential energy ceases to be positive definite. According to the former clinical definition, the instability is noted to be associated with the reduction of the load displacement curve or an increase in the ROM (White and Panjabi, 1990). This highlights the importance of the normal function for the spine, rather than the ultimate load that can be supported.

White and Panjabi, 1990 defined clinical instability as "the loss of the ability of the spine under physiologic loads to maintain relationship between vertebrae in such a way that the spinal cord or nerve roots are not damaged or irritated and deformity or pain does not develop". At this time, upper cervical spine instability is quite well understood and defined both clinically and biomechanically (Cornish, 1968; Effendi et al., 1981; Fielding et al., 1974). However, classification of the lower cervical spine remains controversial (Harris et al., 1986). White et al., 1975 proposed a two-column, which defines one anterior column as the vertebral body, the disc and the anterior and posterior longitudinal ligament, and a posterior column as the ligaments and osseous structures posterior to the posterior longitudinal ligament. If a motion segment has all the anterior elements and one posterior element or all the posterior elements and one anterior element intact it will remain stable under physiologic loads. However, if all the anterior or posterior elements are not functional, the motion segment or FSU should be considered unstable (Panjabi et al., 1975; White et al., 1975). In addition to the disruption of the anterior or posterior elements, horizontal translation of >3 to 5 mm or sagittal plane rotation >11° more than the adjacent level in a motion segment, can be considered as cervical instability (White and Panjabi, 1990).

Thus, it is difficult to define stability or instability of the spine clearly. Definitions published to-date has often been incomplete or confused. In this study, spinal instability is referred to the loss of the ability of the spine under physiological loads to maintain its original pattern of displacement or ROM (White and Panjabi, 1990).

2.3.2 Secondary (Coupled) Motion

The term coupled or secondary motion denotes that the motion about one axis consistently occurs simultaneously with motion about another axis (rotation or translation). In vitro, it occurs in the thoracic and lumbar spine, as well as the cervical spine. Two kinds of coupled motion are especially well known in the cervical spine, axial rotation in the same direction as applied lateral bending, and lateral bending in the same direction as applied axial rotation (White and Panjabi, 1990). FE model developed in this study was validated in both primary and secondary motions (if available).

2.4 Cervical Injuries

Cervical injuries are critical injuries as they have the potential to injure the spinal cord. However, there is a lack of epidemiological data currently for neck injuries, especially for the Asian population. In the United States, cervical injuries have cost the nation approximately $68.7 billion in 1978 and $92.7 billion in 1983 (Yoganandan et al., 1987). In Sweden, Borin and von Holst, 2002 conducted a national survey on cervical injuries of patient data from 1987 to 1999. During the study period, 14,310 non-fatal and 782 fatal cervical injuries occurred. Most of the cervical injuries were caused by transport accidents and falls (Brolin and von Holst, 2002). In Singapore, Yen et al., 1998 carried out a retrospective study of 231 patients admitted between January 1990 and December

1995 to the only spinal rehabilitation centre in Singapore. They found that the most common causes of injuries were fall (50.7%) and road traffic accident (37.2%). Damage to the cervical spine predominated (53.7%), followed by the thoracolumbar junction (23.4%). The overall number of road accidents in 2001 and 2002 resulting in injury or death are 6879 and 7091 cases respectively. Out of these, 145 and 302 suffered serious injuries (Singapore.Police.Force, 2002). It has been shown that injuries accounted for approximately 7.0% (1108 humans) for major causes of death from 1998 - 2002, and are only exceeded by cancer, heart diseases, pneumonia and cerebrovascular disease (Ministry.of.Health, 2003). However, accidents remained the number one (approximately 9.6% or 37000 patients) cause of hospitalisation from 1998 – 2002 (Ministry.of.Health, 2003). Similar trends have been observed in the United States (Yoganandan et al., 1987). It has also been shown that most of the cervical injuries are more often connected with spinal cord injuries, and most of it occurred at the C5-C6 level (Figure 17) (Sances et al., 1984).

2.5 Summary

This chapter reviewed the anatomy and kinematics of the human cervical spine. It was shown that the cervical spine is a mechanical structure composed of multiple spinal motion segments connected in series, and its total behaviour is the composite of the behaviours of the individual spinal motion segments. It was also shown that the cervical spine is in a unique position to receive injury. Therefore, understanding the mechanics of the cervical spine is important for the treatment of these injuries.

Review on the literatures showed that many studies have been conducted in the past to quantify the dimensions of the spinal vertebrae, facets, cortical bone, endplate,

intervertebral disc and even unconvertebral joints. These studies provided better understanding on the spinal dimensions and are important for the development of the current cervical FE model. They allowed comparisons of the current FE model geometry against the data reported in the literatures.

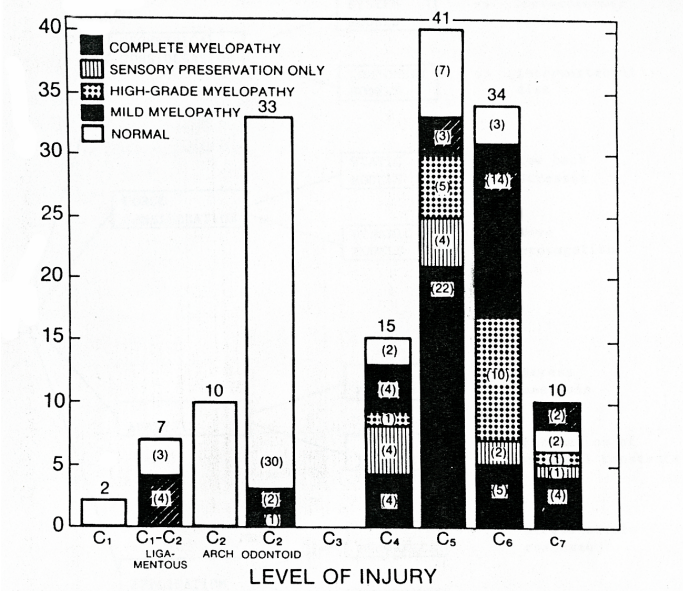

Figure 17: Cervical spine fractures of patients admitted between 1975 and 1980 (Sances et al., 1984).

In the following Chapter, the author reviewed biomechanical studies that were carried out on the human spine, especially the human cervical spine. Their objectives, methodology and results will be highlighted and discussed.

Chapter 3. Review on Biomechanical Models

3.1 Introduction

The spine is a mechanical structure composed of multiple functional spinal units (FSUs) connected in series, and its total behaviour is the composite of the behaviour of the individual FSU, and each FSU may move in any of the six degrees of freedom. The motion mainly arises from a combination of translation along any direction and rotation about any axis in space. Several experimental and biomechanical three-dimensional studies of human FSUs have reported the load-displacement properties of various cervical spinal specimens under different physiological loadings for different purposes. These biomechanical studies have provided basic insights into the functions of the spine and contributed in the development on the definition of clinical instability and diagnostic guidelines. Biomechanical studies help to define the roles of various anatomic elements (e.g., facets and disc) in supporting physiologic and traumatic loads applied to the cervical spine. In 1998, Panjabi provided an extensive overview of the cervical spine models for biomechanical research. Generally, the biomechanical models are divided into four categories depending on their usage: **physical models**, ***in vitro* models**, ***in vivo* models** and **finite element models** (Table 1).

This chapter aims to provide a review of the existing biomechanical models and serves as a guide and idea for current research. Definition, purpose and a brief description of the selected studies from the literature for each model are presented in the following sections. Studies under each category are briefly reviewed to illustrate the diversity of the model's characteristics, with a greater emphasis on the finite element models.

Details, of course, can be easily obtained from the original articles. This chapter ends with a brief discussion on the prevailing gap and problems found in the literature and areas for further research.

Categories	Uses	Advantages	Disadvantages
Physical model	Implant and component testing	Simple, less variable, less expensive, evaluates implant alone	Non-anatomical, un-physiological implant loading
In vitro model	Spinal function studies and implant testing	Actual human anatomy, physical properties and population variability	Difficult to obtain, expensive
In vivo model	Spinal function studies and implant testing	Living phenomena can be simulated	Difficult to obtain, expensive, usually tested on animals
Finite element model	**Simulating situations not modelled by other biomechanical models**	**Capable of simulating real phenomena: effect of muscles, bone healing, tissue adaptation, determining internal loads, strain and stress**	**Difficult to validate**

Table 1: Four categories of biomechanical models with their uses, advantages and disadvantages.

3.2 Physical Models

Physical models are made of artificial materials. These models are used when bony anatomy and physical properties of the soft tissue are less important.

3.3 *In Vitro* Models

In vitro models consist of human cadaveric spine specimens. These models are used when the anatomy is more important. The main uses of such models are to test for the strength, fatigue, stability of the spine specimen and its associated tissues. *In vitro* biomechanical models using a cadaveric spine specimen can be divided further into two

sub-categories. **Basic biomechanics** models help to document the basic movements of the spine in response to applied loads or displacements. The spine's behaviour may be studied in single or multiple directions, under simple or complex loads and in neutral or any other posture. **Clinical biomechanics** models simulate spinal injuries, diseases or surgical decompression procedures and may involve transecting one or more appropriate spinal elements to simulate cervical injuries. Comparative biomechanical responses of the altered and intact states of the specimen quantify the effect of alteration and potential instability. A detailed review of these studies by investigators whose works are used for comparison of results from FE analyses are presented below.

3.3.1 Basic Biomechanics

Moroney et al., 1988 investigated the load-displacement behaviour of 35 fresh adult cervical spine motion segments in compression, shear, flexion, extension, lateral bending and axial torsion tests (Figure 18). The results show that the stiffness of the cervical motion segments in compression was similar to those of the thoracic and lumbar motion segments. However, in other modes of loading, the cervical stiffness was considerably smaller than the thoracic or lumbar stiffness. Removal of the posterior elements (disc segments) decreased cervical motion segment stiffness by as much as 50%.

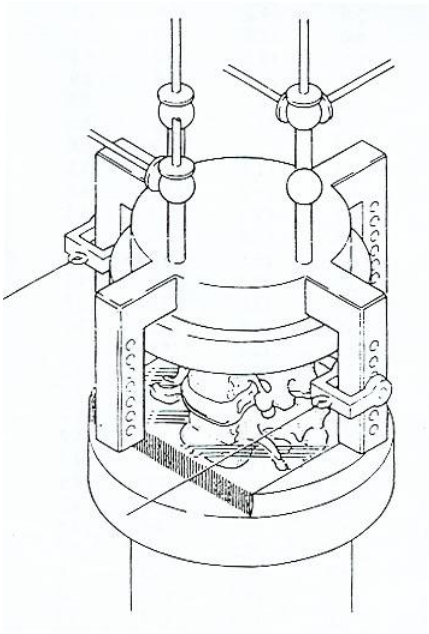

Figure 18: Schematic of an intact motion segment being tested *in vitro* (Moroney et al., 1988).

Shea et al., 1991 determined the biomechanical load-displacement response and strength of the lower cervical spine by using a combination of physiological related loads (Figure 19). During the failure tests, failure in six out of seven mid cervical specimens resulted from flexion alone, while combined compression-flexion was required to fail five of the eight lower cervical specimens. These controlled load-displacement measurements of cervical spine specimens described for the first time the continuous flexion-compression response of the human cervical spine up to failure, and suggest that the results on the three apparently distinct mobile regions of the cervical spine (C1-C2, C2-C5 and C5-T1) may facilitate the interpretation of hazardous conditions and the diagnosis of injury on the cervical region.

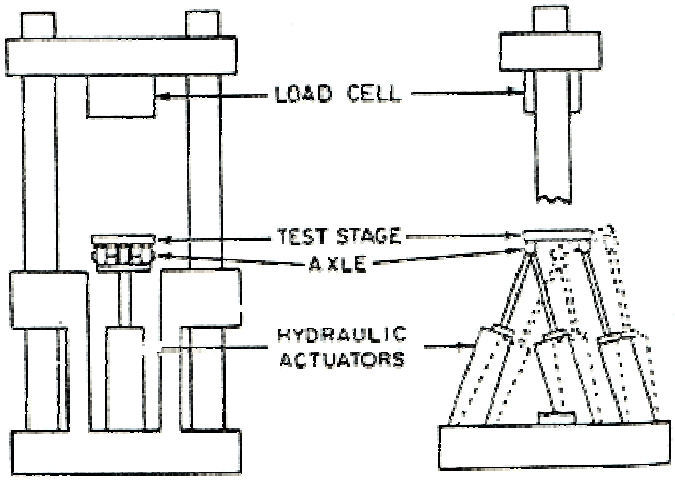

Figure 19: Planar testing apparatus consisting of a three-component load cell, a movable test stage, linear hydraulic actuators and linear variable displacement transducers (below actuators) for displacement feedback (Shea et al., 1991).

In 1993a, Wen et al. conducted experiments (Figure 20) on 56 functional spinal specimens to investigate the biomechanical responses of the cervical spine under pure static moments (flexion/extension, lateral bending and axial rotation). The results clearly demonstrated the non-linearity of the cervical spine load-rotational curves in the three-dimensional space.

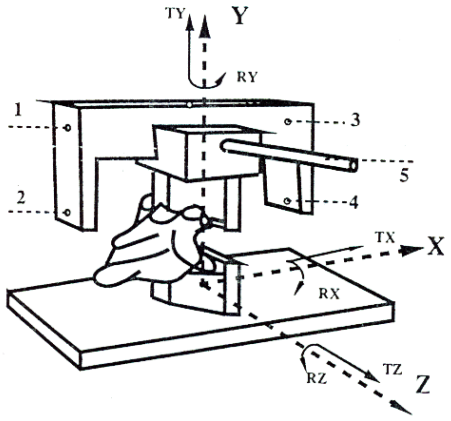

Figure 20: Three-dimensional coordinate systems and experimental setup (Wen et al., 1993a).

Pintar et al., 1995 determined the patterns of localized strain distribution in the anterior aspect of the vertebral body and in the lateral masses of lower cervical three-segment

units. Miniature strain gages were mounted to the middle human cadaveric vertebrae (Figure 21) and exercised under three types of loading mode: compression-flexion, compression-extension and uniform compression at 800 N. The corresponding displacement, strain for the vertebral body and the lateral masses were extracted at four load levels (200, 400, 600 and 800 N).

a) b)

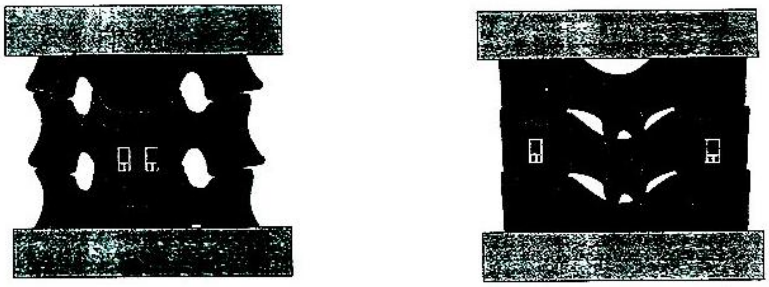

Figure 21: Illustration showing placement of the strain gages on the a) anterior vertebral body and b) on the lateral facet masses (Pintar et al., 1995).

Yoganandan et al., 2000 conducted a study to characterize the geometric and mechanical properties of the cervical ligaments from C2-T1 levels using eight human cadavers. The lengths and cross-sectional areas of the anterior longitudinal ligament, posterior longitudinal ligament, joint capsules, ligamentum flavum, and interspinous ligament were determined. The biomechanical force-deflection and stiffness were obtained using in situ axial tensile tests. Data were then grouped into middle (C2–C5) and lower (C5–T1) cervical levels. The study finally concluded that various FE researchers attempting to incorporate these data into stress-analysis models can choose the specific parameter(s) based on the complexity of the model used to study the biomechanical behaviour of the human cervical spine.

Although a number of *in vitro* studies have attempted to delineate the normal movement patterns of the cervical spine, none has explored the complexity of the whole cervical spine as a three-dimensional structure. In 2001b, Panjabi et al., studied the mechanical properties of multilevel human cervical spines by applying pure rotational moments to each specimen and measuring the intervertebral ROM. Pure rotational moments of flexion-extension, bilateral axial rotation and lateral bending were applied using a specially designed loading fixture (Figure 22). The loading fixture is designed to apply pure moments to the specimens via three round discs: two vertically oriented and one horizontally oriented. The vertical pulleys are used to apply moments of flexion, extension and lateral bending. The horizontal pulley is used to apply axial rotation. The resulting intervertebral motions were recorded as a series of load-displacement curves.

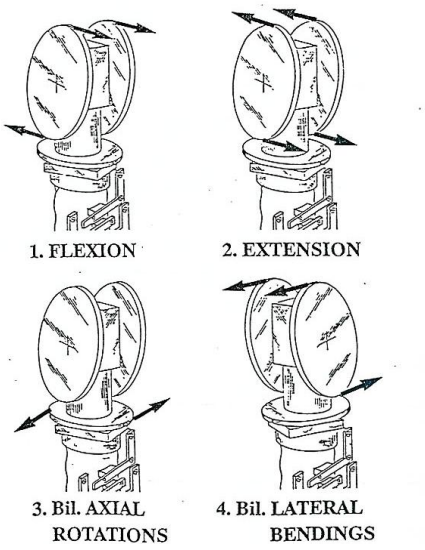

Figure 22: The experimental setup for the flexibility test. (Panjabi et al., 2001).

Cripton et al., 2001 developed a novel technique to measure *in vitro* disc pressures in human cervical spine specimens. A miniature pressure transducer was used and an insertion technique was designed to minimise artefacts due to insertion (Figure 23). The

technique was used to measure the intradiscal pressure in cervical spines loaded in pure axial compression. The resulting pressure varied linearly with the applied compressive force. Peak pressures between 2.4 and 3.5MPa were recorded under 800N of compression.

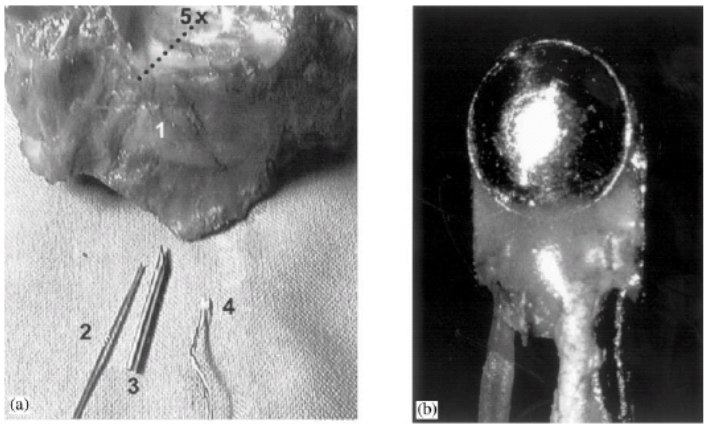

Figure 23: (a) Insertion apparatus, 1-specimen (level C4–5), 2-insertion wire, 3-guide tube, and 4-sensor. The cranial endplate of C4 was used as a ‘‘template’’ as shown (dotted line) from which the guide tube orientation and depth could be determined so that the sensor is implanted at the centre of the disc (point 5); (b) close up of the pressure sensor (Cripton et al., 2001).

3.3.2 Clinical Biomechanics

3.3.2.1 Surgical Stabilization

Schulte et al., 1989 investigated the immediate biomechanical stability of the cervical spine following discectomy and stabilization. The cervical specimen was tested in the intact state, following discectomy at the C5-6 intervertebral level, following insertion of a bone graft in the intervertebral space, and following the application of an anterior metal plate. The load-deformation data of the injured and stabilized tests were normalized with regard to the corresponding results of the intact specimens. At the injured level (C5-6), the load-deformation results indicated a highly significant increase in motion in flexion (66.6%), extension (69.5%), lateral bending (41.3%), and axial

rotation (37.9%). After the insertion of the bone graft, a significant decrease in motion was seen in the effected segment in extension (-45.9%), with similar reductions in lateral bending and axial rotation and a smaller reduction in flexion. The application of an anterior metal plate in addition to the bone graft at the injured level provided significant reduction in motion (-70%) in all load modalities. The data may have clinical relevance regarding the role of internal fixation in cases of severe spine instability.

Pelker et al., 1991 studied the rotational biomechanical responses of the normal and posterior stabilized cervical spine. Before stabilization, a severe ligamentous and bony injury was simulated on the three vertebral body human cervical spine segments. It was mentioned that the load displacement curves of the intact spines were similar to those reported earlier (Panjabi et al., 1988). Good stabilization was noted for all of the repairs in flexion loading.

3.3.2.2 Ligamentous Injury

Richter et al., 2000 investigated the load-displacement properties of the normal and injured lower cervical spine under flexion/extension, axial rotation and lateral bending, using pure moment of 2.5 Nm without axial preload. The specimen was mounted on the spinal loading simulator as shown in Figure 24. Five conditions were investigated consecutively: (1) the intact functional spinal unit (FSU) C5/6; (2) the FSU C5/6 with the anterior longitudinal ligament and the intertransverse ligaments sectioned; (3) the FSU C5/6 with an additional 10-mm-deep incision of the anterior half of the annulus fibrosus and the disc; (4) the FSU C5/6 with additionally sectioned ligamentum flavum as well as interspinous and supraspinous ligaments; (5) the FSU C5/6 with additional

capsulotomy of the facet joints. The results were captured and compared against the intact model. Finally, the investigators concluded that flexion/extension is the most sensitive load-direction for the tested discoligamentous instabilities.

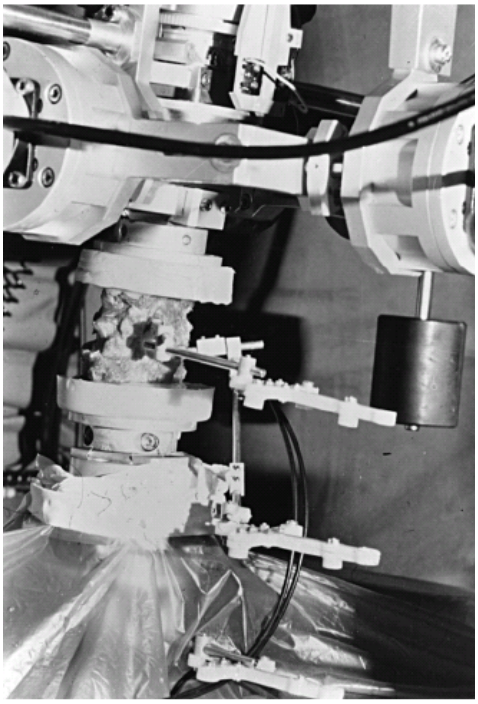

Figure 24: Cervical human specimen fixed in the three-dimensional spinal loading simulation (Richter et al., 2000).

3.3.2.3 Facetectomy

Raynor et al., 1985 tested fourteen cervical spine motion segments consisting of two adjacent vertebral bodies and their connecting ligaments: these were tested in shear. Five specimens had intact facet joints, five specimens had bilateral facetectomy of 50% or less, and four specimens had bilateral 70% facetectomy. The results indicated significant lost of cervical spine shear strength for bilateral resection of more than 50% of the facet joint. In 1987, Raynor et al. repeated the experiment using a single motion segment in an effort to expand on their previous investigation. Complete facetectomy was performed and subsequent motion was measured with non-destructive testing.

Zdeblick et al. 1993 used a four level-segment to investigate the biomechanical effects of graded bilateral facet resections using *in vitro* experiments (Figure 25). Each specimen was tested intact and after sequential resection of 25%, 50%, 75% and 100% of the C5-C6 capsules. They found that cervical segmental mobility increased substantially after facet resection of greater than 50%.

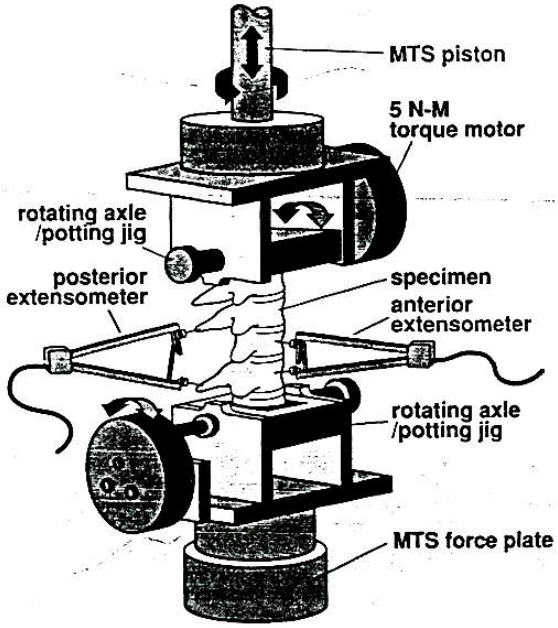

Figure 25: Experimental setup to study the influence of cervical facetectomy (Zdeblick et al., 1993).

Generally, *in vitro* studies have indicated the destabilizing effects of facet resection on the ROM, the relationship between the amount of resection and degree of segmental instability resulted from this resection and the potential contribution to accelerated degenerative changes.

3.3.2.4 Laminectomy

Goel et al., 1984 tested the flexibility of C4-C6 after applying a pure moment of 0.3 Nm on the C2-T2 specimens with spinous ligaments and ligamentum flavum removed at the

C5-C6 level. Effects of stabilization (interspinous wiring and acrylic cement, PMMA) after removal of ligaments on the cervical spine inter-segmental ROM was investigated. A three-dimensional sonic digitizer was then utilized to study the motion in flexion, extension, right lateral bending and right axial rotation. The results indicated an increase of about 25% in flexion-extension, 6% in lateral bending and 3% in axial rotation. Four years later, Goel et al., 1988b studied the effect of multiple-level total laminectomies followed by stabilization on the load-deformation behaviour of the cervical spine. Fresh human ligamentous cervical spines were harvested and a pure moment of 0.3 Nm was applied via a loading frame attached to the C-2 vertebra of the specimen. A set of three light-emitting diodes (LEDs) were attached rigidly to each of five vertebrae (C3-C7) to record their spatial locations after each load step application. They found that the flexion-extension resulted in a significant increase of about 10% in the ROM after two-level laminectomies. The laminectomized specimen was then stabilized, using a facet-wiring construct, across the C4-C7 segment before testing for the final time. The results showed that the facet wiring was an effective technique to stabilize the injured cervical spines (approximately equal to 80% reduction in motion, compared with intact spines).

Double-door type cervical laminoplasty has been widely used in the treatment of multi-segmental stenotic conditions. However, its biomechanical advantages over laminectomy remain controversial. Kubo et al., 2003 evaluated the effects of multilevel double-door laminoplasty and laminectomy as compared with the intact cervical spine. The results indicated that the double-door laminoplasty with hydroxyapatite spacer appears to restore the motion of the decompressed segment to its intact state in all loading modes.

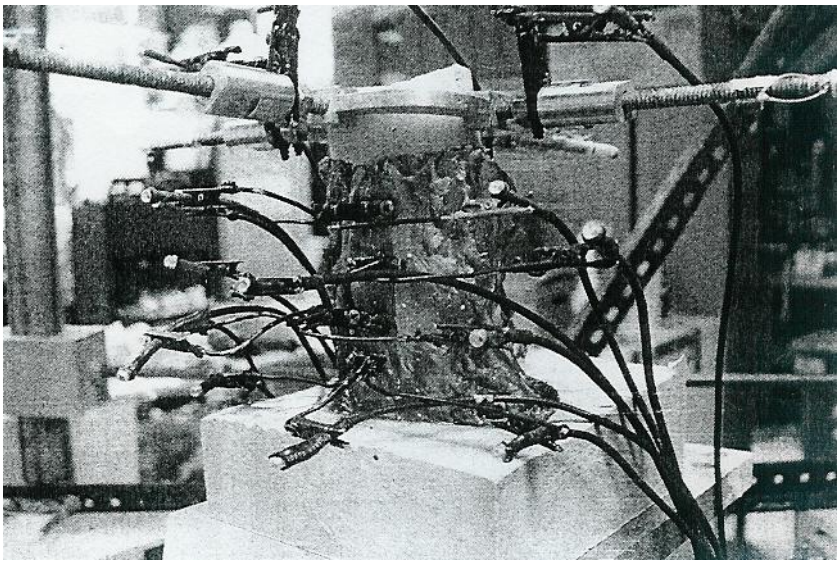

Figure 26: Experimental setup for the testing of the cervical spine (Kubo et al., 2003).

3.4 *In Vivo* Models

There are certain phenomena that cannot be studied using in *vitro* models. In these situations, animal models are used to study phenomena such as fusion in response to spinal instrumentation, degenerative processes adjacent to the fusion and response to an injury to disc and facets. The output of these models consists of stiffness and strength of the specimen. In vivo biomechanical models usually use animal models, with minimum work done using human volunteers.

3.5 Finite Element Models

In vitro and *in vivo* cervical spinal stability analyses usually focus on the analysis of the ROM or to a minor extent, internal stress and strain of the intact, injured and stabilized cervical joints. Any changes to the cervical spinal component either through one of these conditions or a combination of these conditions would then be expected to change the ROM under certain loading conditions. These changes in the ROM may affect the stress, strain and promote degenerative changes in the various spinal components.

Although the ROM is a valuable tool for the study of spinal stability, sole reliance on the ROM may only produce partial results. Predicting the change in both the ROM and internal biomechanics for various situations is important for understanding the magnitude and mechanical nature of the cervical spinal instability. However, due to inherent shortcomings described earlier associated with *in vitro* and i*n vivo models*, it is necessary to use the finite element methods of analysis to investigate and understand the cervical spine clinical biomechanics.

Finite element analysis is an essential part of today's engineering activities. It is a very well tested technique used in the design of numerous products from electronic systems and domestic appliances through cars, aircraft and large civil engineering constructions. Detailed information on the basics of FEA can be found in Appendix A.1 Introduction to FE.

Finite element methods have the advantage that an infinite number and variety of combinations can be developed and investigated. Furthermore, the same model can be used for any types of loading conditions, the model will not be injured or damaged, and the model can be modified to reflect any injury or clinical conditions. Finite element analysis can also provide a wealth of information that *in vitro* studies cannot, such as the load sharing and stress distribution through the soft and hard tissues.

The first application of finite element analysis in the area of biomechanics was probably reported by Brekelmans et al., 1972 The application of musculoskeletal biomechanics method started with thoracic modelling in 1970 (Schultz and Galante, 1970) and the vertebral column in 1973 (Panjabi, 1973). Continuous advancements in numerical

techniques as well as computer technology has made the finite element method a versatile tool for biomechanics applications and allowed simulation of more complex problems (including the biomechanics of the normal, injured and surgically altered spine). FEA also enjoys a distinct advantage over many other mathematical modelling techniques (particularly those involving closed-form equations) in that it can handle, with relative ease, the complex geometries, material and contact nonlinearities encountered in the modelling of spine.

Since 1987, the growing interest in spinal research has contributed to a large increase in the number of published papers. Yoganandan et al., 1987 provided an extensive review of all types of mathematical models of the human spine, including continuum models, discrete and lumped parameter models, as well as models based on the more modern finite element method. Goel and Gilbertson, 1995 presented a review on the applications of the finite element in thoracolumbar spinal research. In the same year, Gilbertson et al., 1995 did another review on the new developments and advantages of mathematical spine biomechanics research. Yoganandan et al., 1996a provided another critical review on the finite element applications in human cervical spine modelling. They focused on the developments in model construction (model generation), constitutive law (material properties) identification, loading and boundary condition details and validation of the finite element modelling. In 2001, Yoganandan et al., provided an extensive summary on the methods and modelling approaches used in the development and analysis of the cervical spine finite element model. Geometrical characteristics such as length and cross-sectional areas, and material properties such as force-displacement and stress strain responses for all components were described in the article. One year later, Fagan et al., 2002a reviewed the development of finite element

analysis in the spine modelling. These reviews highlighted the importance of the FE studies in contributing a wealth of information on the spinal biomechanics, reducing the dependence on animal and cadaveric experiments and at the same time, providing an invaluable complement to the clinical studies.

Generally, there are four ways in which finite element analysis can contribute to cervical spine research;

(a) to provide an assessment and understanding of the cervical spine in health,

(b) to provide an assessment of the cervical spine as altered by disease, degeneration, ageing, trauma or surgery,

(c) to provide an assessment of the cervical spine with instrumentation and

(d) to assist in the design and development of the spinal instrumentation.

The four main areas of cervical spine research using FEA can also be provided by experimental analyses and clinical studies. However, finite element analyses can provide information that cannot be obtained by these studies. For example, it can predict the value of the stress in the various spinal components (discs, vertebra body, etc), as well as detailed rotational motion data. It also allows exploration of an essentially infinite range of various physiological conditions and combinations of these conditions that help in the understanding on the cervical spine biomechanics. Similarly, finite element analysis permits exploration of countless range of different treatment options and surgical interventions and allows ‘testing’ and optimization of any prostheses before it is even manufactured.

Today, finite element models of the human spine can be classified into the following sections;

a) whole spine models

b) single vertebral body models

c) intervertebral disc models

d) lumbar or thoracic spine models

e) cervical spine models

f) other models, (spinal injuries, instrumentation, etc)

Literature reviews for the above finite element spinal models are presented below. Due to a large number of papers reviewed, only selected articles will be presented in the following sections and literature review was concentrated on the published papers regarding the cervical spine.

3.5.1 Whole Spine Models

Belytschko et al., 1978 developed a three-dimensional finite element model of the spine to evaluate the mechanical response of a pilot being ejected from a plane's cockpit. The model shown in Figure 27 consisted of the vertebrae, pelvis, head, and ribs from T1 to T10, upper and lower viscera, ligaments, muscles and connective tissue. It was assumed that all the skeletal components were rigid bodies, with each vertebra being modelled by only one rigid element. Spring elements were used for the ligaments and harness restraints, while beam elements were used for the intervertebral discs. The model was subjected to a non-linear force applied to the base of the model (the seat) to simulate ejection.

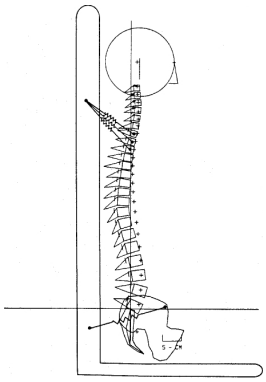

Figure 27: Lateral view of a simplified model to evaluate the mechanical response of a pilot being ejected from an aircraft (Belytschko et al., 1978).

A simplified three-dimensional finite element model (Figure 28) was developed by Dietrich et al., 1991 to look at the behaviour of the complete spine. It included intervertebral discs that were modelled with anisotropic elastic properties for the annulus and an incompressible space for the nucleus pulposus. All bone components were again assumed to be rigid, but both ligament and muscle effects were included. The model was used to estimate the forces and stresses in the different elements for different positions of the spine.

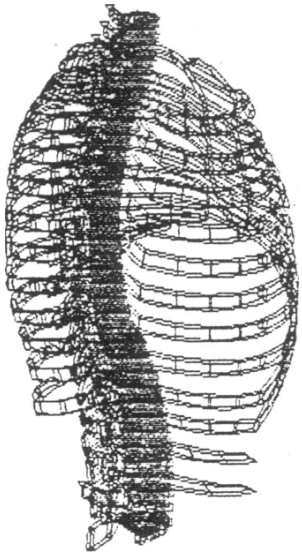

Figure 28: A three-dimensional model of the spine and ribcage that included a simple disc model and some muscle and ligament detail (Dietrich et al., 1991).

In order to study deformity due to laminectomy, Saito et al., 1991 simplified the vertebral geometry by dividing it into four sagittal slices. The first slice accounted for the vertebrae and the discs, the second slice included the cortices of the body and the articular facets, the third slice included the transverse processes and intertransverse ligaments and the fourth slice simulated the lower part of the cranium and the cortex of the atlas (Figure 29). For the postlaminectomy model, slices 3 and 4 were the same as the normal model. However, the spinous processes and spinous ligaments were removed by laminectomy for slice 1 and the laminas were also removed for slice 2. Based on linear elastic material definition, spine deformities were computed. The lower region of T2 was fixed and the lower part of the skull had a free boundary condition in the antero-posterior direction. A load of 150 N (four times the weight of the head) was applied to the C1-C2 facet. No validation results were reported. The simulation analyses revealed that the primary cause of postlaminectomy deformity was the resection of one or more spinous processes and/or posterior ligaments (Figure 30). In the normal model, the stress was diffused, resulting in uniform compression on the spinal bodies, therefore, no deformity occurred. However, in the postlaminectomy model, the tension was transferred to the facets. The resultant imbalanced and increased stress on the spinal bodies led to wedging deformities.

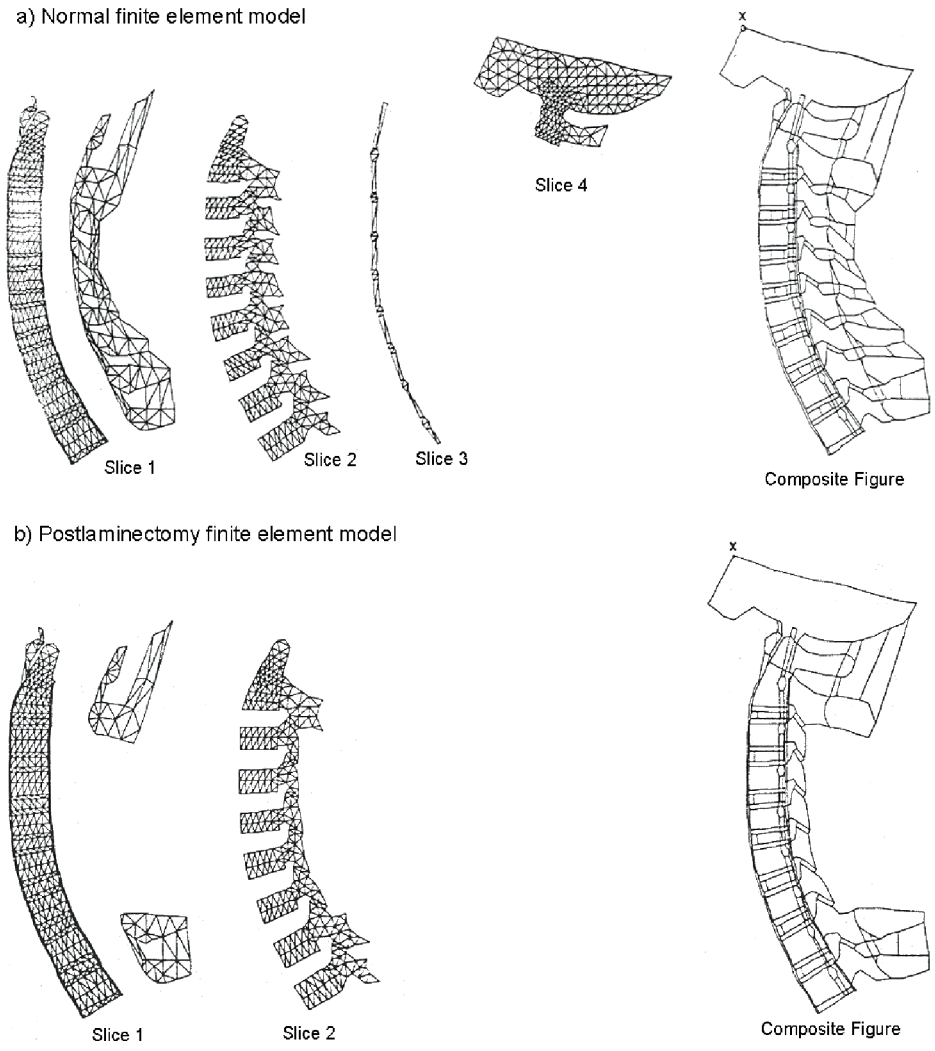

Figure 29: a) Normal and b) Postlaminectomy finite element model of the cervical spinal column (Saito et al., 1991).

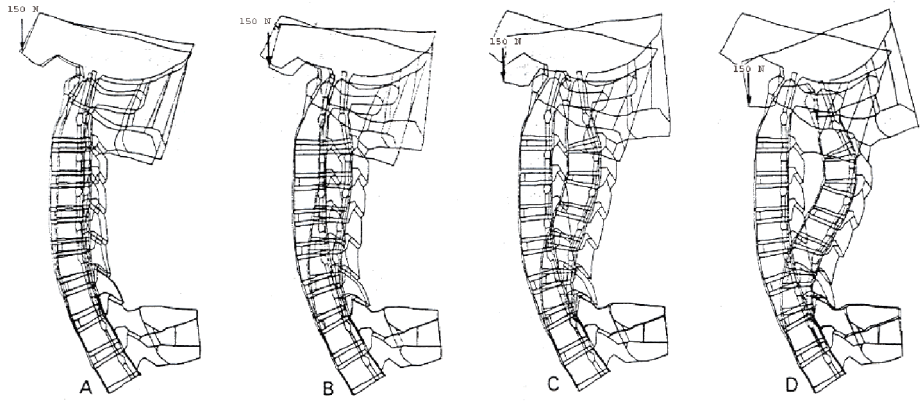

Figure 30: Postlaminectomy finite element model. A-D, Displacement after the 1st, 5th, 10th and 14th loadings (Saito et al., 1991).

Lee et al., 1995 used a linear three-dimensional finite element model (Figure 31) (including the ribcage, thoracolumbar spine and pelvis with their associated soft tissues) to predict the vertebral displacements after manipulative techniques used in the assessment and treatment of spinal disorders. In this model, the intervertebral discs were modelled by beam elements, and it was assumed that the patient was relaxed and hence the muscle forces were negligible.

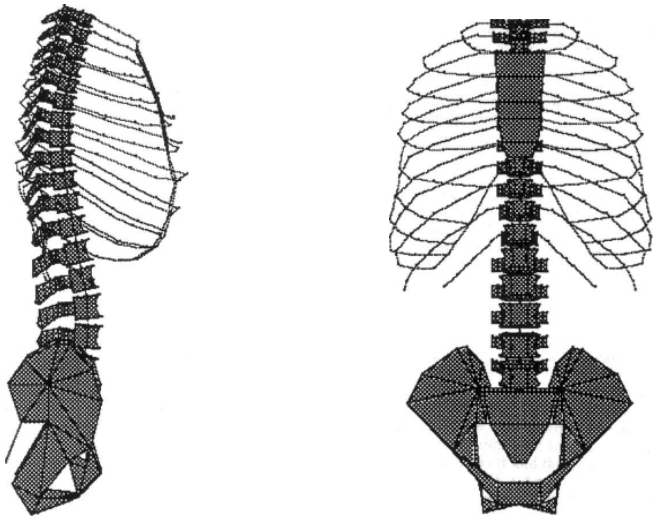

Figure 31: Model of a spine, ribcage and pelvis used to predict responses to lumbar manipulative forces. This model used short beam elements to represent the discs (Lee et al., 1995).

3.5.2 Single Vertebral Body Models

In order to model the spinal structures with more details, single vertebral body has been developed with more complex element idealizations. Therefore, the models reviewed in this and subsequent sections used very high element mesh density to describe the cervical bony vertebra. Take note that the reviews presented here on single vertebral models were limited to single cervical vertebra model only.

Hakim and King, 1978 developed a three-dimensional finite element model (Figure 32) of an isolated vertebra with anatomical details of the bone obtained through sectioning and direct measurement. Some comparisons were made with experimental data and it was observed that significant discrepancies existed because of the very complex nature of the problem and uncertainties in the geometry and material properties of the bone. They were probably the first to consider the facet joints in their model, but the disc was represented by simple linear axial elements. The model was extended later to a full motion segment by including a disc with linear homogeneous isotropic properties.

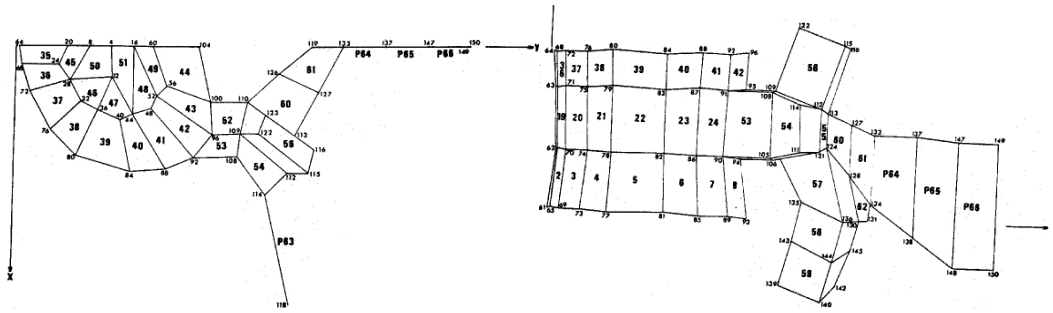

Figure 32: Three-dimensional models of a human vertebra. Only half the body was represented because of planar symmetry, but the model did include the posterior elements (Hakim and King, 1978).

Bozic et al., 1994 constructed a finite element model of the C4 vertebra (Figure 33) using computed tomography (CT) data. Loading was simulated by applying 4 mm axial compressive displacement through spring elements attached to the superior surface (Figure 34). The boundary condition was applied in the superior-inferior, medial, lateral and antero-posterior directions with the use of springs. Based on the maximum shear stress theory, the model predicted the initiation of the vertebral body fracture occurred in the cancellous bone. However, the effects of other spinal components (e.g. articular facets and disc) were not included, thus limiting the usefulness of the model.

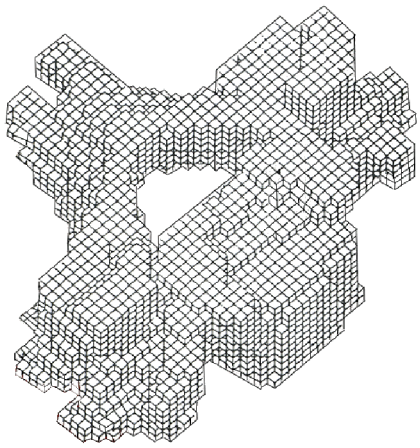

Figure 33: Finite element model of the C4 vertebra (Bozic et al., 1994).

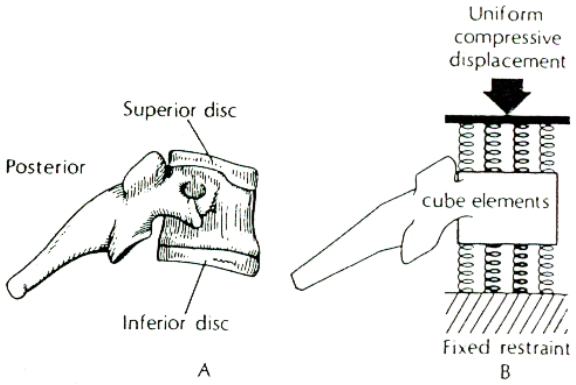

Figure 34: A) Cervical vertebrae with superior and inferior intervertebral discs. B) Schematic representation of the condition simulated by the finite element model (Bozic et al., 1994).

Teo et al., 1994 constructed a finite element model of the C2 vertebra (Figure 35). A coordinate measuring machine was used to capture the geometry of the single vertebra. A force of 1000 N was applied in the antero-posterior direction at 0° or ±45° angles in the sagittal plane distributed over 50 mm^2 on the anterior surface of the dens. Linear material properties for the cortical bone were used to analyze the tensile and compressive stress under these conditions for determination of the mechanism of odontoid fracture. No validation was reported in the study.

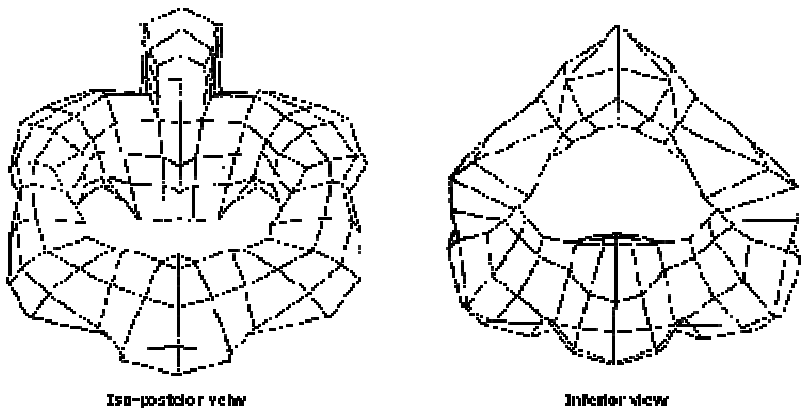

Figure 35: Finite element model of C2 (Teo et al., 1994).

Graham et al., 2000 developed an anatomically accurate three-dimensional model of the C2, generated from the computerized tomography data (Figure 36) using 32,815 triangular elements and 40,969 nodes. The FE model was constrained and loaded to simulate the values used in previous biomechanical studies. A matrix of stress plots was created for comparative analysis.

Recently, Teo and Ng, 2001 developed a geometrically accurate model of the first cervical vertebra (atlas) shown in Figure 37 using a three-dimensional digitizer to investigate fracture mechanisms of the bone. In the same year, Bozkus et al., 2001 developed a finite element model of the C1 (Figure 38) and used it to determine the strain distribution in the C1 during axial static compressive loading.

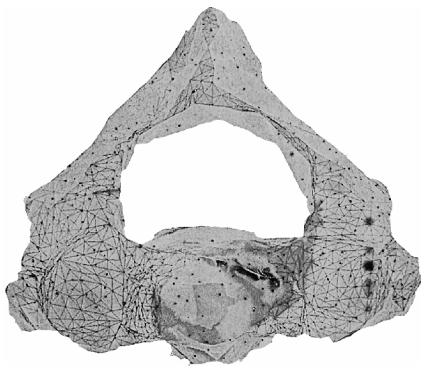

Figure 36: Finite element model of C2, using triangular elements (Graham et al., 2000).

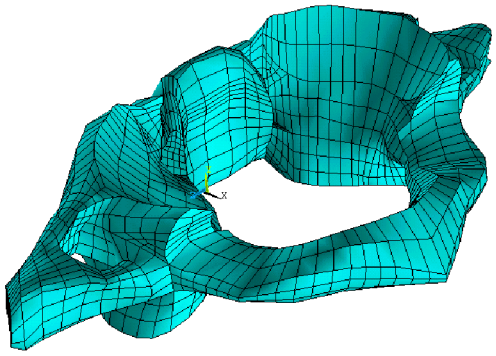

Figure 37: Finite element model of the first cervical vertebra (atlas) developed by direct measurement of a cadaveric specimen and used to examine fracture mechanisms (Teo and Ng, 2001).

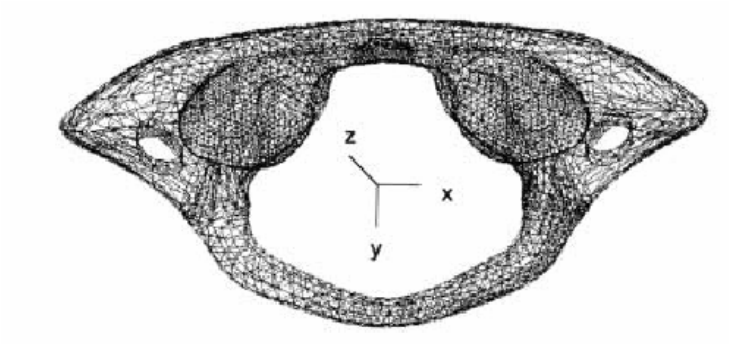

Figure 38: The mesh model of C1 derived from finite element modelling (FEM) (Bozkus et al., 2001).

3.5.3 Intervertebral Disc Models

As mentioned earlier, Belytschko et al., 1974 were the first to present details of a finite element analysis of an intervertebral disc and adjacent vertebrae. They modelled the problem by assuming axial symmetry with linear orthotropic material properties for the disc (Figure 39). The same axial symmetric model was subsequently extended by assuming that the annulus had non-linear orthotropic properties, the actual values of which were derived by comparison with experimental measurements (Kulak et al., 1976).

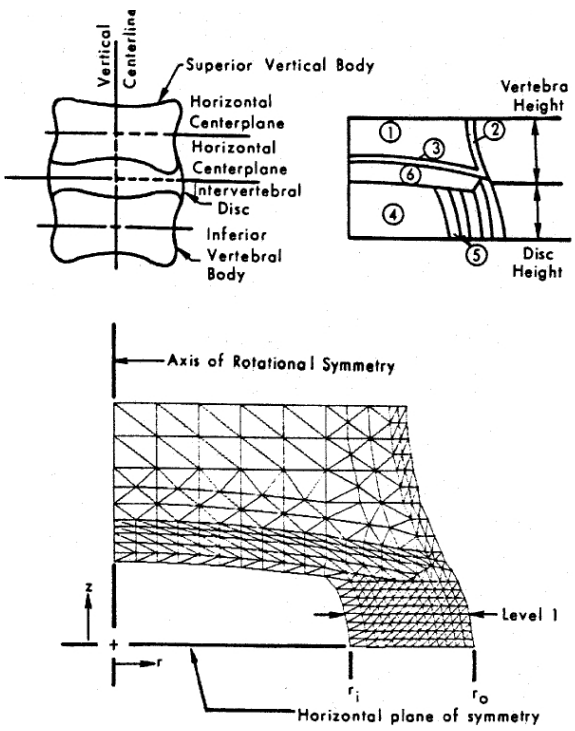

Figure 39: Finite element model of an intervertebral disc and adjacent vertebrae (Belytschko et al., 1974; Kulak et al., 1976).

One of the most significant contributions to the modelling of the intervertebral discs was made by Shirazi-Adl et al., 1984. They developed a three-dimensional nonlinear finite element model of the L2–L3 disc body unit (Figure 40). The model consisted of cortical bone, cancellous bone, bony end plate and the disc. The disc annulus was represented as a composite of collagen fibers embedded in a matrix of ground substance, while the nucleus was modelled as an incompressible fluid. The axial elements used to model the fibers were arranged in a criss-cross pattern around the annulus and defined with non-linear properties to reflect the softening of the fibers at higher strain. Because the disc experiences large displacement and strain under physiological loading, the analysis required both non-linear material and geometry solution. This finite element study has been described as the most comprehensive model by White and Panjabi, 1990. This model formed the basis of further intervertebral disc modelling and the methodology has been used quite extensively.

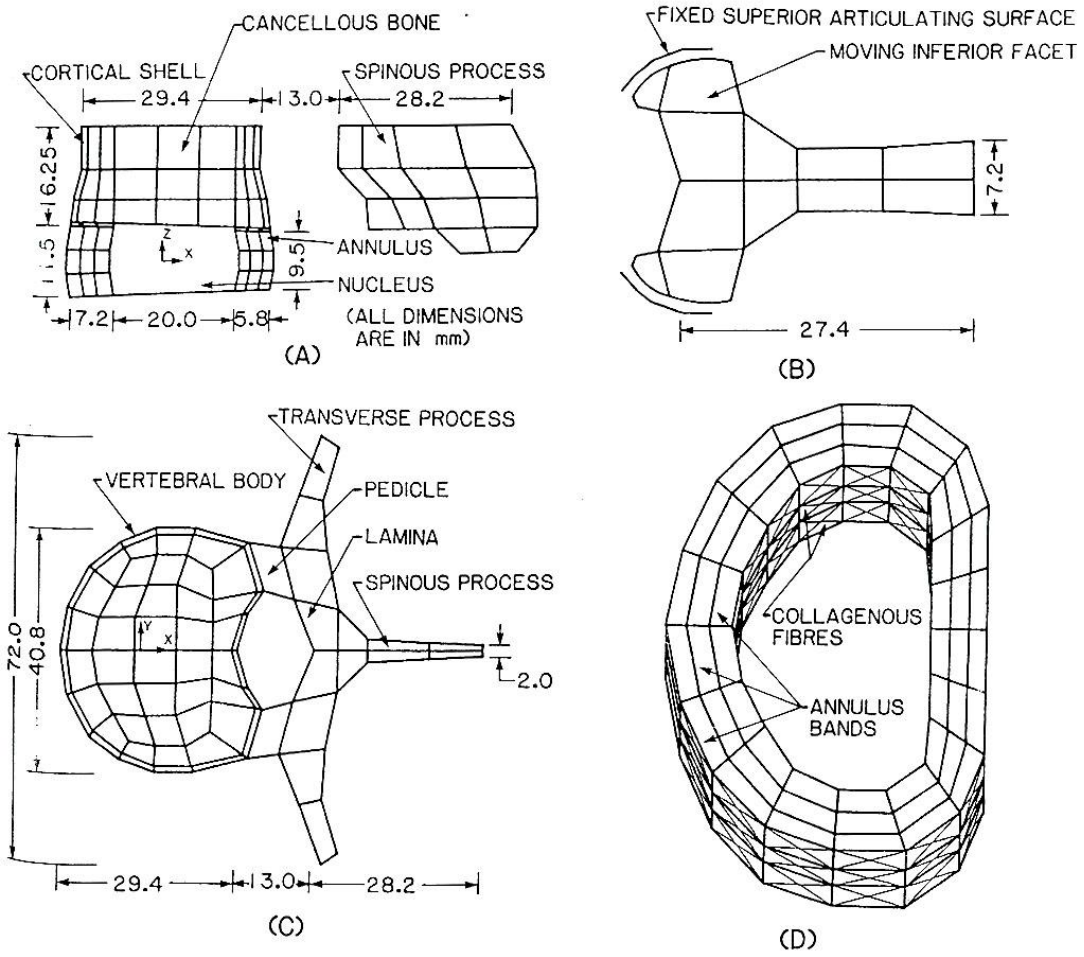

Figure 40: The three-dimensional non-linear model of the L2–L3 disc body (Shirazi-Adl et al., 1984).

3.5.4 Lumbar Spine Models

As most of the earlier finite element studies on the human spine were limited to the thoracic and lumbar regions and some of these articles are presented first in this section to highlight the methods and analyses that are relevant to the study of cervical spine described in (Section 3.5.5 Cervical Spine Models).

Lavaste et al., 1992 designed a parameterized three-dimensional finite element model of the lumbar spine (Figure 41). The model's geometry was constructed using six parameters per vertebra. These parameters were digitized from X-rays of the tested specimen.

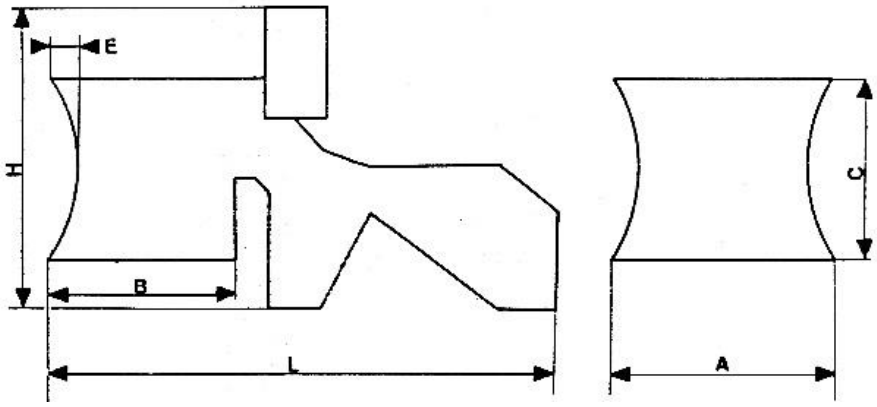

Figure 41: The six parameters used in the reconstruction of the lumbar model (Lavaste et al., 1992).

Rao and Dumas, 1991 developed a simple finite element model of the L5-S1 intervertebral disc body (Figure 42) for material sensitivity studies. The annulus fibrosus of the model was idealized as an inhomogeneous composite of an isotropic ground substance, reinforced by helically oriented collagen fibers so that the model has six different structural components, namely: cortical bone, cancellous bone, endplates, nucleus pulpous, annulus and fibers.

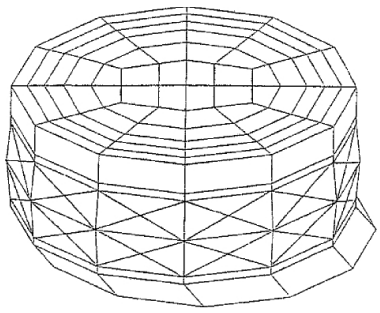

Figure 42: A simple finite element model of the L5-S1 intervertebral disc body (Rao and Dumas, 1991).

Lu et al., 1996 constructed a finite element model of a lumbar motion segment (Figure 43) with the aim of understanding the effect of compression, bending and twisting, and fluid changes in the disc on the propensity to disc prolapses. The three-dimensional

model accounted for the viscoelastic material properties of the annulus fibers and ligaments. In the study, the diurnal fluid exchange was simulated by changing the amount or volume of the fluid content in the disc nucleus. Combined with bending and twisting, a compressive load was applied at different loading rates.

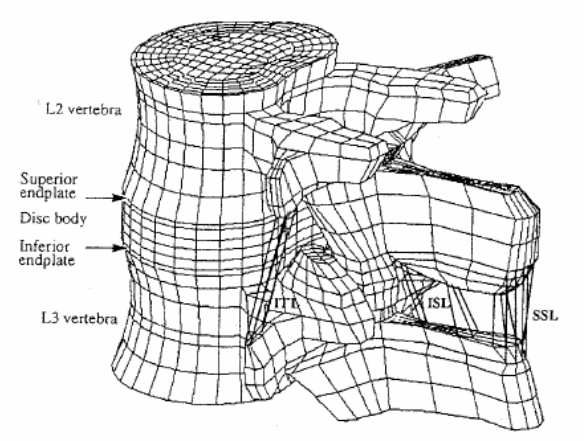

Figure 43: A full three-dimensional finite element model of the L2–L3 (Lu et al., 1996).

3.5.5 Cervical Spine Models

Cervical spine modelling is primary interest to clinicians and biomechanical engineers due to numerous cervical related injuries, degenerations and cervical surgical techniques. However, much less effort has been spent on modelling and analysis of the cervical spine when compared to the lumbar spine. Apart from using the finite element models to broaden our understanding on the kinematics of the cervical spine, the models can also be used to simulate different spinal conditions and their treatment, and to assist in the design and analysis of new spinal instrumentation. Summary of the cervical spinal models reported in the literatures are listed in Table 2.

Author	Year	Model	Type	Analysis type and software	Applications	Geometry	Validation
(Saito et al., 1991)	1991	Occiput-T2	2-D	Linear, static, FEMP	Laminectomy deformity	Assume-simplified	None
(Kleinberger, 1993)	1993	Head-T1	3-D	Linear, static and dynamic, DYNA-3D	Compression, flexion injury biomechanics	Assume-simplified C5 type geometry for all vertebrae	Human volunteer head motion
(Yoganandan et al., 1996b)	1996	C4-C6	3-D	Linear, static, I-DEAS, NASTRAN	Stress analysis of C4-C5-C6 spinal unit	Actual-sagittal, coronal and axial CT scans	(Shea et al., 1991)
(Maurel et al., 1997)	1997	C3-C7	3-D	Non-linear, static, ANSYS	Stress analysis of C4-C5 spinal unit	Assume-simplified	FSU validation using data by (Moroney et al., 1988)
(Voo et al., 1997)	1997	C4-C6	3-D	Linear, static, I-DEAS, NASTRAN	Facetectomy	Actual-sagittal, coronal and axial CT scans	(Moroney et al., 1988)
(Goel and Clausen, 1998)	1998	C5-C6	3-D	Non-linear, static, ABAQUS	Stress analysis of C5-C6	Actual-sagittal axial CT scans	(Moroney et al., 1988)
(Kumaresan et al., 1998)	1998	C4-C6	3-D	Linear, static, I-DEAS, NASTRAN	Modelling techniques for articular facets	Actual-sagittal, coronal and axial CT scans	None
(Maiman et al., 1999)	1999	C4-C6	3-D	Linear, static, I-DEAS, NASTRAN	Anterior cervical fusion	Actual-sagittal, coronal and axial CT scans	None
(Puttlitz et al., 2000b)	2000	C0-C2	3-D	Nonlinear, static, ABAQUS	Upper cervical spine instrumentation	Actual-transverse CT scans	(Goel et al., 1988a)
(Kumaresan et al., 2001)	2001	C4-C6	3-D	Linear, static, I-DEAS, NASTRAN	Disc degeneration under compression	Actual-sagittal, coronal and axial CT scans	(Pintar et al., 1996)
(Ng and Teo, 2001)	2001	C4-C6	3-D	Nonlinear, static, ANSYS	Stress analysis of C4-C6 under axial compression	Actual vertebrae captured using digitizer	(Shea et al., 1991)
(Chen et al., 2001)	2001	C5-C6	3-D	Nonlinear	foraminotomy	None	(Moroney et al., 1988)

Table 2: Finite element models of the cervical spine.

Kleinberger, 1993 developed a head/neck model to study the mechanics of the cervical spine injuries due to automobile collisions (Figure 44). Although validation was performed on a single motion segment, the results were not presented. Based on the validated results, full cervical spine and skull model was developed by replicating the

motion segment throughout the cervical spine with minimum dimensional changes to the individual vertebrae. He was also careful to point out that numerous assumptions and simplifications were made to the model and extensive CPU run times were a limiting factor.

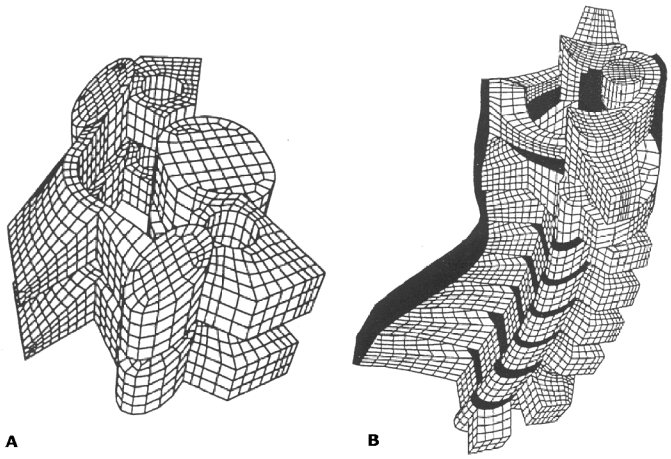

Figure 44: A) Finite element model of the cervical spine function unit. B) Finite element model of the cervical springs column (Kleinberger, 1993).

In 1996, a three-dimensional finite element model of the C4-C6 lower cervical spine unit (Figure 45) based on a cervical specimen and 1 mm CT slices was reported by Yoganandan et al., 1996b. In regions of special interest (ligament insertion points and intervertebral discs), cryomicrotomy procedures were used to obtain greater anatomical detail. Bone geometry in this model was extensively digitized and generated. However, the model did not simulate other structures (collagen fibers and facet contact) appropriately. Fibers were not included and facet contacts were simulated using solid elements. The linear model was then validated in compression.

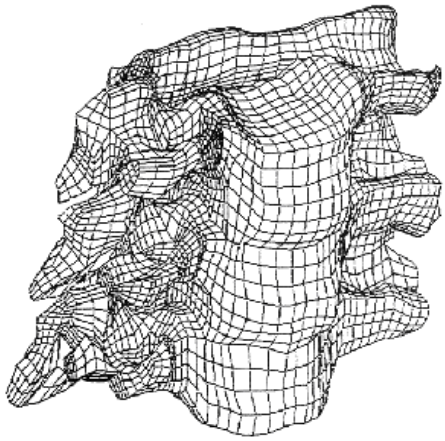

Figure 45: Finite element model of the C4-C6 (Yoganandan et al., 1996b).

Yoganandan and his co-workers used the same C4-C6 model to investigate the effects of facetectomy and laminectomy on the segmental mobility under limited loading types (Figure 46) (Kumaresan et al., 1997; Voo et al., 1997; Yoganandan et al., 1996b). As in the earlier study, the major weakness of these studies was the use of linear analysis.

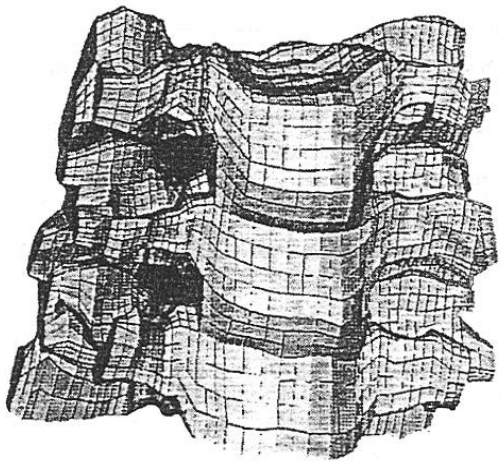

Figure 46: Finite element mode of cervical spine (Kumaresan et al., 1997; Voo et al., 1997).

Based on the experience gained in the development of the parameterized lumbar model (Lavaste et al., 1992), Maurel et al., 1997 presented a parameterized finite element model of the lower cervical spine (Figure 47). Although the C3-C7 model was

presented, only the C5-C6 FSU and disc segment model were validated against the experiment data under sagittal moments and analyzed for the effects of some geometrical parameters. The results showed that the orientation of the facets with regard to the horizontal plane appeared to have a large influence on the coupled rotation, notably in lateral flexion.

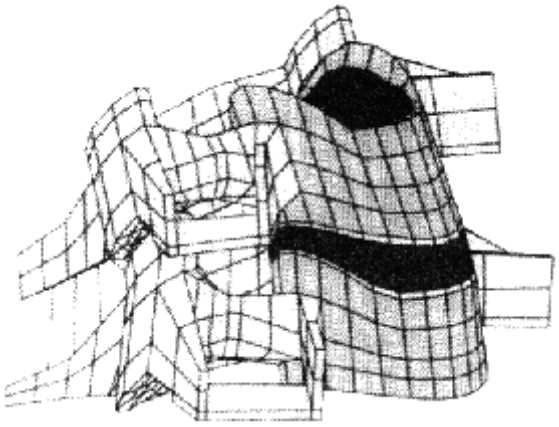

Figure 47: A three-dimensional finite element model of the lower cervical spine (Maurel et al., 1997).

Goel and Clausen, 1998 developed a three dimensional C5-C6 model (Figure 48) from serial CT scans to investigate the biomechanical influence of the uncinate processes and Luschka joints. The model included nonlinear ligament load/deflection definition using bilinear cable, composite intervertebral disc, and fluid nucleus. The model was validated against experimental data and used to predict the load sharing in the cervical spine under various loading modalities.

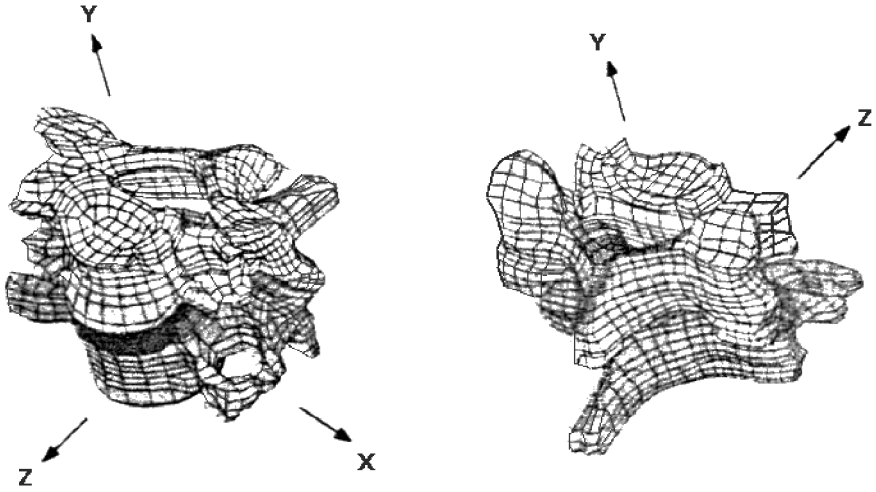

Figure 48: Finite element model of the C5-C6 (Goel and Clausen, 1998).

In 2001, Ng and Teo developed a detailed model of the lower cervical spine using a high-definition digitizer. The model was validated under axial compressive loading of up to 1 mm. A parametric study was also conducted by evaluating the biomechanical response of the cervical spine related to the changes in the modelling techniques and the mechanical properties of the disc annulus.

3.6 Summary

Review on the literatures showed that the biomechanical research of the human cervical spine can be classified into four main areas, and these four areas can help to provide further understanding to the underlying mechanisms of various cervical conditions. *In vitro* studies can be based on animal spines, cadaveric spines or artificial spine models and have been conducted in the past to determine the biomechanics of cervical structures. *In vitro* studies of isolated components such as ligaments and vertebral bodies, single and multilevel functional spinal units and complex systems such as ligamentous columns, intact head-neck complexes and whole body intact human cadavers have enriched our understanding on the cervical spine behaviour. Although *in*

vitro studies provide the most direct and obvious way to obtain information on the cervical spinal biomechanics, it can be expensive and suffers from specimen variability and issues of repeatability. This review showed that the finite element method is an invaluable application tool that can supplement *in vitro* studies in understanding the clinical cervical spine biomechanics. This method may also guide the researchers to define and develop better experimental procedures.

However, it should be noted that the finite element models are not universal models. They are, like all other models, specific to the problem at hand. For example, if a finite element model is used to study the dynamics of a spine, say, in a whiplash simulation in which the goal is to measure the intervertebral motions in response to a horizontal acceleration, then a model may consist of a series of vertebral bodies connected by ligaments and discs. On the contrary, if the model is designed to study the internal stress and strain in the disc, then the vertebra and the disc may be modelled more realistically. In such a formulation, internal stress and strain can be studied. Thus it is important that the specificity of a computer model is designed right from the beginning (Fagan et al., 2002; Gilbertson et al., 1995).

A review on the literatures based on the above criteria showed that the existing models reported in the literatures could not be used to investigate the aims and objectives of the current study. The reasons are listed below and provided the impetus to the **current study**.

1. Whole Spine Models – There is a lack of accurate representations of anatomical details of the spinal components. Therefore, these models cannot be used to

investigate the biomechanics of the cervical spine under various cervical conditions described earlier in Chapter 1.2 Research Aims accurately.

2. Single Vertebral Body Models – Anatomical descriptions of the cervical region range from early simplified models to current detailed models. However, these models cannot be used for the current study due to a lack of intervertebral discs and its associated ligaments.
3. Lumbar Spine Models – Although extensively studied, it should be noted that the geometry and biomechanics of the cervical and lumbar spine vary tremendously. It is also clear that the pathology affecting cervical intervertebral discs is different from that affecting the lumbar discs and the influence of these parameters are still unknown. Therefore, results from lumbar study cannot be used directly for the understanding of the cervical spine biomechanics.
4. Intervertebral Disc Models – same as (3)
5. Cervical Spine Models – Usually consist of one or two FSU. These models cannot be used to investigate the influence of various conditions on the cervical biomechanics of the adjacent levels realistically.

In the next chapter, the author will describe the development process for the finite element modelling of the C2-C7. A straightforward approach with graphical illustrations was adopted to explain the procedures taken to construct the C2-C7 finite element model from the dried cadaver specimens.

Chapter 4. Finite Element Model Details

4.1 Introduction

The FINITE ELEMENT METHOD (FEM) is now firmly established as an engineering tool of wide applicability as described in the preceding chapter. It is no longer regarded as the sole province of the researcher or academic but it is now employed for design purposes in many branches of technology. One of the principal advantages of the FEM is the unifying approach it offers to the solution of diverse engineering problems. Bio-engineering particularly has seen a proliferation of various analyses using FEM both in the fields of prosthetic implants and biological tissue (Goel and Gilbertson, 1995; Yoganandan et al., 1987).

Since the cervical spine constitutes part of a very complex biomechanical system, an understanding of the cervical spinal motion segments mechanics is pertinent to numerous medical problems. Direct comprehensive *in vivo* experimental measurement of the forces, moments and characterization of biomechanical responses, etc would be extremely difficult. Accordingly, there exists a need for a detailed biomechanical analysis to characterize the responses of the cervical spine under simulated injury, disc degeneration and surgical treatments investigated in the later chapters using FEM.

The model developed in this study represents a three-dimensional idealised structure of a human cervical spine, and the various stages, assumptions, difficulties, etc, involved in the modelling of the C2-C7 FE model are presented in the following sections.

4.2 Finite Element Model Generation

4.2.1 General Concept

The development of the finite element models for complete characterization of the human cervical spine requires complex modelling techniques. Important consideration in the cervical spine model development includes

- Hard tissues
  - + Bones
    - § Proper representation of the facet joint area and orientation
    - § Inclusion of various bony components (cortical shell, cancellous bone., etc)
    - § Inclusion of the bone microstructure
  - + Intervertebral discs
    - § Inclusion of endplate, disc annulus, disc nucleus and annular fibrosus
    - § Inclusion of rate dependent viscoelasticity
- Soft Tissues
  - + Soft tissue modelling with the appropriate nonlinear properties
  - + Modelling of active and passive muscles forces
- Articulations
  - + Three-dimensional, unconstrained modelling of the cervical joint

It is apparent that a finite element model incorporating all of these techniques would be very complex in nature. Kostuik and Smith, 1991 mentioned that “Over-sophistication in mathematical models frequently occurs. Over-sophistication can result in agreement between model predictions and experimental data by increasing the complexity of the model. However, this may result in the model predictions that may be erroneous in other situations.” It is not the objective of this research to develop a highly complex

model that provides accurate results only for certain situations, but rather to provide a strong foundation for the complete modelling, analysis and understanding of a cervical spine that is valid for all conditions. The knowledge obtained from these studies will then be applicable for future analyses using patient specific models. Therefore, the model used in the current research will ignore the inclusion of bone microstructures, muscles and viscoelasticity. The results on the influence of viscoelasticity on the cervical spine model will be added and discussed briefly in a sub section (Refer 6.5.4 Post-Surgical Laminectomy) in later chapters.

4.2.2 Digitizing, Coordinates Extraction and Solid Model Development

This section illustrates the procedures for the development of the three-dimensional finite element model of the C2-C7, including the digitizing process, coordinate extraction and solid model development. A commonly used method described in the literature for the cervical spine geometry development is by stacking the computed tomography (CT) images sequentially to develop the 3D solid model (Refer Chapter 8. Development of a Patient Specific Model). However, in this study, a methodology (Figure 49) that was developed previously was utilized to extract the geometry from the dried vertebrae (Ng and Teo, 2001). The cervical vertebrae column (Figure 50) considered in this study were obtained from a 68-year-old man, who died in Singapore General Hospital. Medical records and detailed examinations by independent spine surgeon were performed to ensure the absence of bony abnormalities, spine disease or trauma.

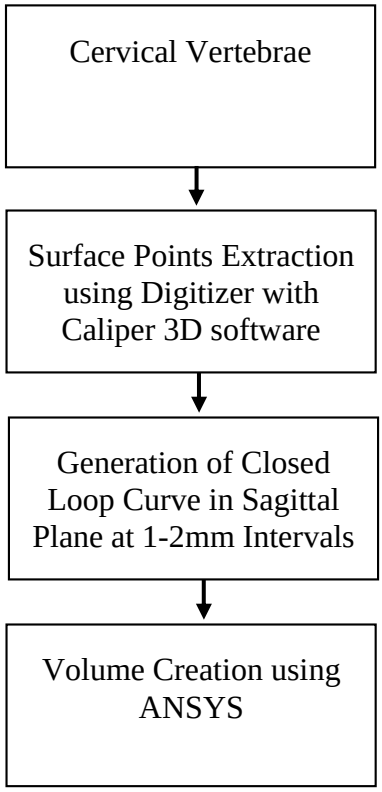

Figure 49: Methodology for the generation of cervical vertebrae volume (Ng and Teo, 2001).

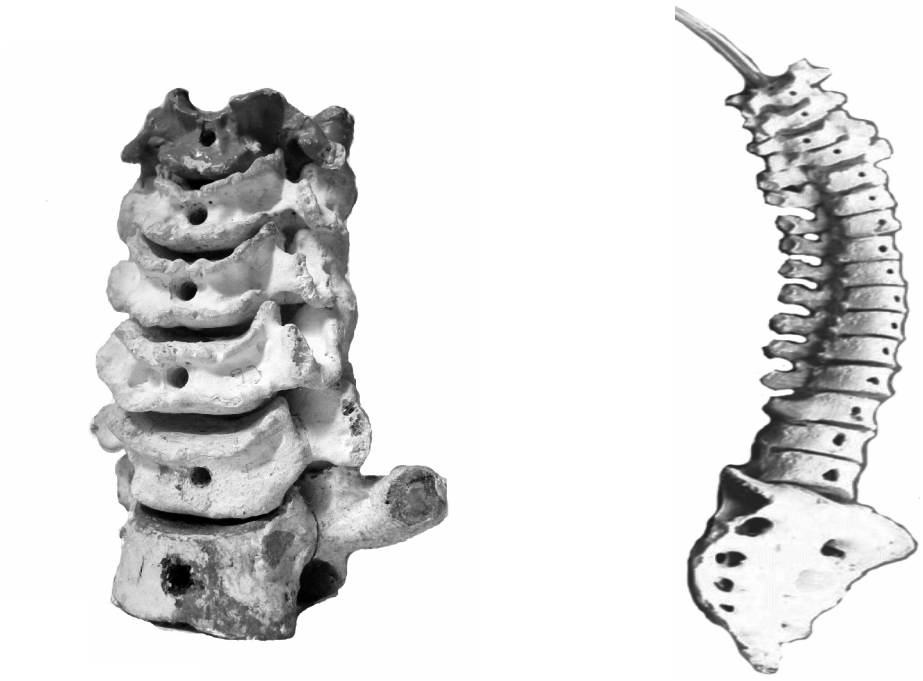

Figure 50: a) Isometric view of C3-T1 vertebrae, b) spine column

The geometry of the cervical spine was obtained from the cervical vertebrae using a digitizer. The digitizer (FaroArm, Bronze Series, Faro Technologies, Inc., Florida, USA) (Figure 51) is a measuring instrument capable of moving in six degrees of freedom. Sphere and point probes attached to the tip of the digitizer were available for measurement, with accuracy of ±0.3 mm. The instrument was connected to a computer and the digitized coordinates were recorded. Prior to the digitization process, the probe was calibrated and a reference point was set at the anterior inferior end of the cervical vertebrae. To ensure the reliability of the measurements taken from the digitizer, accuracy tests were conducted for the linear and angular dimensions according to the user manual (FAROArm, 1997). To prevent any movement during the digitization process, the cervical vertebra was fixed to a vice-clamp via a rod attached to the vertebra body (Figure 52). The probe was then used in digitizing over the surface profile of the dried vertebra to obtain the continuous surface point coordinates. Prior to the digitizing, prominent areas like facets, vertebral body superior and inferior surface that play an important role in the spinal biomechanics were identified and highlighted. The captured three-dimensional coordinates were processed to generate evenly spaced contours of about 1-2 mm in the sagittal plane using a third party computer software, Surfacer 8.0 (Structural Dynamics Research Corporation, Ohio, USA). The contours were then exported to ANSYS (SAS IP, Inc., Canonsburg, USA) using IGES (The Initial Graphics Exchange Specification) format for surfaces and volumes creation.

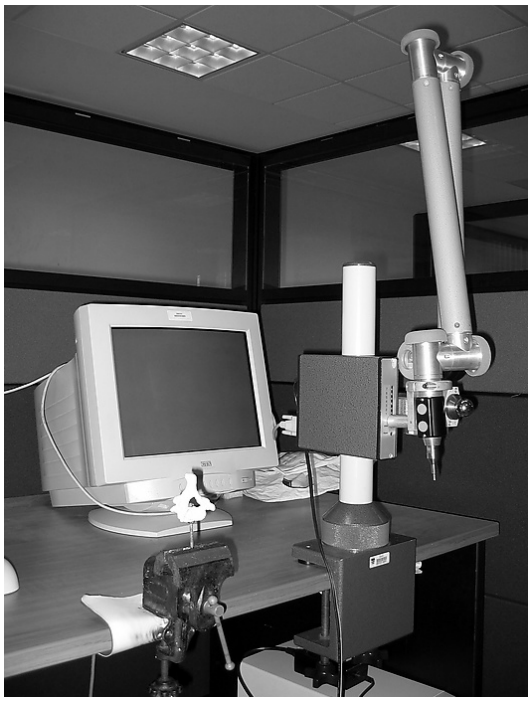

Figure 51: Digitizer FaroArm setup.

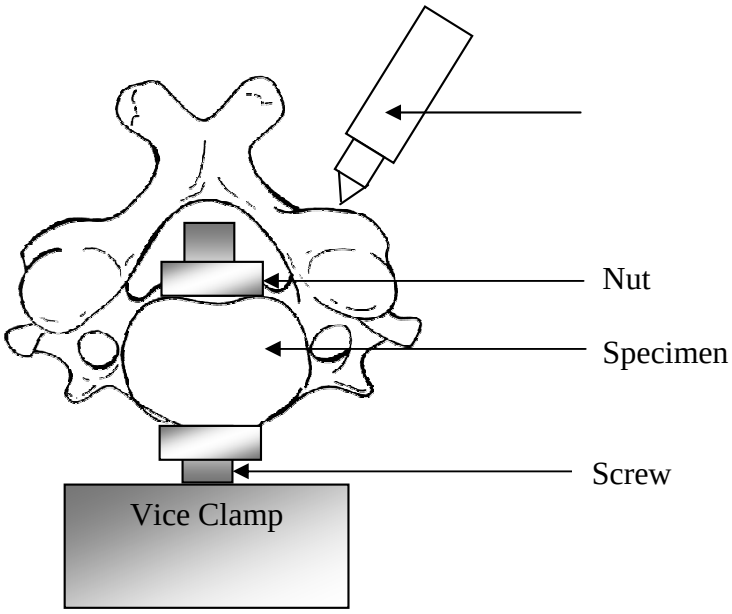

Figure 52: Experimental setup for digitizing and coordinate extraction.

Once the solid vertebrae models were developed, the next step was to create the solid intervertebral disc. In order to model the cervical intervertebral disc accurately, geometrical characteristics have to be quantified. Radiographs, CT, and MRI by other researchers provide reasonably accurate data on the geometrical characteristics of the

disc. Therefore, the author referred to both experimental work and previous finite element models reported in the literatures for the modelling of the intervertebral disc (Goel and Clausen, 1998; Maurel et al., 1997; Mercer and Bogduk, 1999; Yoganandan et al., 2001; Yoganandan et al., 1996b). The vertebrae were then stacked up over each other and intervertebral disc volumes were formed between the vertebrae by connecting the adjacent superior and inferior surface of the two vertebrae.

The solid model (Figure 53) for the entire structure (C2-C7) was thus developed following this procedure and the geometrical dimensions of the solid model were scrutinized against the literature data in the next section. At this stage, the solid model did not include the details of the internal vertebrae (such as cortical and cancellous bone) and intervertebral disc (such as disc nucleus and ground matrix). The solid model only contained the external surface as captured by the digitizer.

a) vertebrae

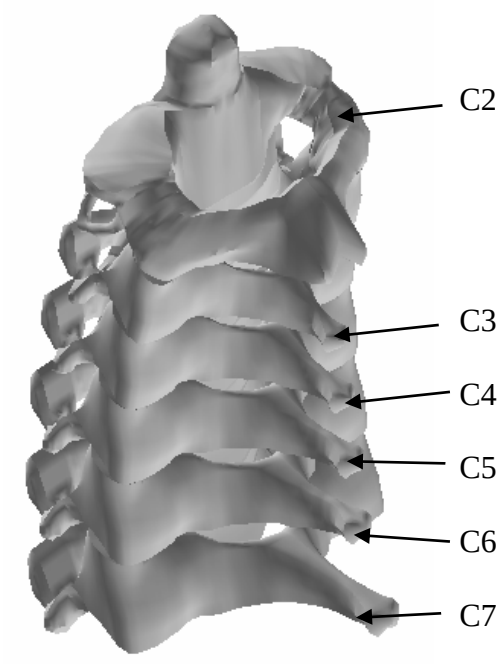

b) intervertebral disc

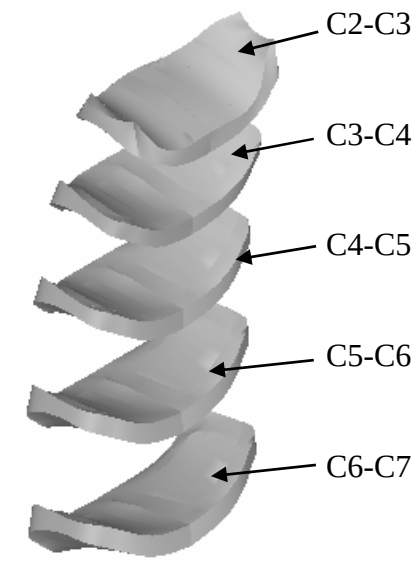

Figure 53: C2-C7 solid model, a) vertebrae, b) intervertebral disc.

4.2.3 Comparison of C2-C7 geometry against published data

Before proceeding to create the finite element model, it was important to verify the dimensions of the C2-C7 solid model were within the range of the quantitative geometry data reported in the literatures (Chua, 1999; Gilad and Nissan, 1986; Panjabi et al., 1991; Panjabi et al., 1993; Tan et al., 2002; Tan et al., 2004). The linear dimensions and areas of various parts of the cervical spine used in the comparisons are shown in Figure 54. Overall, fourteen geometrical parameters used to describe the cervical vertebrae and intervertebral disc are compared and the results are illustrated in Figure 55 to Figure 62. The geometrical data of the current model was obtained through the interface of the ANSYS pre-processor (SAS IP, Inc., Canonsburg, USA), whereas the geometrical data reported in the literatures were obtained from either radiographs or digitized coordinates. These geometrical parameters were also used in quantifying the anatomy of the cervical spine by many biomechanical investigators (Chua, 1999; Gilad and Nissan, 1986; Panjabi et al., 1991; Panjabi et al., 1993; Tan et al., 2002; Tan et al., 2004). Despite the excellent efforts by local investigators to quantity the dimensions of the Asian spinal geometry, there is still a lack of quantitative data on some geometrical parameters. Due to this, some geometrical parameters comparison conducted in this study were done with the corresponding dimensions obtained from the Caucasian spines. Therefore, it should be pointed out that the current FE model is constrained by these limitations.

Generally, the solid models compared well with the experimental data. These comparisons (both Caucasian and Asian) with the data reported in the literatures will ensure that the geometrical dimensions of the solid model were within the mean dimensions of the general adult population. Furthermore, in the mathematical

modelling of the cervical spine, investigators always emphasized the importance of modelling the actual geometry as accurately as possible to obtain reasonable results applicable to clinical and *in vivo* situations as the anatomical structures greatly define the motion of the cervical spine and its related biomechanical response. Therefore, geometrical comparisons will also ensure that the validation studies and further analyses performed on the cervical spine model in the later chapters should produce a realistic representation of the kinematics and biomechanics of the cervical spine for the general adult population.

After the geometrical comparisons, **the next step was to create the finite element model from the solid model.**

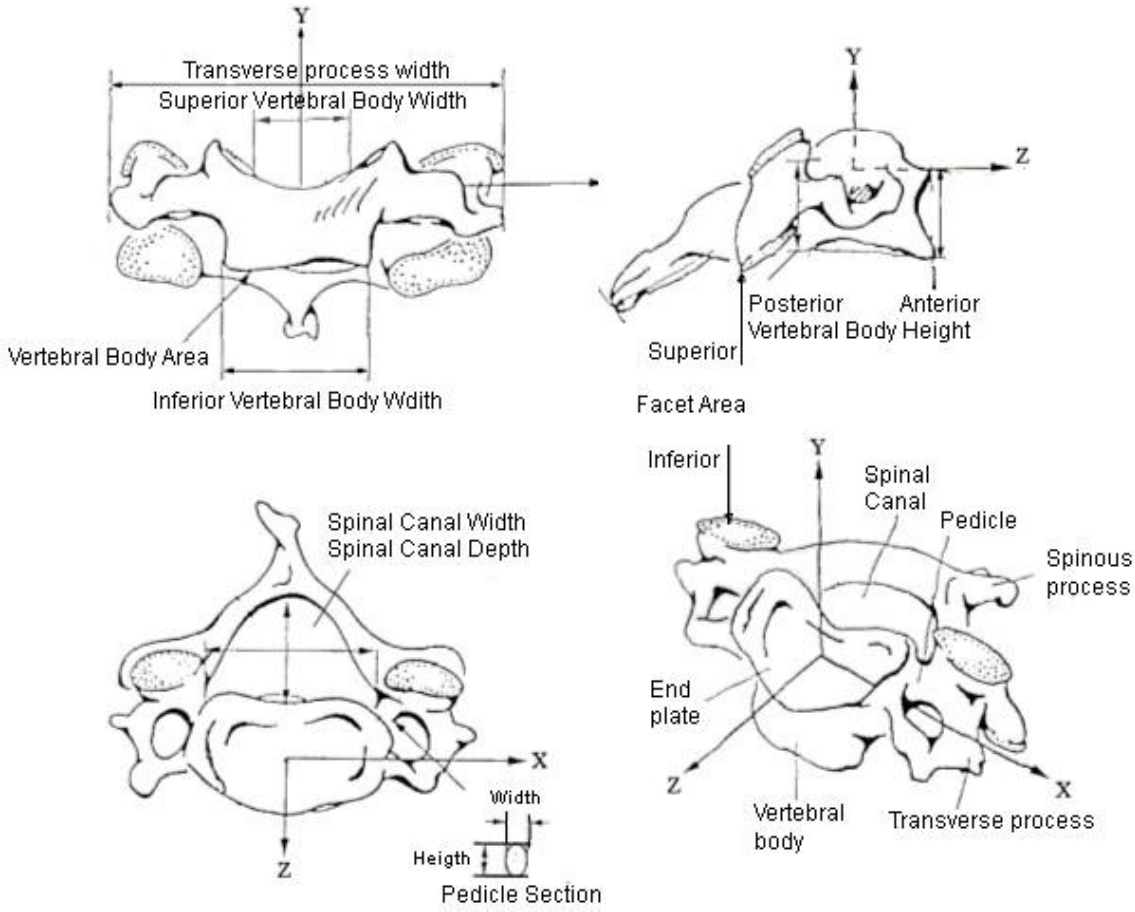

Figure 54: Four views (front, side, top and isometric) of a cervical vertebra showing the dimensions (Panjabi et al., 1991).

a) b)

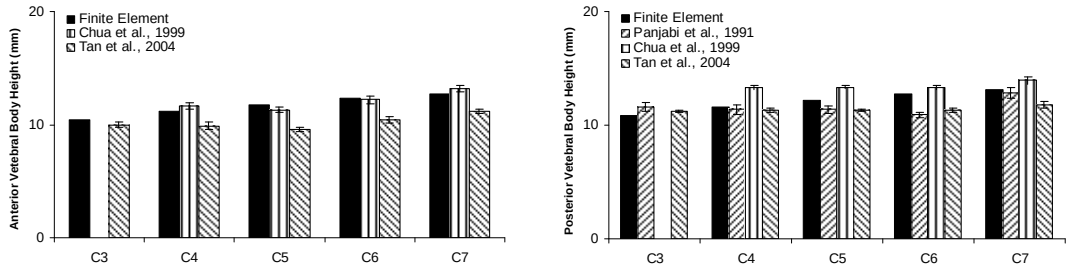

Figure 55: Vertebral body a) anterior, b) posterior height.

a) b)

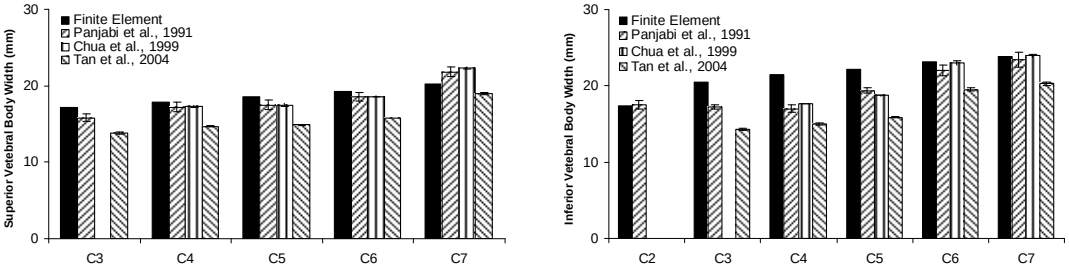

Figure 56: Vertebral body a) superior, b) inferior width.

a) b)

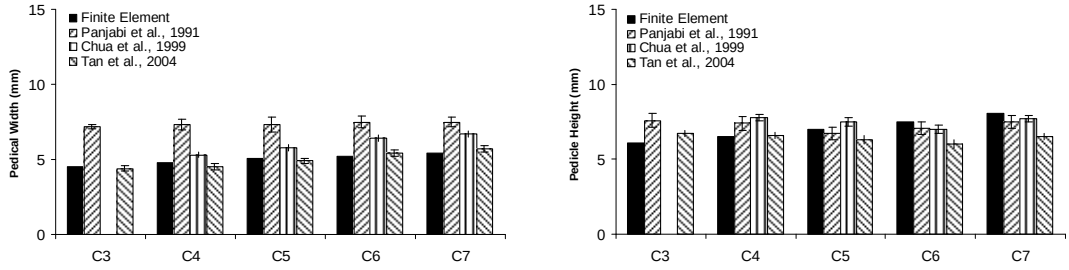

Figure 57: Pedicle, a) width, b) height.

a) b)

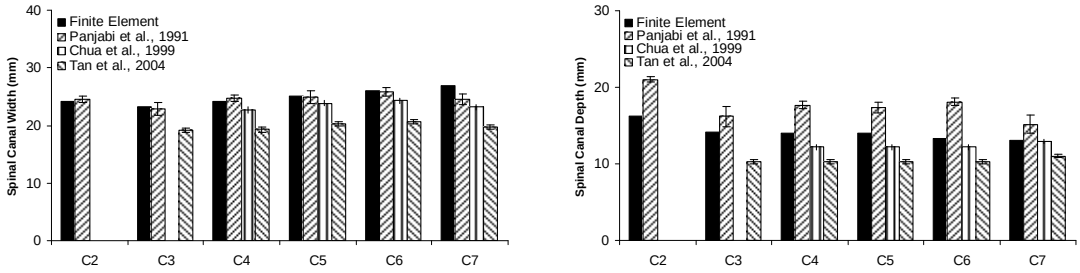

Figure 58: Spinal canal a) width and b) depth.

a) b)

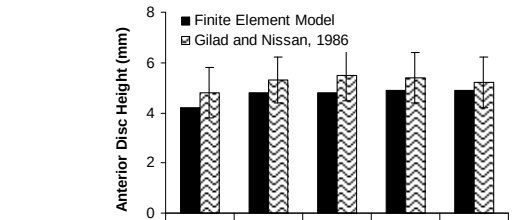

	C2-C3	C3-C4	C4-C5	C5-C6	C6-C7
Finite Element Model	4.2	4.8	4.8	4.9	4.9
Gilad and Nissan, 1986	4.8	5.3	5.5	5.4	5.2

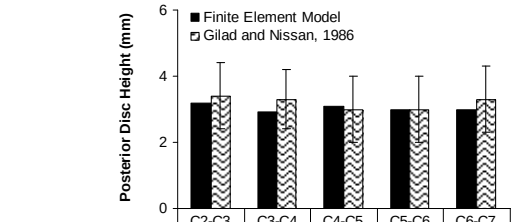

	C2-C3	C3-C4	C4-C5	C5-C6	C6-C7
Finite Element Model	3.2	2.9	3.1	3	3
Gilad and Nissan, 1986	3.4	3.3	3	3	3.3

Figure 59: Intervertebral a) anterior, b) posterior disc height.

a) b)

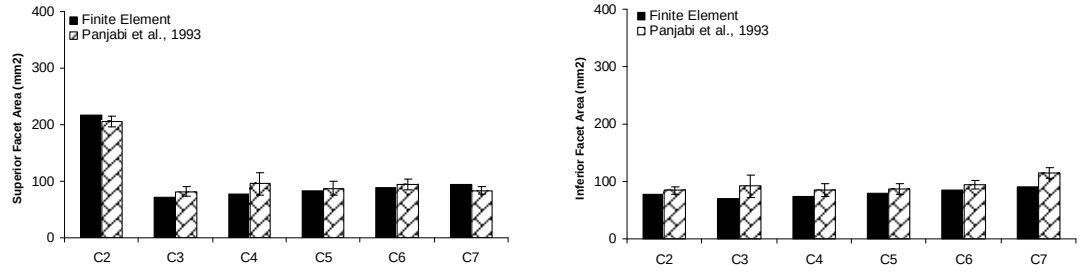

Figure 60: Facet a) superior, b) inferior area.

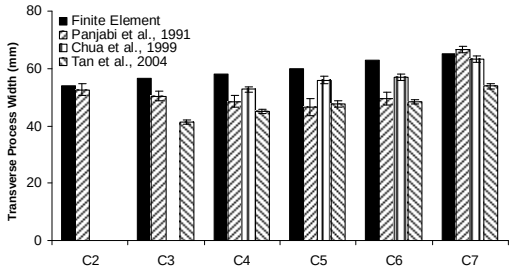

Figure 61: Transverse process width.

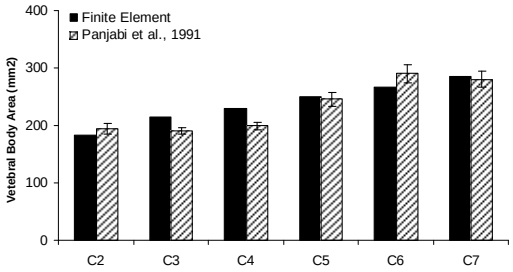

Figure 62: Vertebral body area.

4.2.4 Finite Element Mesh Generation of Bony Vertebrae C2-C7

Once the solid model of the C2-C7 was identified and developed, the next step was to generate the finite element mesh using mapped mesh technique within the solid model. **The finite element model was created from the existing C4-C6 solid model developed in an earlier study** (Ng and Teo, 2001). However, the finite element model was completely redefined in terms of element types, loading modes and validated extensively with experimental data under compression, anterior/posterior shear and pure loading (flexion, extension, lateral bending and axial rotations). New material properties were assigned to the current model and are more consistent with the latest values reported in the literatures. In addition, annulus fibrosus was modelled with fibers reinforcement and the fibers used the tension only cable elements to simulate the fibers. Loading is now applied through a series of rigid beams connected to the surface of the

vertebrae. These arrangement and the new element types allow the use of structural nonlinearity under all loading types.

Previously, solid element that supports both the translational and rotational degrees of freedom was used in the analysis. The use of these old six DOF solid elements allows the application of moment loads directly to the surface of the vertebrae, but it does not support structural nonlinearity due to the changing geometry as it deflects. That is, the stiffness [K] is a function of the displacements (*ANSYS 7.0 Documentation and User Manual*). The stiffness changes because the shape change and/or the material rotate. This refinement in the cervical spine model is critical for injury, surgical technique, etc studies in the later chapters. Detailed information on the methodology of applying pure moments to the cervical models under structural nonlinearity (large displacement and large rotation analysis) can be found in Appendix (A.3 Applying Pure Moments). It is important to understand the features available in the commercial FEA packages that allow the application of pure moments to the spinal models. This understanding will prevent erroneous assumptions and predictions. Furthermore, nonlinear analyses are also needed for the inclusion of material nonlinearities and changing of contact status for the posterior articular facets. The following sections will describe in more detail the finite element model development process of the C2-C7.

4.2.5 Modelling of Associated Spinal Components

The cortical bone, cancellous bone, and posterior elements of each vertebra were delineated during the finite element model generation such that different material properties could be assigned for each region. The vertebrae body was modelled as a soft cancellous bone surrounded by a thin cortical bone of 1.0 mm thickness

(Yoganandan et al., 1996b). Cancellous, cortical and posterior elements were assigned linear elastic Young's modulus of 100 MPa, 10000 MPa and 3500 MPa, respectively (Table 4).

4.2.6 Intervertebral Disc

Each intervertebral disc consisted of disc annulus, disc nucleus, annulus fibers and endplates. The endplate were modelled as double layer of elements between each vertebra and the disc and a thickness of 1 mm was used for each endplate (Yoganandan et al., 1996b). The disc annulus and endplates were modelled as 8-noded brick elements. The nucleus pulposus can be modelled in a number of ways, e.g. as an incompressible solid, as a poroelastic solid or as a fluid as reported in the literatures. The simplest approach used in the present study represents the nucleus pulposus with solid elements with a Poisson's ratio equal to 0.499 (Table 4). Annulus fibers modelled using three-dimensional tension only fiber elements were connected diagonally (Figure 63) between the corner nodes of the inner and outer faces of the annulus elements, consistent with those reported in literatures (Table 3). Material properties for the intervertebral disc were linear, isotropic.

Reference	Element Type	Young's Modulus (E)
(Maurel et al., 1997)	Cable (tension)	10 – 110 MPa
(Goel and Clausen, 1998)	Rebar (tension)	450 MPa
(Kumaresan et al., 1999b)	Rebar (tension)	500 MPa

Table 3: Modelling of annulus fibers reported in literatures.

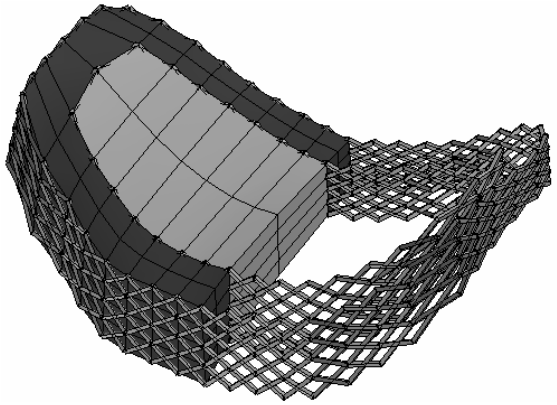

Figure 63: Intervertebral disc with criss-cross annulus fibers.

4.2.7 Ligaments

All ligaments approximating the ligamentous structures in the cervical spine were incorporated into the finite element model as a two noded tension only cable elements: anterior and posterior longitudinal ligaments, interspinous ligament, spinous ligaments, ligamentum flavum and capsular ligaments. This modelling technique was such that there is no axial compression force transmission in the longitudinal direction of the ligament. Attachment sites and orientations for each ligament were determined from spine biomechanics and anatomy texts (Goel and Clausen, 1998; Kumaresan et al., 1999a; Lavaste et al., 1992; Ng and Teo, 2001; Saito et al., 1991; Yoganandan et al., 2000). Their insertion points were chosen to mimic anatomical observations as closely as possible (Figure 64b). Material properties for the six cervical ligaments were determined from the published data (Table 4).

4.2.8 Facet Joints

Facet joints, in the finite element studies of the cervical spine, are often represented by gap elements (Goel and Clausen, 1998). Gap elements in commercial finite element codes are typically modelled as linear springs with a constant stiffness value K and gap G. The analysis is usually iterative and convergence is attained with the closure of all

gaps. However, in reality, the facet contact areas are liable to change during load application. Moreover, the facet cartilage layers have nonlinear stress-strain characteristics. The stiffness resulting from the contact of the cartilage layers on the articular surfaces of the inferior and superior facets is a nonlinear function of the strain experienced by the cartilage. This implies that the modelling of facet articulation with linear spring (constant stiffness) and constant gap width will not be a very realistic representation of the physical problem. In this study, articulations of the facet joints were simulated using three-dimensional surface-surface contact elements. No friction was assumed in the facet joints. The contact areas were digitized at the inferior facets of the superior vertebra and superior facets of the adjacent inferior vertebra were internally generated from the existing mesh. The normal contact stiffness will be updated at every sub-step based on the stress of the underlying elements and allowable penetration, which is set to 0.1 mm.

4.2.9 C2-C7 Finite Element Model

The final intact model consisted of 18732 elements and 21523 nodes. The C2-C7 model (Figure 64 and Table 4) consisted of six vertebrae (C2, C3, C4, C5, C6 and C7), five intervertebral discs (C2-C3, C3-C4, C4-C5, C5-C6 and C6-C7) and included all the critical components of the cervical spine. The global xyz coordinate system was set with the positive y axis acting along the posterior wall of the C2 body pointing up, and the positive x axis was perpendicular to the y axis pointing backwards and the positive z axis was perpendicular to the x and y axes pointing left.

4.2.10 Solving Methods

Once the finite element model was developed, the next step was to analyze the finite element model. In this study, all the analyses were performed using ANSYS 7.0 (SAS IP, Inc., Canonsburg, USA). During the analysis, all the elements used in the current study were capable of possessing geometrical and material nonlinearity. Convergence was obtained for each load step before going to the next load step in the analysis.

a) b)

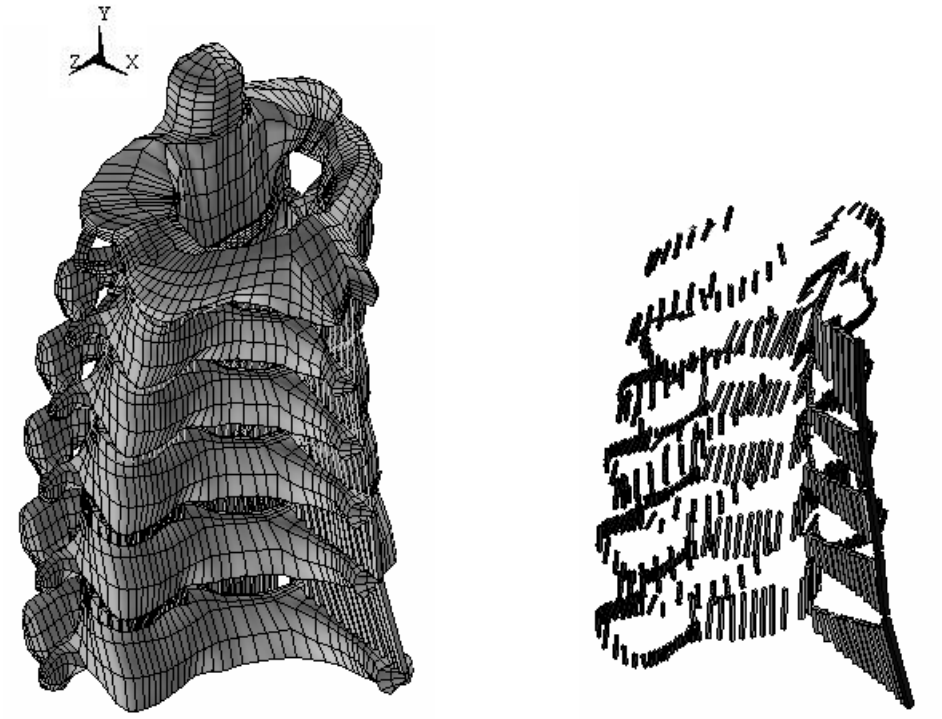

Figure 64: Finite Element model of C2-C7, a) intact model, b) ligaments.

Description	ANSYS Element Type	No of Elements	Young's Modulus (MPa)	Poisson's ratio	Reference:
Hard Tissue					
Cortical bone	8-node (SOLID45)	952	10000	0.29	(Kumaresan et al., 1999a; Yoganandan et al., 1996b)
Cancellous bone		1548	100	0.29	
Posterior elements		7400	3500	0.29	
Endplate		3076	500	0.40	
Soft Tissue					
Disc – annulus	8-node (SOLID45)	1136	3.4	0.40	(Kumaresan et al., 1999a; Yoganandan et al., 1996b)
Disc – nucleus		784	1.0	0.499	(Goel et al., 1995; Halldin et al., 2000)
Fibers	2-node geometrical nonlinear tension only cable (LINK10)	1928	450	-	(Goel and Clausen, 1998)
Ligaments					
Anterior Longitudinal Ligament	2-node geometrical nonlinear tension only cable (LINK10)	950	11.9	-	(Kumaresan et al., 1999a)
Posterior Longitudinal Ligament			12.5	-	
Capsular Ligament			7.7	-	
Ligamentum Flavum			2.4	-	
Interspinous Ligament			3.4	-	
Supraspinous Ligament			3.4	-	
Articulations					
Posterior Facets	Three-dimensional sliding surface (CONTACT174-TARGET170)*	958	-	-	

Table 4: Finite element model characteristics, with element types and number of element indicated. *Contact surface elements were internally generated from the existing mesh, thus they represent opposing faces of brick elements at the mass of posterior articular facets.

4.2.11 Calculation of ROM

Calculation of ROM in the three major anatomically planes are not available in the typical commercial FEA packages. Therefore, a macro was written to automate the process of calculating the rotation automatically based on ANSYS output, using the following Euler equations. If sagittal plane is XOY,

Before rotation: Pt1(x1, y1), Pt2(x2, y2), **Equation 1**

After rotation: Pt3(x1+Ux1, y1+Uy1), Pt4(x2+Ux2, y2+Uy2) **Equation 2**

Angle1=Arctangent (y2-y1/x2-x1) **Equation 3**

Angle2=Arctangent [(y2+Uy2-y1-Uy1)/ (x2+Ux2-x1-Ux1)] **Equation 4**

Rotational Motions =angle2-angle1 **Equation 5**

where Pt1, Pt2, Pt3, Pt4 are points in the global coordinates system, angle1 is the angle between line connecting Pt 1 & Pt 2 and axis X, angle2 is the angle between the connecting Pt 3 & Pt 4 and axis X. For example, to calculate the ROM of C5-C6, with the applied moment at C5, two nodal points on the superior C5 body were selected to determine the rotation of the C5 vertebra with respect to C6 in the plane of moment application.

In this study, many results are presented using normalized values. Normalizing of the data is very common in spinal research and is used by many investigators (Cusick et al., 1988; Goel et al., 1988b; Goel et al., 1984; Kubo et al., 2003). Results are usually normalized as follows:

N = (Vi – Vs) / Vi * 100% **Equation 6**

where N is the normalized result, Vi is the result for the intact model, Vs is the result for the modified model. Thus, a positive value in the normalized result indicated an increase in value with respect to the original intact model.

4.3 Summary

Generally, Chapter 4 began with a brief introduction on the concept on the finite element method of analysis. The author also discussed the procedures (from digitization to modelling) taken in this study to model and simulate the human cervical spine accurately. Generating a C2-C7 model and ensuring that it was a correct description of the problem may be difficult. Firstly, the geometries of the vertebrae and intervertebral disc are irregular and facet contact between the adjacent vertebrae is important and possibly other regions of the geometry will also need to be modelled accurately. In this study, the anatomically realistic C2-C7 model was developed, based on the geometrical data of the embalmed cervical vertebrae, obtained from the three-dimensional multi-axis digitizer. The direct digitizing approach used in the development of the cervical spine model provided an alternative method of modelling the human cervical spine as compared to the current reported method of using the CT scan data. This method also enabled the capture of the highly irregular geometry of the cervical vertebrae efficiently.

It has been pointed out that a mathematical model based on detailed physical data is likely to represent the real structure successfully with a limited validation (Panjabi, 1979). Analyses have revealed that the biomechanical responses of the cervical spine are generally sensitive to changes in its geometrical and material characteristics.

1. Geometry – The author in this study tried to minimize the effects of geometry by comparing the dimensions of the finite element model against quantitative measurements of the cervical spine geometry reported in the literatures (Chua, 1999; Gilad and Nissan, 1986; Panjabi et al., 1991; Panjabi et al., 1992; Tan et al., 2002; Tan

et al., 2004). The close correlation in the geometry comparisons against the general population provided the necessary confidence for subsequent analysis and validations against the literature data using the cervical model.

2. Material - Although the cervical model was very realistic, the results will be limited by the use of linear elastic and homogeneous material properties. For the bony structures, this assumption was supported by the earlier studies on the mechanical behaviour of the bone, which have not revealed signs of nonlinear elasticity (Rohl et al., 1991). In this study, constant material properties were chosen for the various spinal components, although there can be local changes in the mechanical properties (for example, the elastic modulus of the cortical bone may range from 8GPa to 10GPa). Because the aim of this study was to investigate the global responses of the cervical spine exclusively after various conditions, the assessment on the variation in the mechanical properties within a spinal component was therefore excluded in this study. Furthermore, most of the *in vitro* tests preconditioned the specimens (loading and unloading the specimen several times before taking the motion measurements) before actual testing and loads were applied in short durations of less than 30s to minimize the effect of viscoelasticity (time dependent nonlinearity). In some finite element analyses, nonlinearity was defined only as material nonlinearity and the nature of the internal structure contributing to the nonlinearity were neglected. Ignoring the time dependent material properties, the disc structures are complex and contain nonlinear behaviour. This non-linearity arises from a combination of the nonlinear properties of the constituent materials, especially the collagen fibers and geometrical nonlinearity due to a change in orientation of the fibers during loading. Structural nonlinearity will be important when more than one motion segment is considered and the deflections of the vertebrae will be significant in relation to the overall geometry of the model (after

simulated injuries, surgical techniques and degeneration). Thus, a finite element model of the cervical spine may have contact, material and structural nonlinearities. In the present study, the C2-C7 model contained three types of non-linearities: (a) geometric non-linearities: due to large displacements; (b) contact non-linearities: due to nonlinear facet articulation; (c) material nonlinearities: due to nonlinear behaviour of the intervertebral discs, stemming from their composite structure involving the presence of bilinear elements for the annulus fibers. Furthermore, the cable element has a wrinkling capability, i.e., the cable element was incapable of sustaining a load in compression and was only load bearing in tension. This could be considered as a form of material nonlinearity.

In the following chapters, the finite element model was validated against the data reported in the literatures using the cadaveric specimens from the general population and tested under various clinical relevant conditions. The associated load configurations, boundary conditions and the predicted results are presented graphically and discussed. Any conclusions concerning the biomechanics of the human cervical spine and of relevant clinical applications are also presented, where appropriate.

Chapter 5. Validation and Ligamentous Injury Studies

5.1 Introduction

Stability of the cervical spine is provided by a combination of passive ligaments, facet joints, discs and active muscles. However, the ligamentous structures of the cervical spine are often involved in the cervical spine injuries, for example in whiplash injuries that inflict severe cervical ligamentous injuries. Although standard clinical imaging techniques, especially nuclear magnetic resonance imaging (MRI) allow the detection of ligamentous injuries, few biomechanical data exist concerning the significance of the ligamentous structures on the changes in the load-displacements, ROM and internal parameters of the cervical spine under physiological loading conditions (Goel et al., 1984; Panjabi et al., 1978; Wen et al., 1993b). Ligamentous injuries will decrease the mechanical stiffness of the cervical spine, and potentially affecting the internal spinal components. However, the contribution of the cervical ligamentous structures to the cervical spine stability has not been clearly established.

For the clinicians, it is important to know if there is a sudden large change in the cervical spinal flexibility after ligamentous injuries. Knowing this information will help the surgeons to decide whether to fuse the segment or not. However, as Goel and Gilbertson, 1995 pointed out, although the finite element method is increasingly able to simulate a variety of clinical situations in a realistic manner, a great deal of work must precede this (especially **validation studies**). This is true, as FEM analysis of any biological structures usually requires element idealization and assumptions. Thus, prior

to the actual investigations, a series of validation studies were conducted to compare the predicted ROM, stiffness and internal strains against the experimental measurements.

5.2 FE Model Validation

Validation studies form the crucial link between the development of the finite element model and its final intended use. Once the initial validation studies have been completed, the model can be used as a specimen with repeatability and reproducibility characteristics that are ideal for various biomechanical studies, including simulated spinal injuries, surgical treatments, stabilization, etc investigated in the present study. Therefore, the purpose of this study was to test the hypothesis that the assumptions made during the development and formulation of the lower cervical spine model was valid, within the physiological limits and comparable to the *in vitro* data reported in the literatures (Table 5). During the validation studies, the motion segment levels, orientation, loading and boundary conditions were identical to the *in vitro* testing conditions.

Prior to the validation, mesh sensitivity studies (Refer A.2 Mesh Sensitivity Studies) were conducted to determine the optimum element size for the finite element model on the prediction of stiffness/ROM under various loading modes (compression, anterior/posterior shear, flexion and extension, lateral bending and axial rotation). However, a compromise between the computational time and the accuracy of the finite element model prediction will be decided, depending on the nature of the analysis. After serious consideration from the above results, the finite element model with the appropriate mesh density and accuracy was chosen for all the subsequent analysis.

Anatomical Region	Loading		Responses	References
	Force	Mode		
Disc Segment				
C5-C6	73.6 N preload in 1 step and 1.6 Nm in 4 steps	flexion, extension, lateral bending, axial rotation	primary and secondary ROM	(Maurel et al., 1997; Moroney et al., 1988)
Single FSU				
C5-C6	73.6 N preload in 1 step and 1.8 Nm in 4 steps	flexion, extension, lateral bending and axial rotation	primary and secondary ROM	(Moroney et al., 1988)
	50 N in 1 step	compression, anterior shear, posterior shear	force displacement stiffness	
	1 Nm in 4 steps	flexion, extension, lateral bending and axial rotation	ROM	(Goel and Clausen, 1998)
	9.5 N preload in 1 step and 1.5 Nm in 4 steps	Flexion and extension	ROM	(Wen et al., 1993a)
	9.5 N preload in 1 step and 2 Nm in 4 steps	lateral bending		
	9.5 N preload in 1 step and 4.5 Nm in 4 steps	axial rotation		
	2.5 Nm in 4 steps	flexion, extension, lateral bending and axial rotation	ROM	(Richter et al., 2000)
Double FSU				
C4-C5-C6	1mm in 5 steps	compression	force displacement stiffness	(Shea et al., 1991)
	2 mm in 4 steps	anterior shear		
	4 mm in 8 steps	posterior shear		
	2.5 N preload in 1 step and 1.8 Nm in 4 steps	flexion, extension, lateral bending and axial rotation	ROM	(Panjabi et al., 1986; Pelker et al., 1991)
	800 N in 4 steps	compression	force displacement stiffness, internal vertebral body and facet mass strains	(Pintar et al., 1995)

Table 5: Summary of validation studies against experimental data.

5.2.1 Validation against Shea et al., 1991 on C4-C6

The C4-C5-C6 model was used to simulate the in vitro experiments carried out by Shea et al., 1991 under axial compressive loading, anterior and posterior shear. The model was created by removing the C2, C3, C7 vertebrae and the associated soft tissues. Loading and boundary conditions were similar to those reported in the experimental procedure. For the three loading conditions (compressive, anterior and posterior shear), the C6 inferior vertebral body was constrained in all the degrees of freedom. Under compressive loading, a uniform axial displacement of 1 mm was applied incrementally in five equal sub-steps to the superior nodes of C4. Furthermore, uniform anterior and posterior displacements of 2 mm and 4 mm, respectively were applied incrementally in four sub-steps and eight sub-steps to the superior nodes of C4 for the other two loading configurations. For the applied compressive loads at C4, the predicted vertical reaction force at C6 was compared with the experimental results. For the applied anterior and posterior displacements at C4, the predicted horizontal reaction force at C6 was compared with the experimental results (Shea et al., 1991).

The predicted stiffness (Figure 65 - Figure 68) showed close agreement with the *in vitro* data under compression, anterior and posterior shear (Shea et al., 1991). Under posterior shear, FE results are higher and not within experimental range except when the applied displacement is 4 mm.

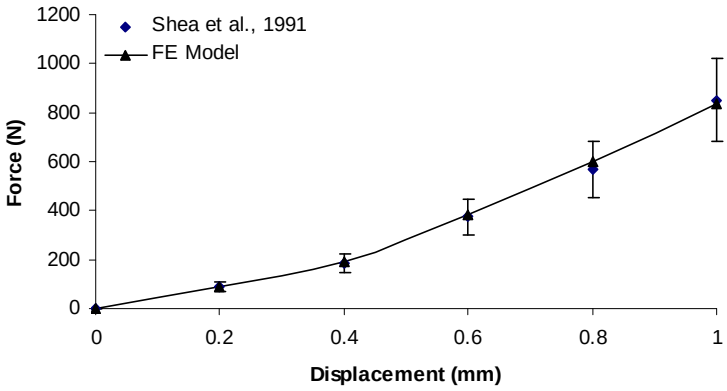

Figure 65: Comparison of C4-C6 model against experimental data under 1 mm compression (Shea et al., 1991).

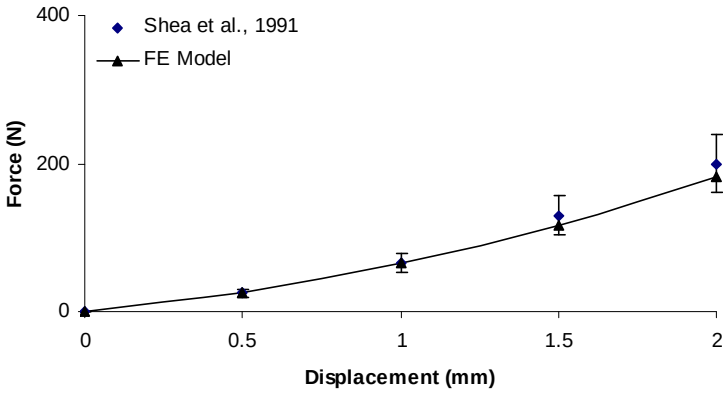

Figure 66: Comparison of C4-C6 model against experimental data under 2 mm anterior shear (Shea et al., 1991).

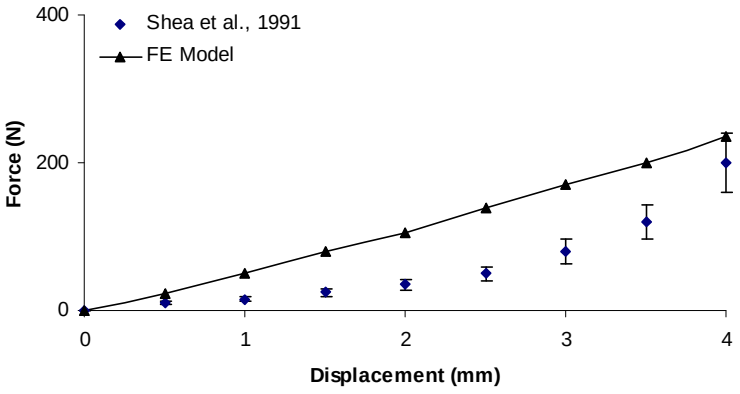

Figure 67: Comparison of C4-C6 model against experimental data under 4 mm posterior shear (Shea et al., 1991).

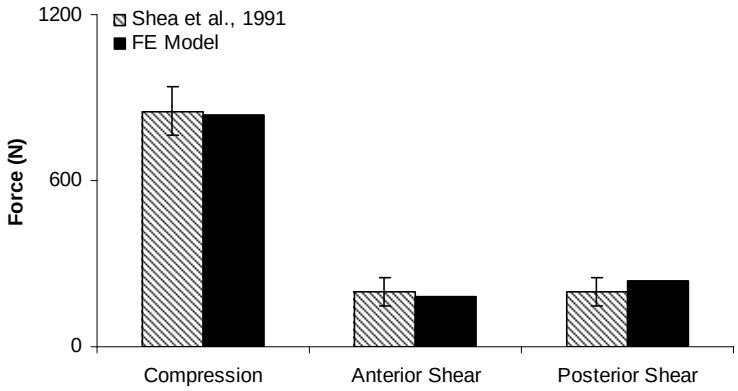

Figure 68: Validation of C4-C6 model against *in vitro* data (Shea et al., 1991).

5.2.2 Validation against Moroney et al., 1988 on C5-C6

In this study, the C2-C7 model with C2, C3, C4 and C7 removed to form the C5-C6 FSU was used for validation against *in vitro* experimental results under a) sagittal moments (flexion, extension, lateral bending and axial rotation) and b) stiffness (compression, anterior shear, posterior shear and lateral shear). The model was adjusted so that the mid-plane of the intervertebral disc was aligned to the horizontal plane, similar to the experimental setup. For sagittal moments, an axial compressive preload of 73.6 N was applied over the surface of the C5 superior vertebra body. After the application of preloads, pure moments of up to 1.8 Nm in flexion, extension, lateral bending and axial rotation were applied to the same surface. Rotational motions arising from the applied moments were calculated using the formulae described earlier (Refer 2.3 Kinematics of the Functional Spinal Unit). For load displacements, a force of 50 N in the four directions (Fy (compression), Fz (anterior shear), -Fz (posterior shear), Fx (lateral shear)) was applied all over the surface of the C5 superior vertebra body. The resulting displacement in the direction of force application was captured. In these series of analyses, constraints were applied in all degrees of freedom to the inferior surface of the C6 vertebra body.

The results predicted in this study were compared (Figure 69 - Figure 73) against the *in vitro* data. The current results indicated the slight non-linearity curve of the cervical spine under various loading mode. The predicted trend agreed well with experimental data throughout the loading range. However, when compared to the ROM under lateral bending, the model predictions were lower, but, fortunately, still within the variation found in the experimental data. Apart from the primary motions, the model also compared well against the experimental data in the secondary motions. It was noted that the ROM for the corresponding secondary motions (for both FE prediction and *in vitro* data) are usually a fraction of the primary motions

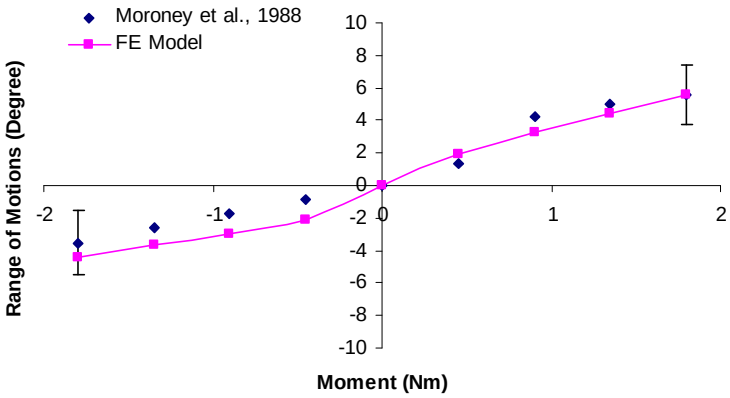

Figure 69: Comparison of C5-C6 against experimental data in flexion-extension (Moroney et al., 1988).

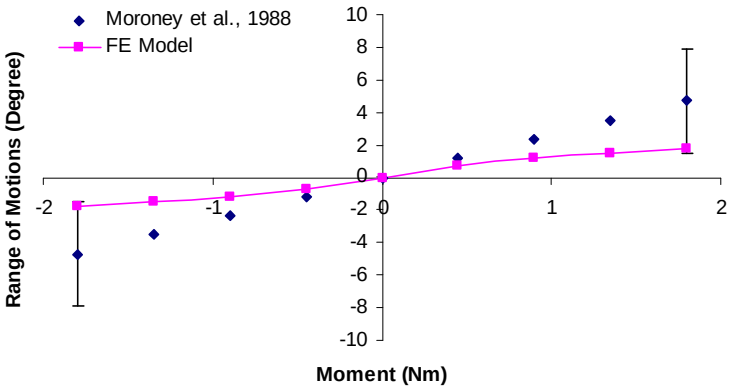

Figure 70: Comparison of C5-C6 against experimental data in lateral bending (Moroney et al., 1988).

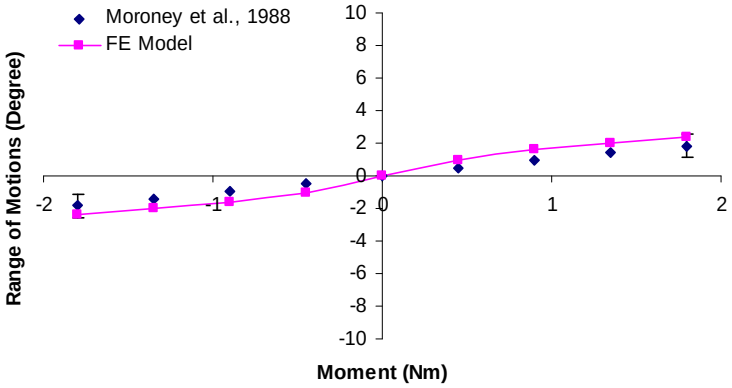

Figure 71: Comparison of C5-C6 against experimental data in axial rotation (Moroney et al., 1988).

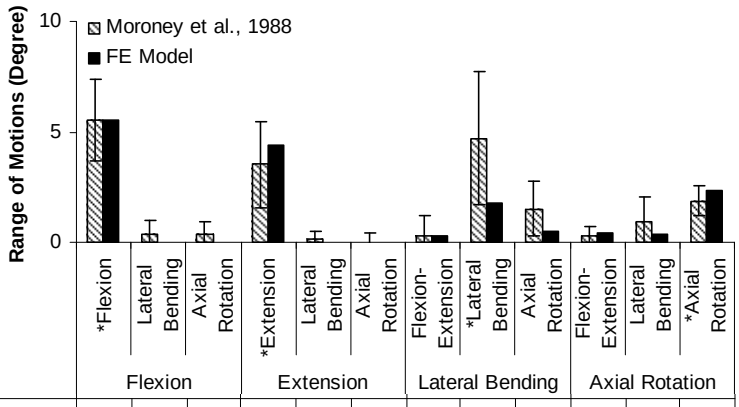

Moroney et al., 1988	5.6	0.3	0.3	3.5	0.1	0	0.3	4.7	1.5	0.3	1	1.9
FE Model	5.6	0	0	4.4	0	0	0.3	1.8	0.5	0.5	0.4	2.4

Figure 72: Validation of C5-C6 FSU against *in vitro* data. *denotes primary motions (Moroney et al., 1988).

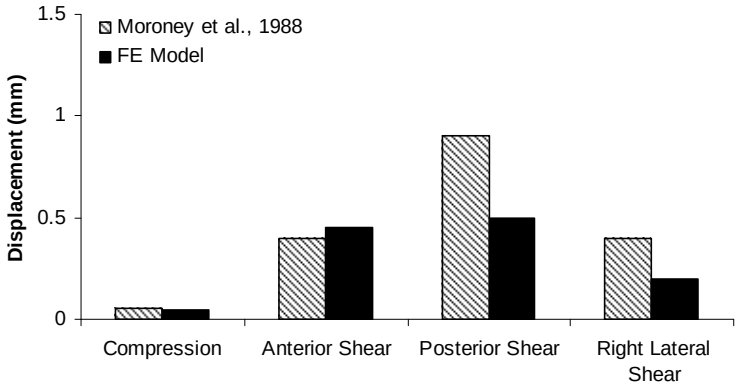

Figure 73: Validation of C5-C6 against *in vitro* data under 50 N force (Moroney et al., 1988).

5.2.3 Validation against Moroney et al., 1988 and Maurel et al., 1997 on C5-C6 Disc Segment

The C5-C6 disc segment was created by removing the C2, C3, C4 and C7 vertebrae, its associated soft tissues and all the posterior structures. The C5-C6 disc segment only contains two vertebral bodies, the intervertebral disc, the anterior longitudinal ligaments and the posterior longitudinal ligaments. During the simulation, the inferior vertebra was rigidly fixed in all directions of movements and the superior vertebra was free to move in response to the loads applied to the superior surfaces of the C5 vertebra. The model was adjusted so that the mid-plane of the intervertebral disc was aligned to the horizontal plane, similar to the *in vitro* setup. An axial compressive preload of 73.6 N was applied and eventually, a pure moment of 1.6 Nm in flexion or extension was applied incrementally in four equal steps over the top surface of the C5 vertebra. The calculated ROM (primary and secondary motions) were compared (Figure 74) with the *in vitro* data (Moroney et al., 1988) and linear FE results (Maurel et al., 1997) reported in the literatures. Generally, a high level of conformance can be seen between the current model and the *in vitro* data under flexion, extension and axial rotation. Under lateral bending, the model falls in the lower range of the experimental data.

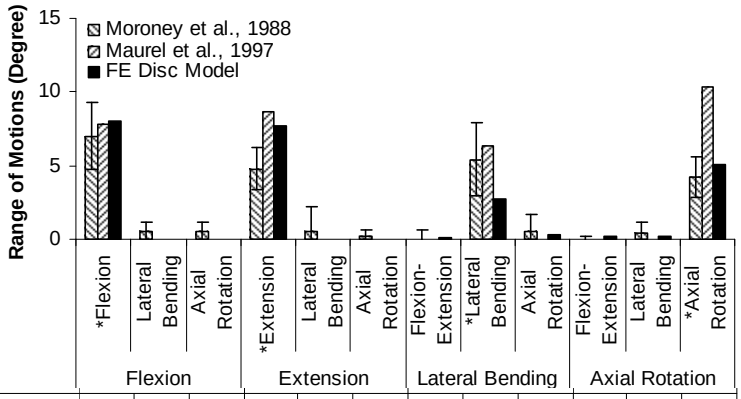

Moroney et al., 1988	7	0.5	0.5	4.8	0.5	0.2	0	5.4	0.5	0	0.4	4.2
Maurel et al., 1997	7.8			8.7				6.3				10
FE Disc Model	8	0	0	7.7	0	0	0.1	2.7	0.3	0.2	0.2	5.1

Figure 74: Validation of C5-C6 disc segment against *in vitro* data. *denotes primary motions (Maurel et al., 1997; Moroney et al., 1988).

5.2.4 Validation against Pelker et al., 1991 on C4-C6

The C4-C6 model was created from the C2-C7 model and was used in this study. Loading and boundary conditions were similar to the setup reported by Pelker et al., 1991. The inferior surface of C6 was fixed in all directions of movements and a constant pure moment of 1.8 Nm was applied to the top surface of the C4 vertebra. Prior to the application of pure moments, a preload of 2.5 N was applied to the same surface. ROM was predicted and compared against the data reported in the literatures (Pelker et al., 1991). The predicted ROMs (Figure 75) are comparable to the *in vitro* data under similar loading and boundary conditions. It should be noted that under axial rotation, the predicted ROM at the upper segment is slightly lower than the lowest *in vitro* data.

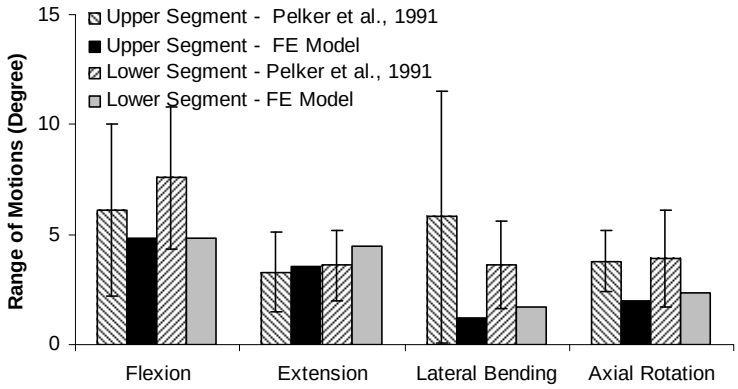

Figure 75: Validation of C4-C6 model against *in vitro* data (Pelker et al., 1991).

5.2.5 Validation against Wen et al., 1993 on C5-C6

In this study, C5-C6 model was used for comparison against *in vitro* data by Wen et al., 1993a. The model was tested under four physiological loading modes, flexion, extension, lateral bending and axial rotation. The setup, loading and constraints were similar to those reported in the literatures (Wen et al., 1993a). The loading was applied to the superior vertebra body of C5 and constraints were provided at the base of C6. Pure moments of up to 1.5 Nm, 2.0 Nm and 4.5 Nm was used to simulate flexion-extension, lateral bending and axial rotation, respectively in four equal sub-steps. Prior to the application of pure moments, a preload of 9.5 N was used in the first load step. The predicted primary motions and secondary motions were obtained (Figure 76) and compared against the experimental data (Wen et al., 1993a). Overall, the C5-C6 model compared well against the data reported by Wen et al., 1993a. However, it should be noted that Wen et al., 1993a did not provide any data on secondary motions. It can be seen that the predicted ROM under lateral bending is lower than the mean experimental data minus the standard deviation. Furthermore, direct comparison (Figure 77) on the motions against the individual specimen under lateral bending indicated better

correlation between the FE and experimental data. The results showed that the motions predicted by FE were closer to the value obtained using Specimen 25.

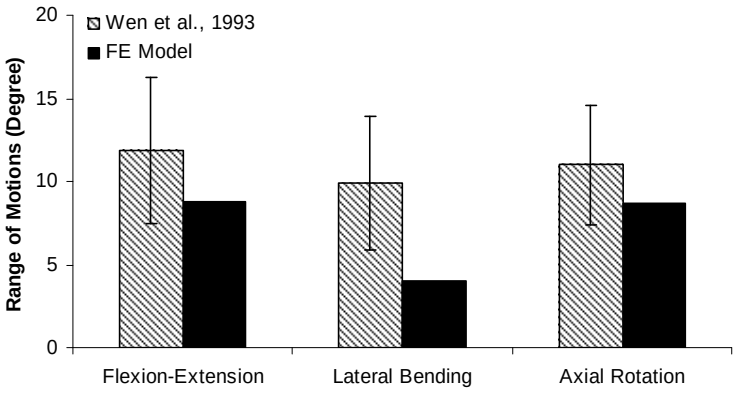

Figure 76: Comparison of C5-C6 FSU against experimental data (Wen et al., 1993a).

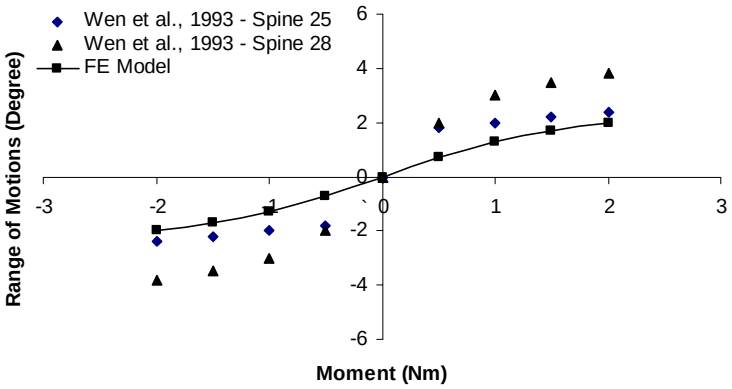

Figure 77: Comparison of C5-C6 FSU against experimental data in lateral bending. Data from two specimens were used in the comparison (Wen et al., 1993a).

5.2.6 Validation against Pintar et al., 1995 on C4-C6

As the cervical spine internal stress, strain and pressure values were obtained from the FE model and used in this study, it was important to validate the model using internal parameters (other than ROM and stiffness). In this study, the C4-C6 data obtained by Pintar et al., 1995 was used for the comparison. The C4-C6 model was created from the

C2-C7 model. Loading and boundary conditions were similar to those used in the experimental procedure. The inferior surface of the inferior most vertebra (C6) was fixed in all degrees of freedom and pure compressive load was applied uniformly to the superior most (C4) vertebra. The computed stiffness and the localized strain data (averaged over a group of elements that covered the respective areas represented by the strain gauges in the experimental) in the anterior region of the middle vertebral body and lateral facet mass (Figure 21) were obtained and compared with the *in vitro* data for validation purposes (Figure 78 - Figure 80). Generally, the predicted results compared well with the *in vitro* data and were within the standard errors obtained by the *in vitro* data. The results showed that increasing the axial compressive force would increase the displacement and the anterior vertebral body and lateral facet mass strains.

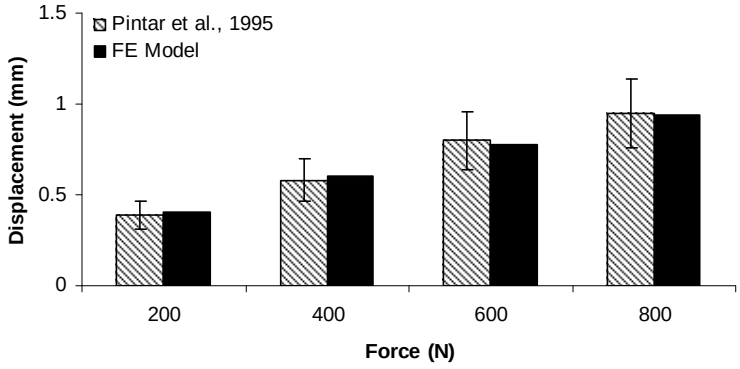

Figure 78: Comparison of the C4-C6 model with *in vitro* data under compression for force-displacement (Pintar et al., 1995).

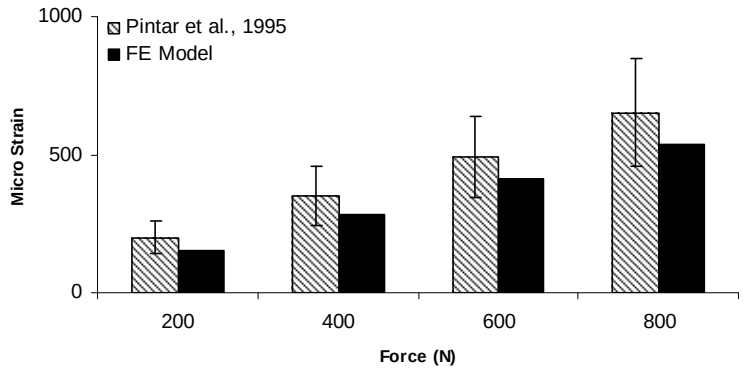

Figure 79: Comparison of the C4-C6 model with *in vitro* data under compression for anterior vertebral body strain (Pintar et al., 1995).

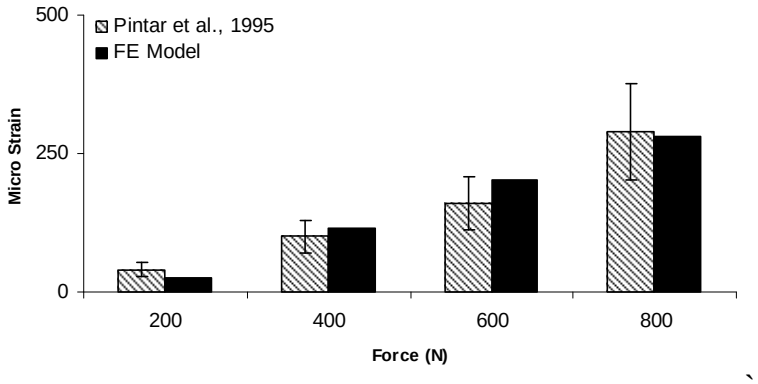

Figure 80: Comparison of the C4-C6 model with *in vitro* data under compression for lateral facet mass strain (Pintar et al., 1995).

5.2.7 Validation against Goel and Clausen, 1998 on C5-C6

In this study, the C5-C6 model was created by removing the C2, C3, C4 and C7 vertebrae and its associated tissues for loading under sagittal moments (flexion, extension, lateral bending and axial rotation). Loading was applied to the superior surface of C5 vertebra body incrementally in four equal steps, up to 1 Nm. Boundary conditions were applied to the inferior surface of C6 vertebra, by fixing the vertebra body in all degrees of freedom. The predicted ROM was compared and correlated well (Figure 81 - Figure 84) against experimental data throughout the whole loading range.

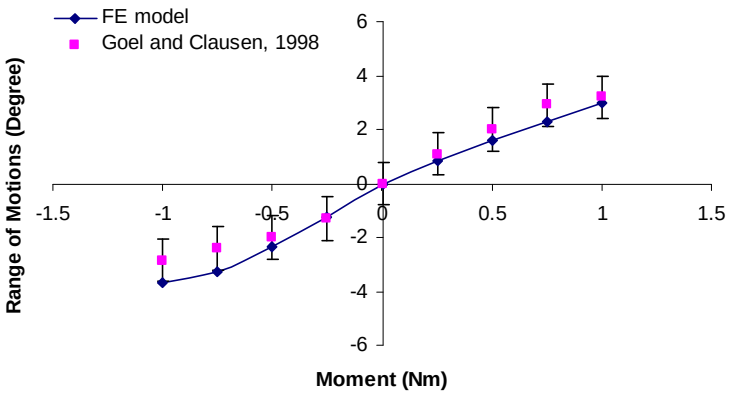

Figure 81: Comparison of C5-C6 FSU against experimental data in flexion-extension (Goel and Clausen, 1998).

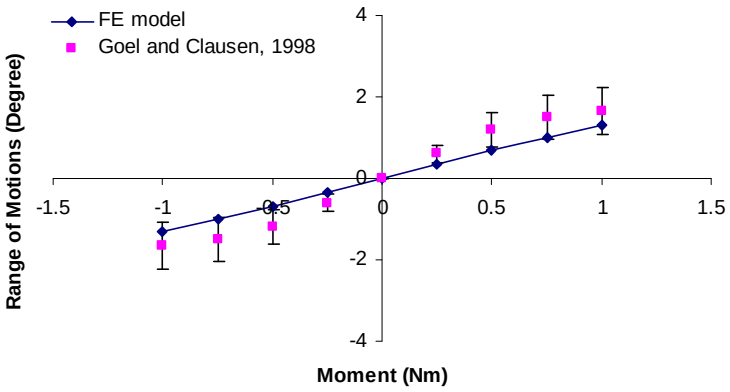

Figure 82: Comparison of C5-C6 FSU against experimental data in lateral bending (Goel and Clausen, 1998).

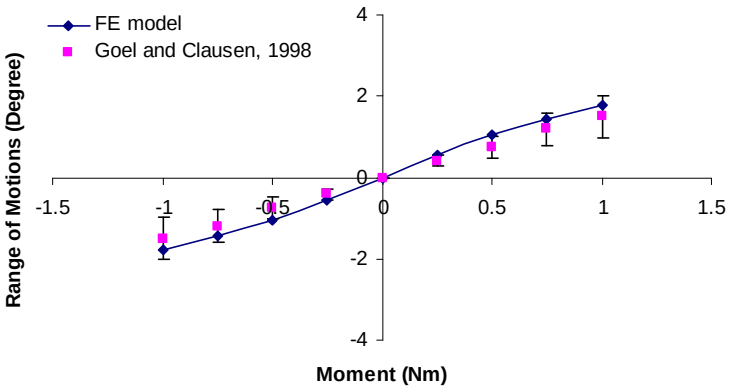

Figure 83: Comparison of C5-C6 FSU against experimental data in axial rotation (Goel and Clausen, 1998).

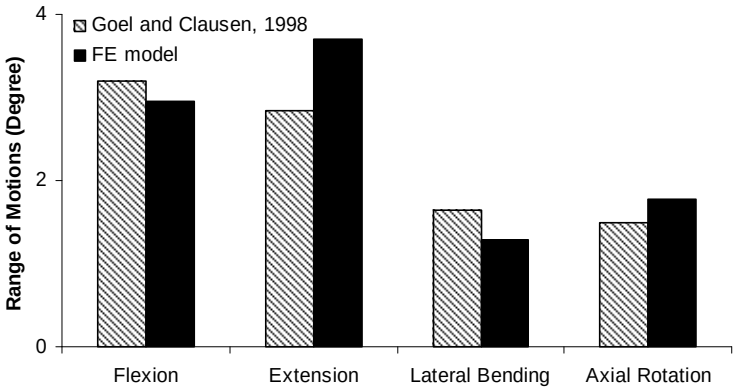

Figure 84: Validation of C5-C6 FSU against *in vitro* data. *denotes primary motions. Goel and Clausen, 1998 did not report any secondary motions, so no comparison can be made (Goel and Clausen, 1998).

5.2.8 Validation against Richter et al., 2000 on C5-C6

The C5-C6 model was used in this series of comparison against experimental data reported by Richter et al., 2000. Flexion/extension, right/left lateral bending and left/right axial rotation moments of 2.5 Nm in each direction were applied to the superior surface of C5 vertebra body. The C6 inferior vertebra body was rigidly fixed in all direction of movements. The results (Figure 85) correlated well with the experimental data under flexion-extension and axial rotation. Under lateral bending, the predicted ROM is slightly lower than the mean minus the standard deviation.

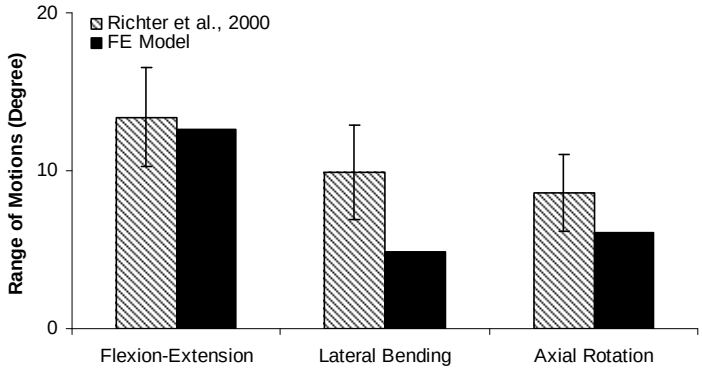

Figure 85: Validation of C5-C6 FSU against *in vitro* data. *denotes primary motions. Richter et al., 2000 did not report any secondary motions, so no comparison can be made.

5.2.9 Regression Analysis

To formulate a functional relationship between the applied moment and angle or force and displacement, the data for each loading case was fitted with a nonlinear function as follows

$$q = \mathbf{A \ln(BM+1)} \qquad \textbf{Equation 7}$$

where θ is the rotational angle, M is the applied moment and A and B are model constants. This function has been widely used to model the nonlinear behaviour of soft tissues (Nightingale et al., 2002). For the C5-C6 model under sagittal moments, four FE validation studies were conducted, each with their own preload values. Since there is a lack of another independent variable (preload) in the equation, it was not possible to average the FE results for the various validation studies prior to curve fitting. Instead, all the FE results were curve fitted individually (Figure 86 - Figure 89). These curve fitted responses were then averaged and curve fitted again to get the final constants. Summary of the final constants used to curve fit the various models under different loading conditions can be found in Table 6. The lowest and highest R2 values are 0.98 and 1 respectively.

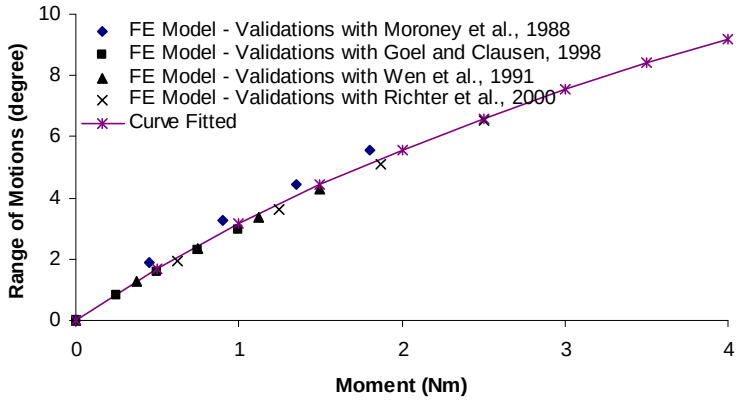

Figure 86: Curve fitted C5-C6 FE predictions under various validation studies in flexion.

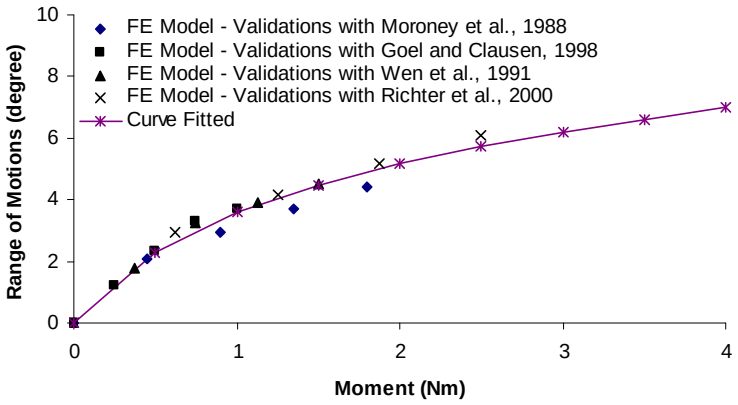

Figure 87: Curve fitted C5-C6 FE predictions under various validation studies in extension.

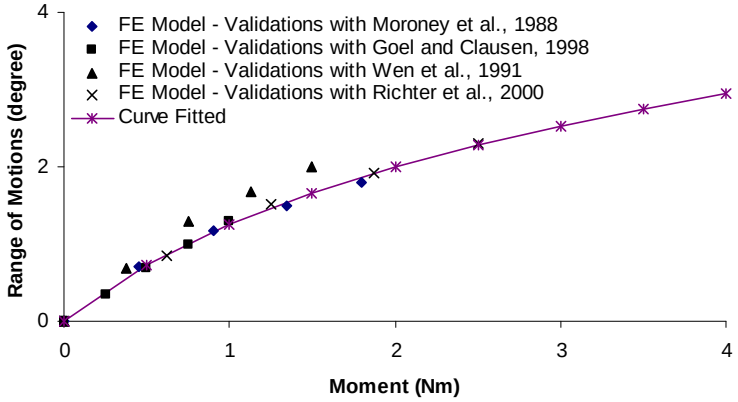

Figure 88: Curve fitted C5-C6 FE predictions under various validation studies in lateral bending.

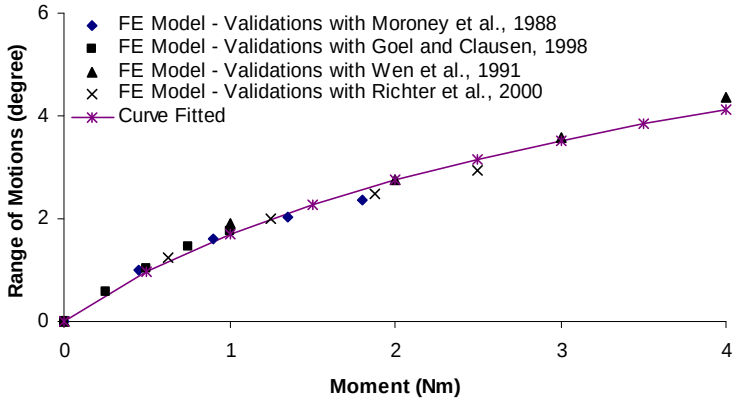

Figure 89: Curve fitted C5-C6 FE predictions under various validation studies in axial rotation.

	C4-C6			C5-C6		
	A	B	R^2	A	B	R^2
Compression	0.69310921	0.00375490	0.99	-		
Anterior Shear	1.64401372	0.01302045	0.99			
Posterior Shear	11.09692877	0.00184341	0.99			
Flexion	22.48814994	0.29772957	1.00	10.52605052	0.34903997	0.99
Extension	4.80618932	2.34054937	1.00	3.02404733	2.26858085	0.98
Lateral Bending	1.99023742	1.54660435	1.00	1.92547025	0.91003445	1.00
Axial Rotation	3.03821053	1.72533515	1.00	2.79936743	0.83912214	0.99

Table 6: Summary of constants used for curve fit the nonlinear behaviour of the cervical biomechanics using the functional relationship described in Equation 6.

The curves created from these final constants were then used to compare against reported experimental results (Figure 90 - Figure 93). It can be seen that the curves generated from equation 7 provide a good fit for flexion, fall in the lower range of experimental data for lateral bending and in the upper range for extension and axial rotation. This can be due to a number of reasons:-

1. Averaging of the *in vitro* data by various investigators may have smoothened the curve. Therefore, direct comparison on the motions against the individual specimen may indicate better correlation between the FE and experimental data.
2. Equation 7 does not account for the influence of preloads, which may have a noticeable effect on the predicted ROM.

Overall, equation 7, using the constants derived from curve fitting the FE predictions, compared well against the experimental data. In the past, stiffness or ROM had been used in the comparison of results among various authors and research groups.

Confusion arises when various authors tried to compare their results against experimental data under different loading magnitudes. Using this methodology, cervical spine biomechanics under similar setup and various loading conditions can be compared efficiently. Furthermore, this equation can also be used to describe the nonlinear behaviour of the cervical spinal biomechanics more easily.

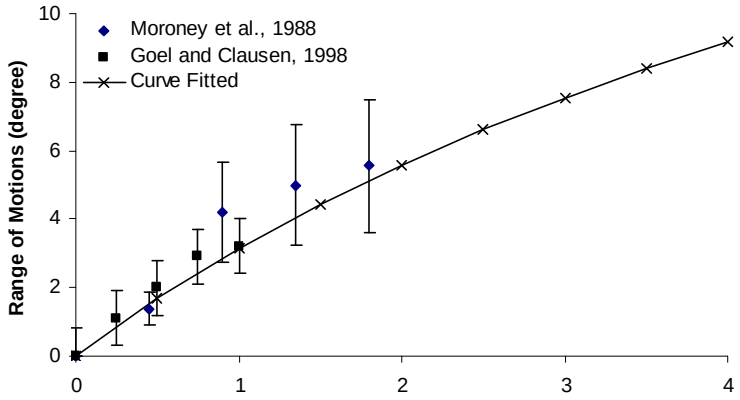

Figure 90: Comparison of fitted curve for C5-C6 against experimental data in flexion.

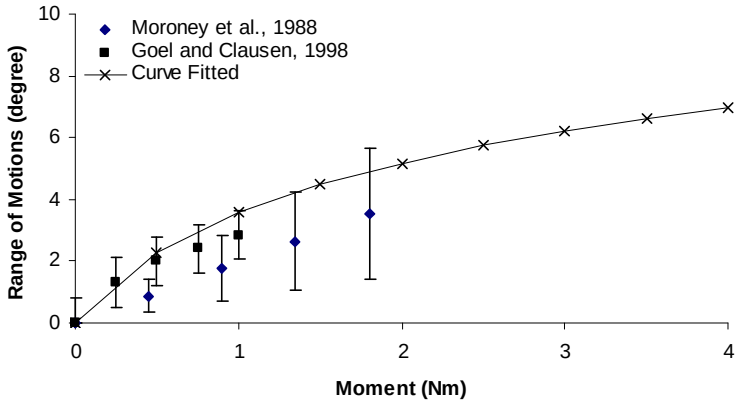

Figure 91: Comparison of fitted curve for C5-C6 against experimental data in extension.

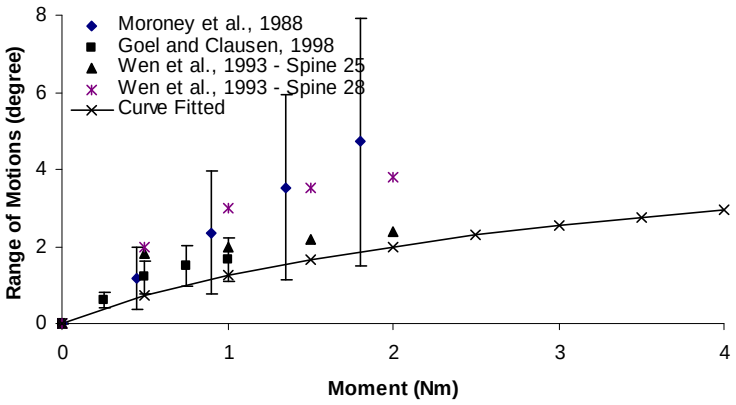

Figure 92: Comparison of fitted curve for C5-C6 against experimental data in lateral bending.

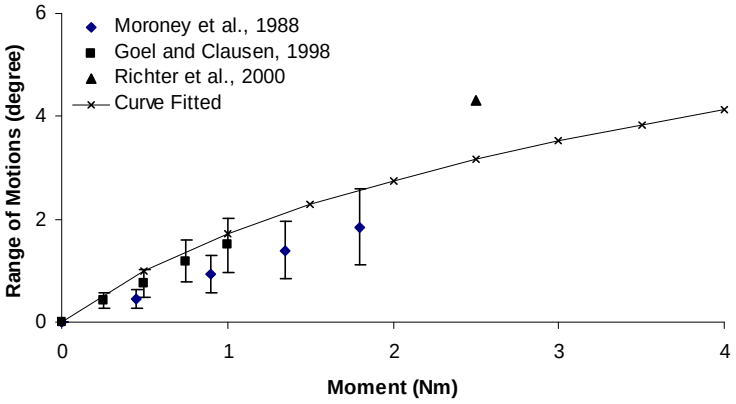

Figure 93: Comparison of fitted curve for C5-C6 against experimental data in axial rotation.

5.2.10 Summary

In this chapter, detailed three-dimensional lower cervical spine FE models **were validated against the various experimental data (external and internal biomechanical responses) reported in the literatures**. To the author's knowledge, no FE models (single or multiple motion segment levels) are currently available or reported in the literatures that are able to the validate various external (ROM and stiffness) and the internal (strains) against many *in vitro* data and under a wide range of loading

conditions (flexion, extension, lateral bending, axial rotation, compression, anterior and posterior shear).

Validation of the cervical spinal model was essential but very difficult, due to the significant physiological and biological variation among the specimens used in the experimental studies. Furthermore, as there were many assumptions and simplifications during the development of the cervical spine model (Refer 4.2 Finite Element Model Generation), validation studies becomes very important and necessary step before they were utilized for further studies in the subsequent chapters. Prior to this, **convergence studies were conducted to investigate the influence of mesh density on the external and internal responses under a wide range of physiological loading modes to ensure that sufficient element mesh density was used to describe the current cervical spine model**. Overall, the FE models predicted not only the primary motions but also the secondary motions, stiffness and internal strains in close agreement with the experimental values reported by various investigators. One reason for this close agreement can be attributed to the close correlation in the geometrical dimensions of the current FE model against the general population. Once the models were validated, results obtained from these models can then be interpreted as an approximation of the *in vitro* and *in vivo* cervical spine responses within this loading range. The model's applicability beyond this level should be treated with caution.

Generally, displacements are more accurately predicted than the internal stress and strains in all finite element models, because the stress and strains are derived from the displacements and are more sensitive to the changes. Currently, FE models reported in the literatures were only validated with the *in vivo* and *in vitro* data by comparing the

ROM or force/displacement stiffness. While this invariably showed that the ROM of the model might be reasonable, it does not ensure the accuracy of the strains within the model. Therefore, the absolute strain values predict by these spine models should be carefully interpreted. In this study, the FE models were not only validated with ROM and stiffness, it was also validated with internal anterior vertebral body and lateral facet mass strains. Subsequently, this model was further refined and validated by comparing the internal intervertebral disc pressure against the data reported in the literatures (Refer Chapter 7.3.2 Internal Disc Pressure).

It is also known that the biomechanical responses of the human cervical spine are nonlinear, with increasing stiffness at higher loads. Therefore, it is important to develop a realistic finite element model that can effectively simulate the general external nonlinear behaviour of the human cervical spine. In the past, several authors had used three-dimensional linear models to validate against published data (Kumaresan et al., 1999a; Kumaresan et al., 1997; Maiman et al., 1999; Voo et al., 1997; Yoganandan et al., 1996b). However, linear results obtained from the analysis prevented them from realistically representing the biomechanical responses of the human cervical spine. The present FE model is able to predict the biomechanical changes in the human cervical spine by utilizing the three nonlinearities. The current study also proposed a new methodology of applying pure moments to the cervical spinal models that support geometrical nonlinearity.

In this study, the close correlations obtained from the validation studies showed that the methodologies and assumptions used in the development and idealisation of the human cervical spine were valid. Furthermore, in order to extent the applicability of the FE

analysis, regression analyses were performed. Despite the variability of the *in vitro* results, the fitted curve was generally within the range of the reported data. This showed that the equation used to predict the behaviour of the soft tissues could be used to describe the general cervical spine external biomechanics. With all the appropriate validations, the finite element model could then be used with confidence to provide further understanding on the cervical spine biomechanics. Validated models can then simulate the effects of injury, degeneration, surgical techniques and trauma within the validated range. The validated model can also help to evaluate new spinal instrumentation or fixation, without actually manufacturing it.

In the next section, the cervical spine model will be further investigated under ligamentous injured condition. The results from the injured model are compared against the *in vitro* data reported in the literatures.

5.3 Ligamentous Injury Studies

The purpose of this study was to test the hypothesis that the lower cervical spine ligaments play an important function in maintaining the cervical stability. A secondary goal of this study was to provide previously unavailable biomechanical data on the internal biomechanical changes after ligamentous injury. The results and finding from this study will assist in the further understanding of the cervical biomechanics. Summary of the loading and boundary conditions can be found in Table 7.

Descriptions	Loading	Steps	Constraints	In vitro
C4-C6				
Compressive	1 mm	5	Fixed at C6 inferior body and apply loads at C4 superior body	(Shea et al., 1991)
Anterior	2 mm	4		
Posterior	4 mm	8		
C5-C6				
Flexion	9.5N/2 Nm	5	Fixed at C6 inferior body and apply loads at C5 superior body	(Wen et al., 1993b)
Extension				
Lateral Bending				
Axial Rotation				

Table 7: Boundary, loading conditions and comparisons used in the injury simulation.

Four models were constructed from the C2-C7 model for used in this study. Two intact C4-C6 and C5-C6 models as well as two ligamentous injured C4-C6 and C5-C6 models. The two ligamentous injured models were constructed from the intact model through the resection of all cervical ligaments. The two C4-C6 models (intact and injured) were tested under compression, anterior shear and posterior shear. The other two C5-C6 models (intact and injured) were loaded under sagittal moments similar to the study reported by Wen et al., 1991. The biomechanical responses under these conditions were predicted and analyzed. Take note there were no *in vitro* ligamentous injury studies carried out under compression, anterior and posterior shear. Therefore, no comparison can be made.

5.3.1 Influence on Rotational Motions

In general, the percentage change in the ROM (Figure 94) increases under flexion, extension, lateral bending and axial rotation after ligamentous injuries.

Under flexion and extension, the injured model was more flexible in flexion (95%) than in extension (27%) at maximum loading of 2.0 Nm. In flexion, the passively stretched ligaments provided the more needed role of cervical stability. Under extension moments, the slight deviation of moment deflection suggested the determinant role of articulating facets and intervertebral disc. Similarly, several investigators also reported that the measured moment deflections increased by about 98% and 58%, respectively (Wen et al., 1993b). The importance of ligamentous injuries can also be seen under lateral bending and axial rotation at 2.0 Nm, where ligamentous injuries resulted in 50% and 88% increase in the rotational motion.

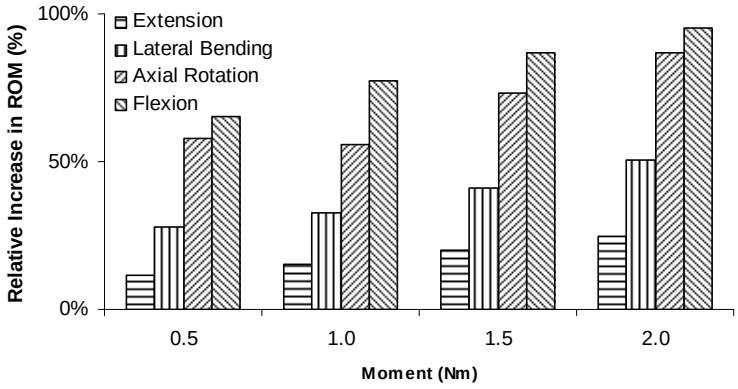

Figure 94: Percentage increase in the ROM of C5 with respect to C6 from the normal model due to ligamentous injuries under flexion, extension, lateral bending and axial rotation.

Figure 95 - Figure 98 show the summary of the percentage change in the biomechanical responses and the corresponding spinal component stress under flexion, extension, lateral bending and axial rotation after ligamentous injuries. The results showed that increases in the ROM were accompanied by increase in the stress in the various spinal components.

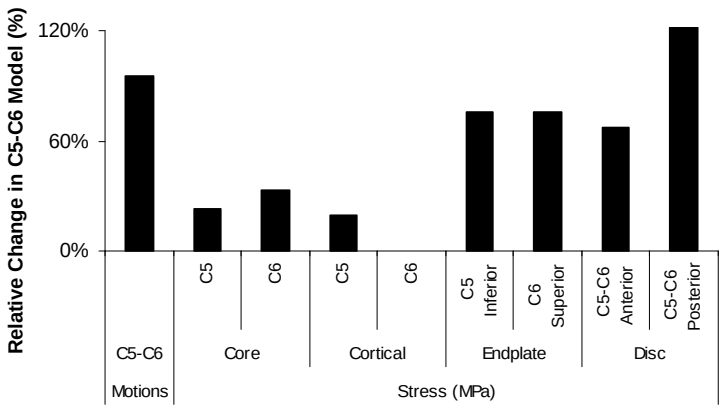

Figure 95: Percentage change in the respective spinal components stress due to ligamentous injuries under flexion.

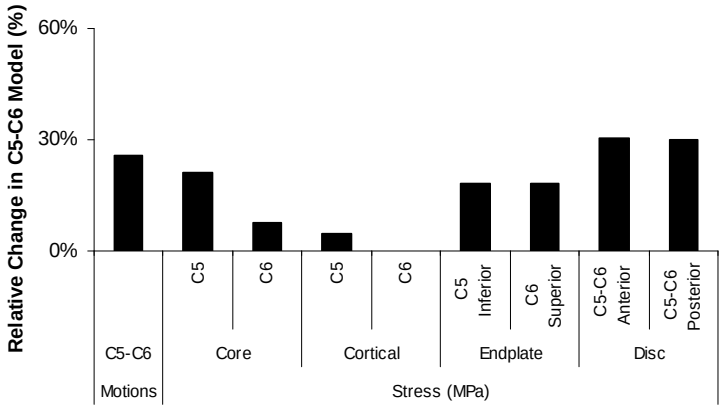

Figure 96: Percentage change in the respective spinal components stress due to ligamentous injuries under extension.

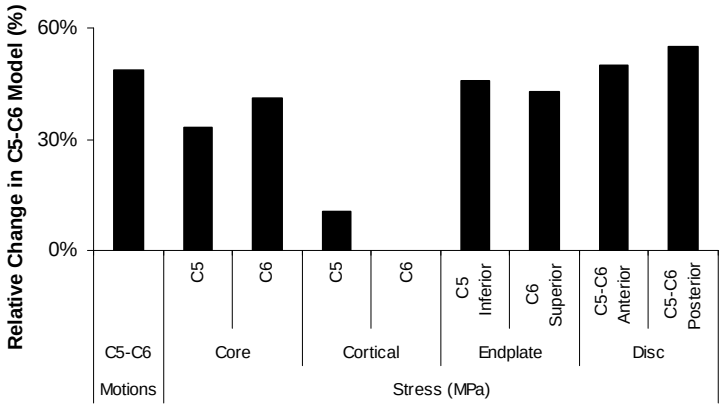

Figure 97: Percentage change in the respective spinal components due to ligamentous injuries under lateral bending.

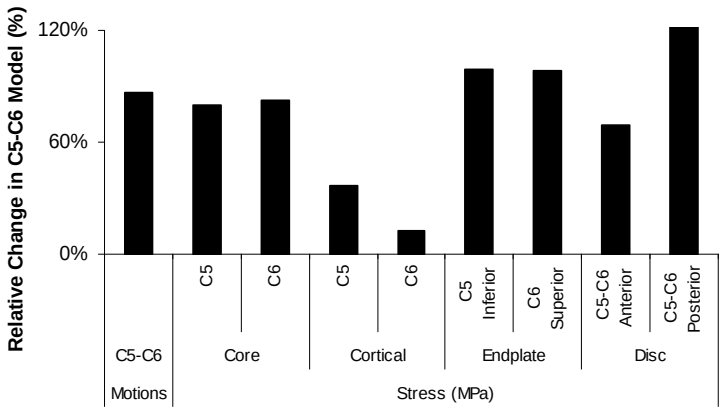

Figure 98: Percentage change in the respective spinal components stress due to ligamentous injuries under axial rotation.

5.3.2 Influence on Load Displacement

Under compressive loading (Figure 99 - Figure 102), the removal of passive ligaments does not affect the stability of the human spine, as these are only active in tension. Under 2 mm anterior shear, an increase in the ROM can be seen after ligamentous injuries. Under 2 mm posterior shear, the magnitude of increase in the ROM is significantly higher than anterior shear. This shows that the posterior articular facets play an important role in resisting anterior shear after ligamentous injuries.

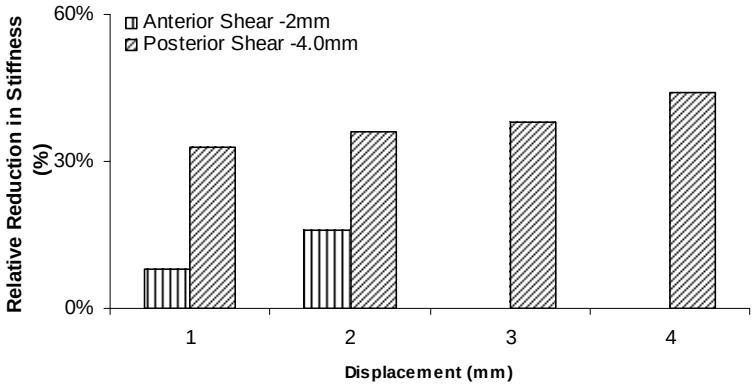

Figure 99: Percentage decrease in stiffness of C4 with respect to C6 from the normal model due to ligamentous injuries under anterior shear and posterior shear.

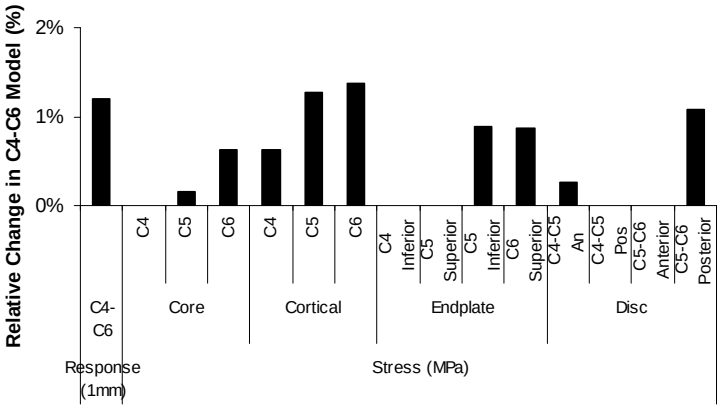

Figure 100: Percentage change in respective spinal components stress due to ligamentous injuries under compression.

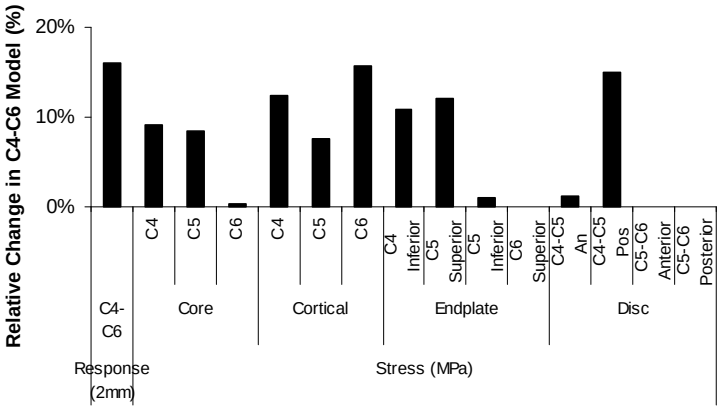

Figure 101: Percentage change in respective spinal components stress due to ligamentous injuries under anterior shear.

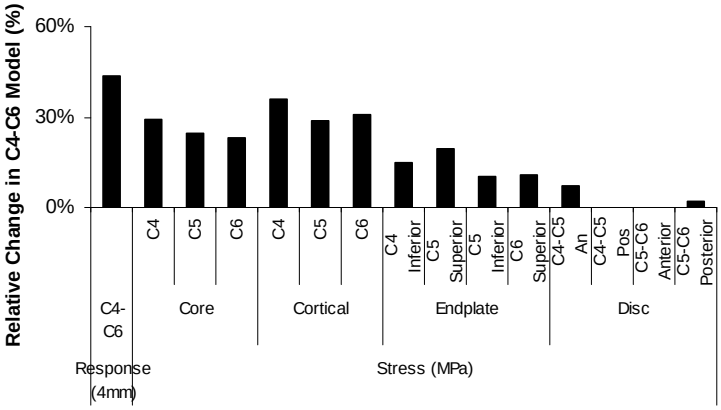

Figure 102: Percentage change in respective spinal components stress due to ligamentous injuries under posterior shear.

5.3.3 Discussion

The author believes that the ligamentous tissues provide a clinical role in the stability of the cervical spine in living subjects. Therefore, the primary objective of this study was to assess the role of ligaments in resisting physiological loads. The significant increases in the cervical spine flexibility after sectioning the ligaments indicated the dominant role of the ligaments in providing stability relates to certain loading modes only. Although comprehensive, the current objective can be better achieved by removing the ligaments belonging to each region (For e.g., anterior longitudinal ligament posterior longitudinal ligament, etc) one at a time or in multiple steps and not removing all in a single step (as carried out in the present study).

This study showed that the ROM of the lower cervical spine after ligamentous injuries increases significantly under flexion, axial rotation, lateral bending and posterior shear but increases mildly under extension and anterior shear. Compression was not affected by the ligamentous injuries. Therefore, where conservative therapy is adopted for this type of injury, treatments for temporary immobilisation of the cervical spine should specifically limit the motions in these directions. If surgical operation is needed, these types of instability can be treated successfully by anterior fixation, which stabilizes the spine in flexion, lateral bending and axial rotation (Richter et al., 1999).

Some authors have already studied the mechanisms of ligamentous injuries to the cervical spine biomechanics under limited loading and injury conditions. Panjabi et al., 1978 found out that if a functional unit has all its anterior elements “plus one” additional posterior structure, or all of its posterior elements “plus one” additional anterior structure, then the functional unit will remain stable in the sagittal plane under

physiological loads. Goel et al., 1984 found the dominant role of the capsular ligaments in flexion, extension, lateral bending and axial rotation of lower human cervical spine segment. Ulrich et al., 1991 found that flexion stability is preserved with posterior ligamentous elements even though the capsular ligaments of the facet joints are severed. Wen et al., 1993 studied the mechanical tolerance and the instability of the cervical spine in some ligamentous injuries showing a significant increase in flexibility after sectioning of some ligamentous structures in certain directions in the intact state. However, it was very difficult to compare previously reported *in vitro* study by Wen et al., because of variations between the applied moments when testing various specimens to failure. For example, the applied moments used in their injury studies vary over a wide range, from 0.3 Nm, up to a maximum of 2 Nm. In our study, in order to obtain consistent readings, a maximum loading of 2 Nm was used.

The injury study was conducted on C5-C6 and C4-C6 as most cervical spine injuries occur at this level. However, the interpretations of these results need to be careful because the neck muscles probably produce additional restrictions, stabilising the cervical spine. The ongoing biological process of healing or biomechanical adaptation after injuries has not been simulated. Thus, these results may only be valid at the time of initial injuries and do not permit a more accurate analysis of delayed instability. Furthermore, this study only assumed total ligamentous resection, but did not take into account the various types of injury patterns suffered by the cervical spine during accidents.

5.4 Summary

This chapter, for the first time, provided the most exhaustive comparison against experimental data. This kind of exhaustive FE comparison studies has never been reported in the literatures. This may be due to the complexity and difficulty of generating FE models based on single cadaveric specimen that are able to compare against such a wide range of *in vitro* experiments. Fortunately, the FE model based on a single cadaveric specimen (geometry comparable to the general population) compared well against the external and internal responses of the data reported in the literatures. Regression analyses were then performed by using a nonlinear equation used to describe the soft tissues. This equation can be used to describe the general biomechanics of the cervical spine FSU. Subsequently, the cervical spine model was used to investigate the influence of ligamentous injuries on the cervical spine biomechanics.

Although these findings were interesting and comprehensive, the modelling and analysis procedures used in this study have some limitations. One major limitation of the present study is the lack of neck muscles in the FE model. It is well known that the cervical spine must maintain mechanical stability in both static and dynamic situations. This stability is composed of the passive stability of the spinal column and active stability provided by the muscles. The current study does not account for the stabilizing role of neck muscles in cervical spinal responses and is only interested in the passive stability of the ligamentous cervical spine. This study only investigated the mechanical factors that may cause segmental instability. The biological response to these mechanical situations must also be investigated to gain a clearer understanding of cervical spine biomechanics. Nevertheless, the significance of this study lies in the successful validation of the FE models under various conditions and the advancement

on the further understanding of the intact and ligamentous injured cervical biomechanics.

Chapter 6. Investigation of Surgical Techniques

6.1 Introduction

Cervical stenosis causes narrowing of the spinal canal, which places additional pressure on the spinal cord. Stenosis often occurs in patients over the age of 50. In these patients, stenosis is the gradual result of aging and "wear and tear" on the spine during everyday activities. As people age, the ligaments of the spine thicken and harden (called calcification). Bones and joints may enlarge, and bone spurs (called osteophytes) may form. When these conditions take place in the spinal area, they can cause the spinal canal to narrow, creating pressure on the spinal nerve. Spinal canal components that contribute to the cervical stenosis include facets, ligamentum flavum, posterior longitudinal ligament, vertebral body and the intervertebral disc. Cervical stenosis may cause pain or numbness. The pain may move from one part of the body to another but is often most noticeable in the neck. Patients experiencing pain or disability from stenosis often develop a less active lifestyle (An, 1998a; Dillin and Simeone, 1998; Eidelson, 2002; Ishida et al., 1989; Whitecloud and Dunsker, 1993).

Severe cases of stenosis often require surgery. Different surgical options are available for the treatment of cervical spinal stenosis: these include anterior approach, posterior approach, and sometimes a combined anterior and posterior approach. Posterior approaches like laminotomy, laminectomy or facetectomy require the removal of tissue from the affected motion segment. Since the operation involves structural changes to the spine, it should be possible to offer biomechanical explanations for these post surgical changes. The goal of the surgery is to relieve pressure on the spinal cord or

spinal nerve by widening the spinal canal. This is done by removing, trimming, or realigning the involved parts that are contributing to the pressure. Surgical procedures of the cervical spine require removal of tissue from the motion segment, for example facetectomy, laminotomy, laminectomy and discectomy. When large amounts of tissue are removed, the stiffness of the motion segment is reduced and the rotational motions increased. To compensate for this decrease in stiffness and increase in rotational motion, which, in addition to creating pain, may present a risk to neurological structures, fusion surgery is sometimes performed. Currently, there is still a clinical controversy about weather a fusion should or should not be performed. The question of whether to fuse or not is very important since fusion procedure increases the morbidity from spinal surgery. Furthermore, when one motion segment is fused the adjacent segments may receive increased stress, placing these segments at risk of future injury. Unfortunately, existing literatures does not provide a clear answer to this.

Saito et al., 1991 used a simplified two dimensional model to study the postlaminectomy deformities. The simulation analyses revealed that the primary cause of postlaminectomy deformity was due to the resection of one or more spinous processes and/or posterior ligaments. However, the deformity of the spine after postlaminectomy was only described using graphical illustrations. There was no mention of the percentage increase in the biomechanical responses due to the laminectomy. Voo et al., 1997 used a two-level segment (C4-C6) model to investigate the biomechanical effects of cervical facetectomy at C5 and C6 levels under sagittal moments. However, the use of linear model limited their accuracy in doing cervical instability studies. Kumaresan et al. 1997 used a human lower cervical spine (C4-C6) model to investigate the biomechanical effects of the cervical laminectomy and bilateral

facetectomy. Laminectomy was performed on C5, and bilateral facetectomy was performed on C5 and C6. The overall stiffness and intervertebral disc stress were obtained for the surgically altered models. However, it was impossible to determine the behaviour of the unaltered neighbouring components realistically using these models. This was due to the loading and boundary conditions applied to the superior surface of C4 and inferior surface of C6. These constraints will induce additional end-effects to the model, and therefore, restrict the applicability of the results. Therefore, the instability simulations of these surgical procedures should be carried out in a model with multiple motion segments to justify the actual *in vivo* behaviour of the cervical spine.

This chapter will attempt to simulate the common clinical procedures used to decompress the spinal canal and determine the influence of these clinical procedures on the biomechanics of the cervical spine on the altered and unaltered motion segments. Four types of clinical situations were evaluated in this section; 1) unilateral and bilateral facetectomy; 2) laminectomy with progressive unilateral and bilateral facetectomy, 3) one/two-level laminotomies and laminectomies, 4) post-surgical laminectomy. The increase in the flexibility of these surgically altered models was evaluated by comparing it against the original model and experimental data.

6.2 Model Refinements

It has been pointed out that the material and geometric properties are the two most important factors in the development of a finite element model of the human cervical spine (Panjabi, 1979). However, before converting to a completely nonlinear and complex model, it was necessary to identify the critical spinal components that will

affect the external responses (stiffness and ROM), and to better define them in the refined model. Since a dimensionally accurate description of the cervical model already exists. Therefore, the first logical step was to conduct material sensitivity studies to identify the critical spinal components that have significant influence on the external responses. Furthermore, material properties of the human cervical spine components reported in the literatures vary drastically depending on the approach, method and specimen preparation (Table 8). This kind of scatter is inherent and varies among different specimens due to age, disease, gender and population. It is neither physically possible nor ethically acceptable to eliminate the scatter of material properties. Furthermore, it is becoming recognised that these uncertainties can cause changes to the biomechanical responses, resulting in an associated degree of uncertainty in the predicted results. Hence, accepting the existence of this scatter and dealing with it is more reasonable and acceptable.

Accordingly, several investigators (Table 9) have studied the effects of material variation of the human spine by varying the modulus of a limited numbers of the spinal components one at a time using a non-statistical approach. However, sensitivity studies of the human cervical spine have not been done comprehensively or systematically, and little attempt was made to assess the sensitivity of the model to variation in input parameters or possible interactions between them. Fortunately, there are also available statistical methods for design analysis, called factorial designs, by which a large number of variables, each of which can assume a range of values, can be analysed much more efficiently than the common approach of varying one at a time while keeping the others fixed (Manson, 1991). In the following sections, two techniques (Full Factorial Analysis and Probabilistic Design Analysis) were employed to understand the influence

of material sensitivity of one or more spinal components on the external responses (ROM and stiffness) and internal stress. Encouraging and important results from the first statistical analysis (factorial analysis) motivated the author to conduct a second and more complicated sensitivity study using Probabilistic Design Analysis. These ensured a better understanding on the important parameters affecting the cervical biomechanical responses and these understanding would translate to a better model definition, giving rise to a more accurate analysis in the subsequent chapters.

Description	**Young's Modulus (MPa) / Poisson's Ratio**				
	Saito et al., 1991	**Maurel et al., 1997**	**Goel and Clausen 1998**	**Kumaresan et al 1999**	**Ng and Teo, 2001**
Hard Tissue					
Cortical bone	10000 / 0.29	12000 / 0.30	10000 / 0.30	10000 / 0.29	10000 / 0.29 *
Cancellous bone	450 / 0.25	100 / 0.20	450 / 0.25	100 / 0.29	100 / 0.29 *
Posterior elements	-	6000 / 0.30	3500 / 0.25	3500 / 0.29	3500 / 0.29 *
Endplate	600 / 0.3	300 / 0.30	2000 / 0.20	500 / 0.40	500 / 0.40 *
Soft Tissue					
Disc – annulus	40 / 0.49	2.5 / 0.45	4.2 / 0.45	3.4 / 0.40	3.4 / 0.40 *
Disc – nucleus	200 / 0.49	-	-	3.4 / 0.49	1.0 / 0.499 *
Fibers	-	110	450	-	-
Ligaments					
Anterior Longitudinal Ligament	-	10	15 – 30	11.9 *	-
Posterior Longitudinal Ligament	-	20	10 – 20	12.5 *	-
Capsular Ligament	-	20	7 – 30	7.7 *	-
Ligamentum Flavum	-	50	5 - 10	2.4 *	-
Interspinous Ligament	-	3	4 – 8	3.4 *	-
Supraspinous Ligament	-	3	4 - 8	3.4 *	-

Table 8: Variation of the material property for the human cervical spine finite element model. * denotes the material properties used in the basic finite element model.

Description	Investigators				
	1984	**1986**	**1991**	**1999**	**2002**
	Shirazhi-ADL et al., 1984	Spilker et al., 1986	Rao and Dumas, 1991	Kumaresan et al ., 1999a	Fagan et al., 2002b
Model	Lumbar Disc Segment	Disc Segment	L5-S1	C4-C6	Lumbar Disc Segment
Type	3-D	3-D	3-D	3-D	3-D
Material sensitivity Study	Basic analysis of disc	Fiber composite annulus	cortical bone, cancellous bone, cartilaginous endplates, nucleus pulposus, ground substance and collagen fibers	Vertebra plus posterior elements, discs, endplates, facets and ligaments considered as a single unit	Disc annulus, Nucleus pulposus, Collagen Fibers
Geometry	Assume-simplified	Assume-simplified	Assume- simplified	Detail	Assume-simplified
Loading	compression	compression, axial rotation, shear, and moment loading	compression	flexion, extension, lateral bending and axial rotation	compressive, flexion and axial rotational

Table 9: Summary of sensitivity studies reported in the literatures.

The second step was to simulate all the structural components accurately. In this study, the digitizer was used to develop the cervical spine model and the model dimensions compared well with the data reported in the literatures (Gilad and Nissan, 1986; Panjabi et al., 1991; Tan et al., 2002; Tan et al., 2004). Nevertheless, the geometrical element idealization of the cervical finite element model was further refined in a subsequent section based on the findings from the material sensitivity studies. These refinements included a more detailed finite element representation of the cortical bone, unconvertebral joints and intervertebral discs.

6.2.1 Material Sensitivity Studies of both Hard and Soft Tissues

6.2.1.1 Factorial Design Analysis

6.2.1.1.1 Methods

Factorial analysis was carried out to determine the influence of six parameters (modulus of cortical shell, vertebral body, posterior elements, endplate, disc annulus and disc nucleus) of the C4-C6 finite element model on the predicted internal and external biomechanical responses under axial compressive loading, anterior, posterior shear (Manson, 1991). The model was created by removing the unnecessary components from the C2-C7 model.

In the current work, the modulus of each spinal component was varied ±20% from the basic and most widely used values reported in the literatures (Table 8). A single full factorial analysis consists of 64 runs (Table 10), totalling 192 runs for the three loading conditions. The loading and boundary conditions were chosen to mimic the experimental study by Shea et al., 1991. For each run, the stiffness and key stress values in the various spinal components at the final loadings were recorded and collected. A total of 2880 output parameters (six factors, three loading conditions, and fifteen output variables) were evaluated. Variation in the modulus of a single spinal component will result in two responses, the lowest and the highest. Data obtained from the highest outputs were then used to normalize against the lowest outputs. The graph (Figure 104) was then formed by stacking up the normalized data of all the spinal components considered in this study under similar loading conditions. A longer bar in the graph means larger effect.

6.2.1.1.2 Results

The computed results from the material sensitivity analysis of the C4-C6 model using the highest/lowest value obtained from the factorial analysis under the three loading types agreed reasonably well with the published experimental data at final loadings (Figure 103). The predicted results showed that the percentage variation due to material

property changes falls within the experimental scatter data reported in the literatures at the final loading. These showed that the different material properties used in the previous FE studies reported in the literatures were still within the acceptable range, in terms of predicting the stiffness. Figure 104 showed that changes in the disc annulus modulus have the largest influence on the stiffness under the three loading types. Changing the posterior element modulus also influenced the stiffness of the cervical spine under compression and anterior shear only. Generally, variations in the spinal components modulus (Figure 105 - Figure 107) had a significant impact on the respective component stress. Overall, changes in the disc annulus modulus affect the disc annulus stress and the stress of its neighbouring components.

Runs	Pattern	Modulus (MPa)					
		Core	Cortical Shell	Endplate	Posterior Elements	Disc Annulus	Disc Nucleus
1	-++---	80	12000	600	2800	2.72	0.8
2	+++-++	120	12000	600	2800	4.08	1.2
3	--+--+	80	8000	600	2800	2.72	1.2
4	+-----	120	8000	400	2800	2.72	0.8
5	-++-+-	80	12000	600	2800	4.08	0.8
6	-++-++	80	12000	600	2800	4.08	1.2
7	++-+++	120	12000	400	4200	4.08	1.2
8	-+++-+	80	12000	600	4200	2.72	1.2
9	-----+	80	8000	400	2800	2.72	1.2
10	+-++++	120	8000	600	4200	4.08	1.2
11	-+-++-	80	12000	400	4200	4.08	0.8
12	+-+---	120	8000	600	2800	2.72	0.8
13	---+-+	80	8000	400	4200	2.72	1.2
14	--+-++	80	8000	600	2800	4.08	1.2
15	--++++	80	8000	600	4200	4.08	1.2
16	-++++-	80	12000	600	4200	4.08	0.8
17	++++++	120	12000	600	4200	4.08	1.2
18	++++--	120	12000	600	4200	2.72	0.8
19	-+---+	80	12000	400	2800	2.72	1.2
20	-++--+	80	12000	600	2800	2.72	1.2
21	+-++--	120	8000	600	4200	2.72	0.8
22	+-+--+	120	8000	600	2800	2.72	1.2
23	-+-+++	80	12000	400	4200	4.08	1.2
24	++++-+	120	12000	600	4200	2.72	1.2
25	-+-+--	80	12000	400	4200	2.72	0.8
26	--+-+-	80	8000	600	2800	4.08	0.8
27	+----+	120	8000	400	2800	2.72	1.2
28	++-++-	120	12000	400	4200	4.08	0.8
29	+-+++-	120	8000	600	4200	4.08	0.8
30	++----	120	12000	400	2800	2.72	0.8
31	+--+++	120	8000	400	4200	4.08	1.2
32	------	80	8000	400	2800	2.72	0.8
33	++-+-+	120	12000	400	4200	2.72	1.2
34	+--+--	120	8000	400	4200	2.72	0.8
35	+-+-+-	120	8000	600	2800	4.08	0.8
36	+-+-++	120	8000	600	2800	4.08	1.2
37	++--++	120	12000	400	2800	4.08	1.2
38	--++--	80	8000	600	4200	2.72	0.8
39	+-++-+	120	8000	600	4200	2.72	1.2
40	--++-+	80	8000	600	4200	2.72	1.2
41	-+----	80	12000	400	2800	2.72	0.8
42	---++-	80	8000	400	4200	4.08	0.8
43	-+--+-	80	12000	400	2800	4.08	0.8
44	---+--	80	8000	400	4200	2.72	0.8
45	----++	80	8000	400	2800	4.08	1.2
46	+---++	120	8000	400	2800	4.08	1.2
47	----+-	80	8000	400	2800	4.08	0.8
48	-+--++	80	12000	400	2800	4.08	1.2
49	-+++--	80	12000	600	4200	2.72	0.8
50	---+++	80	8000	400	4200	4.08	1.2
51	+++-+-	120	12000	600	2800	4.08	0.8
52	+++--+	120	12000	600	2800	2.72	1.2
53	++---+	120	12000	400	2800	2.72	1.2
54	--+---	80	8000	600	2800	2.72	0.8
55	--+++-	80	8000	600	4200	4.08	0.8
56	+---+-	120	8000	400	2800	4.08	0.8
57	+--++-	120	8000	400	4200	4.08	0.8
58	-+++++	80	12000	600	4200	4.08	1.2
59	++-+--	120	12000	400	4200	2.72	0.8
60	+++---	120	12000	600	2800	2.72	0.8
61	-+-+-+	80	12000	400	4200	2.72	1.2
62	++--+-	120	12000	400	2800	4.08	0.8
63	+++++-	120	12000	600	4200	4.08	0.8
64	+--+-+	120	8000	400	4200	2.72	1.2

Table 10: Factorial analysis of the six critical spinal components evaluated in the present study. + denotes high value, - denotes low value.

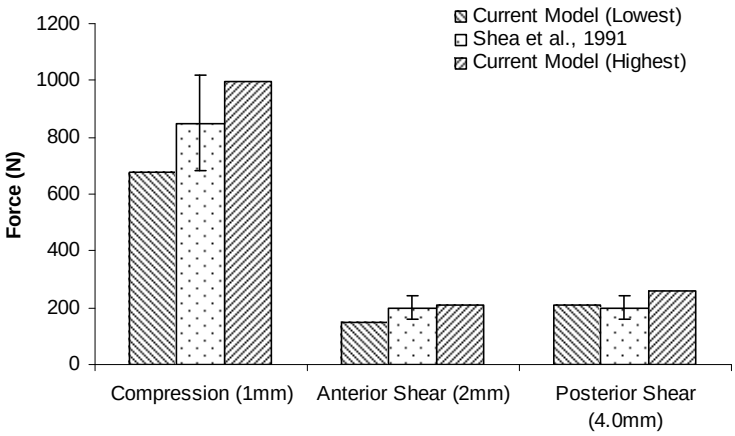

Figure 103: Comparison of finite element model responses using the highest value and lowest value obtained from factorial analysis with experimental values at final loading under axial compressive loading, anterior and posterior shear.

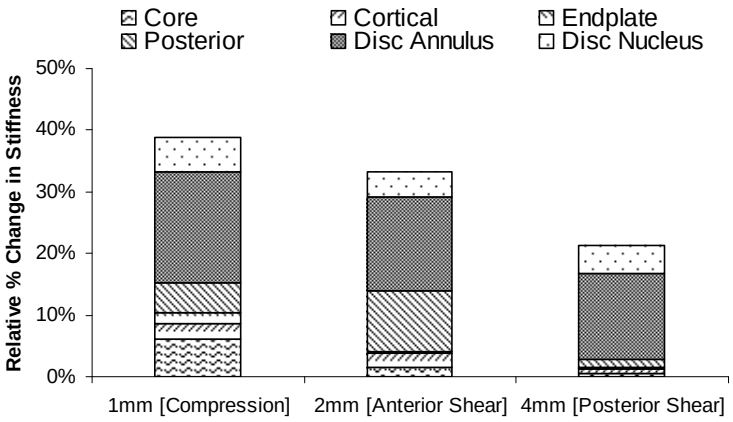

Figure 104: Relative percentage change of the C4-C6 force/displacement due to material variations. (A longer bar means larger effect).

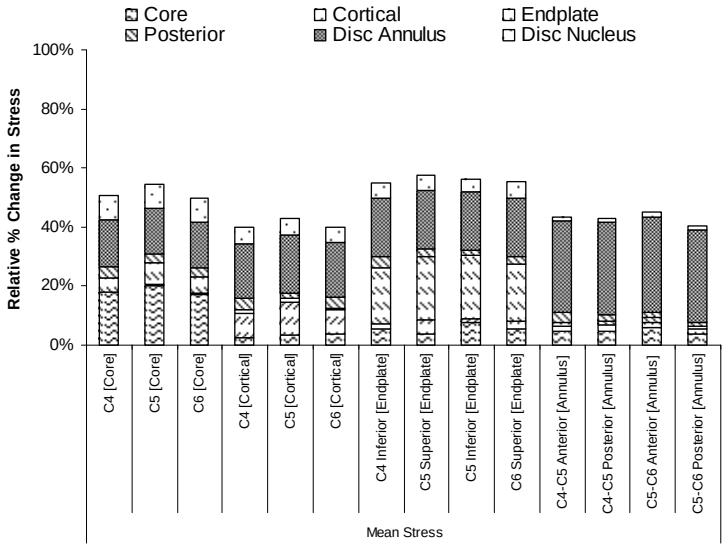

Figure 105: Relative percentage change of C4-C6 stress to material variations under compression. (A longer bar means larger effect).

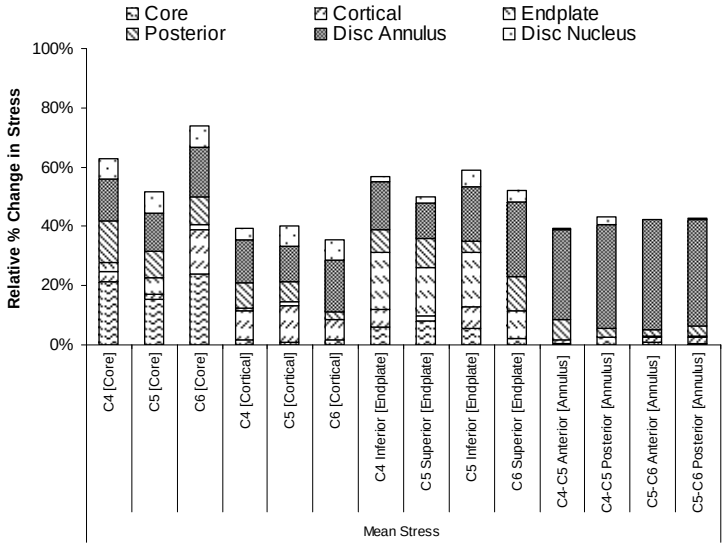

Figure 106: Relative percentage change of the C4-C6 stress due to material variations under anterior shear. (A longer bar means larger effect)

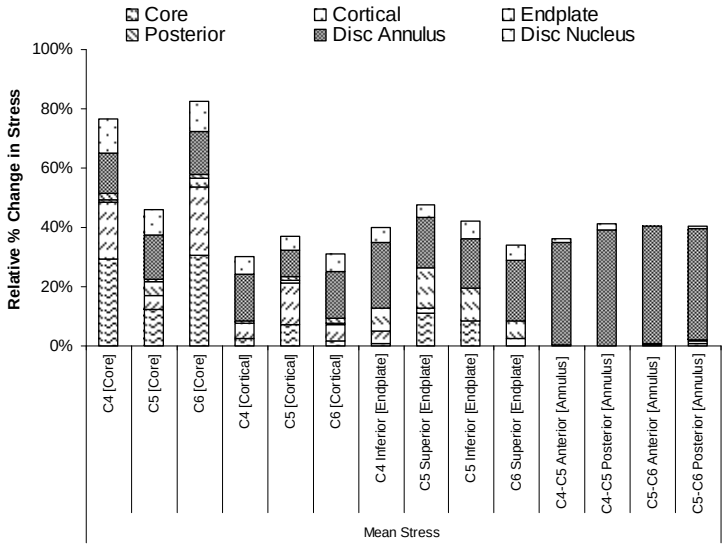

Figure 107: Relative percentage change of the C4-C6 stress due to material variations under posterior shear. (A longer bar means larger effect)

6.2.1.1.3 Discussion

A sensitivity study based on engineering statistical approach was used to determine the effects of variations in the material properties of the spinal components on the external and internal responses of the of C4-C5-C6 finite element model under three loading conditions. The methodology and results underscored the importance of material variations of multiple parameters. The author believes that this is the first study to incorporate a factorial analysis to understand the influence of material properties changes of two or more spinal components on the biomechanical responses and stress. This approach also allows the delineation on the effects of an individual factor on the biomechanical responses (Figure 104).

Variation of the material properties of the cortical bone revealed its negligible influence in the responses under the three loadings. This can be related to the fact that the cortical bone was the stiffest material used in the finite element model. This study showed that the cancellous bone exerts some influence under compression, secondary only to the

disc annulus while the effects of varying endplate show negligible influences. This demonstrated that although the endplates were relatively soft when compared to the bone, they were relatively stiffer than the adjacent disc annulus. Varying the material properties of the posterior structures played a mild role in affecting the stiffness under compression and anterior shear. This demonstrated the influence of the facets joints in the load transfer under these two loading modes Apart from material variation in facets contribution to cervical spine stability, the importance of geometrical parameters like dimensions of the facets in resisting physiological loads cannot be neglected as well.

The findings showed that changes in the material properties of the disc-annulus have the highest influence on the force-displacement response of the cervical spine under the three loads considered. The stiffness of the cervical spine segment increases with increase in the Young's modulus. In the presence of a nearly incompressible disc nucleus modelled using a Poisson ratio of 0.499, the stiffening behaviour becomes more evident. Furthermore, an increase in displacement causes the transverse bulge to increase, thus resulting in an increase in the collagen fibers tensile resistance. This becomes very prominent under compression, and to a lesser extent, under anterior and posterior shear as displayed in the results which showed that the differences due to material changes was highest under compression, followed by anterior and posterior shear (although different displacement is applied to the model). Material properties variation of the disc nucleus showed a slight difference in the predicted results under all modes of loading. It was well known that the disc nucleus is entrapped in the annulus and changes to the material properties should not alter the overall response significantly.

In the area of lumbar spine investigation, Keller et al., 1989 conducted an experiment on twelve lumbar vertebral segments to determine the compressive mechanical properties of the human lumbar vertebral trabecular bone on the basis of anatomic origin, bone density and intervertebral disc properties. The results showed that the trabecular bone compressive strength and stiffness increase with increasing bone density (elastic modulus). The results also suggested that interdependency of the trabecular bone and intervertebral disc properties may exist. Their findings showed close correlation with our analytical results, which clearly demonstrated a higher cancellous core modulus leading to higher compressive responses (Figure 104). Furthermore, the present results showed that increasing the disc annulus modulus also lead to an increase in the bony structures stress. The increase in the neighbouring spinal stress may have enhanced stress-related remodelling, resulting in overgrowths of osteophytes. This phenomenon is further investigated in Chapter 7. Investigation of Disc Degeneration.

Overall, the results showed that variations in the disc annulus have a significant effect on both the external biomechanical responses and internal stress of the disc itself and neighbouring hard tissues. Material variations in the hard tissues generally affect only the primary spinal components and have insignificant impact on the neighbouring hard and soft tissues. The current results correlated well with the literature data reported on the human lumbar spine and human cervical spine studies but extended it further by including additional modes of loading which have never been published (Kumaresan et al., 1999a; Rao and Dumas, 1991).

Due to the interesting findings obtained from the current study, another more in-depth study using probabilistic design analysis method was conducted to understand the influence of these parameters.

6.2.1.2 Probabilistic Design Analysis

6.2.1.2.2 Methods

In the current section, Probabilistic Design System based on Monte Carlo Simulation methods using Latin Hypercube Sampling (LHS) techniques available in ANSYS 7.0 (SAS IP, Inc., Canonsburg, USA) was used to analyze the material sensitivity of C4-C6 cervical spine model involving thirteen uncertain input parameters. These input parameters consisted of material properties of varies spinal components. The variations of these input parameters (Table 11) were defined as random input variables and were characterized by triangular distribution type and by their distribution parameters (mean values, standard deviation, etc.

For the random input variables (Young's modulus of various spinal component), a triangular statistical distribution function was used to describe its randomness as well as the parameters of the distribution function. Three values were used for each input variables, the minimum value x_{min} (50%-80% of the basic value), the most likely value limit x_{mlv} (basic value) and the maximum value x_{max} (120%-150% of the basic value). For cortical shell, cancellous core, posterior structure, endplate, disc annulus and nucleus pulposus, ±20% from the basic value. For all ligaments and annulus fibers, values chosen were ±50% from the basic value.

Name	Type	Young's Modulus (MPa)			
		Minimum	Basic	Maximum	Standard Deviation
Hard Tissue					
Cancellous	Triangular	80	100	120	8.199
Cortical	Triangular	8000	10000	12000	819.600
Endplate	Triangular	400	500	600	40.860
Posterior	Triangular	2800	3500	4200	286.900
Soft Tissue					
Disc Annulus	Triangular	2.72	3.4	4.08	0.279
Disc Nucleus	Triangular	0.8	1	1.2	0.082
Annulus Fibers	Triangular	225	450	675	91.970
Ligament					
Anterior Longitudinal	Triangular	5.95	11.9	17.85	2.435
Posterior Longitudinal	Triangular	6.25	12.5	18.75	2.563
Capsular	Triangular	3.85	7.7	11.55	1.573
Ligamentum Flavum	Triangular	1.2	2.4	3.6	0.491
Interspinous	Triangular	2.72	3.4	4.08	0.279
Supraspinous	Triangular	2.72	3.4	4.08	0.279

Table 11: Input variables of the thirteen spinal components evaluated.

During a probabilistic analysis, the model underwent multiple iterations to compute the random output parameters as a function of the set of random input variables. The values for the input variables were generated randomly (using Monte Carlo simulation).

The loading types and range of values were as follows: flexion, extension, lateral bending and axial rotation, 0 to 1.8 Nm. These loading values were chosen based on the typical values used in the validation studies. The inferior body of C6 was fixed in all direction of movements. For each case, ROM at various spinal components was

recorded after each load step. However, only the ROM at the final load step was presented here. A single probabilistic analysis for each loading type consists of 140 runs, totalling 980 runs for the four loading conditions.

6.2.1.2.3 Results

As the probabilistic design analysis is capable of capturing many types of results, only the ROM under maximum loading for each loading type is presented here. The evaluation of the probabilistic sensitivities was based on the correlation coefficients between all random input variables and a particular random output parameter. Spearman rank order correlation coefficients based on 95% confidence level are used in these series of results. To plot the sensitivities of a certain random output parameter, the random input variables were separated into two groups: significant (important) and insignificant (not important). Using a lower confidence level will increase the number of significant factors. Throughout the seven types of loading carried out, only the disc annulus has the most significant impact (Table 12).

Out\Inp	Core	Cortical	Endplate	Posterior	Disc Annulus	Disc Nucleus	ALL	PLL	CL	LF	ISL	SSL	AF
Flexion	0.14	0.07	-0.17	0.01	**-0.78**	-0.08	0.04	-0.04	**-0.55**	0.05	**-0.29**	-0.02	**-0.38**
Extension	0.06	0.04	-0.15	0.06	**0.61**	0.11	0.07	0.07	**0.19**	-0.01	-0.03	-0.08	**0.67**
Lateral Bending	0.12	-0.03	-0.01	0.04	**0.69**	0.07	0.02	-0.03	**0.40**	-0.16	-0.10	0.09	**0.63**
Axial Rotation	0.07	-0.05	-0.12	0.06	**0.54**	**0.19**	0.10	-0.09	**0.29**	0.01	0.02	**-0.21**	**0.77**

Table 12: Spearman Rank Order Correlation Coefficients between input variables and the ROM. Values in bold denotes significant input factors at 95% confidence level. (ALL is anterior longitudinal ligaments, PLL is posterior longitudinal ligaments, CL is capsular ligaments, LF is ligamentum flavum, ISL is interspinous ligaments, SSL is Supraspinous ligaments, AF is annular fibers).

6.2.1.2.4 Discussion

In the probabilistic design analysis, the overall results showed the soft tissues have a higher influence on the cervical ROM than the hard tissues. Among the soft tissues, the disc annulus modulus has the highest influence for all loads modes (flexion, extension, lateral bending and axial rotation). The magnitudes of influences on the ROM for the remaining soft tissues differ, depending on the loading modes. Among the loading modes, the influence of disc annulus on the ROM was the highest under flexion, followed by lateral bending, extension and finally axial rotation. Although structurally different from the lumbar spine intervertebral disc, the results indicated that the cervical spine intervertebral disc plays an equally important role in the spinal stability, similar to those reported for the lumbar spine.

The nucleus pulposus was defined as an incompressible solid element in the current model (Poisson's ratio equal to 0.499, lowest modulus is 0.8 MPa and highest modulus is 1.2 MPa). Its presence has a very significant effect on the C4-C6 ROM. The results demonstrated that the nucleus pulposus has the highest influence on the ROM under axial rotation, followed by extension, flexion and lateral bending. Apart from material sensitivity of the disc nucleus, the geometrical influence of disc nucleus had been demonstrated in other experimental and finite element studies of intact and denucleated intervertebral discs (Shirazi-Adl et al., 1984).

The annulus fiber has a rather significant effect on the ROM that is higher or comparable to disc annulus under flexion, extension, lateral bending and axial rotation. Rao and Dumas, 1991 reported similar findings for the lumbar spine in compression, flexion, and extension. Some earlier papers reported in the literature showed higher influence of the annulus fibers under higher applied compressive displacements

(Shirazi-Adl et al., 1984; Ueno and Liu, 1987). This is due to the strengthening of the stiffness of the annulus fiber of the lumbar spine at higher loads. Furthermore, the annulus fiber orientation in the cervical spine is also different from the lumbar spine.

Overall, the combined effects of all the cervical ligaments on the ROM under the flexion, extension, lateral bending and axial rotation are enormous. The correlation coefficients are almost equal to or slightly less than the disc annulus. However, not all ligaments contribute equally to the cervical spinal stability. Furthermore, some ligaments only contributed under certain loading modes. The inter-spinous ligament has some effect under flexion. Anterior longitudinal ligaments and posterior longitudinal ligament have negligible impact on the ROM. Ligamentum flavum has some influence on the ROM under lateral bending. Capsular ligaments have a large influence under all loading modes considered in this study.

6.2.1.3 Summary

Two approaches (Full Factorial Analysis and Probabilistic Design Analysis) were used independently to explore the material sensitivity of the cervical spine. However, these methods were computationally very expensive, as a large number of models have to be analyzed (due to large number of input variables, each having an associated uncertainty). However, using the two approaches together enabled the main factors to be identified first using Factorial Analysis and then only the uncertainty in these has to be modelled using Probabilistic Design Analysis. Nevertheless, the current study has demonstrated the feasibility of using the systematic statistical approach, which should result in more realistic modelling of the human cervical spine and better assessment of the sensitivity of the cervical spine model to the input parameters.

In 1999, Kumaresan et al., investigated the material sensitivity of the cervical spine by varying the modulus of the ligaments as a single unit and exercised the linear model under physiological conditions. Their results revealed the important role of the ligaments in maintaining stability. All these studies clearly underscore the need to accurately model and study the effect of individual ligament due to material variations. Therefore, we conducted a study to understand the roles of individual ligament due to material variation. The material property variations considered in this study consisted of material variations for all the spinal ligaments in the lower cervical spine as well as the hard tissues and intervertebral disc.

A limitation of these studies were due to the insufficient values chosen for variability of input parameters, where range of the minimum and maximum values chosen for the sensitivity study are less than those found in literatures. Because of this reduced range, the study cannot represent the wide variation of parameters among individuals. Therefore there may be present a real risk of bias in the conclusions drawn for the study, with some parameters which may be considered of small importance only because their values do not change enough (for example, disc annulus, disc nucleus or ligaments).

It was also known that the vertebrae strength decreases with age. The decrease in the vertebrae strength is due to the reduction in the bone mineral content (Figure 108). The bone mineral content is then divided by the area to calculate the bone mineral density or BMD. Assuming a constant area, a reduction in the bone mineral content will decrease the bone mineral density. The elastic modulus of the vertebra can then be computed from the bone mineral density using the following empirical equation developed by Carter and Hayes (Carter and Hayes, 1977).

$$E = 3790\, e^{0.06} r^{3} \qquad \textbf{Equation 8}$$

for $0.001 \leq \varepsilon \leq 10.0\ s^{-1}$, $0.20 \leq \rho \leq 0.50\ g\ cm^{-3}$, where E is the elastic modulus (MPa), ε is the strain rate (assumed to be 0.01 for the entire bone) and ρ is the bone mineral density for the human trabecular bone (Lanyon et al., 1975). There are two major types of bone in the cervical spine, cancellous bone (also known as trabecular bone) and cortical bone. Using the equation described above, the cancellous bone modulus ranged from 25MPa to 360MPa. The cancellous modulus is affected by two events, osteoporosis and aging. Furthermore, osteoporosis is present in many pathological conditions and is commonly found in bedridden or elderly patients. In all types of osteoporosis, the bone becomes thin and sparse (Carter and Hayes, 1977). Under either of these conditions, the bone modulus decreases. Therefore, decreasing the elastic modulus of the vertebrae structures of the cervical spine used in the current FE model can effectively simulate old age or osteoporosis. However, the influence of osteoporosis due to reduced vertebral body modulus on the cervical FSU ROM remains unknown.

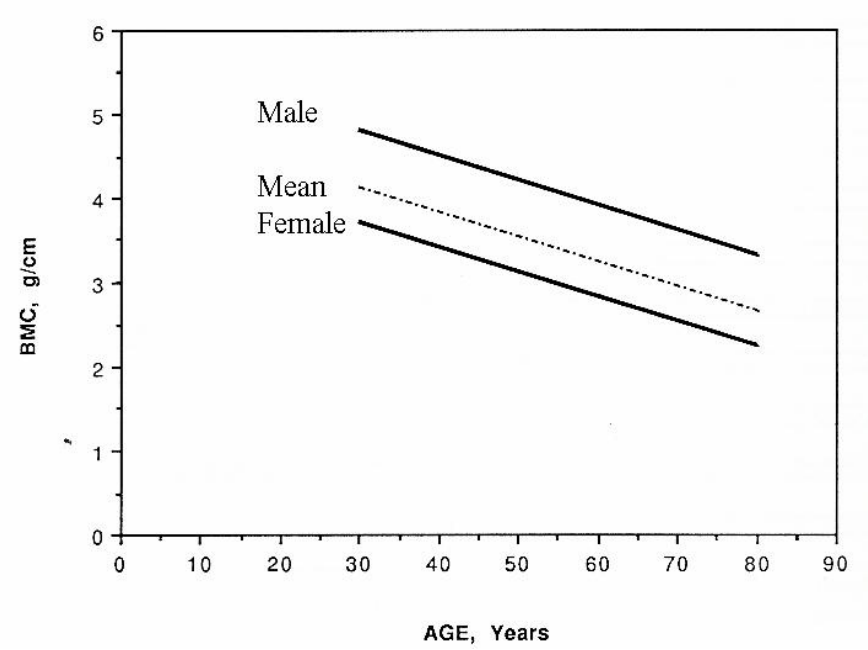

Figure 108: Bone mineral content versus age (White and Panjabi, 1990).

Nevertheless, this study has demonstrated a systematic approach of using statistical methods to study the material sensitivity of the cervical spinal components. Generally, variation of the material properties of the disc annulus has the highest influence on both the external responses and internal stress of the disc annulus and its neighbouring hard bones.

6.2.2 Geometry Refinements

6.2.2.1 Cortical Bone

The vertebral body played an important role in the spinal stability. Therefore, it was important to model the thickness of the cortical shell accurately. In previous studies, cortical bone thickness of 1 mm was used to construct the finite element models and was consistent with the cervical models reported in the literatures (Goel and Clausen, 1998; Maurel et al., 1997; Yoganandan et al., 1996b). However, recent quantitative measurements by Panjabi et al., 2001a showed that the cortical bone thickness of the

cervical spine was 0.5 mm, instead of 1 mm. Therefore, the current model using 1 mm cortical bone thickness was modified (Figure 109) to reflect the new dimensions.

a) 1.0 mm b) 0.5 mm

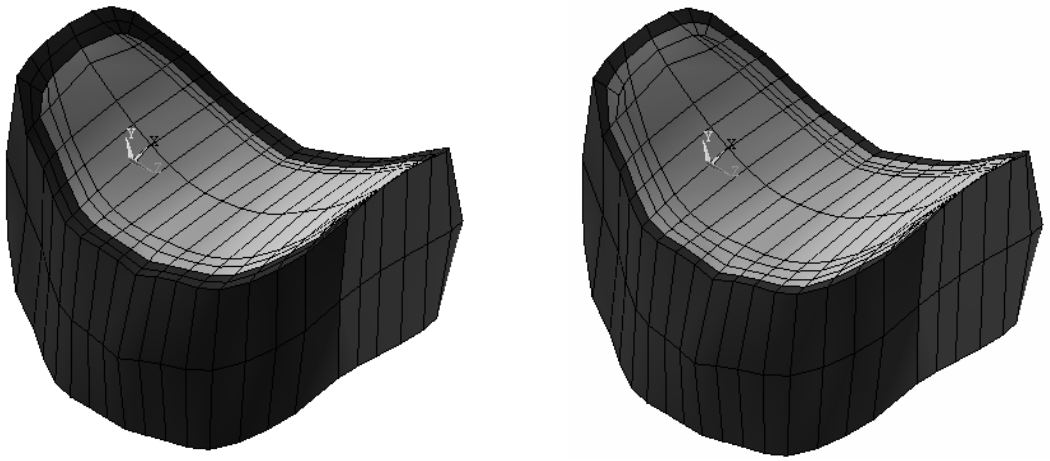

Figure 109: Illustration of the various cortical bone thicknesses. a) 1.0 mm, b) 0.5 mm

6.2.2.2 Unconvertebral Joint

The unconvertebral joints are located in the vertebral body-disc-vertebral body medium, from C2 to T1 (Refer Chapter 2.2.3.1.2 Unconvertebral Joints). Previously, geometries of the unconvertebral joints were included during the development of the finite element model from the dry vertebrae. The intervertebral disc was then formed between the vertebrae by connecting the disc to the adjacent superior and inferior surface of the vertebrae body (reaching the edges of the uncinate processes as well). Goel and Clausen, 1998 have used approaches similar to those used for the facet joints (gap elements), in simulating the articular contacts of the unconvertebral joints. The results indicated slightly lower ranges of rotational motions when compared to the normal model (without the gap elements) under all loading modes (flexion, extension, lateral bending and axial rotation). As the earlier study was not related to the influence of uncinate processes and to save computational time, gap elements were not included to

simulate the potential contact of the uncinate process of the inferior vertebral body (say C4) with the superior vertebral body (say C5).

Therefore, the current model was modified to include unconvertebral joints, modelled within the disc annulus by bordering the lateral edges of the inferior vertebral body, the corresponding superior vertebral body and medially by the outer layer of the lateral circumference of disc annulus (Figure 110). Figure 111 shows the schematic diagram of the idealized joints. The dimensions of the refined FE model with the unconvertebral joints was compared (Figure 112) against the experimental measurements (Yoganandan et al., 2001). Generally, the unconvertebral geometry of the FE model is close with the data reported in the literatures.

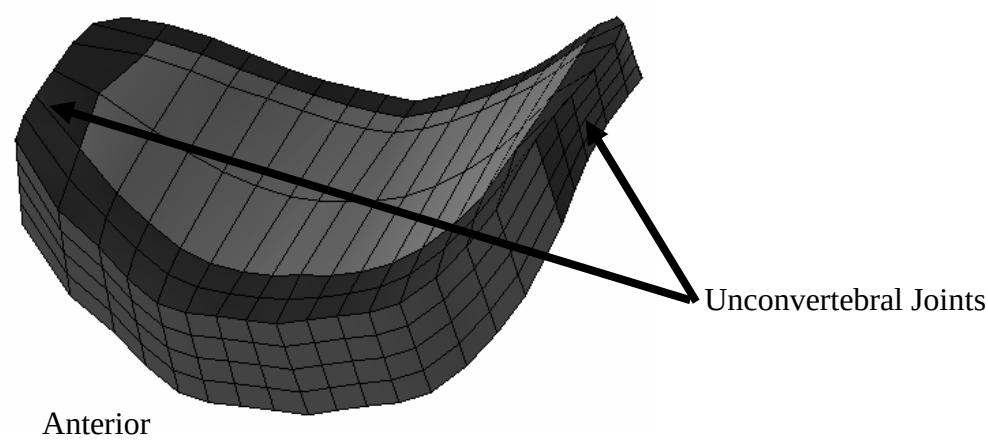

Figure 110: C5-C6 intervertebral disc with unconvertebral joints located bilaterally.

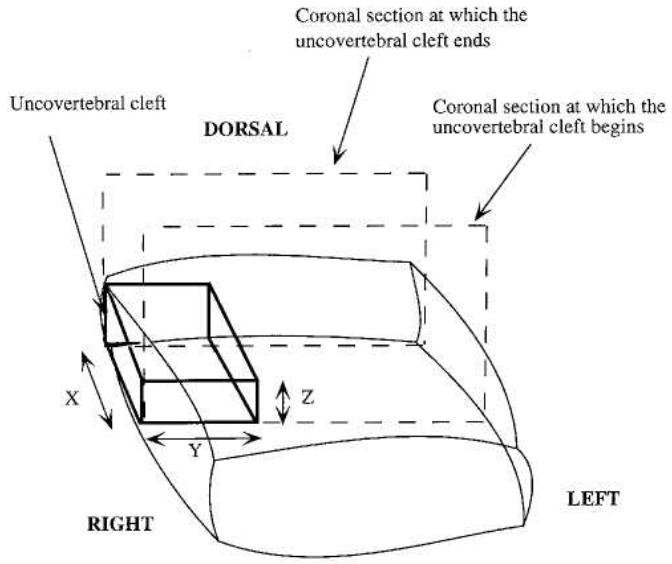

Figure 111: Schematic of the idealized unconvertebral joint (Yoganandan et al., 2001).

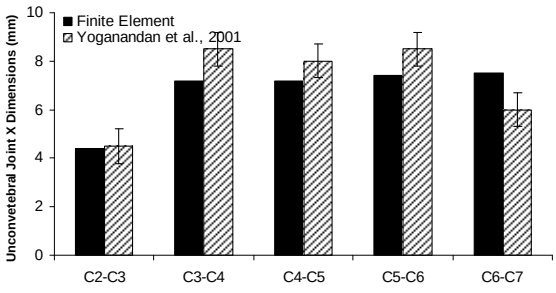

a)

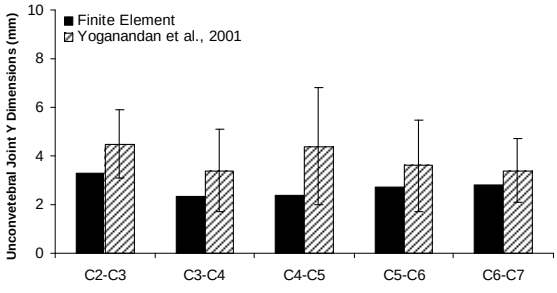

b)

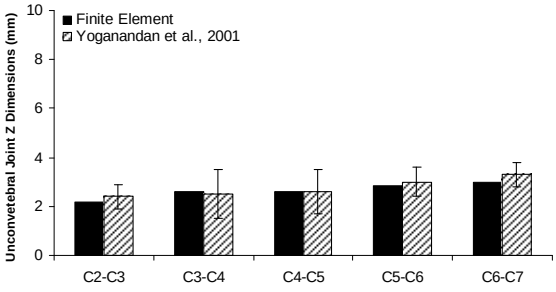

c)

Figure 112: Unconvertebral joint dimensions in a) x directions, b) y directions and c) z directions.

6.2.2.3 Intervertebral Disc

Currently, all the cervical spine models reported in the literatures simulated the cervical disc as a ring of ground substance enclosing the disc nucleus (Refer Chapter 3. Review on Biomechanical Models). However, a micro-dissection and qualitative study performed recently showed that the morphology of cervical intervertebral disc (Figure 113) is more like a crescentic anterior ligament (thicker anteriorly and thinner posteriorly) than a ring of fibers surrounding the nucleus pulposus (Mercer and Bogduk, 1999). The current model was redefined (Figure 114) to incorporate the new disc structure, the most important component bearing the biomechanical features of an FSU (Panjabi & White, 1990). Thus, a more realistic prediction of biomechanical behaviour of the cervical spine could be expected from the current model.

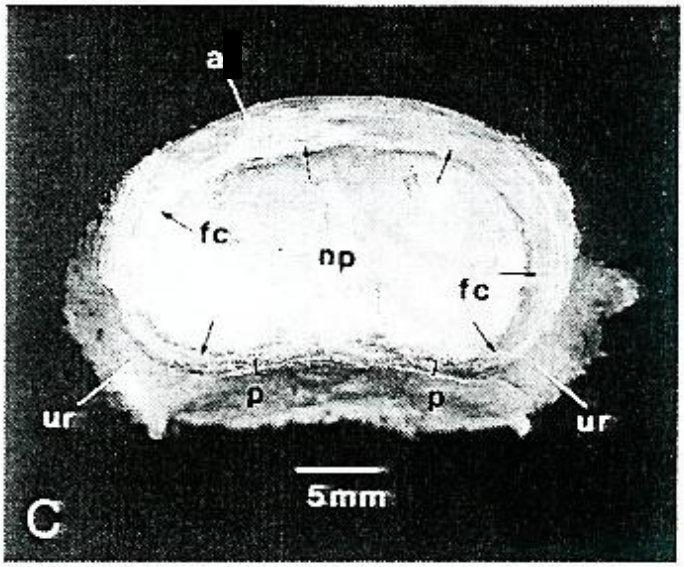

Figure 113: Photographs showing the top view of a 39-year old disc. The disc annulus (a & p), uncinate region (ur), nucleus pulposus (np) and fibrosus cartilage (fc) (Mercer and Bogduk, 1999).

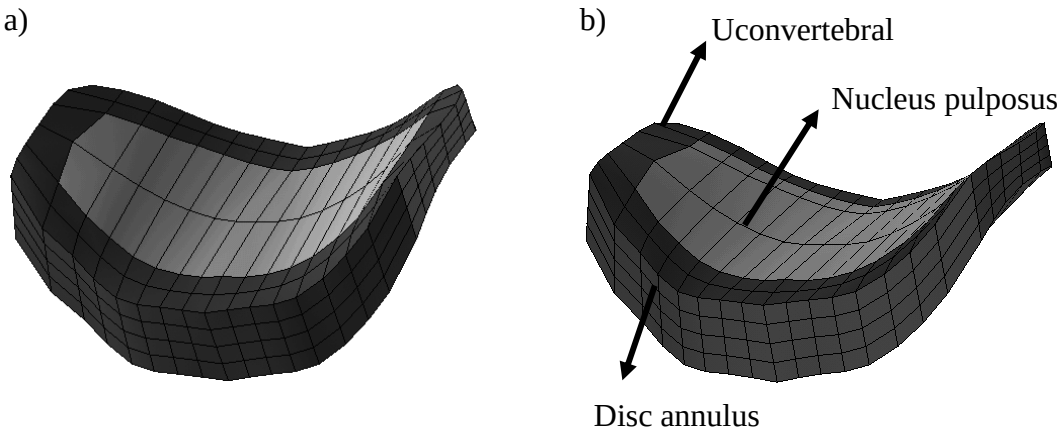

Figure 114: Finite element model of the cervical intervertebral disc. a) old model, b) refined model.

6.2.3 Material Refinements

6.2.3.1 Nonlinear Ligaments

Ligaments are uniaxial structures that resist only tensile or distractive forces (Figure 115). Table 13 shows a summary of the recent approaches used in modelling of the human cervical spine ligaments. Various assumptions have been used for simulating the cervical ligaments. Spring elements use a force-deflection curve or stiffness as material property input, whereas cable and membrane element uses a stress-strain curve or modulus of elasticity as the input. As a first step, only linear material properties simulated with tension only cable elements were used in the earlier chapters to describe the behaviour of the cervical ligaments and these element idealizations were consistent with the studies reported in the literatures. However, since ligaments are sensitive interconnecting structures and plays an important role in maintaining cervical spinal stability (Chapter 5. Validation and Ligamentous Injury Studies). Therefore, it is important to incorporate their complex characteristics into the refined finite element model.

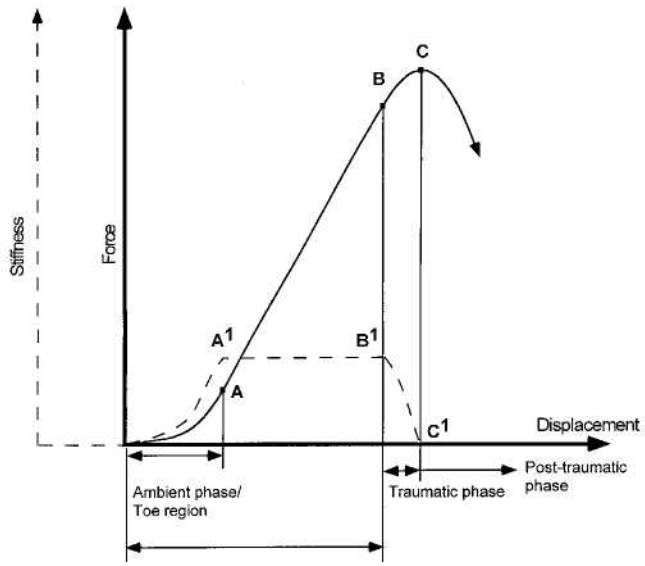

Figure 115: Typical force-displacement (solid line) and stiffness displacement (dotted line) responses of a ligament. Non-linearity in the force-displacement behaviour is apparent (White and Panjabi, 1990).

In this study, material properties of the ligaments for the refined model were adopted from *in vitro* studies conducted by Yoganandan et al., 2000. In this study, nonlinear spring elements were chosen to simulate the force-deflection data obtained *in situ*. Verification tests using spring elements were conducted to test the accuracy and effectiveness of the element in simulating the cervical ligaments. The spring was fixed in all directions of movement at the bottom and a tensile displacement was applied to the top incrementally. The reaction force at the bottom was obtained (Figure 116 - Figure 117) and compared against *in vitro* data. Generally, the predicted results compared well with the experimental data. This showed that the use of nonlinear spring element can effectively simulate the nonlinear characteristics of the cervical ligaments.

Author	Ligaments	Element Type	Material properties
Saito et al., 1991	ALL, PLL, ISL, SSL, LF	Two dimensional linear triangular	Same properties for all ligaments: Tension, E: 170 – 185 MPa, υ: 0.36 and compression, E: 1.0 MPa, υ: 0.45
Kumaresan et al., 1997b	ALL, PLL, CL, LF, ISL	Linear cable	E (MPa) – ALL: 54.5, PLL: 30, LF: 1.5, CL: 1.5, ISL: 1.5
Voo et al., 1997	ALL, PLL, CL, LF, ISL	Linear cable	E (MPa) – ALL: 54.5, PLL: 30, LF: 1.5, CL: 2.0, ISL: 1.5
Maurel et al., 1997	ALL, PLL, CL, LF, ISL, SSL	Linear Cable	E (MPa) – ALL: 10, PLL: 20, LF: 50, CL: 20, ISL: 3, SSL: 3
Goel and Clausen, 1998	ALL, PLL, CL, LF, ISL	Bi-Linear Cable	E (MPa) – ALL: 15(<12%) 30(>12%), PLL: 10(<12%) 20(>12%), LF: 5(<25%) 10(>25%), CL: 7(<12%) 30(>12%), ISL: 4(20-40%) 8(>40%)
Maiman et al., 1999	ALL, PLL, CL, LF, ISL	Linear Cable	E (MPa) – ALL: 11.9, PLL: 12.5, LF: 2.4, CL: 7.7, ISL: 3.4
Natarajan et al., 1999	ALL, PLL, CL, LF, ISL	Bi-Linear Cable	E (MPa) – ALL: 15(<12%) 30(>12%), PLL: 10(<12%) 20(>12%), LF: 5(<25%) 10(>25%), CL: 7(<12%) 30(>12%), ISL: 4(20-40%) 8(>40%)
Chen et al., 2001	ALL, PLL, CL, LF, ISL	Bi-Linear Cable	E (MPa) at 0.3 strain – ALL: 7, PLL: 13, LF: 1.5, CL: 1.5, ISL: 1.5

Table 13: Summary of recent finite element models with cervical spinal ligaments

C2-C5

Anterior Longitudinal

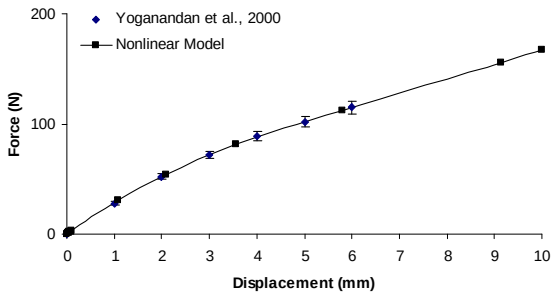

Posterior Longitudinal

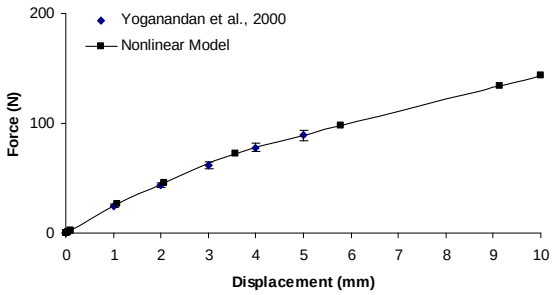

Capsular

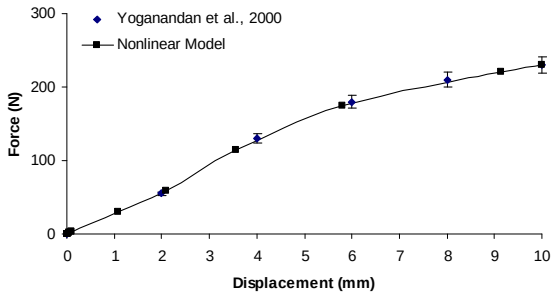

Ligamentum Flavum

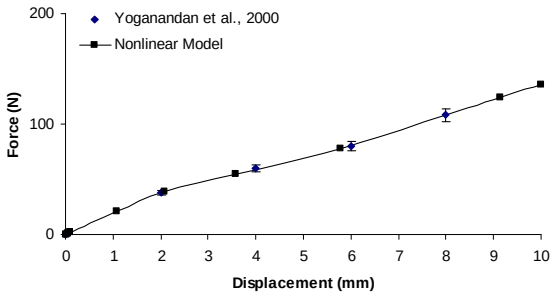

Interspinous

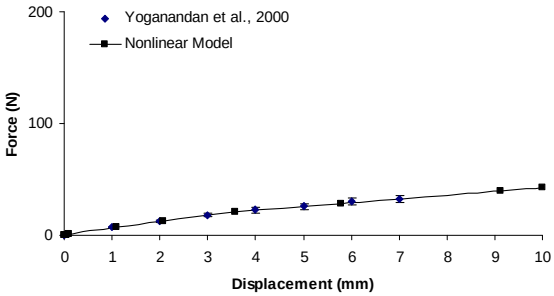

Figure 116: Validation of C2-C5 ligaments against *in vitro* data (Yoganandan et al., 2000).

C5-C7

Anterior Longitudinal

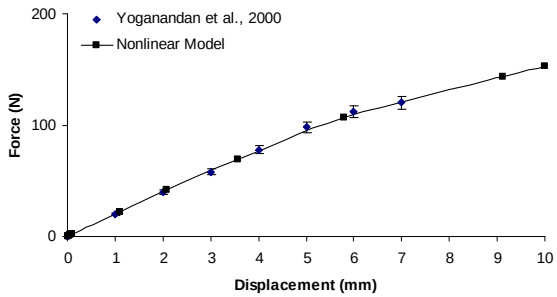

Posterior Longitudinal

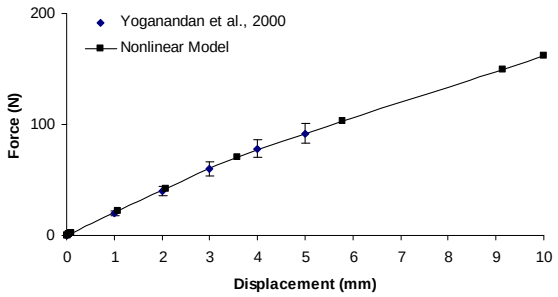

Capsular

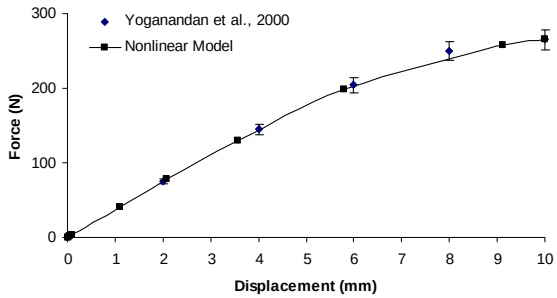

Ligamentum Flavum

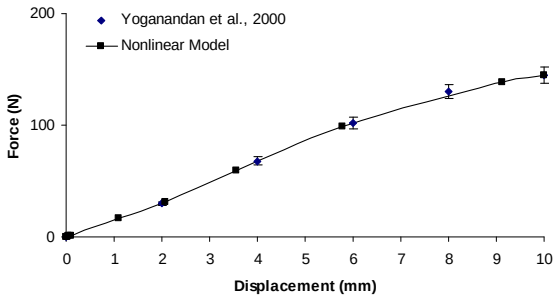

Interspinous

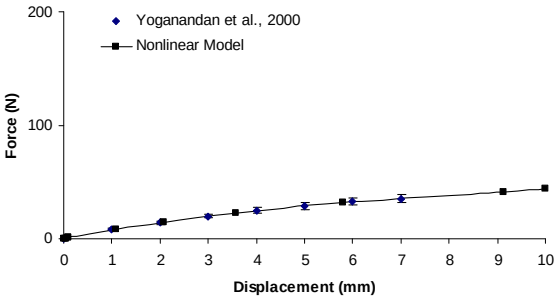

Figure 117: Validation of C5-C7 ligaments against *in vitro* data (Yoganandan et al., 2000).

6.3 Preloads and Orientations

The next important factor affecting the biomechanical response of the cervical spine was the orientation of the cervical spine during testing. Standardization of the testing

criteria for the lumbar spinal implants has been recommended, using approximate orientation found *in vivo* (Wilke et al., 1998). That is, the mid-plane of L3-L4 was recommended to be aligned horizontally. However, in the area of cervical spinal testing, various investigators used various orientation techniques. Pelker et al., 1991 tested the spinal flexibility in flexion, extension, lateral bending and axial rotation. The specimens were mounted in a quick setting epoxy resin and a line joining the geometrical center of top and bottom vertebral bodies was aligned perpendicular to the horizontal plane (Table 14). Moroney et al., 1988 tested several functional spinal units (FSU) in the same loading directions by aligning the mid-plane of the disc to the horizontal plane. Wen et al., 1993a reported a study on the cervical FSU normal ROM. However, there was no information on the orientation of the FSU during the *in vitro* testing. Various orientation techniques influence the rotational motions of the cervical spine. However, the extent of these influences has not been investigated and reported in the literatures.

Another important factor is the preload magnitudes. The human cervical spine supports compressive load arising from head weight and muscle forces. During flexion and extension, preload magnitude can reach a maximum value of 155 N (Hattori et al., 1981). However, *in vitro* experiments have demonstrated that in the absence of muscle forces, the ligamentous cervical spine becomes unstable at compressive loads magnitudes far below those seen *in vivo*. This was due to the buckling of the spinal column under small compressive preload. Panjabi et al., 1998b showed that the critical load for the ligamentous cervical spine column (C0-T1) in the frontal plane was 10.5 N (±3.8), which is about one-fifth to one-quarter the weight of the average head. Thus,

most of the studies on three or more segmental models do not apply compressive preload (Table 14).

Investigator	Description	Orientation	Preload	Moment (Nm)
Wen et al., 1993a	C2-C7 FSU. For e.g., C2-C3, C3-C4, C4-C5, C5-C6 or C6-C7	No information on the orientations	9.3 N	1.5 – 4.5 depending on loading directions
Moroney et al., 1988	C2-T1 FSU, For e.g., C2-C3, C3-C4, C4-C5, C5-C6, C6-C7 or C7-T1	Mid-plane of the disc aligned to the horizontal plane	73.6 N	1.8
Pelker et al., 1991	C2-C4 and C5-T1	Line joining the geometric centres of the top and bottom vertebral bodies was aligned perpendicular to the horizontal plane	2.5 N	1.8
Panjabi., 2001b	C0-C7	Origin at the inferior posterior end of the moving vertebrae (C0), with the positive Y axis pointing up, along the posterior wall and positive Z axis pointing posteriorly and positive X axis pointing laterally	No	1.0

Table 14: Summary of in vitro studies reported in the literatures.

Patwardhan et al., 2003 reported a technique to apply compressive load to multiple-lumbar spine specimens without buckling. This technique was also applicable to multiple-cervical spine specimens. However, an earlier study by Cripton et al., 2000 showed that axial force applied in this manner reduces the lumbar spinal motion differentially in different directions. With a particular magnitude of compression on a single lumbar motion-segment, flexion-extension was unaffected while axial rotation and lateral bending motions decreased slightly. In addition, there was little consensus about how axial preload should be incorporated in spinal flexibility tests in order to simulate the compressive loads naturally present *in vivo* (White and Panjabi, 1990). Some preload application methods used *in vitro* were suspected of producing unwanted

forces as the specimen rotates and, in doing so, influencing the resulting kinematics (Cripton et al., 2000). Generally, many investigators have found out that preload significantly influences the stiffness of the lumbar spine (Cripton et al., 2000; Edwards et al., 1987; Janevic et al., 1991; Panjabi et al., 1977; Patwardhan et al., 2003; Patwardhan et al., 2000; Patwardhan et al., 1999; Patwardhan et al., 2001). However, the influence of preload magnitudes on the cervical spinal biomechanics remains unknown.

Therefore, a study was conducted to understand the influence of various orientation and preload magnitudes on the cervical FSU incorporating the refinements mentioned earlier.

6.3.1 Methods

The C5-C6 model used in this section was created from the refined C2-C7 model and tested under three different orientations (rotation about Z axis) (Figure 118a); normal, -10 degree and +10 degree. Normal orientation represented the mid-plane of the disc aligned directly to the transverse plane (XZ). +10 degree represented the orientation of the disc at 10 degree in the positive direction (+Z) from the normal orientation.

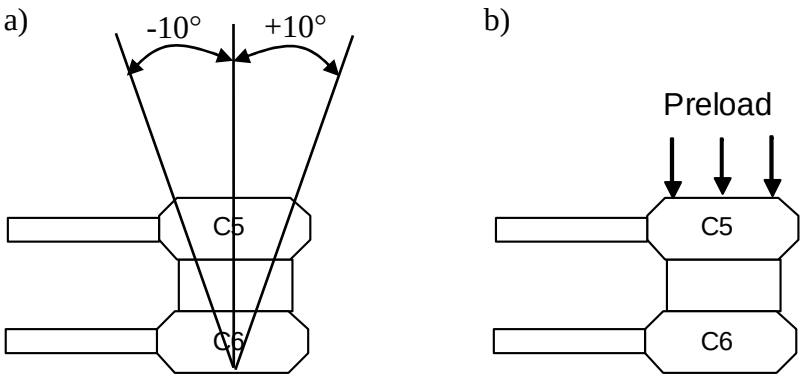

Figure 118: Illustrations on the a) various orientations and b) application of preload.

For every orientation considered in this study, four different preload magnitudes (ranging from 0 N to 150 N) were applied in the first load step to simulate physiologic compressive loads (Figure 118b). These preload magnitudes were calculated using *in vivo* disc pressure data reported by Hattori et al., 1981. The highest pressure was measured in the neck extension position and were approximately equivalent to a compression force of 155 N, assuming a disc cross-section area of 255 mm^2 (Hattori et al., 1981). In the neutral position, the force was approximately 75 N. Thus, various preload magnitudes used in this study represented the corresponding compression loads that exist in the neutral and slightly extended position. They also fall within the ranges of compressive preloads used in the experimental studies (Moroney et al., 1988; Pelker et al., 1991). A summary of the material properties used in the current study is shown in Table 15.

In the second load step, pure moments of 1.8 Nm (flexion (+MZ), extension (-MZ), lateral bending (MX) and axial rotation (±MY)) were applied to the superior surfaces of C5 in four incremental sub-steps. Overall, four different preload magnitudes and three orientation modes were investigated in this study. A single loading direction required twelve runs (four preload types x three orientation modes), resulting a total of forty eight runs. In these series of analyses, the inferior surface of C6 was fixed in all degrees of freedom, similar to experimental studies (Moroney et al., 1988; Pelker et al., 1991). The ROM was delineated from the analysis results. The C5-C6 intact model under various preloads was also validated by comparing the external behaviour with those reported in the literatures (Moroney et al., 1988; Pelker et al., 1991).

Description	Element type	Young's Modulus (MPa)	Poisson's ratio	Sources
Hard Tissue				
Cortical bone	Linear isotropic 8- node solid	10000	0.29	(Clausen et al., 1997; Goel and Clausen, 1998; Yoganandan et al., 1996b)
Cancellous bone		100	0.29	
Posterior elements		3500	0.29	
Endplate		500	0.40	
Soft Tissue				
Disc – annulus	Linear isotropic 8- node solid	3.4	0.40	(Clausen et al., 1997; Goel and Clausen, 1998; Yoganandan et al., 2001)
Disc – nucleus	Linear isotropic 8 – node solid with selective reduced integration method that prevent volumetric locking in nearly incompressible cases	1.0	0.499	
Unconvertebral Joint		1.0	0.499	
Fibers	Two node nonlinear tension only cable	450	-	

Ligaments - Two node nonlinear tension only spring element

C5-C7 (Yoganandan et al., 2000)

Anterior Longitudinal		Posterior Longitudinal		Spinous		Ligamentum Flavum		Capsular	
Deflection (mm)	Force (N)	Deflection (mm)	Force (N)	Deflection (mm)	Force (N)	Deflection (mm)	Force (N)	Deflection (mm)	Force (N)
0	0	0	0	0	0	0	0	0	0
1	20	1	20	1	8	2	30	2	75
2	40	2	40	2	14	4	68	4	145
3	58	3	60	3	20	6	102	6	204
4	78	4	78	4	25	8	130	8	250
5	98	5	92	5	29	10	145	10	265
6	112			6	32.5				
7	120			7	35				

Table 15: Material property for the C5-C6 model.

6.3.2 Results

Under all loading modes, the model using various preload magnitudes and under normal orientation compared well (Figure 119) with the data reported in the literatures (Moroney et al., 1988; Pelker et al., 1991). The predicted results were within the standard deviation of the respective *in vitro* results.

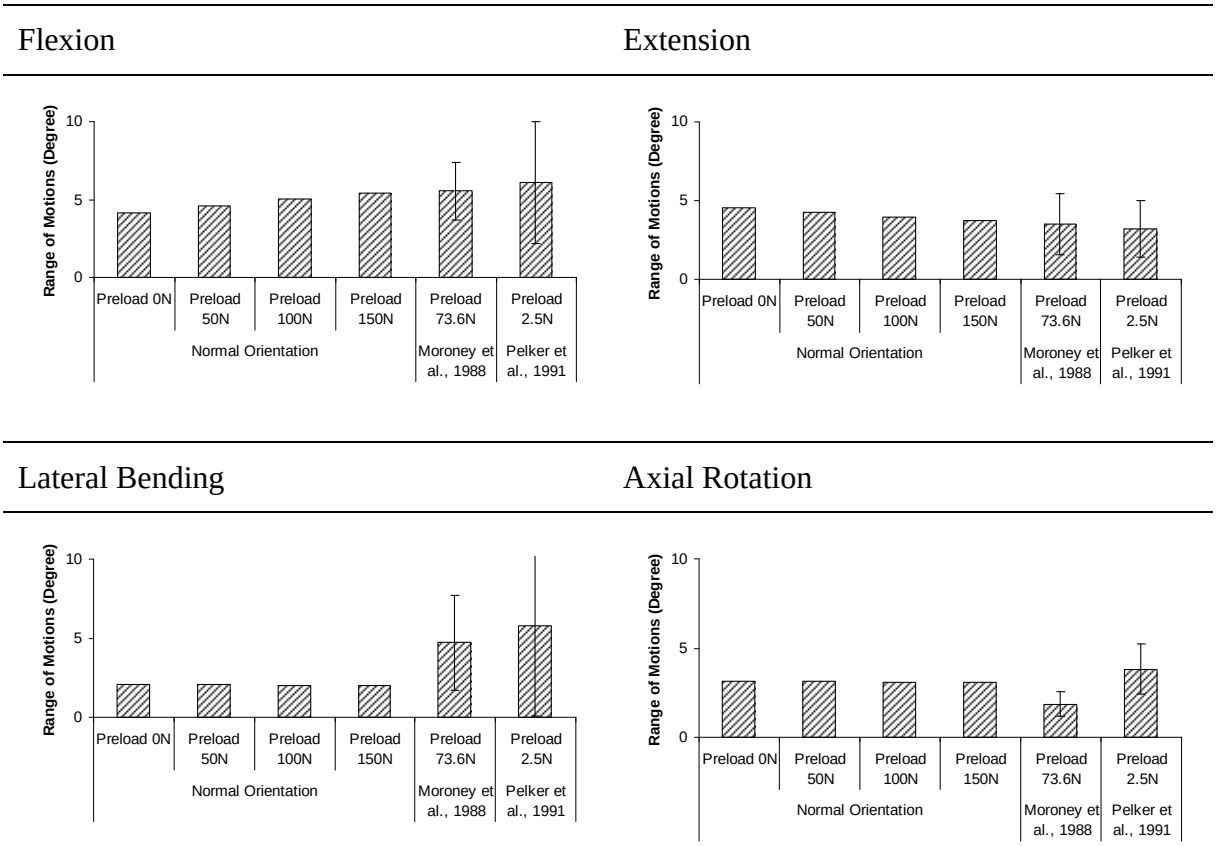

Figure 119: Comparison of the predicted results under normal loading with the data reported in the literatures (Moroney et al., 1988; Pelker et al., 1991).

Changes in the orientation of the C5-C6 only affect the ROM mildly in flexion (Figure 120a). This was caused by the changes in the orientation of the ligaments. However, increasing the preload magnitudes from 0 N to 150 N increases the ROM at 1.8 Nm under all the three orientation modes. This showed that the initial application of axial compressive forces causes the ligaments to slacken. Subsequent applications of pure moments to the C5-C6 model with slacked ligaments resulted in higher increases in the ROM.

a) b)

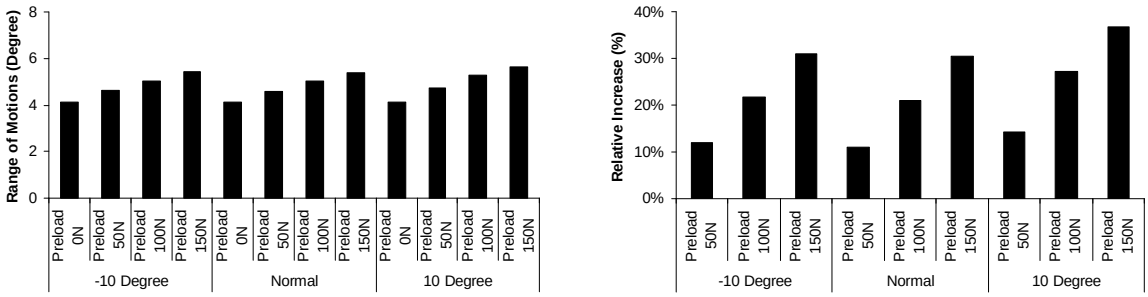

Figure 120: Influence of preload on the a) rotational motions and b) normalized value of the C5-C6 under different orientation in flexion.

The three orientation modes do not have any significant effect on the ROM of the C5-C6 under extension and no preload (Figure 121). The presence of preload compressed the articular facets, decreases the ROM of the C5-C6 model under extension, with the largest decreases seen at +10 degree orientation, +10 degree orientation also resulted in the alignment of the facet orientation towards the horizontal plane, which provides even higher resistance to extension.

a) b)

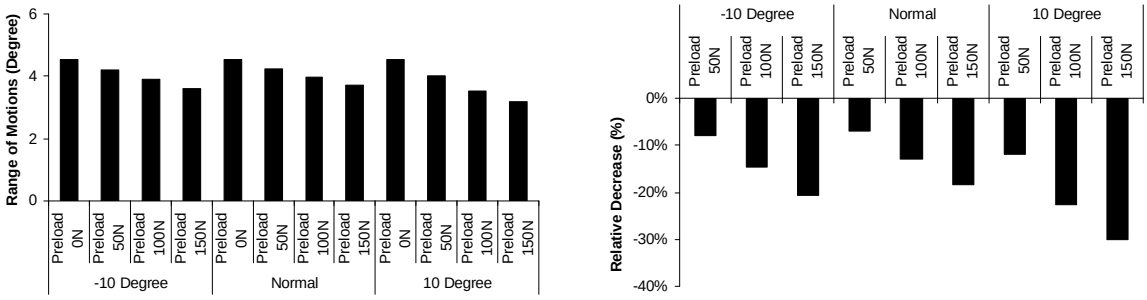

Figure 121: Influence of preload on the a) rotational motions and b) normalized value of the C5-C6 under different orientation in extension.

Under no preload and lateral bending, the ROM of the C5-C6 varied considerably under the three orientations (Figure 122). The results showed that increasing the positive

orientation reduces the C5-C6 ROM. Furthermore, with increasing positive orientation, increasing the preload magnitudes increases the contact between the superior and inferior articular facets, thereby decreases the ROM.

a) b)

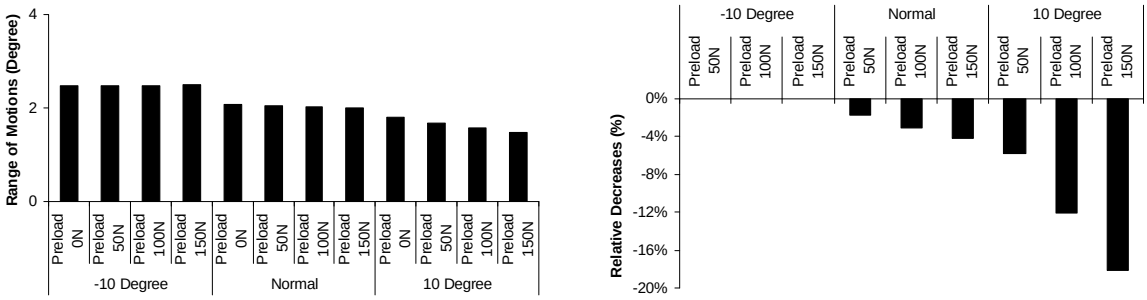

Figure 122: Influence of preload on the a) rotational motions and b) normalized value of the C5-C6 under different orientation in lateral bending.

Under no preload and axial rotation, the ROM of the C5-C6 increase with increasing positive orientation (Figure 123). Increasing the preload magnitude at +10 degree orientation caused the largest decrease in the C5-C6 ROM. Increasing the C5-C6 positive orientation flattens the facets orientation towards the horizontal plane. This provides more resistance under lateral bending and less resistance under axial rotation.

a) b)

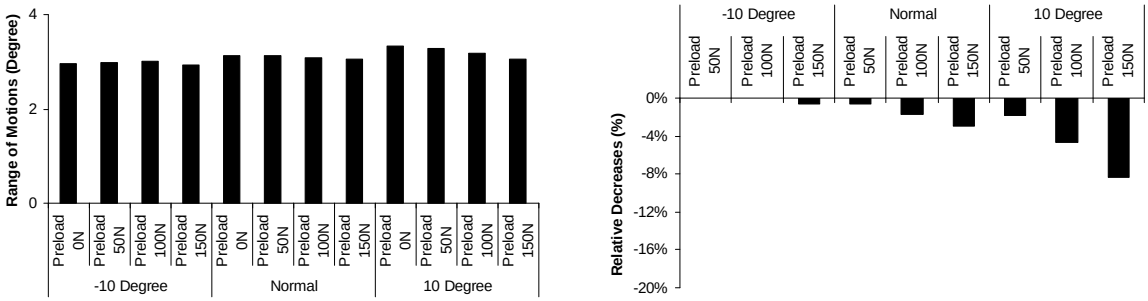

Figure 123: Influence of preload on the a) rotational motions and b) normalized value of the C5-C6 under different orientation in axial rotation.

6.3.3 Discussion

This study has established the influence of different preload magnitudes and orientations on the biomechanics of the cervical spine. Several authors have studied the effects of compressive preload on the responses of the lumbar spinal segments (Cripton et al., 2000; Edwards et al., 1987; Janevic et al., 1991; Panjabi et al., 1977; Patwardhan et al., 2003; Patwardhan et al., 2000; Patwardhan et al., 1999; Patwardhan et al., 2001). However, the changes in the ROM of the cervical spinal segments due to various preload magnitudes and orientations have not been investigated.

It was shown that under normal orientation and increasing preload magnitudes (Figure 119), the predicted ROM increases under flexion and decreases under extension, lateral bending and axial rotation. These changes were found to be influenced by several spinal components: posterior facets, passive ligaments and stiffening of the intervertebral disc. Due to this, it is necessary to establish a standard for *in vitro* testing. However, till date, various *in vitro* studies are still using different orientation during the testing of cervical spinal biomechanics (Kubo et al., 2003; Moroney et al., 1988; Panjabi et al., 2001; Pelker et al., 1991). The best approach is to align the cervical spine in the physiological position. For the testing of C5-C6, the model should be aligned in the positive orientation (+Z) to mimic actual *in vivo* position.

Biomechanical studies are most useful if it can provide information and answers to the clinical problems. To achieve this, preload magnitudes experience during *in vivo* should be used in the future spinal flexibility tests. However, if the cervical spinal biomechanics are to match the *in vivo* behavior by applying physiological preload, current results suggest that the applied moments under different directions should be

varied to compensate for the changes in the rotational motions magnitudes due to the application of preloads. Wen et al., 1993a obtained *in vitro* results using small preloads of 9.3 N and 1.5 Nm, 2.0 Nm and 4.5 Nm in flexion-extension, lateral bending and axial rotation, respectively. They reported good agreement with the *in vivo* data but lower rotational motions under flexion-extension loading. Miura et al., 2002 tested C2-T1 using 100 N preload and 2 Nm and 4 Nm in flexion-extension, lateral bending and axial rotation. Their reported values were within 12-15% in flexion-extension, lateral bending, and 22% in axial rotation of the representative *in vivo* average.

However, it is difficult to define what the desired preload should be acting *in vivo*. The load acting on the cervical spine is a complex combination of the muscle forces and the weight of the head. Complexity of this system has partially resulted in the widespread practice of *in vitro* flexibility test using pure moments (Moroney et al., 1988; Panjabi et al., 2001; Pelker et al., 1991). This is not believed to represent the *in vivo* situation but allows quantitative comparison of surgical techniques and devices and allows repeatable data to be produced (Cripton et al., 2000). Therefore, only pure moments will be applied to the C2-C7 model in the analysis documented in the subsequent chapters, consistent with those reported in the literatures using three or more multiple segments.

With all the in-depth studies on the material, geometry, loading and orientations completed, the next step was to validate the refined C2-C7 model (additional validations using the refined model has been included can be found in Appendix A.4 Validations Using Refined FE Model).

6.4 Validation of C2-C7 Model

This study was performed on a three-dimensional nonlinear model of the intact C2-C7 model. The model was first compared against the data (Table 16) by Schulte et al., 1989, Panjabi et a., 2001b and Kubo et al., 2003. Finally, in order to increase the database with which the C2-C7 model can be compared, three loading values (1.0 Nm, 1.5 Nm and 2.0 Nm) were applied to the intact model. These represent the most commonly used load values reported in the literatures. Extensive validation and studies conducted earlier provided the necessary understanding and experience to use this approach. Moments were applied to the superior surface of the C2 to cause flexion (+MZ), extension (-MZ), left + right lateral bending (±MX) and left + right axial rotation (±MY). The inferior surface of the C7 vertebra was fixed in all directions to prevent movements. The inter-segmental ROM were obtained from the simulation and compared against the *in vitro* data.

Anatomical Region	**Loading**		**Responses**	**References**
	Force	**Mode**		
C2-C7	0.45 Nm in 4 steps	flexion-extension, lateral bending and axial rotation	primary ROM	(Schulte et al., 1989)
	1.0 Nm in 4 steps	flexion, extension, lateral bending and axial rotation	primary ROM	(Panjabi et al., 2001)
	1.5 Nm in 4 steps	flexion-extension	primary ROM	(Kubo et al., 2003)
	1.0 Nm, 1.5 Nm and 2.0 Nm in 4 steps	flexion, extension, lateral bending and axial rotation	primary ROM	(Clausen et al., 1997; Moroney et al., 1988; Nowinski et al., 1993; Panjabi et al., 1986; Pelker et al., 1991; Wen et al., 1993a)

Table 16: Summary of validation studies on C2-C7 model.

Figure 124 compared the FE results against the *in vitro* data by Panjabi et al., 2001b on the inter-segmental ROM under flexion-extension. Take note that the standard deviation from the *in vitro* data was only available at the final load step. It can be seen that the FE results compared well against the *in vitro* data at the respective cervical levels. The results indicated higher inter-segmental motions at the middle regions (C3-C4, C4-C5 and C5-C6) and lower inter-segmental motions at the two ends (C2-C3 and C6-C7). This is consistent with the observation obtained from *in vitro* study. Under lateral bending (Figure 125), the predict ROM for the C5-C6 and C6-C7 falls at the lower range of the experimental data. The inter-segmental ROM for the C2-C3, C4-C5 and C5-C6 are slightly lower than the mean minus the standard deviation. This may be due to the averaging of the experimental results. One of the possible reasons for the slightly lower prediction under lateral bending was discussed earlier (Refer Chapter 5.2.5 Validation against Wen et al., 1993 on C5-C6). Under axial rotation (Figure 126), the predicted inter-segmental ROM compared well against the in vitro data at all the cervical levels (C2-C3, C3-C4, C4-C5, C5-C6 and C6-C7).

Under flexion, the predicted C3-C4, C5-C6 and C6-C7 ROM (Figure 127) compares relatively well against Schulte et al., 1989. Schulte et al., 1989 did not present any data on C2-C3. Therefore, no comparison can be made. The predicted C4-C5 ROM is slightly lower than the *in vitro* results. Under extension and axial rotation, the predicted ROM compares well against the *in vitro* data. Under lateral bending, the FE results are within mean ± the standard deviation for C5-C6 and C6-C7. Under C4-C5, the predicted ROM is slightly lower than the mean minus the standard deviation. Take note that *in vitro* data are not available for C2-C3 and C3-C4 ROM under lateral bending and axial rotation.

C2-C3

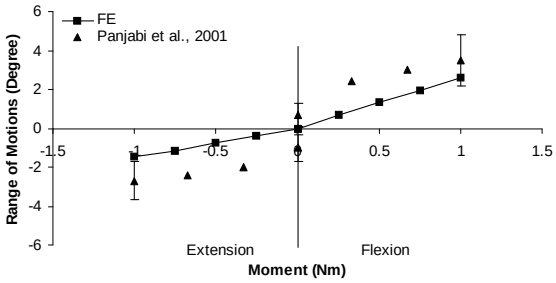

C3-C4

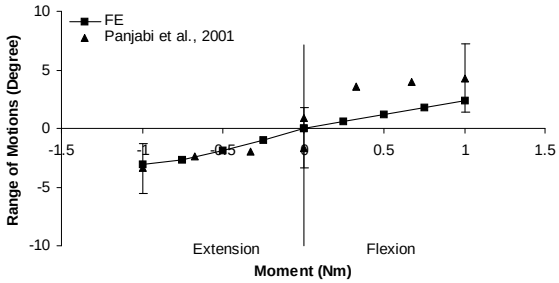

C4-C5

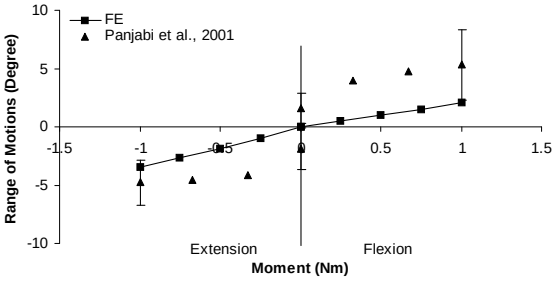

C5-C6

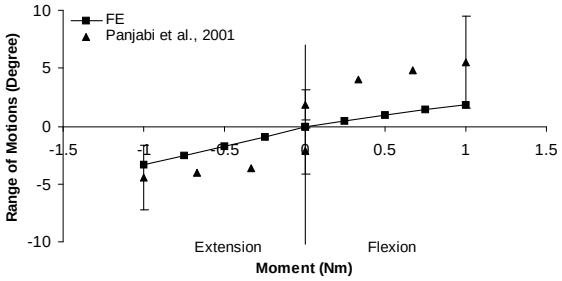

C6-C7

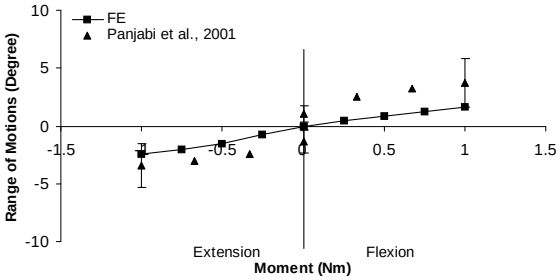

Figure 124: Validation of the C2-C7 model in flexion-extension with experimental data (Panjabi et al., 2001).

C2-C3

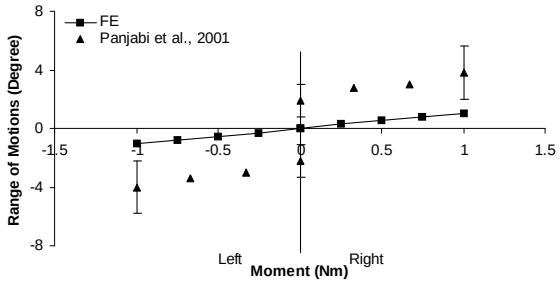

C3-C4

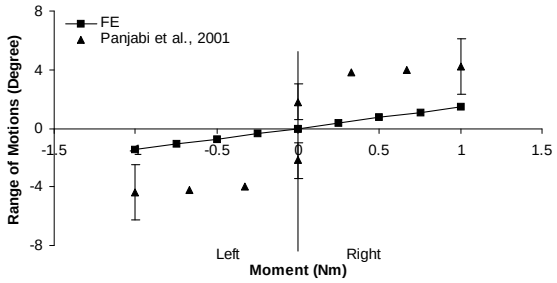

C4-C5

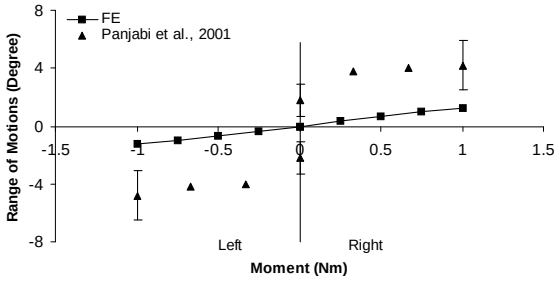

C5-C6

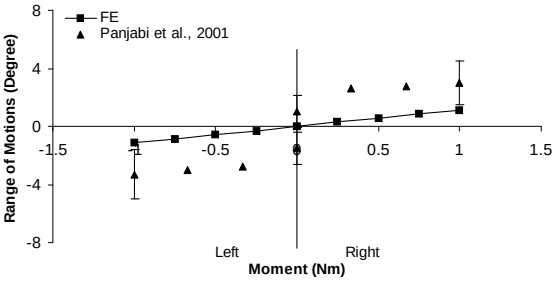

C6-C7

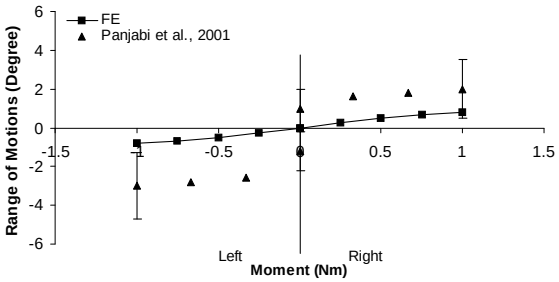

Figure 125: Validation of the C2-C7 model in left and right lateral bending with experimental data (Panjabi et al., 2001).

C2-C3

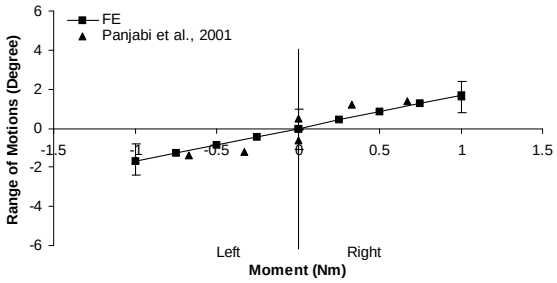

C3-C4

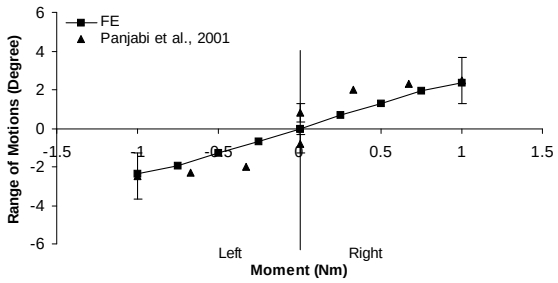

C4-C5

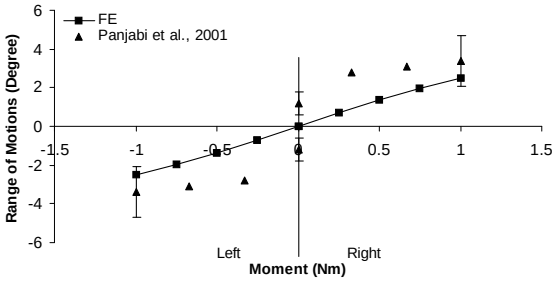

C5-C6

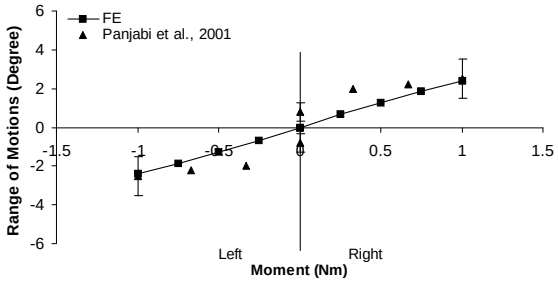

C6-C7

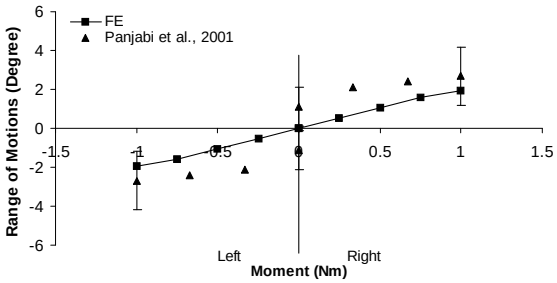

Figure 126: Validation of the C2-C7 model in left and right axial rotation with experimental data (Panjabi et al., 2001).

Flexion

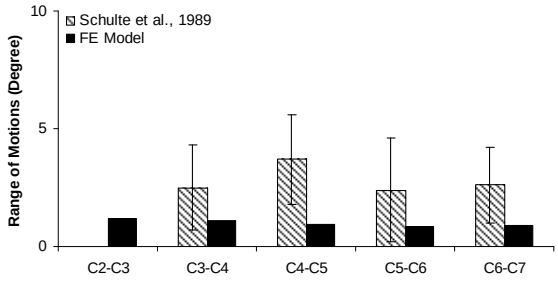

Extension

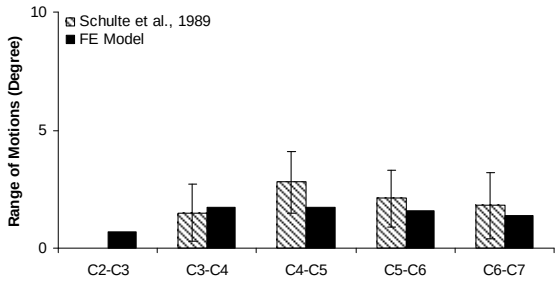

Left Lateral Bending

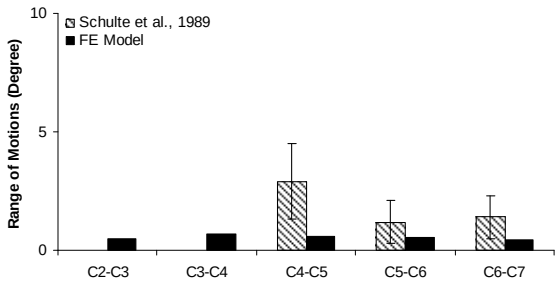

Left Axial Rotation

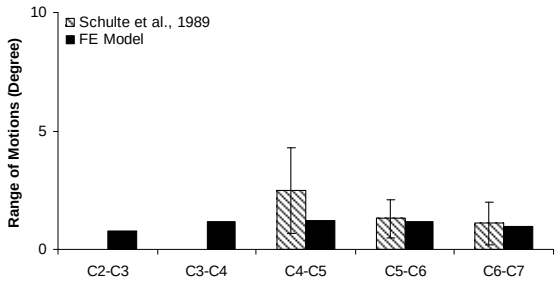

Figure 127: Validation of the C2-C7 model against experimental data at 0.45 Nm (Schulte et al., 1989). Only C4-C7 FSU inter-segmental ROMs are available for comparisons.

Under flexion-extension (Figure 128), the predicted inter-segmental ROM range from 5.7 to 7.4 degree at 1.5 Nm. These results are comparable to in vitro data obtained by Kubo et al., 2003. The computer predicted a slightly lower C3-C4 and C6-C7 ROM than the experimental data. One reason can be due to the higher ROM obtained from the *in vitro* data for C3-C4 and C6-C7 than C2-C3, C4-C5 and C5-C6.

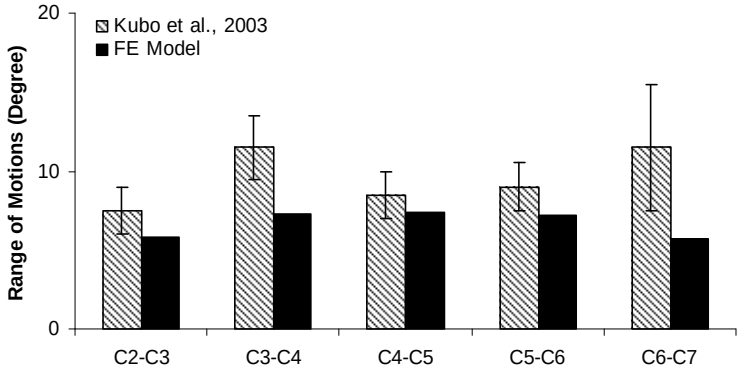

Figure 128: Validation of C2-C7 model against experimental data at 1.5 Nm in flexion-extension (Kubo et al., 2003).

Finally, the predicted inter-segmental ROM due to 1.0 Nm, 1.5 Nm and 2.0 Nm was obtained and summarized together with *in vitro* results published in the literatures and used in earlier comparison studies (Figure 129 - Figure 131).

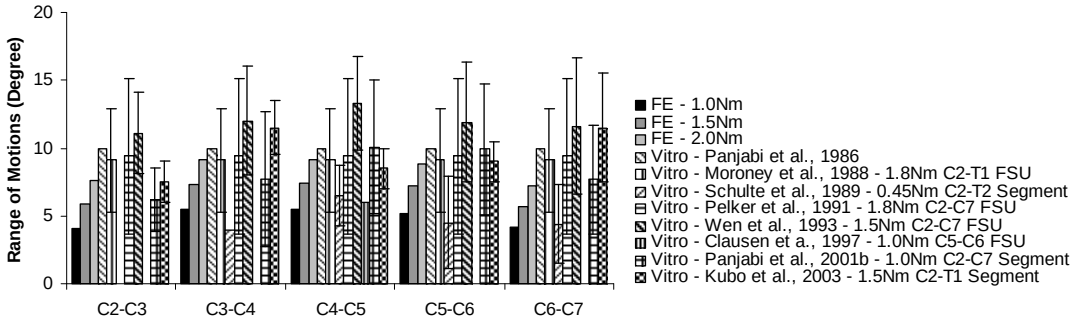

Figure 129: Summary of published results and current FE predictions on the ROM in combined flexion-extension.

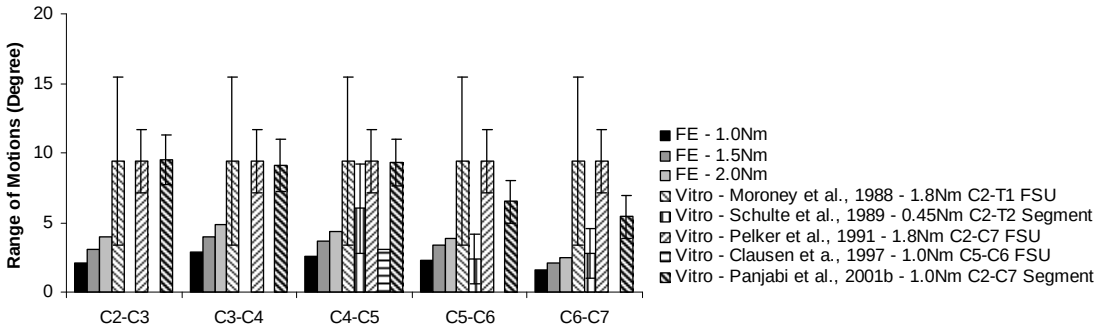

Figure 130: Summary of published results and current FE predictions on the ROM in left and right lateral bending.

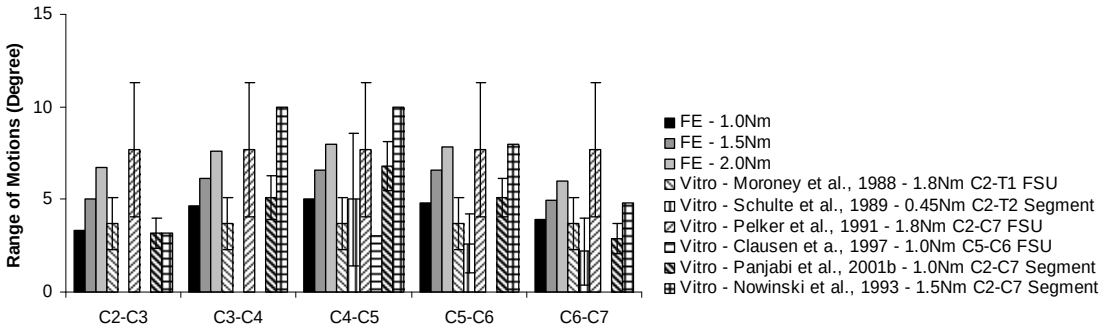

Figure 131: Summary of published results and current FE predictions on the ROM in left and right axial rotation.

6.5 Surgical Procedures

6.5.1 Progressive Unilateral and Bilateral Facetectomy

Cervical spinal stenosis requires surgical procedures to relieve the spinal canal or nerve roots pressure. Facetectomy is used for cervical nerve root decompression using a posterior approach. During facetectomy, a portion of the cervical facet joint must be removed in order to decompress the nerve root. The degree of facet resection is usually determined by the level of nerve root compression. Facetectomy provides better visualization of the nerve roots and their surrounding structures than anterior approaches. Early biomechanical studies on cervical spine facetectomy focused on the testing of a single-motion segment (Panjabi et al., 1975; Raynor et al., 1987; Raynor et

al., 1985). However, the influence of these surgical techniques on the internal stress remained unknown.

Therefore, the purpose of this study was to quantify the inter-segment instability and internal responses of the C2-C7 cervical spine during commonly used surgical techniques of graded unilateral and bilateral facetectomy through analytical simulation.

6.5.1.1 Methods

With this intact model, progressive unilateral and bilateral facetectomy were simulated at the C5-C6 level of the C2-C7 model (Figure 132). Eight surgically altered models (graded unilateral and bilateral facetectomy models) were developed based on the surgical procedures described in the literature (Raynor et al., 1985; Zdeblick et al., 1993; Zdeblick et al., 1992). To simulate facetectomy at the C5-C6 level, the intact model was modified by removing the facet of the inferior process of the C5 and superior process of C6 along with the associated ligaments (capsular ligaments). The facets were removed progressively and each removal represents about 25% of that facet joint (25%, 50%, 75% and 100%). For unilateral facetectomy, only one side of the facet joint was removed progressively.

The inferior surface of C7 was fixed in all degrees of freedom. The model was loaded under pure moments of 1.5 Nm (flexion (+MZ), extension (-MZ), left + right lateral bending (±MX) and left + right axial rotation (±MY)) applied to the superior surfaces of C2 in four incremental steps. The external biomechanical behaviour and internal stresses were delineated from the analysis results. The stress in the various spinal components was obtained by dividing the total von Mises stress over the volume of the

respective spinal components. The averaging of the internal stress will help to prevent localised peak stress at irregular vertebrae surfaces affecting the accuracy of the predicted results. The stresses were also normalized similarly with respect to the corresponding values of the intact model.

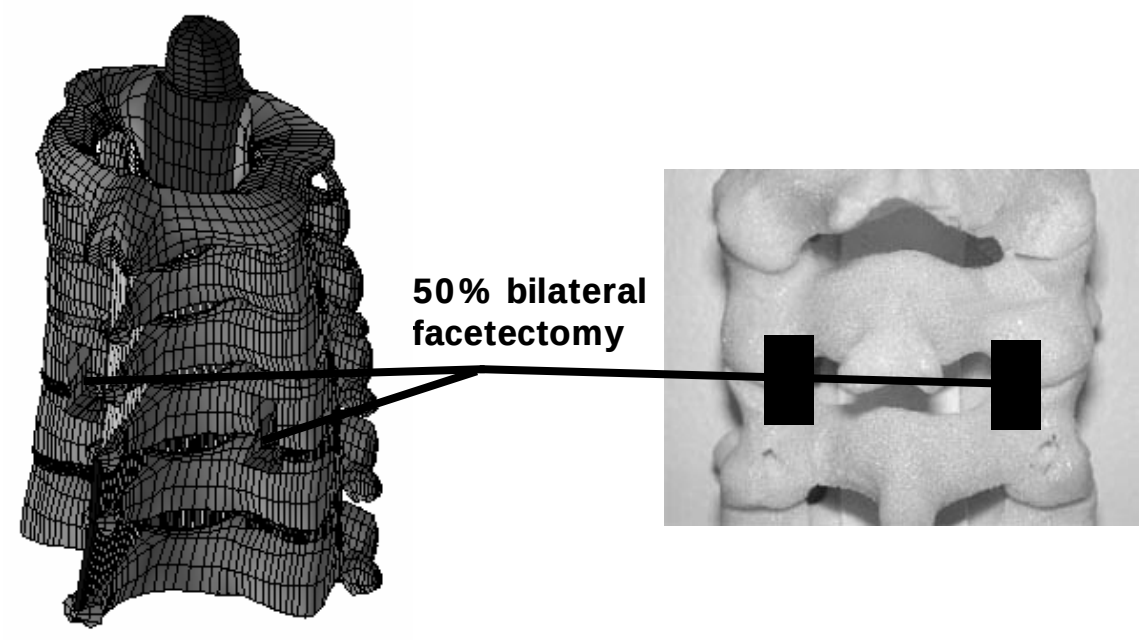

Figure 132: Illustrations on the 50% bilateral facetectomy model.

6.5.1.2 Results

The predicted ROM was normalized as a ratio to that found in the intact spine (Figure 133). In all cases, increasing the facet resection increases the rotational motions at the affected joint (C5-C6). No significant increase is seen at other cervical levels as C5-C6 facetectomy only involved the removal of ligaments and facets at the affected joint only (C5-C6). After 25% facet resection, there were a 1% (unilateral facetectomy) and 2% (bilateral facetectomy) increases in the C5-C6 ROM under combined flexion-extension. After 75% resection, this increased to 3% and 7%, for unilateral and bilateral facetectomy: 6% and 12% increases were observed after 100% resection. Furthermore,

substantial increases in the rotational motions can be seen at C5-C6 level with more than >50% unilateral or bilateral facetectomy. This pattern was more prominent under lateral bending and axial rotation. It is interesting to see that facetectomy performed at C5-C6 levels affects the rotational motions of the adjacent segments by approximately 1-2%. The maximum increase in the ROM at C5-C6 was 18% for 100% bilateral facetectomy in left or right lateral bending and 7% for unilateral facetectomy under the same loading mode. Increases in the ROM after unilateral facetectomy were consistently lower than the increase after bilateral facetectomy for the same direction of loadings and same degree of facet resection.

The percentage changes in the disc stress were well related to the increases in the rotational motions at the affected segments (Figure 134). Under combined flexion-extension, the disc stress increases by a maximum percentage of 9% and 15%, for 100% unilateral and bilateral facetectomy, respectively. It is interesting to note that the percentage increase in the C5-C6 posterior disc stress is approximately two times higher than the C5-C6 anterior disc stress. Under right lateral bending, the maximum percentage increases in the disc stress are 11% (100% unilateral) and 15% (100% bilateral). Under left lateral bending, 100% unilateral facetectomy did not result in any significant increase (<1%) in the disc stress. Under right axial rotation, the C5-C6 disc stress increase by 7% and 12%. Under left axial rotation, C5-C6 disc stress increases by 2% and 12%, respectively.

Combined flexion-extension

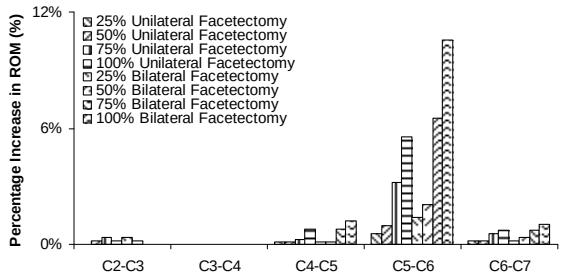

Right Lateral Bending

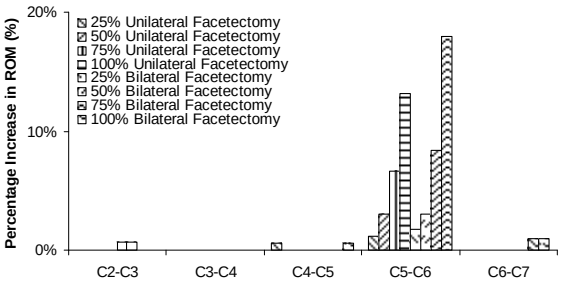

Left Lateral Bending

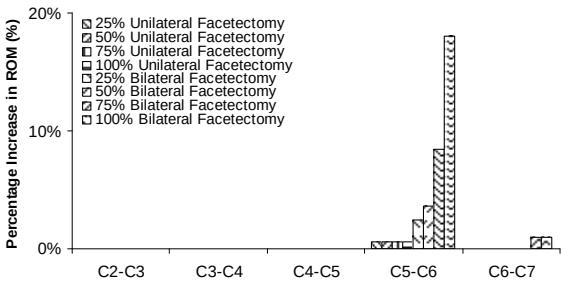

Right Axial Rotation

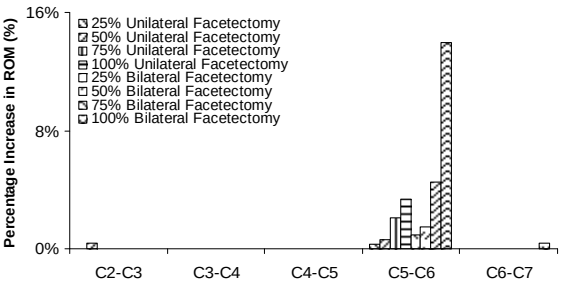

Left Axial Rotation

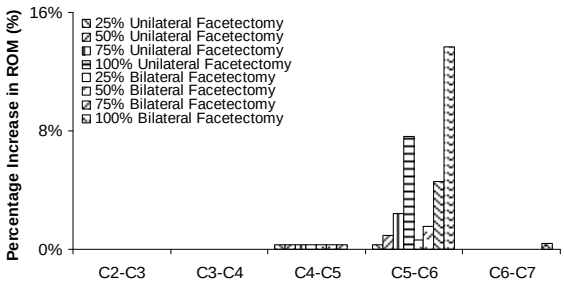

Figure 133: Percentage increase in the inter-segmental ROM due to graded unilateral and bilateral facetectomy.

Combined flexion-extension

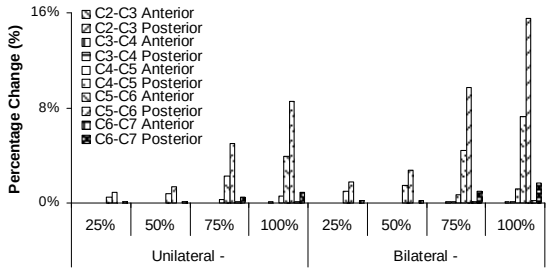

Right Lateral Bending

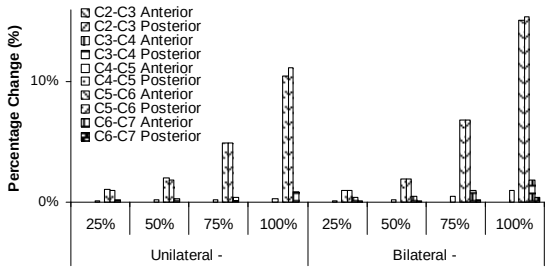

Left Lateral Bending

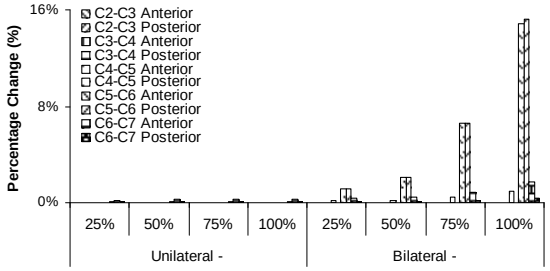

Right Axial Rotation

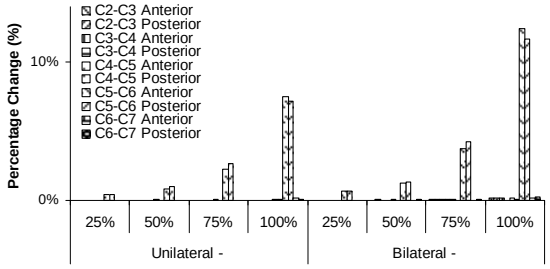

Left Axial Rotation

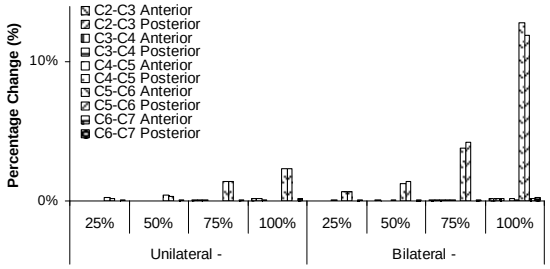

Figure 134: Percentage increase in the disc annulus stress after graded unilateral and bilateral facetectomy.

Overall, significant increases in the cortical bone stress were observed after unilateral or bilateral facetectomy of greater than 50% (Figure 135). C5 and C6 cortical bone stress showed significant increases after facetectomy. Under combined flexion-extension, maximum increases were 33% for bilateral facetectomy and 17% for unilateral facetectomy. The maximum increases in the cortical bone stress were higher than the maximum increases in the ROM and disc stress. Under right axial rotation, the stress

only increases by 7% and 3%, respectively: whereas left axial rotation stress increases by 7% and 6%, respectively.

Combined flexion-extension

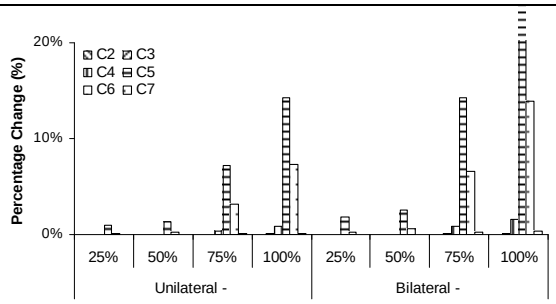

Right Lateral Bending

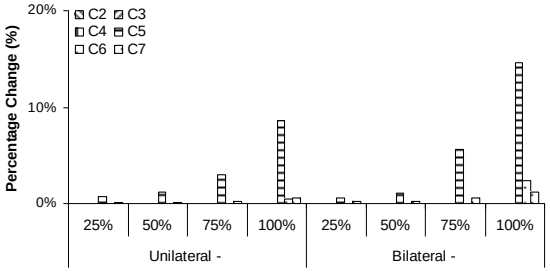

Left Lateral Bending

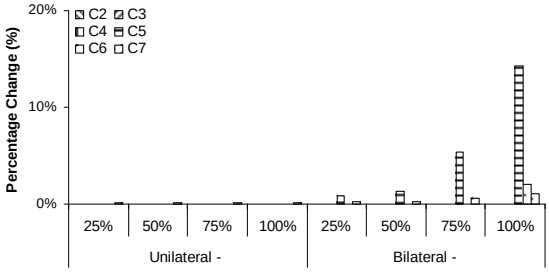

Right Axial Rotation

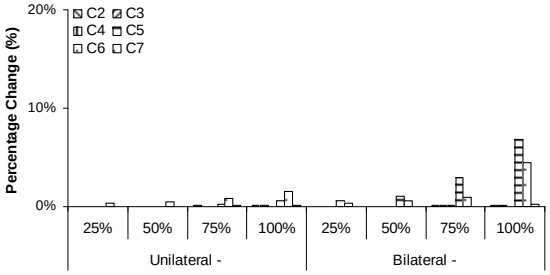

Left Axial Rotation

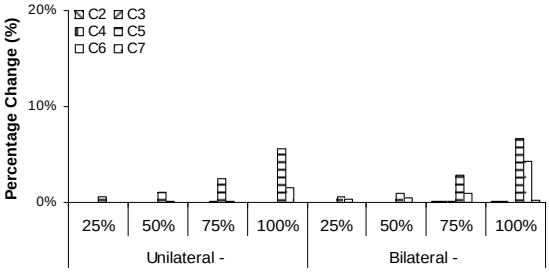

Figure 135: Percentage increase in the cortical bone stress after graded unilateral and bilateral facetectomy.

6.5.1.3 Discussion

The external behaviour of the cervical spine after facetectomy has always attracted the attention of clinicians and biomechanical researchers. Understanding the behaviour after this surgical procedure provides a corridor to better treatment and prevention of spinal instability.

In this study, the refined C2-C7 model was used to determine the effects of unilateral and bilateral facetectomy under sagittal plane moments (combined flexion-extension, left + right lateral bending and left + right axial rotation). The results indicated the significant increase in the ROM after bilateral facetectomy. The increase in the ROM after progressive bilateral facetectomy was considerably greater than the increase after progressive unilateral facetectomy. For both unilateral and bilateral facetectomy, a significant increase in the ROM was observed after facet resection of more than 50%. The current results (Figure 133) correlated well with the experimental findings, which also indicated substantial increases in the rotational motions with unilateral or bilateral facet resection of greater than 50% under all loading modes (Raynor et al., 1987; Raynor et al., 1985; Zdeblick et al., 1993; Zdeblick et al., 1992).

In 1975, Panjabi et al. first assessed the contribution of the facet and its capsule to the stability of the cervical spine. They reported on the responses of the cervical spine segments after disruption of some of the spinal elements. They found that the horizontal translation of the vertebra increased significantly after removal of the facet joint. Raynor et al. investigated the effects of resection of the facet on spinal stability. They tested a cervical single vertebra motion segment under shear loading only. The results showed that bilateral resection of more than 50% of the facet joint significantly compromised the shear strength of a cervical spine motion segment (Raynor et al., 1985). In 1987, Raynor et al. repeated the experiment again using a cervical single motion segment in an effort to expand on their previous investigation. Complete facetectomy was performed and subsequent motion was measured with non-destructive testing (Raynor et al., 1987). White and Panjabi, 1988 and Cusick et al., 1988 demonstrated that the cervical instability increase with progressive facetectomy. In

another *in vitro* study, Zdeblick et al., 1993 showed that bilateral facetectomy of more than 50% caused a significant loss of stability. After 100% facet resection, they reported an increase of 22% under combined flexion-extension and 13% under axial rotation. Their results were comparable to the present study, which indicated an overall increase of 12% under combined flexion-extension and 14% under axial rotation. However, for these studies, changes in flexibility of the motion segments under lateral bending and flexion along remain unclear. Our results correlated well with their findings, which indicated substantial increases in the rotational motions with facet resection of greater than 50% under axial rotation (Zdeblick et al., 1993; Zdeblick et al., 1992). Present results also demonstrated that the increases in the inter-segmental motions caused by surgical procedures were accompanied by higher stress in the disc annulus and cortical shell. This showed that the present finite element model is capable of delivering additional results, which are difficult or even impossible to acquire experimentally.

Voo et al., 1997 tested the biomechanical effects of cervical facetectomy at C5 and C6 levels with a two-level segment (C4-C6) FE model under sagittal moments. The overall stiffness (C4 with respect to C6) was obtained for the surgically altered models. However, their findings (Figure 136) contradicted the current FE results and *in vitro* studies conducted by Zdeblick et al., 1993. One of the reasons for predicting such a low increase in the rotational motions after facetectomy in their model was the use of linear analysis with small displacement options. In the past, many FE studies validated or compared their intact models against *in vitro* data. Subsequently, they used this validated intact model to perform injury or surgical studies. Most of the FE were only validated in the intact form and may not have performed realistically and accurately

during simulated injury studies. Therefore, it is important to compare the model in the both intact and injury stages. The current intact model was validated extensively and sensitivity studies were conducted before performing any surgical studies. Furthermore, the accuracy of the model during surgical studies was also compared against experimental measurements. These comparisons will ensure the validity and accuracy of the current FE predictions.

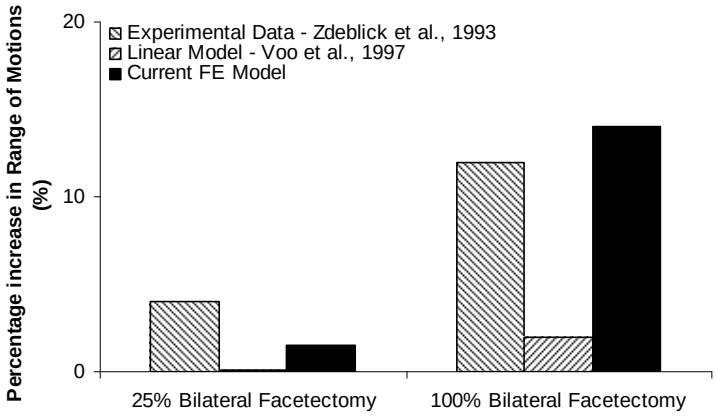

Figure 136: Comparison against data reported in the literatures after total bilateral facetectomy in axial rotation (Voo et al., 1997; Zdeblick et al., 1993).

As a next step, the influence of facetectomy on the internal stress was studied. Generally, increasing the facet resection increases the disc and cortical stress. However, a higher magnitude of increase can be seen in the cortical bone stress. The trend in the increase in the disc stress and cortical bone stress is similar to the increase in the ROM. The trend is similar to the increases in the ROM.

6.5.2 Laminectomy with Unilateral and Bilateral Facetectomy

In the earlier study, the results indicated significant increase in the ROM after 50% resection. However, facetectomy is not conducted alone and is occasionally

accompanied by laminectomy. Laminectomy is needed for decompression of the spinal cord and facetectomy is needed for decompression of the nerve-roots. Although laminectomy with facetectomy effectively decompresses the spinal cords and nerve roots, this procedure poses the risk of postoperative instability and kyphosis.

Therefore, the purpose of this study was to quantify the inter-segmental motions and internal responses of the C2-C7 cervical spine after the commonly used surgical techniques of laminectomy with graded unilateral and bilateral facetectomy.

6.5.2.1 Methods

The C2-C7 intact model was modified to simulate C5 laminectomy with progressive C5-C6 unilateral and bilateral facetectomies. Eight models were developed based on the clinical procedures described in the literatures (Raynor et al., 1985; Zdeblick et al., 1993; Zdeblick et al., 1992).

1) Spinous resection: removal of the spinous process. The spinous ligaments were removed between C4 and C6.
2) C5 laminectomy: removal of the spinous process and left + right lamina. The spinous and flavum ligaments were removed between C4 and C6 (Figure 137a).
3) Unilateral facetectomy: same as (1) + removal of the facet of the superior process of C6 and inferior process of C5. The associated capsular ligaments were removed between the C5 and C6. Each removal represents about 25% of the right facet joint (Figure 137b).
4) Bilateral facetectomies: same as (1) + removal of the facets of the superior process of C6 and inferior process of C5. The associated capsular ligaments were removed between the C5 and C6. Each removal represents about 25% of the left + right facet joint.

The models were then exercised under similar loading and boundary configurations described in Section 6.5.1.1 Methods.

a) b)

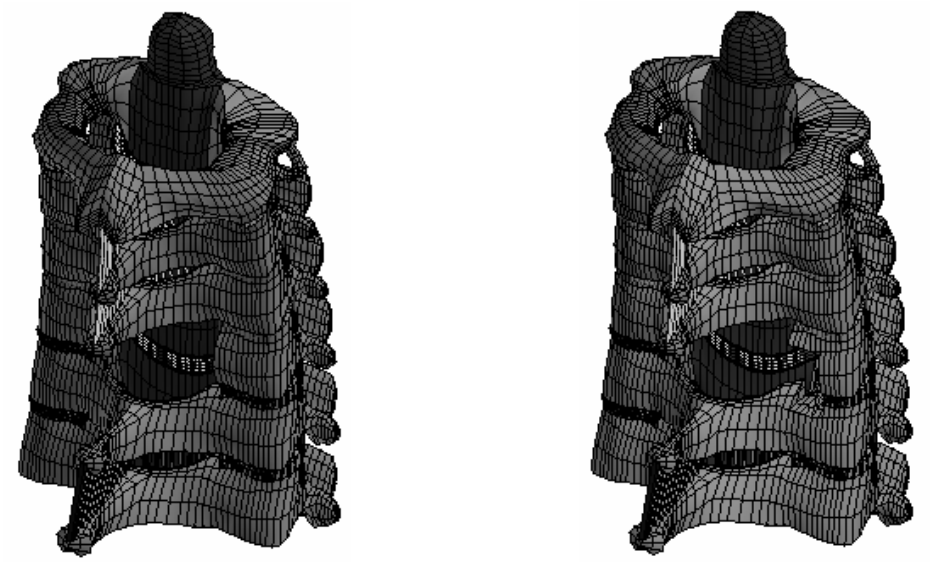

Figure 137: Iso-posterior view of the a) C5 laminectomized model, b) laminectomized model with 50% unilateral facetectomy.

6.5.2.2 Results

Figure 138 show the percentage increase in the ROM due to laminectomy with progressive unilateral and bilateral facetectomy. Under all loading types, most of the changes in the ROM due to surgical techniques occurred at the C4-C5 and C5-C6 segments. The largest magnitude of increase in the ROM was observed under combined flexion-extension. Under combined flexion-extension, spinous resection and laminectomy increase the C4-C5 and C5-C6 ROM significantly. Subsequent progressive facetectomy performed on the laminectomized model only increase C5-C6 ROM. In general, increasing the facet resection increases the ROM at the affected joint. Substantial increase in the ROM can be seen for models with more than 50% facetectomy. For the laminectomized model with more than 50% facetectomy,

subsequent bilateral facetectomy causes higher spinal instability as compared to unilateral facetectomy. It should be noted that the spinous resection and laminectomy do not have a noticeable effect on the ROM under lateral bending and axial rotation.

The maximum percentage increases in the disc stress occurred under combined flexion-extension (Figure 139). The relative change in the disc stress was well related to the increase in the ROM. Under combined flexion-extension, the C5-C6 posterior disc stress increase by 12%, 25%, 40% and 54% for spinous resection, laminectomy, laminectomy with 100% unilateral and laminectomy with 100% bilateral facetectomy. It should also be noted that the spinous resection and laminectomy do not have a noticeable effect on the disc stress under lateral bending and axial rotation.

Under combined flexion-extension, the C4, C5 and C6 cortical stress increase significantly after spinous resection and laminectomy (Figure 140). Furthermore, the cortical stresses in the C5 and C6 increase progressively after subsequent facetectomy. A greater increase in the cortical bone stress was observed after facetectomy of more than 50%. However, the cortical bone stress under lateral bending and axial rotation did not react actively to these surgical procedures as compared to flexion-extension. Overall, the cortical bone at the affected level (C5) experienced the highest increases in the stress.

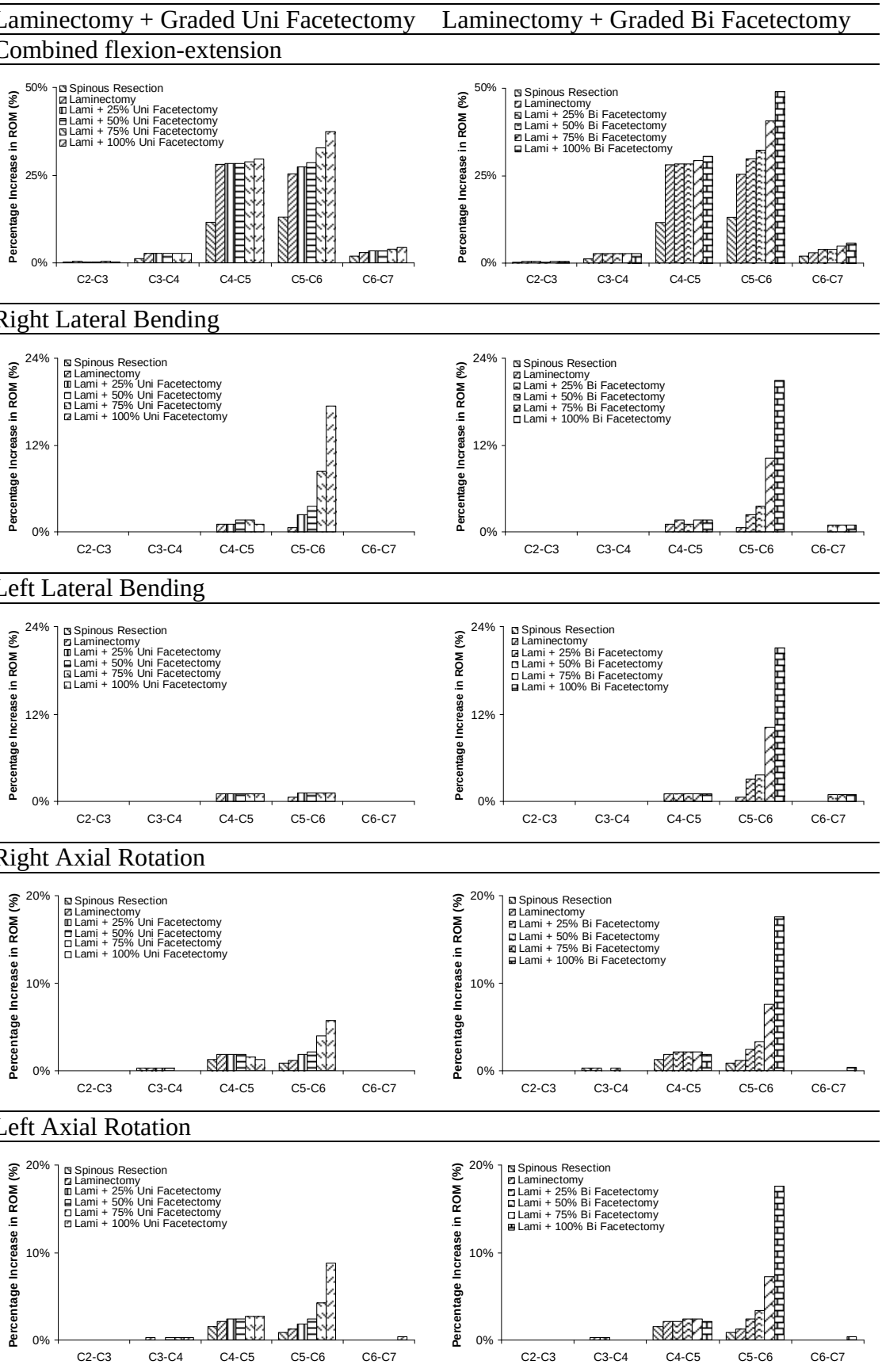

Figure 138: Percentage increase in the ROM due to laminectomy with progressive unilateral and bilateral facetectomy.

Laminectomy + Graded Uni Facetectomy	Laminectomy + Graded Bi Facetectomy

Combined flexion-extension

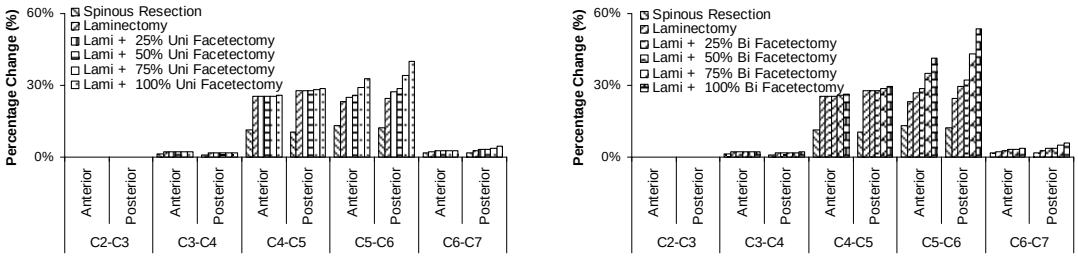

Right Lateral Bending

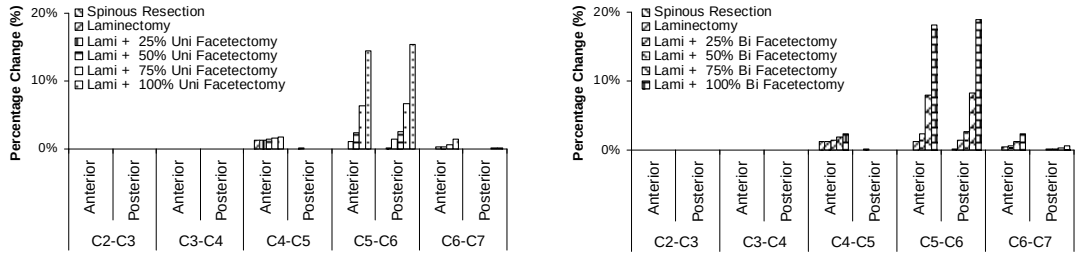

Left Lateral Bending

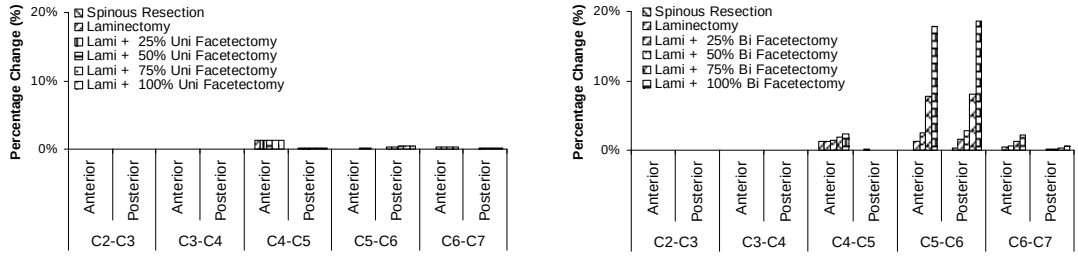

Right Axial Rotation

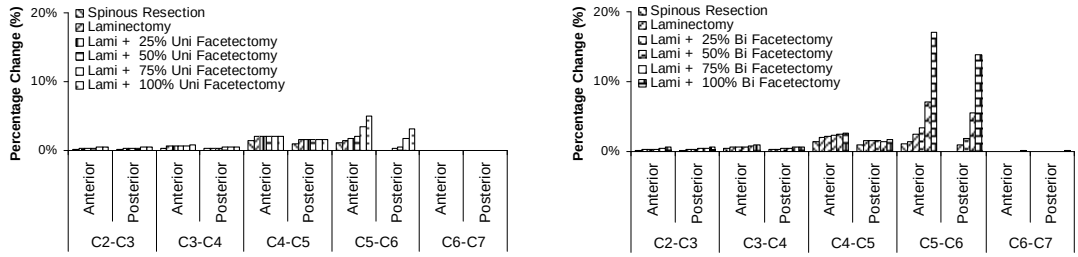

Left Axial Rotation

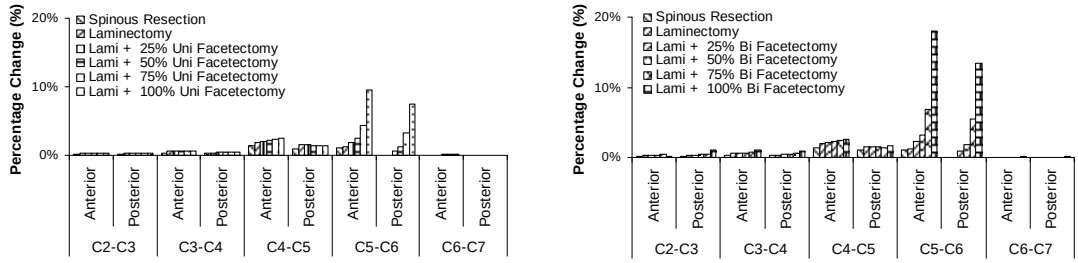

Figure 139: Relative percentage change in the disc annulus stress of the C2-C7 model due to laminectomy with progressive unilateral and bilateral facetectomy.

Laminectomy + Graded Uni Facetectomy	Laminectomy + Graded Bi Facetectomy

Combined flexion-extension

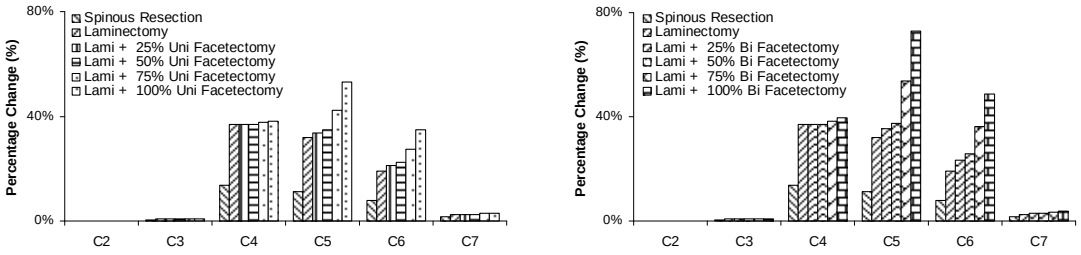

Right Lateral Bending

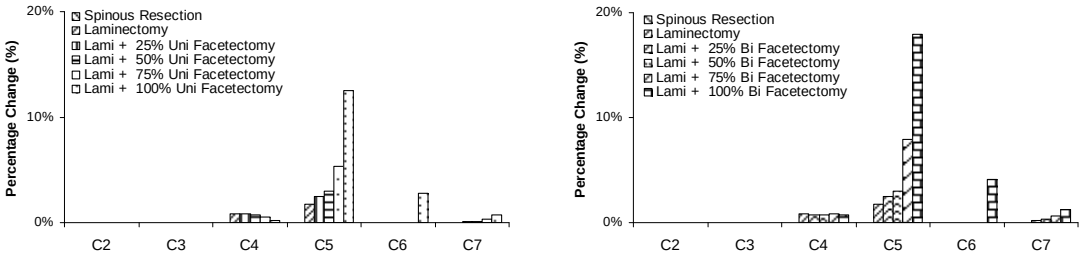

Left Lateral Bending

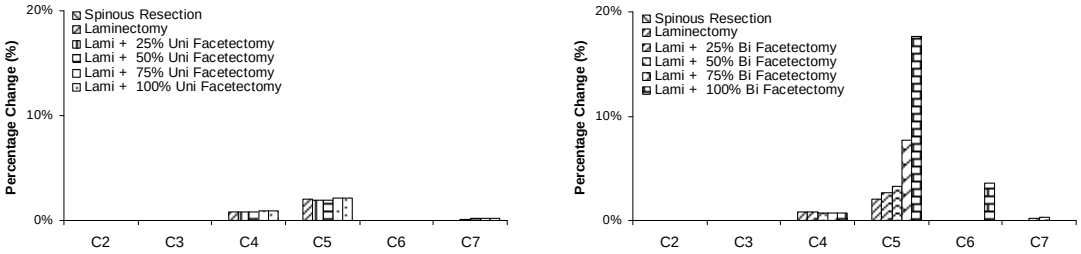

Right Axial Rotation

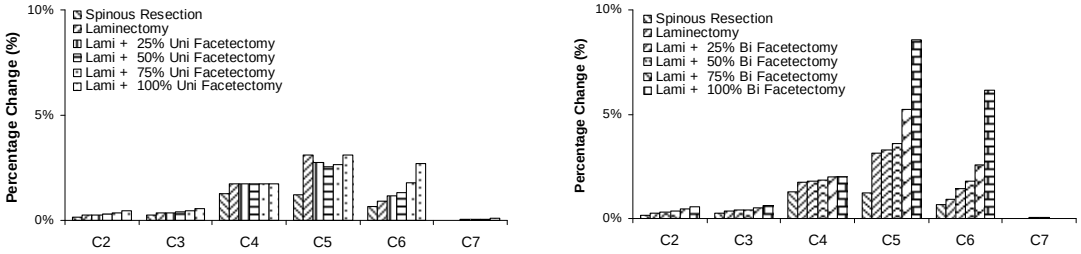

Left Axial Rotation

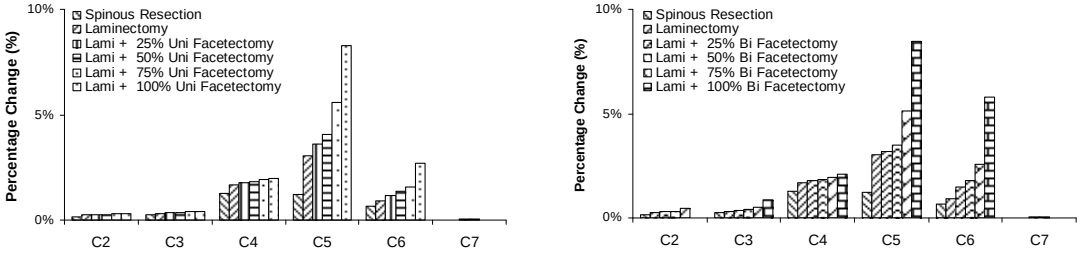

Figure 140: Relative percentage change in the cortical bone stress of the C2-C7 model due to laminectomy with progressive unilateral and bilateral facetectomy.

6.5.2.3 Discussion

In this study, a C2-C7 model was developed to determine the effects of spinous resection, laminectomy and laminectomy with progressive unilateral and bilateral facetectomy under physiological loads.

Goel et al., 1984 tested the flexibility of C4-C6 after applying a pure moment of 0.3 Nm on the C2-T2 specimens with spinous ligaments and ligamentum flavum removed at the C5-C6 level. The results indicated an increase of about 25% in flexion-extension, 6% in lateral bending and 3% in axial rotation. Four years later, Goel et al., 1988b found that flexion-extension loading using a pure moment of 0.3 Nm resulted in a significant increase of about 10% in the ROM after a two-level laminectomies. In 2003, their group, Kubo et a., 2003 repeated the experiment again using pure moments of 1.5 Nm. The results indicated an increase of 22% (±15) in flexion-extension, 8.4% (±6.6) in lateral bending and 23.7% (±13.8) under axial rotation after multiple level laminectomies. Ding et al., 1991 applied complex load simulating 1.0 Nm to four specimens with an increase of 15% in the ROM for the whole specimens under axial rotation after a two-level laminectomy. These findings are consistent with the current results, which indicated an increase in the C4-C5 ROM of 28% in flexion-extension, 1.08% in lateral bending and 2% in axial rotation after a single level laminectomy (Figure 138). In another study, Cusick et al., 1995 showed that a three-level laminectomy on C4-C6 induced significant increase of 120% (3.6º ±1.0 to 8.0º ±2.0) in total column flexibility using complex loading force of compression-flexion.

The current findings also agreed with clinical observations that postlaminectomy deformities occurred mainly in the sagittal plane with rotation and lateral bending being

negligible (Batzdorf and Batzdorff, 1988; Butler and Whitecloud, 1992; Mikawa et al., 1987).

The influence of facetectomy with or without laminectomy on the stability of cervical spine has been reported previously. Zdeblick et al., 1992 studied the biomechanical effects of graded bilateral facet resections after laminectomy. They measured the posterior displacement under flexion and rotational motions under axial rotation. They found that facetectomy of more than 50% after laminectomy caused a statistically significant loss of stability in flexion and axial rotation. However, changes in flexibility of the motion segments under flexion-extension and lateral bending remain unclear. Nowinski et al., 1993 tested several C2-C7 specimens to study on the influences of laminaplasty and laminectomy with 25% to 75% facetectomy. They reported that as little as 25% facetectomy adversely affects the cervical stability after multilevel laminectomy. However, changes in the cervical spinal stability after laminectomy without facetectomy remain unclear. It should be noted that previous *in vitro* studies indicated substantial increases in flexibility after laminectomy (Cusick et al., 1995; Goel et al., 1988b; Goel et al., 1984; Kubo et al., 2003). The present study also showed significant increase in flexibility after laminectomy and subsequent facetectomy with 50% resection. The results also demonstrated that increase in the inter-segmental ROM caused by surgical procedures is accompanied by higher disc annulus and cortical bone stress. This showed that the present finite element model is capable of delivering additional results, which are difficult or even impossible to acquire experimentally.

Degeneration of the spine manifests itself in many different ways. Osteophytes, facet degeneration and disc degeneration are some examples. Theories of bone remodelling

have shown that bony out-growth stems from higher stress or strain energy density (Brown et al., 1990; Kim et al., 1991). In the area of lumbar spine degenerative disc studies, Keller et al., 1989 conducted an experiment on twelve lumbar vertebral segments to determine the compressive mechanical properties of the human lumbar vertebral trabecular bone based on the anatomic origin, bone density and intervertebral disc properties. Goel et al., 1995b demonstrated that the strain energy density in the vertebral cortex and cancellous bone induced the remodelling processes in the form of external shape optimization and internal variations in elastic modulus, respectively. The present results indicated significantly increases in the disc annulus and cortical stress at C4, C5 and C6 levels under combined flexion-extension. Increase in the disc annulus stress magnitude may lead to degenerative changes and altered the structural properties as an adaptation to a higher stress environment. Furthermore, with the combination of increased cortical stress, the current results may partially explain the nature of accelerated degenerative process and formation of osteophytes after laminectomy with or without graded facetectomy. The influence of surgical techniques on the adjacent unaltered levels has been observed clinically (Takagi et al., 2002). As noted in the earlier clinical studies, the effectiveness of laminectomy in the management of cervical spondylosis, exclusive of the degenerative disease process that in itself contributes to progression of myelopathy or radiculopathy has been estimated to range from 22% to 60% (Epstein, 1988; Rowland, 1992). These studies indicated that the worsening of the clinical situation usually occurs by 24mths. This worsening is usually due to recurring of myelopathy or radiculopathy, especially after further osteophytes formation. Their observations were consistent with the current findings of increasing cortical bone and disc annulus stress after laminectomy alone.

6.5.3 One/Two Level Laminotomies and Laminectomies

Cervical stenosis can be managed by various surgical approaches such as laminotomy and laminectomy (Epstein, 2002). During these procedures, in order for the neurosurgeon to reach the affected nerves, it is necessary to remove either the lamina completely or part of it. Laminectomy involves removing the entire lamina completely. However, laminectomy may lead to segmental instability and kyphotic deformity (Epstein, 1988). Earlier studies also indicated significant increases in the ROM after laminectomy (Goel et al., 1988b; Goel et al., 1984; Nowinski et al., 1993; Zander et al., 2003). Therefore, various techniques have been explored to reduce surgical induced injury to the posterior structures while adequate cervical decompression is achieved. One of them is called laminotomy. Laminotomy is preferred over laminectomy to preserve the stability of the cervical spine. During laminotomy, only a small area of the lamina is extracted. The degree of stenosis usually determines the indication for either laminotomy or laminectomy on either single or two-level (Allen et al., 1987; An, 1998a; Dillin and Simeone, 1998; Eidelson, 2002; Ishida et al., 1989). Since these operations involve structural changes to the spine, it should be possible to offer biomechanical explanations for these post-surgical changes.

Some surgeons think that little can be gained by performing a multiple-level laminotomies compared with laminectomy for decompression. Because these surgeons think that the majority of the spinal stability is provided by the intervertebral disc and facets joints (Albert and Vacarro, 1998). However, there are no existing clinical studies in which a clear biomechanical advantage of laminotomy over laminectomy is shown. In addition, comparisons on the influences of the cervical biomechanics after laminotomy and laminectomy were not investigated. Furthermore, there is a lack of

consensus on the minimum numbers of motion segments needed to perform laminectomies accurately during *in vitro* experiments. The inclusion of five motion segments enabled the capture of these post-surgical changes on the adjacent unaltered spinal components realistically.

Therefore, the purpose of this study was to evaluate the inter-segmental rotational motions and stress of the C2-C7 spine after one/two-level laminotomies and laminectomies through analytical simulation. The author believes that improved understanding on the effect of post-surgical responses would help to develop better surgical techniques for the treatment and management of the cervical spine.

6.5.3.1 Methods

The C2-C7 intact model was modified to simulate one/two-level laminotomies and laminectomies at the C4 and C5 levels. Six models were created based on the various dorsal procedures used to decompress the nerve roots (An, 1998a; Dillin and Simeone, 1998; Epstein, 2003; Goel et al., 1988b; Kubo et al., 2003; Zdeblick et al., 1992).

1. One-level C4 laminectomy: removal of the C4 spinous process and left + right lamina. The spinous and flavum ligaments between C3 and C5 were removed.
2. One-level C5 laminectomy: removal of the C5 spinous process and left + right lamina. The spinous and flavum ligaments between C4 and C6 were removed.
3. Two-level C4 and C5 laminectomies: removal of the C4 and C5 spinous process and the associated left + right lamina. The spinous and flavum ligaments between C3 and C6 were removed.

4. One-level C4 laminotomy: removal of approximately 80% of the inferior laminae of C3 and approximately 20% of the superior laminae of C4, along with the connected ligamentum flavum.
5. One-level C5 laminotomy: removal of approximately 80% of the inferior laminae of C4 and approximately 20% of the superior laminae of C5, along with the connected ligamentum flavum.
6. Two-level C4 and C5 laminotomies: removal of approximately 80% of the inferior laminae of C3, entire C4 laminae and finally, approximately 20% of the superior laminae of C5, along with all the connected ligamentum flavum.

The models were then exercised under similar loading and boundary configurations described in Section 6.5.1.1 Methods. Since the postlaminectomy deformities found in patients due to large rotational motions occurred mainly in the sagittal plane with axial rotation and lateral bending being negligible, this section will focus on presenting and discussing the results under combined flexion-extension (Batzdorf and Batzdorff, 1988; Butler and Whitecloud, 1992; Mikawa et al., 1987). Additional results under lateral bending and axial rotation can be found in the Appendix (A.5 Additional Results for One/Two Level Laminotomies and Laminectomies).

a) b)

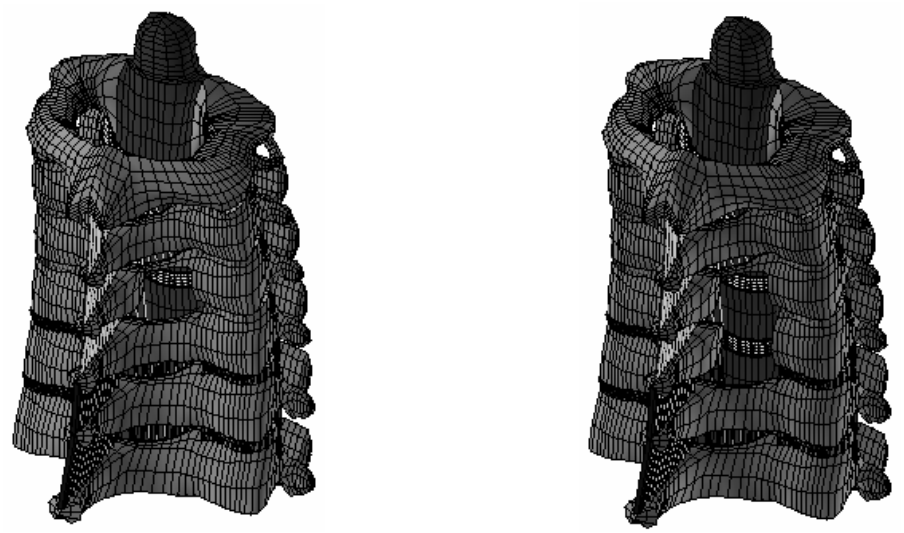

Figure 141: Iso-posterior view of the a) one-level C4 laminotomized model, b) two-level C4 and C5 laminotomized model.

6.5.3.2 Results

The results indicated the significant influence of one and two-level laminectomies under combined flexion-extension (Figure 142). Furthermore, laminectomy performed on a single vertebra (e.g. C4) would influence the inter-segmental ROM at the affected levels (C3-C4 and C4-C5) significantly, while the adjacent levels (C2-C3 and C5-C6) were only slightly affected. The results also showed a slight increase in the inter-segmental ROM after one-level and two-level laminotomies. Overall, the C2-C7 ROM due to two-level removals was about 50% (laminotomies) and 40% (laminectomies) higher than the one-level resection.

The relative increase in the ROM (Figure 143) due to laminectomies correlated well against published data (Goel et al., 1988b; Goel et al., 1984; Kubo et al., 2003). For the C2-C7 model after C5 laminectomy, the predicted increase in the C4-C5 ROM is 28% and C5-C6 ROM is 25%, respectively. This is consistent with the results obtained by

Goel et al., 1984, who obtained a 25% increase in the inter-segmental ROM. For the C2-C7 model after a two-level C4 and C5 laminectomies, the predicted increase in the C3-C6 ROM is 25%. The current results are very close to the experimental data obtained by Kubo et al., 2003. Kubo et al., 2003 obtained a 22% increase in the C2-C7 ROM after a four-level C3, C4, C5 and C6 laminectomies.

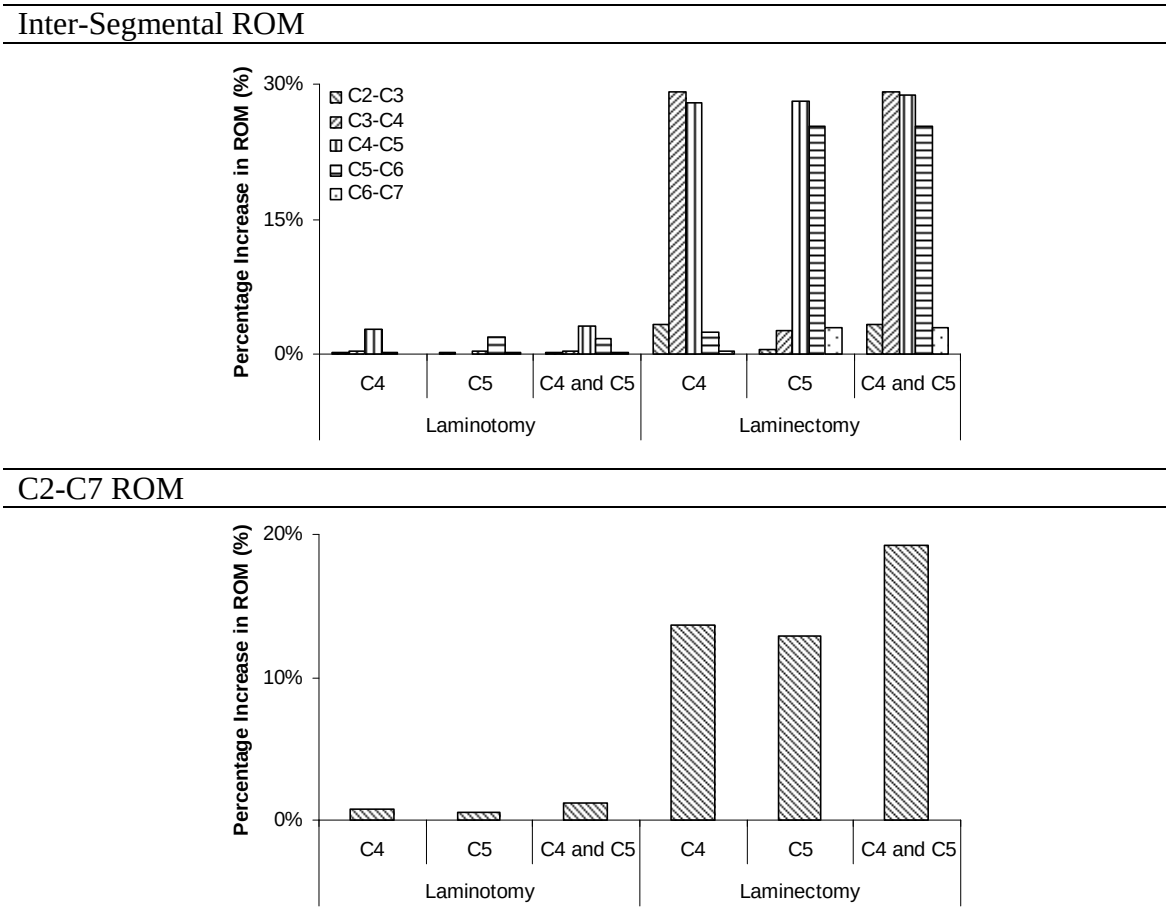

Figure 142: Percentage increase in the ROM after one or two level laminotomies and laminectomies under combined flexion-extension.

Overall, significant increase in the disc annulus stress at the affected levels was observed after laminectomies under combined flexion-extension (Figure 144). It should be noted that the disc annulus were calculated from two regions, anterior and posterior regions. The predicted results correlated well with the increase in the ROM at these levels. Although these surgical procedures involved the removal of posterior structural

elements, it is interesting to note that the increase in the predicted stress at the anterior and posterior region of the disc annulus was very close. After C5 laminotomy, the predicted C4-C5 and C5-C6 disc stress showed minor increase of about 1%. After C5 laminectomy, the predicted C4-C5 and C5-C6 disc stress increased by approximately 25%.

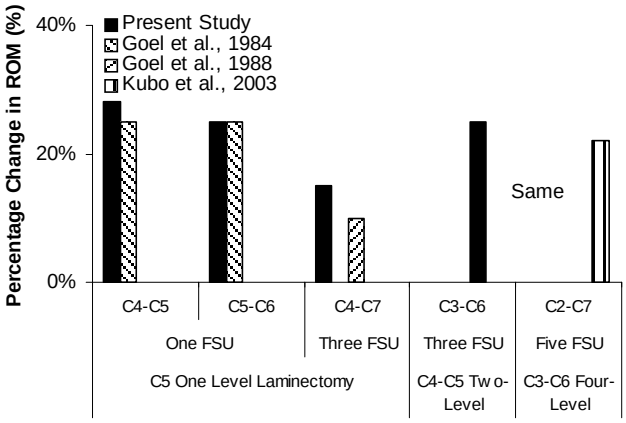

Figure 143: Comparing the relative increase in the rotational motions after laminectomies against experimental data (Goel et al., 1988b; Goel et al., 1984; Kubo et al., 2003). Goel et al., 1984 only removed the spinous ligaments and ligamentum flavum.

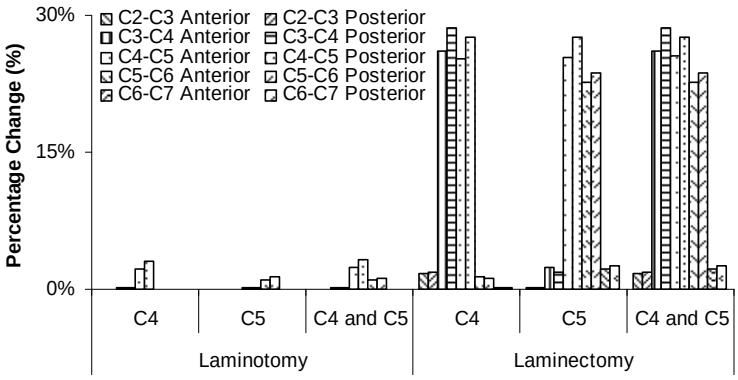

Figure 144: Percentage increase in the disc annulus stress after one or two level laminotomies and laminectomies under combined flexion-extension.

The cortical bone stress increases significantly at the affected levels (C3 – 35%, C4 – 28% and C5 – 15%) and slightly at the adjacent levels (C2, C6 and C7) after a one-level C5 laminectomy under combined flexion-extension (Figure 145). For a two-level C4 and C5 laminectomies, the C3, C4, C5 and C6 cortical bone stress increases by about 26%, 31%, 28% and 15%, respectively while C2 and C7 cortical stress only increases very slightly. One-level or two-level laminotomies increase the cortical stress at the affect levels by approximately 5-7%.

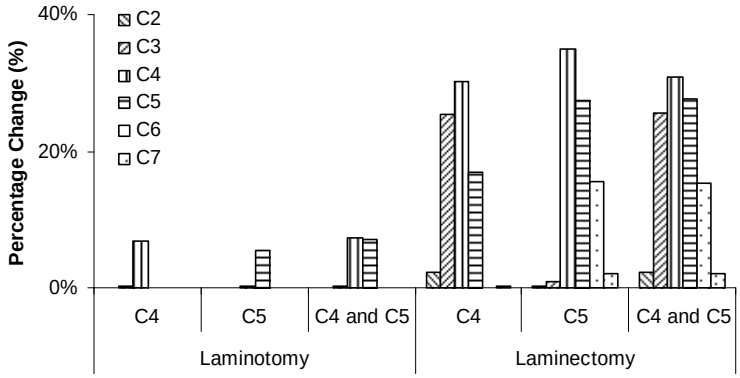

Figure 145: Percentage increase in the cortical bone stress after one or two level laminotomies and laminectomies under combined flexion-extension.

6.5.3.3 Discussion

Decompression of the cervical spinal cord can be accomplished through surgical techniques like laminotomies or laminectomies. One/multi-level laminectomies effectively decompress the spinal cord, but may cause severe spinal instability. In this regard, accurate assessment of spinal stability is an important clinical parameter. The magnitude of spinal instability dictates the necessary treatment protocol (e.g., external implant devices or surgical intervention). The mechanical nature of the instability is important in determining the treatment technique that would most effectively reduce the instability.

In this study, an anatomically accurate C2-C7 finite element model was developed to determine the biomechanical influence of laminotomies and laminectomies. The results showed that one/two-level laminectomies performed on the C2-C7 model influence the cervical spinal biomechanics significantly under combined flexion-extension. This is in agreement with the experimental findings and clinical observations of postlaminectomy kyphosis reported in the literatures. Yasuoka et al., 1981 and 1982 described the development of spinal deformities in all his patients after cervical laminectomy. Mikawa et al., 1987 noted a 14% occurrence of kyphosis after cervical laminectomy for the treatment of spondylosis. Recently, Kaptain et al., 2000 found out that up to 21% of patients who have undergone laminectomy may develop kyphosis. This increase in the flexibilities due to the various surgical techniques may potentially influence the motion segments to alter the load distribution, hence accelerating the process of disc degeneration and osteophyte formation. This can be seen by the increase in the cortical stress at the affected levels after laminotomies or laminectomies and under combined flexion-extension. The losses of these normal motions under combined flexion-extension may also place the cervical musculature at a significant mechanical disadvantage, requiring constant muscular contraction to maintain upright head posture (Albert and Vacarro, 1998).

There also exists confusion among the various researchers concerning the minimum number of motions segments needed to perform laminectomy studies (Table 17). The FE results indicated the influence of laminectomy on the rotational motions of the adjacent levels. The influence of surgical techniques on the adjacent levels had been observed clinically as well (Takagi et al., 2002). This is in good agreement with Goel et al., 1984 who showed that the C4-C5 and C5-C6 inter-segmental ROM increases after

the resection of spinous and flavum ligaments. However, subsequent researchers failed to recognize the influence of these adjacent segments and chose to constrain them (Kubo et al., 2003; Kumaresan et al., 1997; Nowinski et al., 1993; Saito et al., 1991). Furthermore, computing the relative changes using gross ROM will neglect the impact of various surgical techniques on the respective levels or inter-segmental ROM. Therefore, the minimum numbers of cervical vertebrae needed to perform cervical laminectomy studies are proposed as follows:

$$S = NL + UL + LL \qquad \textbf{Equation 9}$$

where S is the minimum number of cervical vertebrae for laminectomy studies, NL is the number of laminectomy levels, UL is the minimum number of cervical levels above the laminectomy levels and LL is the minimum number of cervical levels below the laminectomy levels. In this case, UL and LL have a constant value of two. To analyze a one-level laminectomy, a minimum of five vertebrae are needed, whereas a two-level laminectomies requires a minimum of six vertebrae. For a C5 laminectomy study, a minimum of five vertebrae are needed. Two vertebrae (C3 and C4) above C5 and two vertebrae (C6 and C7) below C5. For a two-level C4 and C5 laminectomies, a minimum of six vertebrae are needed. Two vertebrae (C2 and C3) above C4 and two vertebrae (C6 and C7) below C5. Equation 9 is only applicable to the lower cervical spine, extension of this equation to other regions (thoracic and lumbar) or transition spine (cervico-thoracic and thoraco-lumbar) for laminectomy studies will require further testing and analysis.

Investigator	In Vitro					FEM	
	Goel et al., 1984	Goel et al., 1988	Zdeblick et al., 1992	Nowinski et al., 1993	Kubo et al., 2003	Saito et al., 1991	Kumaresan et al., 1997
Segments	C1-T2	C2-T2	C3-C7	C2-C7	C2-T1	C0-T2	C4-C6
Surgical Techniques	Resection of supraspinous, interspinous and flavum ligaments	Two level (C5 and C6) laminectomies	One level C5 laminectomy with progressive bilateral C5-C6 facetectomies	Four level (C3, C4, C5 and C6) laminectomy with 25%, 50% and 75% facetectomies	Four level (C3, C4, C5 and C6) laminectomies	All level laminectomies	C5 laminectomy
Rotational Motions	C4-C5 and C5-C6	C4-C7	Only C3-C7 torsional stiffness	C2-C7 intersegment	C2-C7	-	C4-C6
Remarks	Posterior arch not removed	Posterior arch not removed	No information on unilateral facetectomy	No results based on laminectomy only. Constraints placed on adjacent level	Constraints placed on adjacent level	No validation. Only graphical illustrations, constraints placed on adjacent level	Linear model, constraints placed on adjacent level

Table 17: Summary of *in vitro* studies on laminectomies.

Currently, there is a significant interest to develop minimally invasive cervical spinal surgical procedures to treat patients with cervical stenosis adequately while the structural preservation of the spine is maximized. In an effort to eliminate these negative aspects of conventional laminectomy, a surgical technique called laminotomy has been used (Ishida et al., 1989). Clinical studies performed by Ishida et al., 1989 showed a smaller incidence of postoperative spinal deformity with laminotomy as compared to laminectomy. Their findings agreed with the present results of minimal increase in the ROM after one and two-level laminotomies.

6.5.4 Post-Surgical Laminectomy

The studies on the various surgical techniques in the earlier sections (Section 6.5.1 to 6.5.3) only considered the immediate post-surgical responses as only static nonlinear analyses were performed. However, to investigate the long-term post-operative changes

under constant loading, it is necessary to develop a viscoelastic cervical spine model, using time-dependent material properties and nonlinear transient analysis. The viscoelastic behaviour of the lumbar intervertebral disc has been well classified and studied for many years using *in vitro* experiments or finite element simulations (Best et al., 1994; Hakim and King, 1979; Lu et al., 1996; Lu et al., 1998; Marchand and Ahmed, 1990; Skaggs et al., 1994; Wang et al., 2000; Wang et al., 1997). However, in the cervical spine modelling, no consideration has been given to understand the viscoelastic behaviour of the intervertebral disc on the cervical ROM. Thus, the rate dependent nature of the cervical segments cannot be simulated and the effect of long-term post-operative changes cannot be evaluated. One reason is due to the lack of material classification on the viscoelastic material properties of the cervical intervertebral disc.

6.5.4.1 Methods

In order to establish the viscoelastic simulation capabilities on the cervical spine model, viscoelastic material properties from the lumbar spine was adopted in the present study. This initial element idealization is justifiable because of the similarities in the time-dependent material composition of the cervical components with the lumbar spine (Yoganandan et al., 1996a). As structural and material properties on the cervical spine were developed through *in vitro* testing, better element idealization can be incorporated into the current finite element model though further refinements. Therefore, in the current study, the intervertebral disc is refined and modelled as a nonlinear, homogeneous and viscoelastic structure.

The Prony series (*ANSYS 7.0 Documentation and User Manual*, 2002) was used to simulate the viscoelastic behaviour of the disc annulus. The shear and bulk moduli are expressed in the form:

$$G_R(t) = G_o\left(1 - \sum_{i=1}^{n} g_i(1 - e^{\frac{-t}{t_i}})\right) \qquad \textbf{Equation 10}$$

$$K_R(t) = K_o\left(1 - \sum_{i=1}^{n} k_i(1 - e^{\frac{-t}{t_i}})\right) \qquad \textbf{Equation 11}$$

where $G_R(t)$ and $K_R(t)$ is the normalized shear and bulk modulus respectively, g_i and k_i are the modulus ratio of the shear and bulk modulus respectively, t_i is the relaxation time constant, t is the time and G_o and K_o is the instantaneous shear and bulk modulus respectively at t = 0. The viscoelastic material properties used for the intervertebral disc are listed in Table 18. The material properties of the remaining cervical spinal components are identical to the values described earlier (Table 15).

The loads were applied to the C2-C7 viscoelastic model in two parts. In the first part, steady state analysis was performed and 1.5 Nm in flexion or extension was applied to the superior surface of the moving vertebrae, similar to the loading described in Section 6.5.1.1 Methods. In the second part, transient analysis was performed, the time was set to 3600s and the pure moment applied during the first part was kept constant. The steady state analysis in the first load step can help to reduce the computational time tremendously. Two models were used, an intact and C5 laminectomized model. The C5 laminectomized model was created based on the techniques described earlier (Refer

6.5.3 One/Two Level Laminotomies and Laminectomies). The inter-segmental ROM against time relationship was obtained and analyzed.

	Elastic Modulus (MPa)	Poisson's Ratio	Shear	Bulk	Relaxation Time(s)
Disc Annulus	4.2	0.45	g_1=0.3991	k_1=0.3991	t_1=3.45
			g_2=0.0000	k_2=0.300	t_2=100
			g_3=0.3605	k_3=0.149	t_3=1000
			g_4=0.1082	k_4=0.150	t_4=5000
Disc Nucleus	1.0	0.499	g_1=0.6375	k_1=0	t_1=0.141
			g_2=0.1558	k_2=0	t_2=2.21
			g_3=0.1202	k_3=0	t_3=39.9
			g_4=0.0383	k_4=0	t_4=266
			g_5=0.0000	k_5=0.8	t_5=500

Table 18: Viscoelastic material properties of the intervertebral disc (Wang et al., 1997).

6.5.4.2 Results

The results showed that the C2-C7 ROM increase by about 44% after post-surgical changes from time 0 to time 3600s under flexion (Figure 146). The results are obtained by normalizing the ROM obtained at the final time (3600s) with respect to the ROM obtained at the start time (0secs). Overall, the percentage increase in the C3-C7, C4-C7, C5-C7 and C6-C7) ROM from time 0 to time 3600s is very close to the percentage increase seen on the C2-C7 ROM. Under extension, the C2-C7 ROM increase by at a lower magnitude of approximately 25% from time 0 to time 3600s (Figure 147) This was due to the presence of the facet joint in resisting extension motion, thereby reducing the load transfer through the intervertebral disc. The results indicated that the

viscoelastic behaviour of the intervertebral disc under constant flexion and extension loads has a high influence on the C2-C7 ROM.

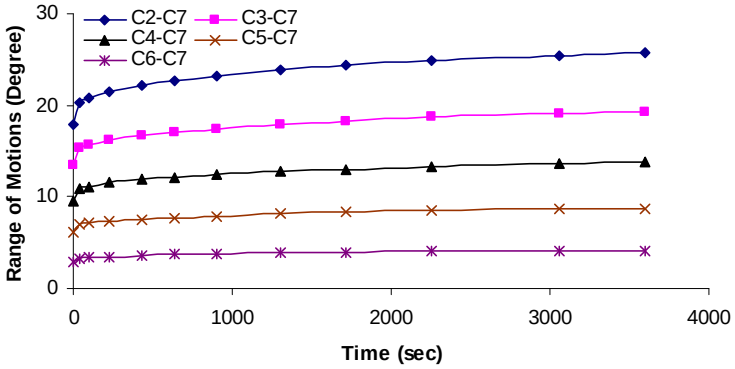

Figure 146: Predicted ROM against time for the intact model in flexion.

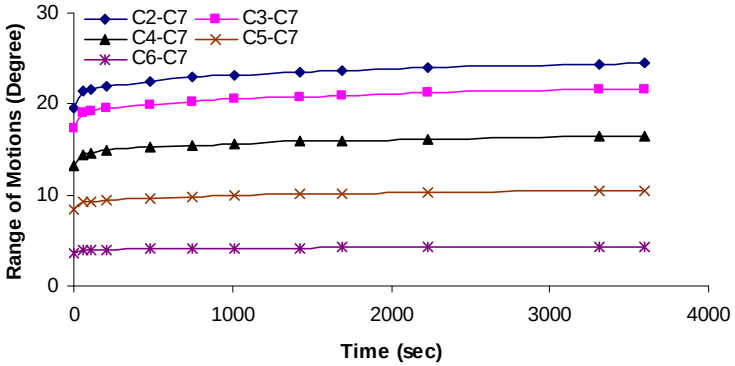

Figure 147: Predicted ROM against time for the intact model in extension.

For the laminectomized model, the C2-C7 ROM increase by about 58% from time 0s to time 3600s (Figure 148). The percentage increases in the C2-C7 ROM from 0s to 3600s are higher in the laminectomized model (58%) as compared to the intact model (44%). At the start of the time cycle, the C2-C7 ROM for the laminectomized model is about 32% higher than the normal intact model. This increased to about 44% at the end of the time cycle. This showed that laminectomy, which requires the removal of ligaments

(spinous ligaments, ligamentum flavum) and spinous process increase the load transfer through the intervertebral disc under flexion. Under extension, the difference between the predicted ROM of the intact and laminectomized model over time were found to be minimal (Figure 149).

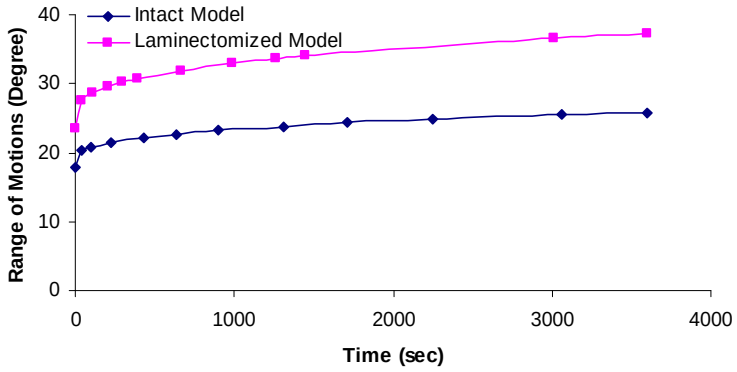

Figure 148: Comparison between the intact and laminectomized model in flexion.

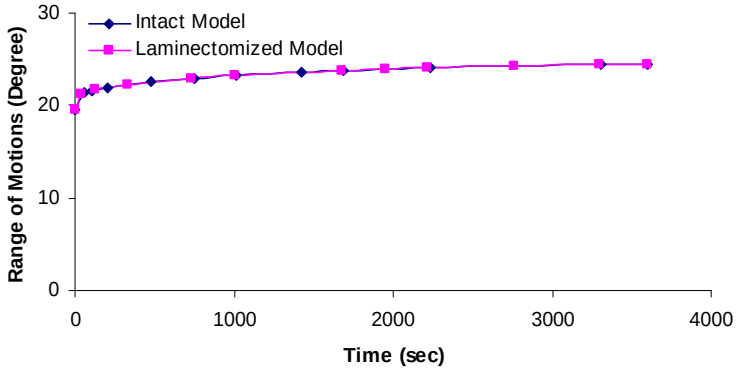

Figure 149: Comparison between the intact and laminectomized model in extension.

6.5.4.3 Discussion

In this study, a nonlinear viscoelastic C2-C7 FE model was used to predict the time-varying behaviour of the intact and surgically altered cervical spine under flexion and extension. The previous static FE models would not be able to predict the variation of

ROM with time. Hence, the current viscoelastic model represented advancement in providing the time and history dependencies on the ROM subjected to the same loading conditions.

However, several limitations and assumptions were applicable to the current model. Firstly, it was noted that the viscoelastic material properties was taken from the lumbar spine. Secondly, the lack of validation on the viscoelastic model, because all the viscoelastic studies (*in vitro* and FE) reported in the literatures were related to the lumbar spine (Best et al., 1994; Lu et al., 1998; Wang et al., 2000; Wang et al., 1997). Nevertheless, these analyses have provided some understanding on the biomechanical behaviour of lumbar spine under long-term conditions, but the behaviour of the cervical spine remains unknown. Third limitation was that the material properties of hard tissues were assumed to be linear and not time dependent. This model idealization was reasonable because the contribution of the hard tissue to the overall ROM was relatively small as demonstrated in the earlier study. Another limitation was that immediately following surgery, patients are often placed in controlled conditions (e.g., Halo) to minimize loading on the altered spine until certain strength/stability level is reached. Due to this, the viscoelastic model was only subjected to 3600s of loading.

6.6 Summary

Overall, the modulating effects of muscles, changes in material properties of spinal structures due to various degenerative processes and the narrowing of the canal due to stenosis were not considered in this study. In this study, the biomechanical responses of the C2-C7 model in flexion, extension, lateral bending and axial rotation after various surgical techniques were investigated. Prior to the analysis, the C2-C7 was refined

geometrically and materially. The refined model was then use to investigate the effects of preload and orientation on the cervical spine responses. Furthermore, previous FE studies on the cervical spine has focused on linear analysis and using limited numbers of motion segments, which may potentially limit the accuracy of the predictions. Fortunately, the inclusion of five-level motion segments allowed the study of various surgical techniques in a more realistic manner.

The salient findings are summarized as follows:

1. Material Sensitivities
    a. Soft tissue has a higher impact on the ROM than hard tissue
2. Effects of preloads and orientations
    a. Under normal orientation and increasing preload magnitudes, the predicted ROM increases under flexion and decreases under extension, lateral bending and axial rotation.
    b. Due to this, it is necessary to establish a standard for *in vitro* testing. The current study recommended biomechanical investigators to align the cervical spine in the physiological position during testing.
3. Progressive unilateral and bilateral facetectomy
    a. First study reported in the literatures using multiple cervical spine motion segments and conducted using nonlinear analysis.
    b. Percentage increase in the ROM after facetectomy correlated well with the data reported in the literatures.
    c. Substantial increase in the ROM can be observed with unilateral or bilateral facet resection of greater than 50% under all loading modes
4. Laminectomy with unilateral and bilateral facetectomy

a. *In vivo* and *in vitro* studies currently lack the capacity for documenting the external and internal biomechanical changes of the surgically altered cervical spine.
b. First study reported in the literatures using multiple cervical spine motion segments and conducted using nonlinear analysis.
c. Percentage increase in the ROM after laminectomy compared well against experimental data
d. Most of the biomechanical changes occurred at the C4-C5 and C5-C6 segments, but some also occurred at C3-C4 and C6-C7 segments.
e. With combined flexion and extension loading, C5 laminectomy significantly affected the stability of the cervical spine at the C4-C5 and C5-C6 levels. Subsequent progressively facetectomy performed at C5 and C6 levels only affected the C5-C6 inter-segmental ROM.
f. Increases in the ROM caused by surgical procedures were accompanied by higher stress in the intervertebral disc and cortical shell.

5. One/Two Level laminotomies and laminectomies
    a. Development of the research relevant equation regarding the number of motion segments needed to perform laminectomy studies
    b. Multi-level laminotomies are preferred over one-level laminectomies based on the biomechanical parameters obtained in the study.
6. Post-Surgical Laminectomy
    a. A viscoelasticity cervical model has been developed and used to understand the effects of post-surgical laminectomies on the cervical spinal ROM.
    b. Laminectomized model caused a higher percentage increase in the C2-C7 ROM in flexion as compared to the intact model at the end of the loading

time. This showed that laminectomy, which requires the removal of spinous ligaments and ligamentum flavum, increase the load transfer through the intervertebral disc under flexion after extended period of time.

Chapter 7. Investigation of Disc Degeneration

7.1 Introduction

Cervical spondylosis is a common degenerative condition affecting all levels of the cervical spine. Cervical spondylosis encompasses a sequence of degenerative changes in the intervertebral discs. During the degeneration process, the disc undergoes progressive structural changes in the form of dehydration of the nucleus pulposus and collapse of the annulus fibrosus resulting in decreased disc height (Figure 150). These changes affect the biomechanics of the cervical spine. Dehydration of the nucleus increases the compressive stiffness of the lumbar and cervical spine (Kim et al., 1991; Kumaresan et al., 2001). However, the influence of the disc degenerative process on the biomechanical responses under flexion, extension, lateral bending and axial rotation remains unknown.

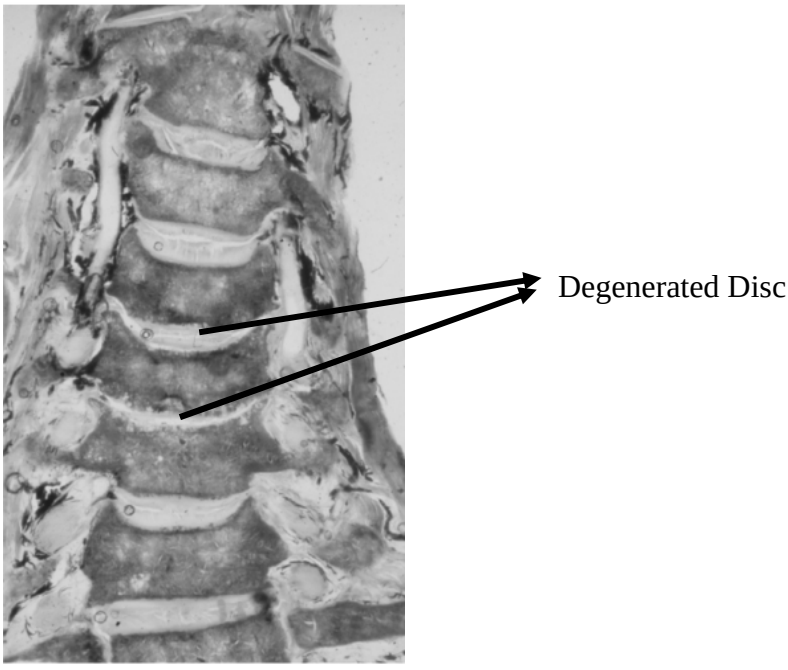

Figure 150: Illustration of the C4-C5 and C5-C6 degenerated cervical disc (Yoganandan et al., 2001).

Because bones remodel in relation to mechanical stress, the degenerative disc process response may lead to the formation of osteophytes or bone spurs in most instances. Theories of bone remodelling phenomena have also shown that bony outgrowth stems from higher stress or strain energy density (Brown et al., 1990; Kim et al., 1991). Osteophytes by themselves may ultimately stabilize the degenerative disc segment over time. However, osteophytes may potentially compress the spinal cord or a spinal nerve, resulting in myelopathy and radiculopathy (Lestini and Wiesel, 1989). However, the formation of osteophytes due to degeneration under physiological loading is not well understood.

Therefore, the current chapter aims to provide further understanding on the influence of disc degeneration on the biomechanics of the cervical spine, including the formation of osteophytes under combined flexion-extension, lateral bending and axial rotation. It was mentioned earlier (Refer 6.1 Introduction) that laminectomy and facetectomy are usually performed after cervical spondylosis is diagnosed, which caused myelopathy and radiculopathy. Several studies have been conducted using FE to investigate the influence of the various surgical techniques of a normal cervical disc. However, till now, the influence of disc degeneration after these surgical techniques remains unknown. Therefore, a secondary objective in this chapter includes the investigation on the influence of disc degeneration after various surgical techniques.

7.2 Disc Nucleus

Disc nucleus can be modelled in a number of ways. Earlier researchers choose the simplest way and modelled it using solid elements (Table 19). This element idealization was consistent with other FE reported in the literatures. However, in order to simulate

the disc nucleus better, it was necessary to model it using fluid elements. Thus, fluid elements were used to model the disc nucleus contained within annulus ground substance having no net flow rate. This improvement relative to previous models enabled a more realistic representation of the disc nucleus.

Authors	Element Type	Material properties
(Saito et al., 1991)	Two dimensional linear triangular	-
(Kumaresan et al., 1997)	Three-dimension solid	E (MPa) – 1.0, υ - 0.49
(Voo et al., 1997)	Three-dimension solid	E (MPa) – 1.0, υ - 0.49
(Goel and Clausen, 1998)	Three-dimensional Fluid	Bulk Modulus 1667
(Maiman et al., 1999)	Three-dimension solid	E (MPa) – 3.4, υ - 0.49
(Natarajan et al., 1999)	Three-dimension solid	E (MPa) – 3.0, υ - 0.49
(Chen et al., 2001)	Three-dimension solid	E (MPa) – 3.4, υ - 0.499

Table 19: Summary of the finite element modelling on disc nucleus.

7.3 Validations

7.3.1 External Biomechanical Responses

This study was performed on a new three-dimensional nonlinear intact C2-C7 model. Predicted biomechanical responses from the new model was compared against the earlier validated model (Refer 6.4 Validation of C2-C7 Model) and in vitro data under similar loading and boundary conditions (Panjabi et al., 2001). The results shown in Figure 151 - Figure 153 compared well against the earlier models and in vitro data. As noted in the earlier comments (Refer 6.4 Validation of C2-C7 Model), the old model generally predicted a lower ROM under lateral bending as compared to the *in vitro* data. The higher predicted ROM under lateral bending using the current model provided a more accurate assessment of the actual cervical spine biomechanics.

C2-C3

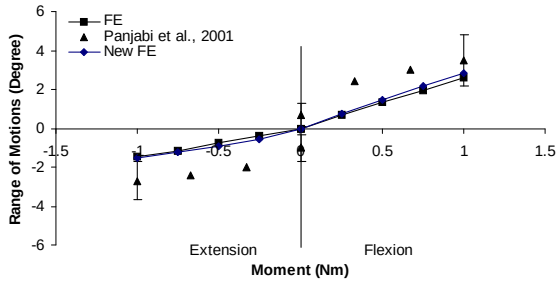

C3-C4

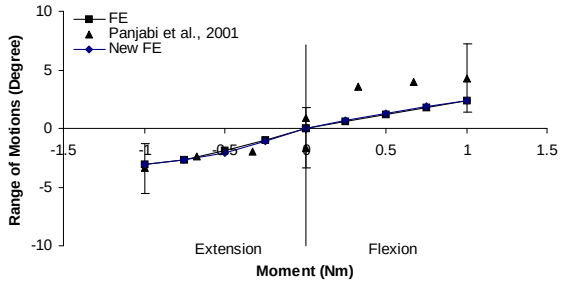

C4-C5

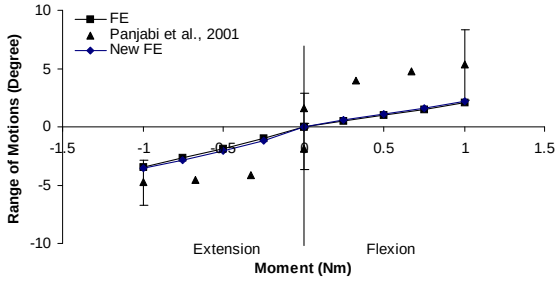

C5-C6

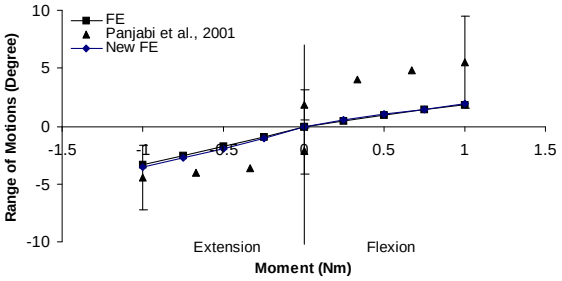

C6-C7

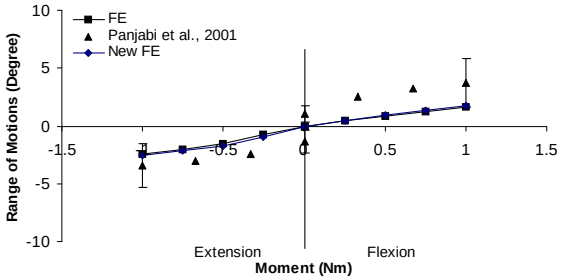

Figure 151: Comparison of the new, old FE models and in vitro data under flexion-extension.

C2-C3

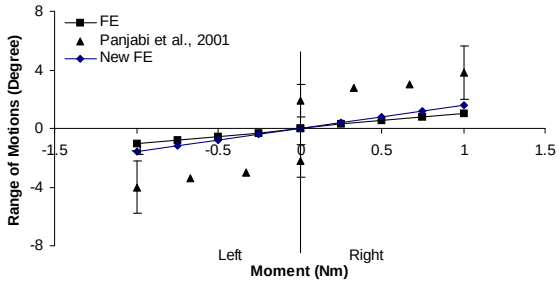

C3-C4

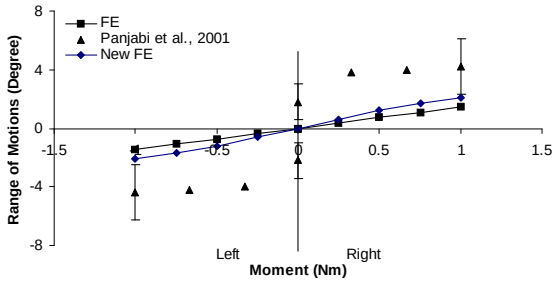

C4-C5

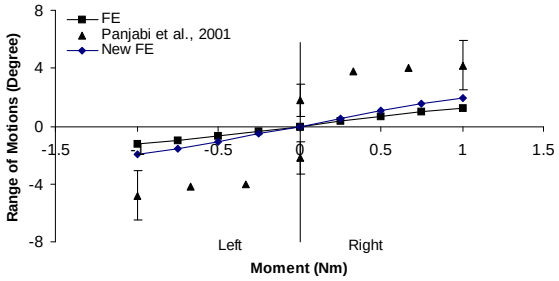

C5-C6

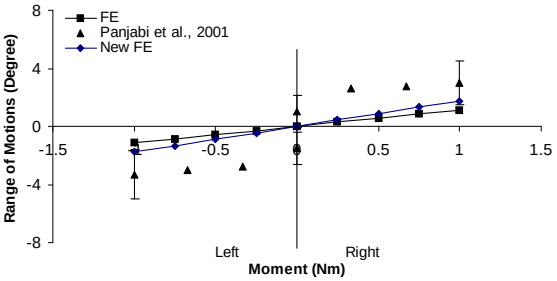

C6-C7

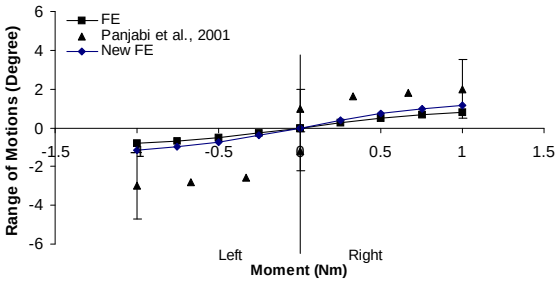

Figure 152: Comparison of the new and old FE models under lateral bending.

C2-C3

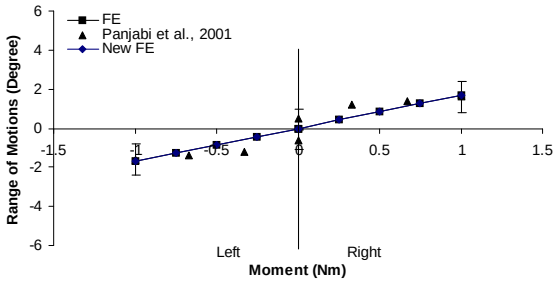

C3-C4

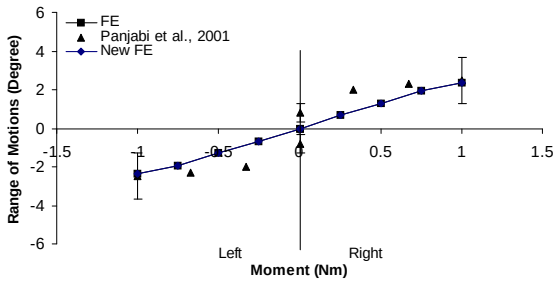

C4-C5

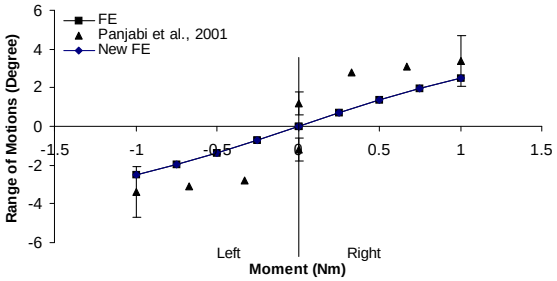

C5-C6

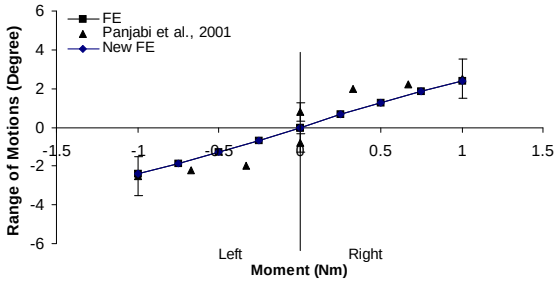

C6-C7

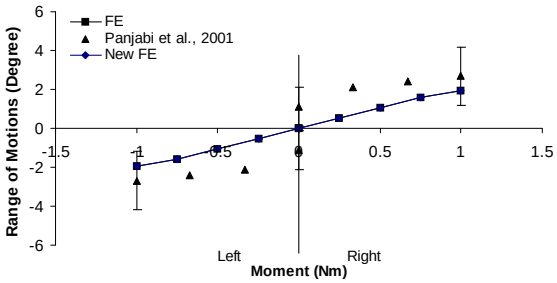

Figure 153: Comparison of the new and old FE models under axial rotation.

7.3.2 Internal Disc Pressure

This study was performed on C2-C3 and C4-C5 FSU models (Figure 154). These models were created from the intact C2-C7 model by removing the unnecessary vertebrae, intervertebral disc and its associated soft tissues. The two FSUs were tested under axial compression. Loading forces were applied to the superior moving vertebra

and the lower vertebra was fixed in all directions of movements. The resulting internal disc nucleus hydrostatic pressure were obtained and compared against *in vitro* obtained by Cripton et al., 2001 (Figure 155 - Figure 156).

a) b)

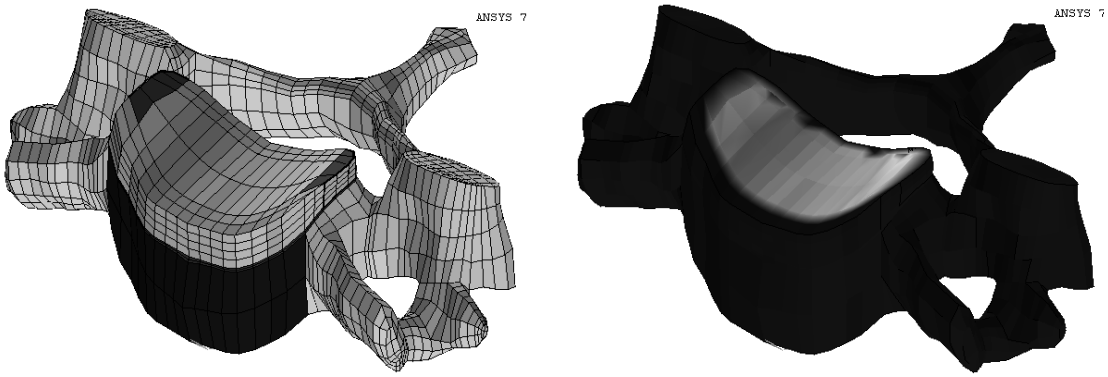

Figure 154: C4-C5 FSU. a) intact FE model and b) disc nucleus hydrostatic pressure under axial compression.

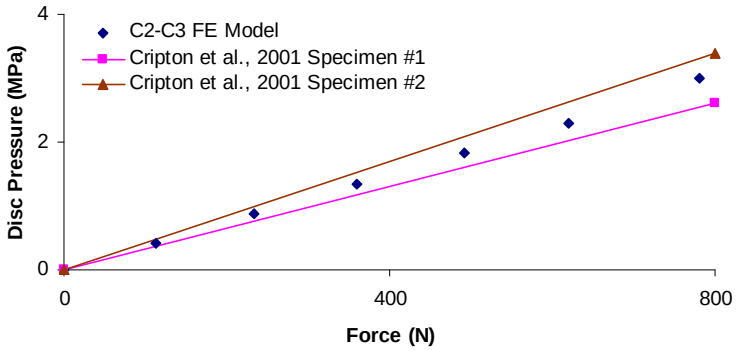

Figure 155: Comparisons of the C2-C3 intervertebral disc pressure against literature data (Cripton et al., 2001).

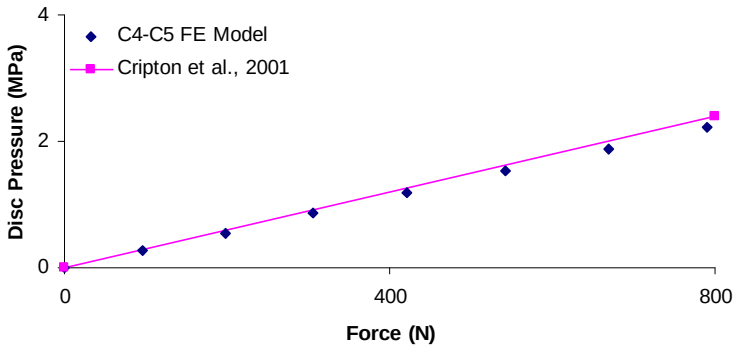

Figure 156: Comparisons of the C4-C5 intervertebral disc pressure against literature data (Cripton et al., 2001).

The predicted results showed that the disc pressure increased linearly with applied axial compression. This behaviour was consistent with the findings obtained through *in vitro* studies reported in the literatures (Cripton et al., 2001; Nachemson, 1960). However, the predicted and measured cervical disc pressures were considerably higher than those of the lumbar spine. For example, Nachemson reported pressures of 0.67 MPa and 0.82 MPa using L3–L4 and L2–L3 discs, respectively, under 800 N of compression (Nachemson, 1960). McNally and Adams reported a pressure of 0.5 MPa for a L2–L3 disc under 500 N of compression (McNally and Adams, 1992). This phenomenon was not surprising since the disc pressure for a given force is known to be inversely proportional to disc cross-sectional area and the cervical disc cross-sectional area is significantly smaller than the lumbar disc. To the author's knowledge, validation of the cervical spine model using internal disc pressure has never been investigated using FEM nor has it been reported in the literatures. These additional validations showed that the current FE model of the cervical is an accurate replica of the actual human cervical spine in terms of the external and internal biomechanical responses.

7.4 Disc Degeneration

7.4.1 Methods

In this study, degenerative changes in the intervertebral disc were classified as slight and moderate based on the mechanical changes reported in the literatures (Kumaresan et al., 2001; Lestini and Wiesel, 1989; Natarajan et al., 1994). These two progressive grades of disc degeneration were simulated at the C5-C6 level in the intact C2-C7 model. Grade 1 (slight degeneration) was represented by the alteration of the material properties to represent the actual *in vivo* dehydration process of the nucleus pulposus. To model Grade 1 disc degeneration, the three-dimensional incompressible fluid elements were replaced with stiffer three-dimensional solid elements that support structural nonlinearity. The modulus of the disc nucleus was changed to two times the modulus of the disc annulus in the intact model (Kim et al., 1991; Kumaresan et al., 2001; Lestini and Wiesel, 1989). Grade 2 (moderate degeneration) included Grade 1 changes and added modification of the fiber content and material properties of the annulus fibrosus representing the disintegrated nature of the annulus. The modulus of the disc annulus was assigned two times the value of the disc annulus in the intact model, and the annulus fiber volume was reduced by 25% from the value of the intact model (Ghosh, 1988; Kumaresan et al., 2001). Finally, the C2-C7 models with two types of C5-C6 disc degeneration were analyzed using similar loading and boundary conditions described earlier (Refer 7.3 Validations).

7.4.2 Results

The results (Figure 157) showed that C5-C6 disc degeneration would significantly influenced the ROM at the affected C5-C6 levels in all modes of loading studied. Under combined flexion-extension, Grade 1 disc degeneration reduced the C5-C6 ROM

by 40% whereas Grade 2 reduced the C5-C6 ROM by 52%. The highest percentage reduction can be seen under lateral bending. Generally, the percentage reduction in ROM increases with progressive disc degeneration.

Combined flexion-extension

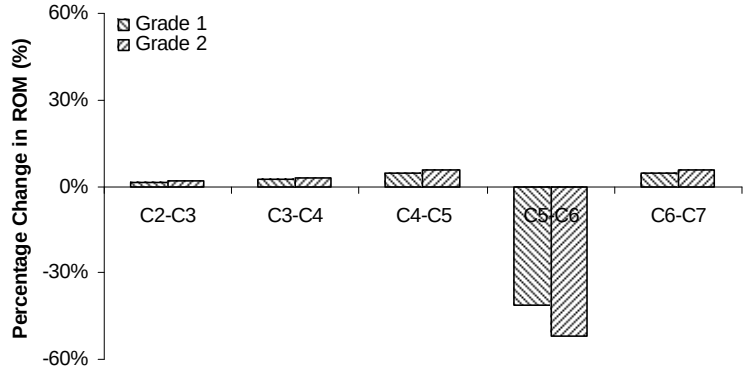

Lateral Bending

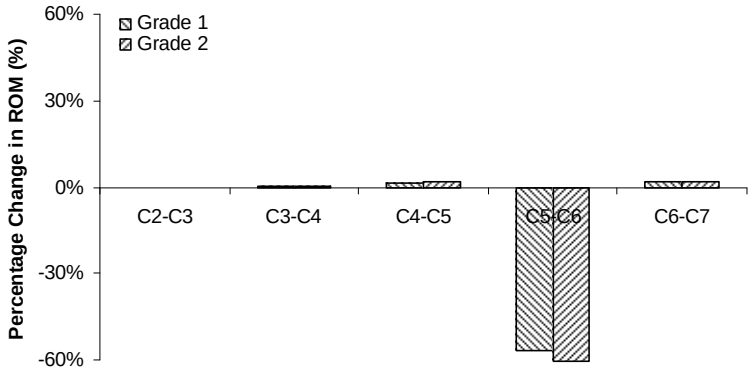

Axial Rotation

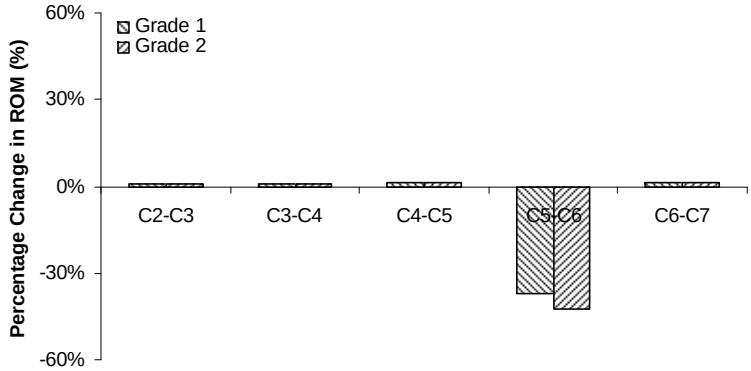

Figure 157: Influence of C5-C6 disc degeneration on the ROM.

Similarly, the responses of the intervertebral disc (Figure 158) varied considerably at the degenerated level. The results showed that the disc annulus stress significantly decreased initially and increased slightly subsequently.

Combined flexion-extension

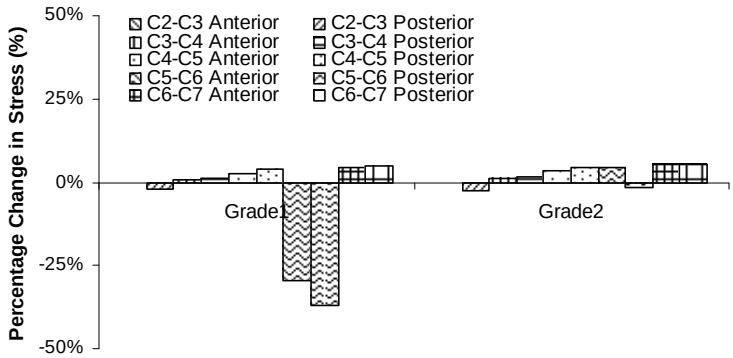

Lateral Bending

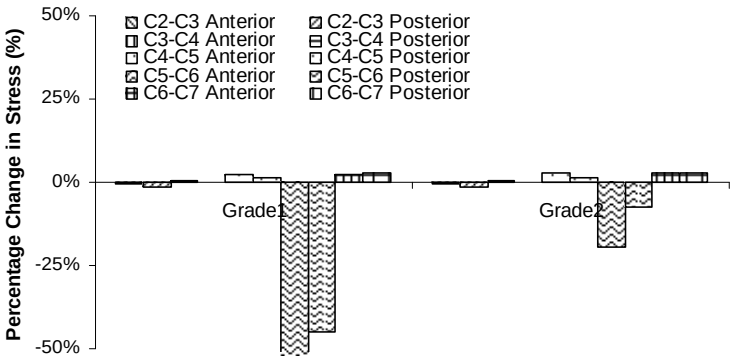

Axial Rotation

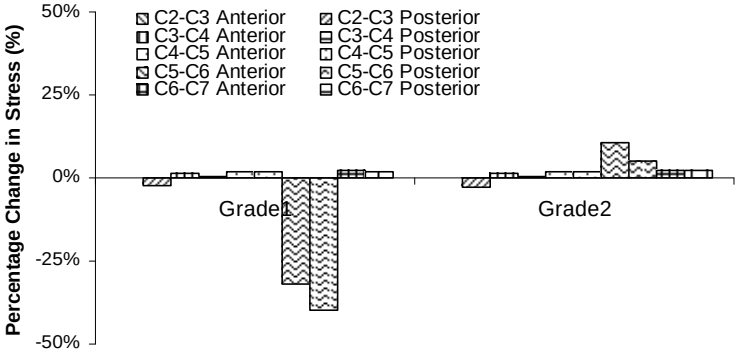

Figure 158: Influence of C5-C6 disc degeneration on the intervertebral disc annulus stress.

While the intervertebral discs stress varies with progressive disc degeneration, the adjacent cancellous bone stress increases (Figure 159). The stress increases by about 65% after grade 1 and grade 2 disc degeneration in combined flexion-extension. Under the three loading modes, the highest percentage increases in stress can be seen under lateral bending.

Combined flexion-extension

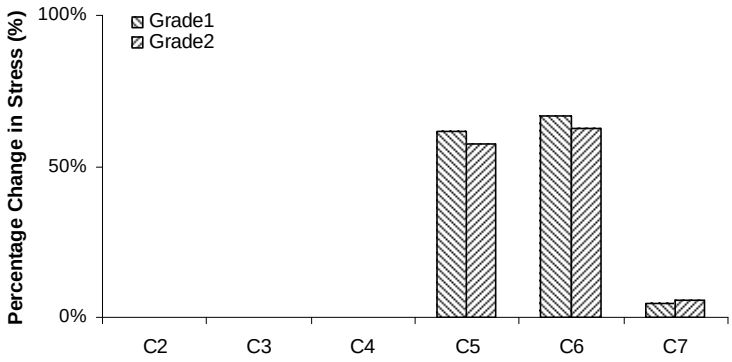

Lateral Bending

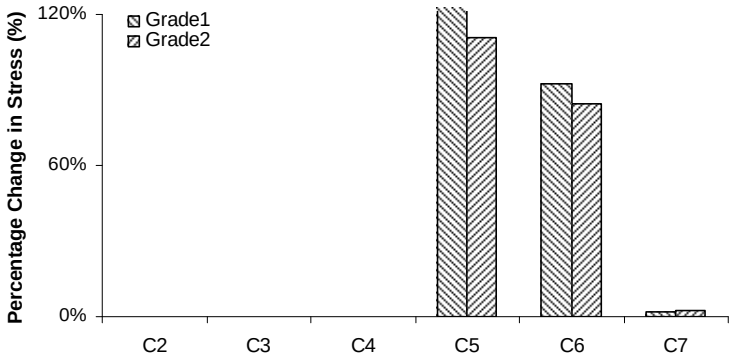

Axial Rotation

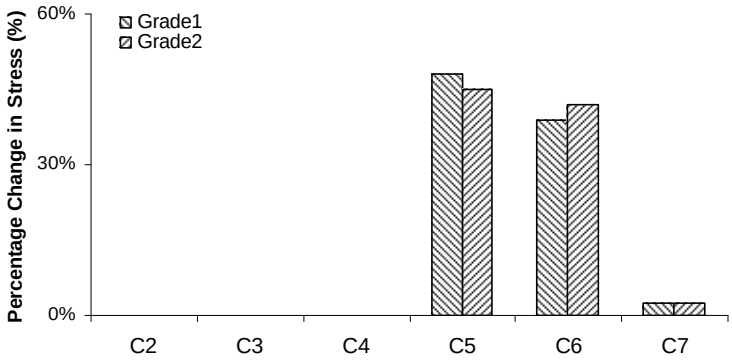

Figure 159: Influence of C5-C6 disc degeneration on the cancellous bone stress.

Generally, progressive disc degeneration affects the cortical stress at the affected C5 and C6 levels (Figure 160). The remaining cervical levels like C2, C3, C4 and C7 are not affected by progressive disc degeneration significantly. The highest percentage increases in cortical stress at these levels are only ~6%.

Combined flexion-extension

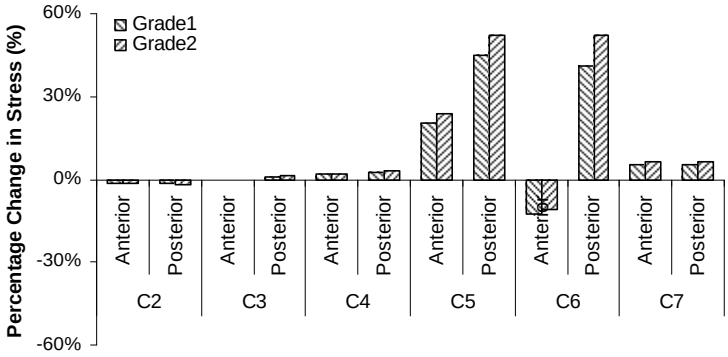

Lateral Bending

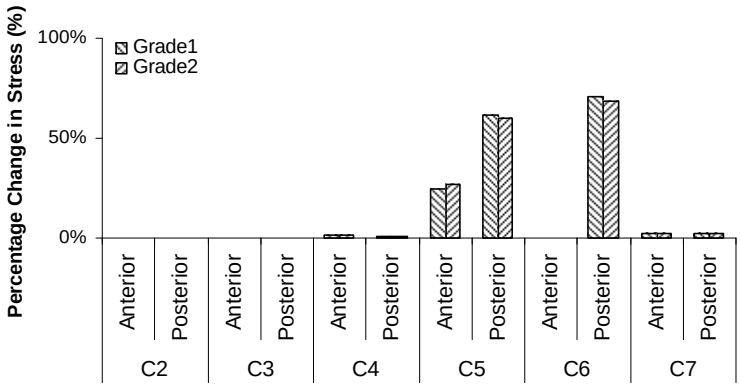

Axial Rotation

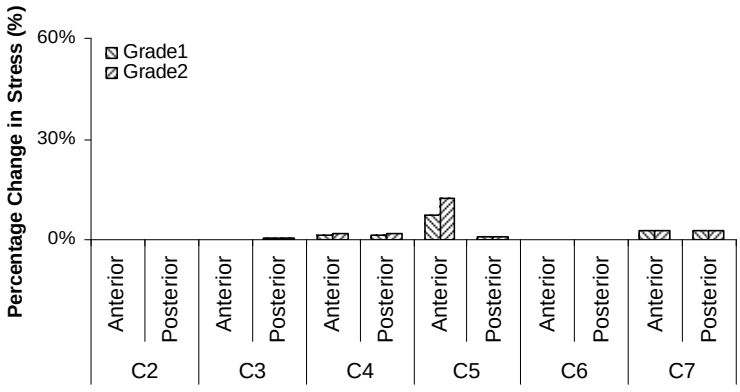

Figure 160: Influence of C5-C6 disc degeneration on the cortical bone stress.

7.4.3 Discussion

To date, there has been a large number of finite element studies delineating the influence of intact and degenerated intervertebral disc on the biomechanical responses of the lumbar spine (Kim et al., 1991; Kurowski and Kubo, 1986; Shirazi-Adl, 1992). Kim et al., 1991 investigated the effects of disc degeneration, simulated at the L4-L5 level, on the biomechanical behaviour of the adjacent intact L3-L4 motion segment. The results indicated lower disc stress as compared with the intact model under the same magnitude of compressive loading force. Shirazi-Adl, 1992 studied the effect of alteration in the disc nucleus fluid content on the mechanics of a lumbar motion segment under compression, anterior shear and axial rotation. The results showed that the vertebral body underwent markedly different stress distributions (Shirazi-Adl, 1992). Kurowski and Kubo, 1986 studied the influence of disc degeneration on the mechanism of load transmission through the lumbar vertebral body. The results showed that the highest effective stresses are concentrated near the cancellous bone. However, it should be noted that the geometry and biomechanics of the cervical disc varied tremendously. It was also clear that the pathology affecting cervical intervertebral discs is different from that affecting lumbar discs. In the lumbar disc, prolapses are common. In the cervical spine, prolapse is uncommon and degenerative changes are reported to occur through the development of osteophytes from the margins of the vertebral body, unconvertebral or facet joints (Kumaresan et al., 2001). Therefore, results from lumbar study should not be used directly for the understanding of the cervical spine biomechanics.

In the area of cervical spine disc degeneration studies using finite element methods, Kumaresan et al., 2001 evaluated the effects of disc degeneration at the C5-C6 level of a

linear C4-C6 cervical spine model under a small axial compressive force of 73.6N. The results indicated that the maximum disc annulus stress decreases initially and increases subsequently, while the cortical stress and strain energy density increases. The current results correlated well with the above findings of varying intervertebral disc annulus stress and increasing cortical bone stress after progressive disc degeneration. The increase in the cortical stress may potentially result in the formation of osteophytes.

Dai, 1998 conducted an imaging study using magnetic resonance imaging to investigate the influence of Grade 1 and Grade 2 disc degeneration on the cervical segmental stability. Two hundred and sixty consecutive patients with suspected cervical spine disorders were analyzed for horizontal and angular displacements on lateral flexion and extension. Their results showed that the grade of disc degeneration increased significantly ($P < 0.01$) with age. The results also indicated the reduction of motion at the affected segments. Current results compared well with the data reported, which indicates the significant reduction in the ROM at the C5-C6 levels.

Overall, the results suggested that the progressive C5-C6 disc degenerative disease led to a change in the biomechanical parameters at the C5-C6. Furthermore, the C5-C6 ROM and disc annulus stress reduces and the cortical stress increases with the severity of disc degeneration (From Grade 1 to Grade 2).

Although comprehensive, the present study only included the degenerative changes in the disc component although changes such as osteoporosis occur in the remaining components of the spine.

7.5 Disc Degeneration and Surgical Intervention

The goal of the surgery is to relieve pressure from the spinal cord or nerve roots caused by cervical spondylosis, which result in disc degeneration. Till now, most of the cervical FE studies have been conducted to understand the influence of various surgical techniques on a normal healthy cervical spine model (Kumaresan et al., 1997; Voo et al., 1997). In addition, there are numerous limitations in these models that were mentioned earlier, such as linear analysis, limited motion segment, etc. Experimental studies also failed to recognize the influence of the cervical disc degeneration on the biomechanical responses after various surgical techniques (Goel et al., 1988b; Goel et al., 1984; Kubo et al., 2003; Nowinski et al., 1993; Saito et al., 1991; Zdeblick et al., 1993; Zdeblick et al., 1992). Furthermore, most of the in vitro experiments did not identify the types of disc degeneration present in the specimens prior to performing the tests. Cusick et al., 1995 noted that the specimens used in the study contained degenerative disc disease ranging from Grade 1 to Grade 3. However, the averaging of the results for different disc degeneration grades after simulated laminectomy added noise to the data. Therefore, the influence of disc degeneration after various surgical techniques on the cervical spine biomechanics remains unknown.

7.5.1 Methods

In this study, two types of C5-C6 cervical disc degeneration were considered. For the normal and two degenerated models, two types of surgical techniques were applied. Laminectomy was performed at C5 and subsequently, total bilateral facetectomy was performed at C5-C6 level. The results from the various surgical techniques were normalized to the respective models (normal disc, Grade 1, Grade 2). The C2-C7

models were analyzed using similar loading and boundary conditions described earlier (Refer 7.3 Validations).

7.5.2 Results

The predicted results demonstrated the influence of disc degeneration after laminectomy and facetectomy. Under combined flexion-extension, laminectomy and facetectomy increase the C2-C7 ROM by about 12% and 18%, respectively, for a normal disc, (Figure 161), 10% and 12%, respectively, for a C5-C6 Grade 1 disc and 9.5% to 10.5%, respectively, for C5-C6 Grade 2 disc. Generally, progressive disc degeneration reduces the percentage increase in the C2-C7 ROM after laminectomy and facetectomy. Similar trend can be observed under other modes of loading (lateral bending and axial rotation).

7.5.3 Discussion

In vitro studies conducted by many investigators showed significantly increase in the ROM or decrease in the stiffness after laminectomies or/and facetectomies for cervical spine (Goel et al., 1988b; Goel et al., 1984; Kubo et al., 2003; Nowinski et al., 1993; Saito et al., 1991; Zdeblick et al., 1993; Zdeblick et al., 1992). However, all these studies failed to recognize the influence of cervical disc degeneration on the biomechanical responses after various surgical treatments. Therefore, the influence of disc degeneration on the ROM laminectomy or/and facetectomy was investigated in this study. The results correlated well with the experimental findings of substantial increase in the ROM after laminectomies and facetectomies.

Combined flexion-extension

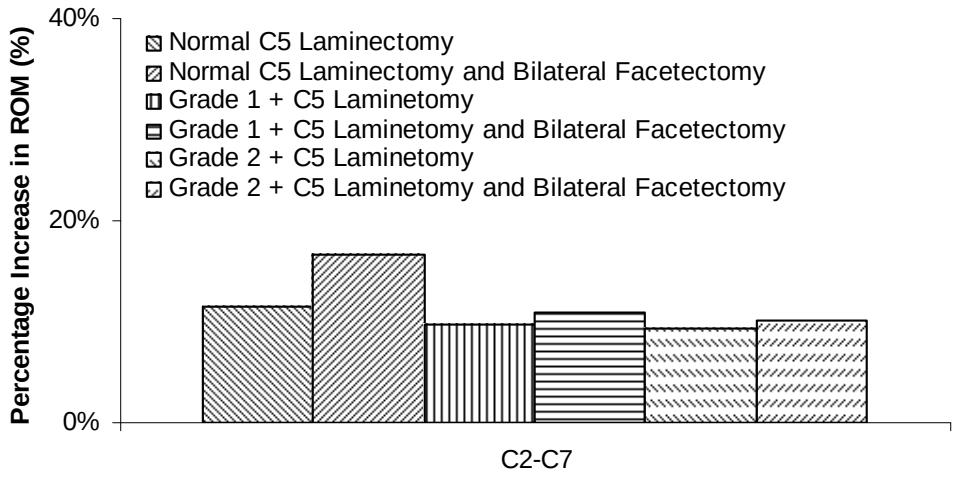

Lateral Bending

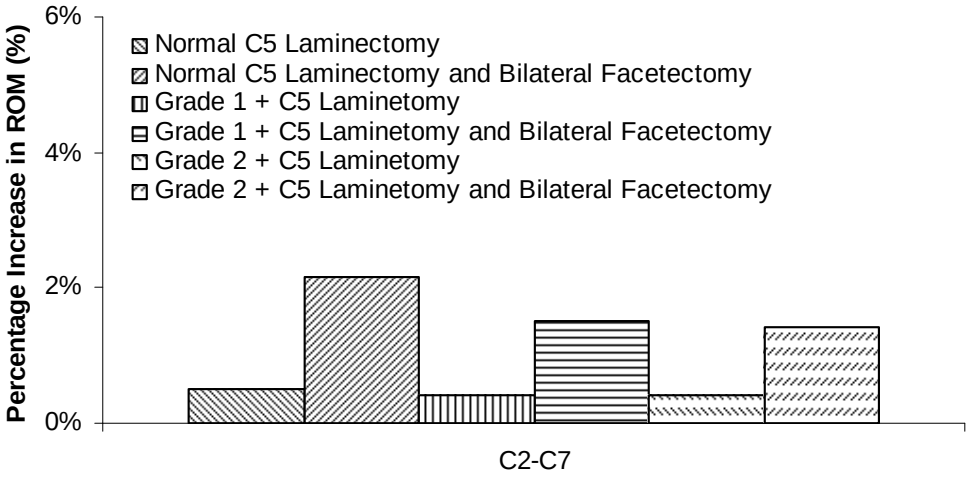

Axial Rotation

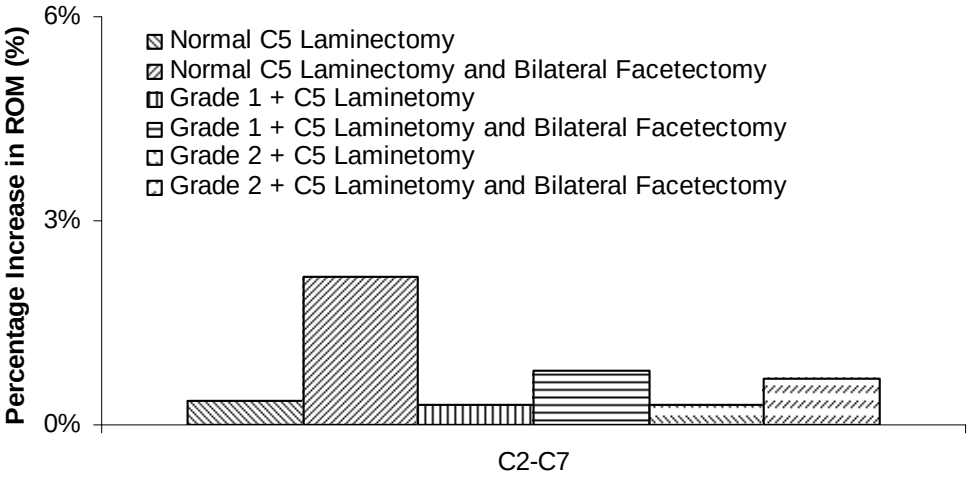

Figure 161: The influence of disc degeneration on the C2-C7 ROM after laminectomy with or without total bilateral facetectomy.

Furthermore, short-term follow-up clinical studies frequently reported the extensive deformation of the cervical spine after laminectomy. Ishida et al., 1989 reported a series of 50 patients and found changed curvatures in 42% at the last follow-up. Miyazaki et al., 1987 found diminished cervical lordosis in 16% and the development of kyphosis in 17% of a series of 127 patients. The current studies simulating immediate post-surgical operation also indicated significant increase in the ROM after laminectomies. However, long-term follow-up clinical studies found that the ROM actually decreased after laminectomy (Yugue et al., 2003). Barnes and Saunders also observed reduced mobility of the cervical spine after extensive laminectomy and suggested that it was a feature of better neurological recovery (Barnes and Saunders, 1984). Current study also indicated an increase in ROM and stress after laminectomy. Increase in the disc stress may potentially accelerate the degenerative process. Disc degenerative processes will affect the cervical stiffness and reduce the percentage increase in the ROM.

Furthermore, it is interesting to see that the influence of facetectomy on the ROM reduces considerably after disc degeneration under combined flexion-extension and axial rotation and slightly under lateral bending (Figure 161). Current findings were consistent with the data reported in the literatures. Kim et al., 1991 and Kumaresan et al., 2001 demonstrated the reduction of facet contribution after degenerative disc disease under compressive loading only. It is a well known that facet, intervertebral disc and ligaments are the primary medium of load transmission in the cervical spine under various directions of physiological loading. While the influence of facet joints diminish, the load transmitted through other spinal components will increase, depending on the direction of movements.

7.6 Summary

A general three-dimensional C2-C7 model has been used to analyze the effect of disc degeneration and surgical techniques (laminectomy or/and facetectomy) subjected to various physiological loads.

The salient findings are summarized as follows:

1. For the intact model
    a. ROM for the intact model decreases with progressive disc degeneration under all direction of loading
    b. Disc degeneration reduces the disc annulus stress and increases the cortical and cancellous bone stress.
    c. Disc degeneration disrupts the normal function of the intervertebral disc and reduces the load sharing of the facets.
2. For the surgically altered models
    a. Percentage increase in the C2-C7 ROM after laminectomy or/and facetectomy reduces with progressive disc degeneration. This is due to the increased cervical spine stiffness, which in turn reduces the function of the facets in providing stability.

Chapter 8. Development of a Patient Specific Model

In the development of any finite element model, it is important to define exactly what information is required from the model and which are the critical parameters and characteristics for that application and then to construct the model accordingly.

For a general-purpose finite element model to simulate a wide range of clinically related biomechanical behaviour of the human cervical spine, it must accurately represent the cervical spine in the following aspects:

- Geometry or anatomy, which includes identifying the geometry of the vertebrae, intervertebral disc and ligaments;
- Material properties of the spinal components;
- Boundary conditions and loading considerations.

Previously (Refer 4.2 Finite Element Model Generation), an accurate description of the human cervical spine geometry was obtained by using the digitized coordinates of dry human cervical vertebrae. The geometry of the specimen chosen for the development of the generic finite element model was compared against the data reported in the literatures. A high conformance was found and the specimen can be used to represent the average adult population. This generic model was able to provide qualitative understanding and assessment of the cervical spine under various situations. However, to provide a clinical solution and accurately predict the ROM based on patient information, there is a need to develop a patient specific model for realistic geometry representation. However, the methodology employed currently by NTU research group

does not allow the creation of the model from a CT scan. Furthermore, there is also a lack of simple modelling techniques reported in the literatures for the development of the patient specific cervical spine model. Therefore, it was necessary to optimize and redefine the existing modelling techniques.

This chapter aims to use the advanced techniques developed in image processing to advance the accuracy and reduce the development time for biomechanical modelling of the patient specific cervical spine model, in particular, to import the 3D reconstruction data obtained from computer tomography (CT) scan images into FEA software for analysis.

8.1 Review on the Existing Modelling Techniques

Currently, cervical spinal geometries may be obtained either through the use of radiographs, coordinate-measuring machines or three-dimensional digitizers, or directly from CT images.

8.1.1 Radiographs

Radiographs have been used extensively by many investigators throughout the early years to generate two dimensional or parameterized models of the human spine. For the parameterized model, the model's geometry was constructed using six parameters per vertebra. These parameters were digitized from two X-rays (antero-posterior and lateral), thus yielding an individualized model (Lavaste et al., 1992).

8.1.2 Dry Vertebrae

8.1.2.1 Coordinate Measuring Machine

Teo et al. 1994 created a simple model of the second cervical vertebra (Figure 35) through the use of a Coordinate Measuring Machine (CMM) (UMC550S, Carl Zeiss, Germany). The finite element model was created by digitizing the points on the surface of the vertebra.

Based on the experience gained in developing the parameterized model mentioned earlier, Maurel et la., 1997 extended their expertise to create a parameterized model of the lower cervical spine (Figure 47). The three-dimensional surface coordinates of the dry vertebrae were measured using a spatial measuring machine.

8.1.2.2 Three-Dimensional Digitizer

A much more geometrically accurate model of the first cervical vertebra (Figure 37) was constructed by Ng and Teo using a three-dimensional digitizer to investigate the fracture mechanism (Teo and Ng, 2001). This method has also been used successfully to capture the geometry of the C4-C5-C6 cervical spine vertebrae.

8.1.3 Computed Tomography Images

The most accurate and efficient way of developing the spine model's geometry was to input the data directly from CT images. CT produces closely spaced axial slices of q patient's anatomy that, when rejoined in the appropriate manner, fully describes a volume of tissue. In CT imaging, a 3-D image of an X-ray absorbing object is reconstructed from a series of two-dimensional (2-D) cross-sectional images. An X-ray beam penetrates the object, and the transmitted beam intensity is measured by an array

of detectors. Each such 'projection' is obtained at a slightly different angle as the scanner rotates about the object. Each CT slice image is composed of tiny picture elements (pixels). Each pixel, in turn, is actually a small volume element (voxel) of the patient's tissue sampled by the CT scanner (Panjabi, 1998). Out of all the existing methods for generating an anatomical model of a physical part, only CT can non-destructively dimension internal as well as external surfaces. CT scan is very popular and has been used extensively in recent years. Currently, many modelling approaches reported in the literatures used CT data to develop the finite element model of the human cervical spine. Bozic et al., 1994 developed a solid three-dimensional finite element model of a cervical vertebra from a CT image to investigate burst fracture mechanisms. Each voxel of the scan data was converted directly to a cube-shaped finite element of size 1.25 mm (Figure 33).

Goel and Clausen, 1997 created the finite element models of the cervical spine, with ligaments using the images from computed tomography. The scans, at 1.5 mm intervals, were printed out, digitized and assembled approximately above one another to generate the three dimensional models. Similar methods of generating the model were used again by for their subsequent studies (Goel and Clausen, 1998; Puttlitz et al., 2000a; Puttlitz et al., 2001).

Another popular and easier way of developing the cervical spine model involves converting the two-dimensional sagittal and coronal CT images into a rasterized computer graphics image and processed in graphics software like Corel Draw 6.0 (Corel Corp.) or Adobe Photoshop 7.0 (Adobe, Inc) using an edge-detection algorithm to extract accurate outlines of the vertebral cross-sections. These two-dimensional

geometric bony boundary data files are converted into a universal graphics data format. The processed outline is vectored by AutoCAD V.12 (Autodesk Inc.) and the three-dimensional wire frame model of the vertebra is created by stacking the sequential two-dimensional cross-section outlines using CAD software like I-DEAS 4.0 (SDRC). This method of creating the finite element model is also used by many investigators (Bozkus et al., 2001; Kumaresan et al., 1999a; Kumaresan et al., 1997; Maiman et al., 1999; Voo et al., 1997; Yoganandan et al., 1996b). A summary of the current and proposed modelling techniques used in the development of cervical spine models is shown in Table 20. However, all the approaches mentioned earlier and used for the development of the human cervical spine required a lot of manual work and were very time consuming.

8.2 Redefined Existing Modelling Techniques

The redefined modelling techniques drop the digitizer approach adopted previously in the development of the cervical spine model (Ng and Teo, 2001; Teo and Ng, 2001). Instead, images from CT scan will be used. CT scan data is widely available and contain necessary information for the development of the patient-specific models for health, injury and implant assessment. The two proposed approaches (Figure 162) are categorized into three-dimensional contour based method and three-dimensional volume based method. To test the efficacy of these two modelling approaches, data files from human visible projects were used.

8.2.1 CT Data

The data used in the current study were CT images. The visible human project female CT dataset consisted of axial CT scans of the entire body taken at 1 mm intervals at a

resolution of 512 pixels by 512 pixels where each pixel is made up of 12 bits of grey tone. There were total 1871 cross-sections of CT obtained from the female cadaver. The software chosen to do the visualization and 3D reconstruction was the Visualization Toolkit, which is a C++ class library with a built-in Tcl/Tk interpreter for visualization and 3D graphics (Schroeder et al., 1998). Visualisation deals with the transformation and representation of data. The CT scan data provided by the visible human project was used to generate the surface structures.

Descriptions	Radiographs	Dry Vertebrae				CT		
		CMM		Digitizer				
Investigators	(Lavaste et al., 1992)	(Teo et al., 1994)	(Maurel et al., 1997)	(Teo and Ng, 2001)	(Bozic et al., 1994)	(Kumaresan et al., 1999a; Voo et al., 1997; Yoganandan et al., 2001; Yoganandan et al., 1996b)	(Clausen et al., 1997; Goel and Clausen, 1998; Puttlitz et al., 2000a; Puttlitz et al., 2001)	Present Study
Geometry	Simplified	Simplified	Simplified	Detailed	Detailed	Detailed	Detailed	Detailed
Procedure	Simple	Simple	Simple	Simple	Simple	Difficult	Difficult	Moderate
Automated	Manual	Manual	Manual	Manual	Semi-Auto	Semi-Auto	Manual	Semi-Auto
Equipment	X-Ray CMM	CMM	CMM	Digitizer	CT Scanner	CT Scanner	CT Scanner Digitizer	CT Scanner
Software	Commercial FE	Commercial FE	Commercial FE	Commercial Graphics Software Commercial FE	Commercial Graphic Software Commercial FE	Commercial Graphic Software Commercial CAD Commercial FE	Commercial FE	Commercial FE Microsoft C++ Microsoft Visual Basic VTK
Techniques	Radiographs ↓ Digitized six parameters ↓ FE Mesh	Dry vertebrae ↓ Captured Surface Points ↓ FE Mesh	Dry vertebrae ↓ Captured Surface Points ↓ Determine Parameters ↓ FE Mesh	Dry vertebrae ↓ Digitizer ↓ Contours ↓ Surfaces ↓ Volumes ↓ FE Mesh	CT Data ↓ 2D Contours using Contour Detection Algorithms ↓ Stack ↓ FE Mesh	CT Data ↓ 2D Outlines using Edge Detection Algorithms ↓ Conversion to Vectored Format ↓ Stack ↓ WireFrame ↓ Surfaces ↓ Volumes ↓ FE Mesh	CT Data ↓ 2D Contours using Digitized Coordinates ↓ Surfaces ↓ Volumes ↓ FE Mesh	CT Data ↓ 2D Segmentation ↓ 3D Surface Reconstruction ↓ Geometry Optimization ↓ Volumes Creation ↓ FE Mesh Automated Contour Generation ↓ Surfaces ↓ Volumes ↓ FE Mesh

Table 20: Summary of modelling techniques used in the creation of cervical models.

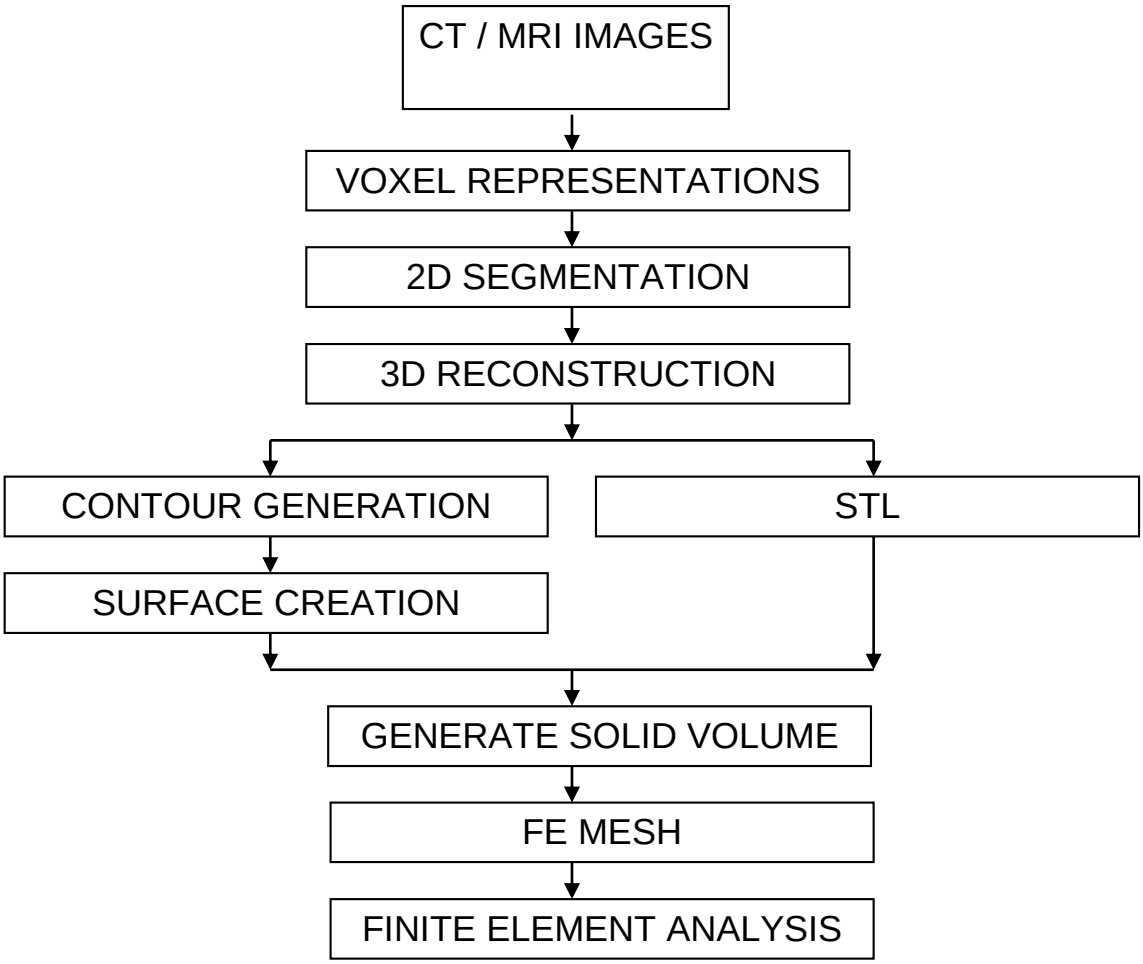

Figure 162: From CT to FE model.

Three algorithms were used for the generation and display of the surfaces. All the three algorithms used in the current study are described in the following sections.

8.2.2 Marching Cubes

The Marching Cubes algorithm designed by Lorensen and Cline to extract surface information from three-dimensional values was used in the current research to develop the spinal model (Cline and Lorensen, 1988; Lorensen and Cline, 1987). The algorithm commences by moving or marching to one voxel or cube at a time and performing a binary classification of each vertex of the current voxel. While marching cubes can

produce very accurate surface representations, it does so at the cost of high polygon counts. A graphical illustration of the human head created through marching cubes using the female dataset from the visible human project is shown in Figure 163.

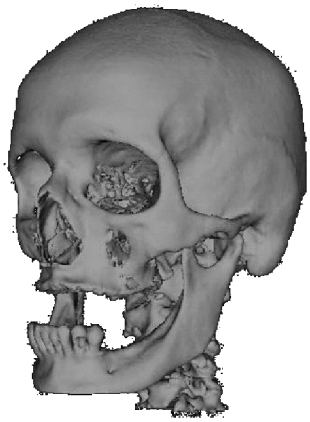

Figure 163: Human head created using marching cubes algorithms (Cline and Lorensen, 1988; Lorensen and Cline, 1987).

8.2.3 Decimate

Marching cubes created huge numbers of polygons. This may potentially overload the system due to the image displayed being too large. Therefore, polygon reduction was needed to reduce the number of polygons required to model the object. One polygon reduction technique is the decimation algorithm. The goal of this algorithm is to reduce the total number of triangles in the triangle mesh, which approximates the original geometry without destroying the original topology (Figure 164).

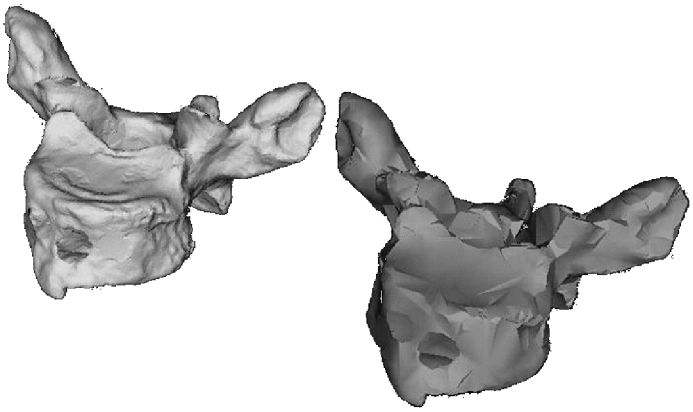

Figure 164: Reduction in mesh density of the single vertebrae.

8.2.4 Smoothing

Laplacian smoothing (Figure 165) is the most commonly used and simplest mesh smoothing method. This method adjusts the location of each mesh vertex to the geometric centre of its neighbour vertices. This method is inexpensive to use but it does not guarantee an improvement in the mesh quality, since repositioning a vertex by Laplacian smoothing sometimes results in poor quality elements.

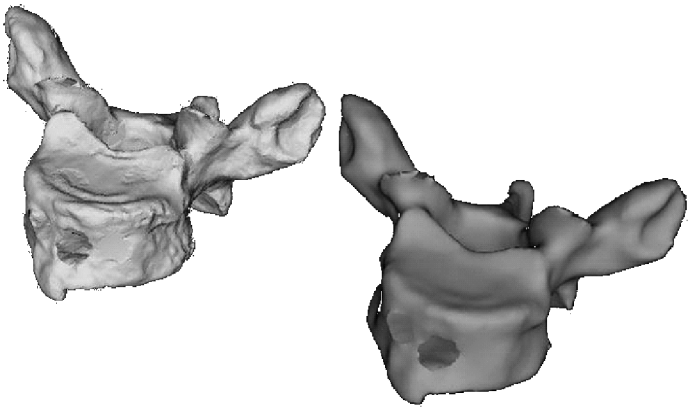

Figure 165: Laplacian surface smoothing of the spinal vertebrae.

8.2.5 Development of Interactive Tools

The steps to 3D surface reconstruction, display and then creation of the wireframe from the 3D surface model are as follows:

1. Define the medical imaging slice parameters and read the RAW data
2. Generate iso surface from the RAW data using Marching Cubes
3. Decimate and smooth the polygons
4. Render and visualize the model for defects
5. Generate sliced wire-frame models and output to VTK format
6. Convert VTK data format to ANSYS scripting language file

Following the steps above, an interactive tool using Microsoft C++ was developed based on the VTK (Figure 166). The tool consists of three parts. The first part deals with the creation of 3D cervical spine models, including the generation of polygonal files from the original CT data using the Marching Cubes algorithm, which provides a high-resolution 3D surface reconstruction. This CT image can be processed by using a simple threshold value of 1224.1, which corresponds to the value of the bone. Tissue classification may be achieved by using very simple method, i.e. thresholding or more complex algorithms (i.e. region growing). For simple thresholding classification used in the present study, the tissue can be classified into two major categories of hard tissue and soft tissue. At this point, the demands of representing the entire surface can require either a large amount of computational power or extreme sophistication in data organization and handling. Therefore, decimate and smoothing algorithms were used to reduce and smooth the surfaces.

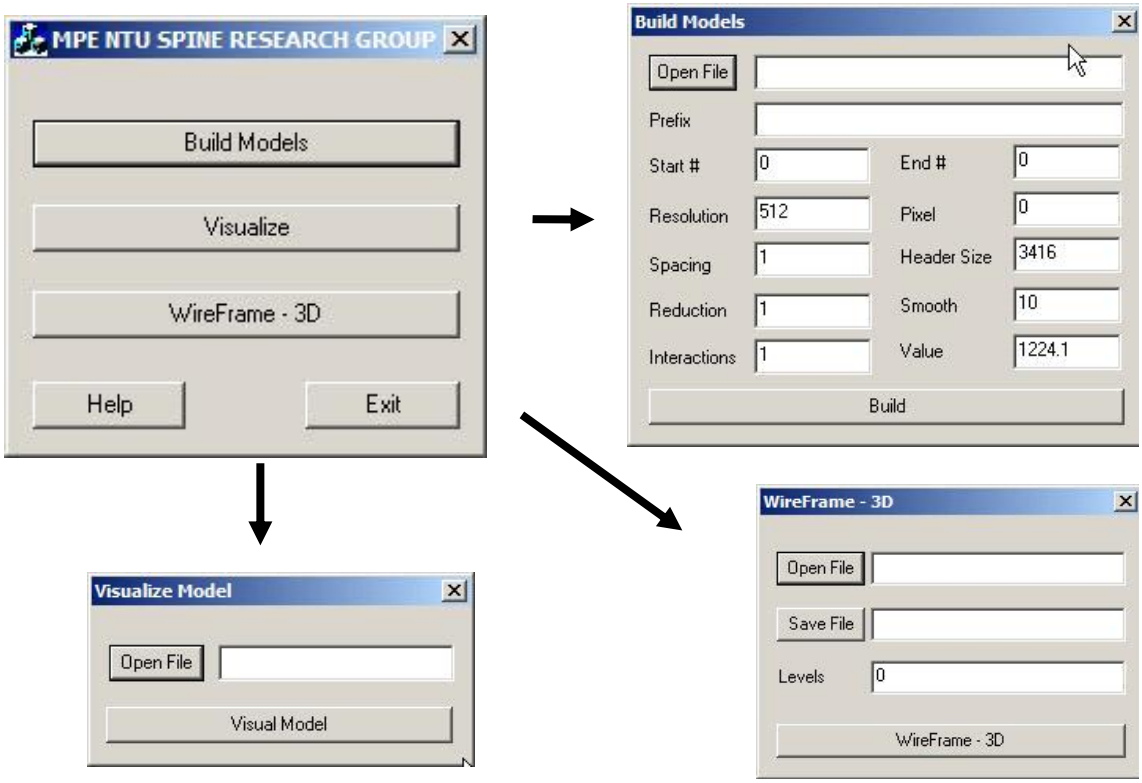

Figure 166: 3D medical image reconstruction software using Microsoft C++.

Thresholding is based on the notion that regions corresponding to different tissue types can be classified by using a range function applied to the intensity value of image pixels. The assumption is that different tissue types will have a distinct frequency distribution and can be discriminated based on the mean and standard deviation of each distribution (Figure 167).

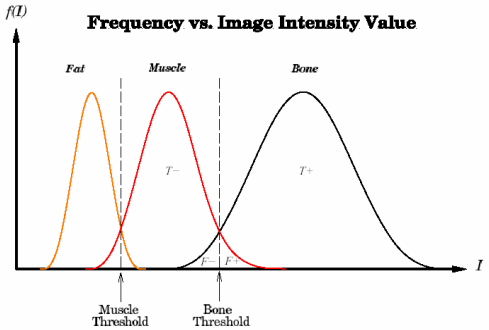

Figure 167: A hypothetical frequency distribution *f*(I) of intensity values I(x,y) for fat, muscle and bone in a CT image.

The second part of the interactive tool renders and displays the 3D models created from the first part. The third part is the generation of wire-frame models for export to FE packages. The wire-frame model (Figure 168) consisting of series of close loop curves can be generated in any planes or orientation.

a) b)

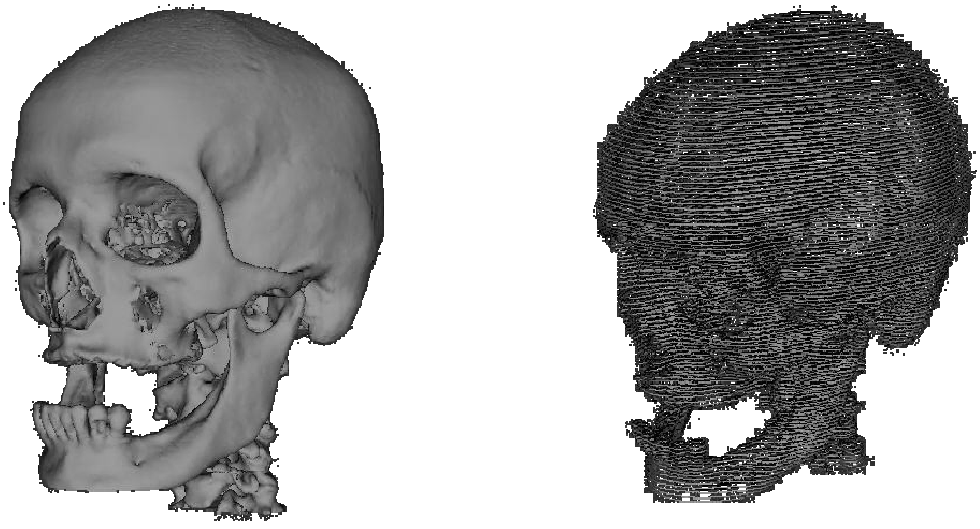

c)

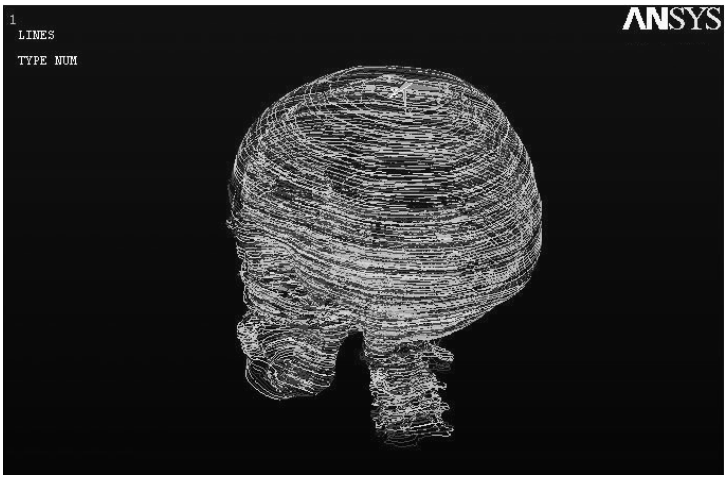

Figure 168: Redefined modelling approaches. A) iso surface, B) wireframe, C) splines in ANSYS.

8.2.6 Finite Element Model

The conversion of VTK format to ANSYS format was done with a program written in the Microsoft Visual Basic language (Figure 169). This programming language offers powerful text manipulation techniques. VTK offers the possibility to write the file into an ASCII file format. The file consists of four parts: the header, a polydata set that contains an array of points, an array of polygons and an array of normals. For the ANSYS input file format, only the array of points and the array of polygons are important and needed. From these, contours can be generated in ANSYS. The script for this program is inserted into Appendix B Programs. The program opens a VTK file and searches for specific details containing the points. The array of points is output to an ASCII text file as keypoints using ANSYS native file structure. The program then opens another VTK file containing the polygons. With the file opened, the array of polygons is output to an ASCII text file as SPLINES. Using ANSYS import function, a list of splines can be created by joining the keypoints.

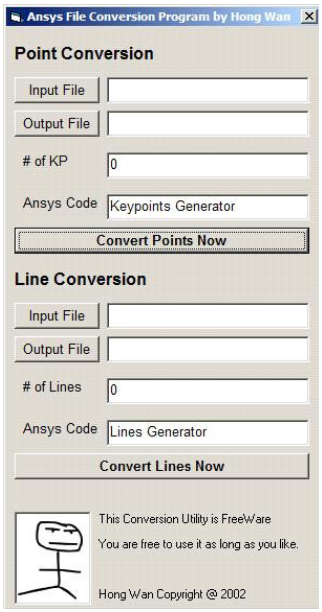

Figure 169: Conversion software written in Microsoft Visual Basic to convert the data to ANSYS scripting language.

The SPLINES were transformed into surfaces by connecting adjacent slice contour segments. ANSYS uses the so-called 'boundary representation' (B-REP), in which a solid object is defined by the surfaces which bound it. These surfaces are mathematically described using special polynomial functions such as non-uniform rational B-spline (NURBS) functions. NURBS make it possible to construct the computer model using fewer numbers of digitized points, which would significantly decrease the size of the files. It would also facilitate operations such as intersection and closure of the boundary surface. Volumes were then created by enclosing all the surfaces for meshing. Generally, this redefined procedure demonstrated improvement over previously reported modelling methodologies for the creation of the cervical spine model. Most importantly, the reconstructed model (Figure 170) in ANSYS has a much higher resolution and requires much less processing time than those done manually. However, the transformation from contours to surface is sometimes complicated, often requiring manual editing when connecting contours from adjacent slices.

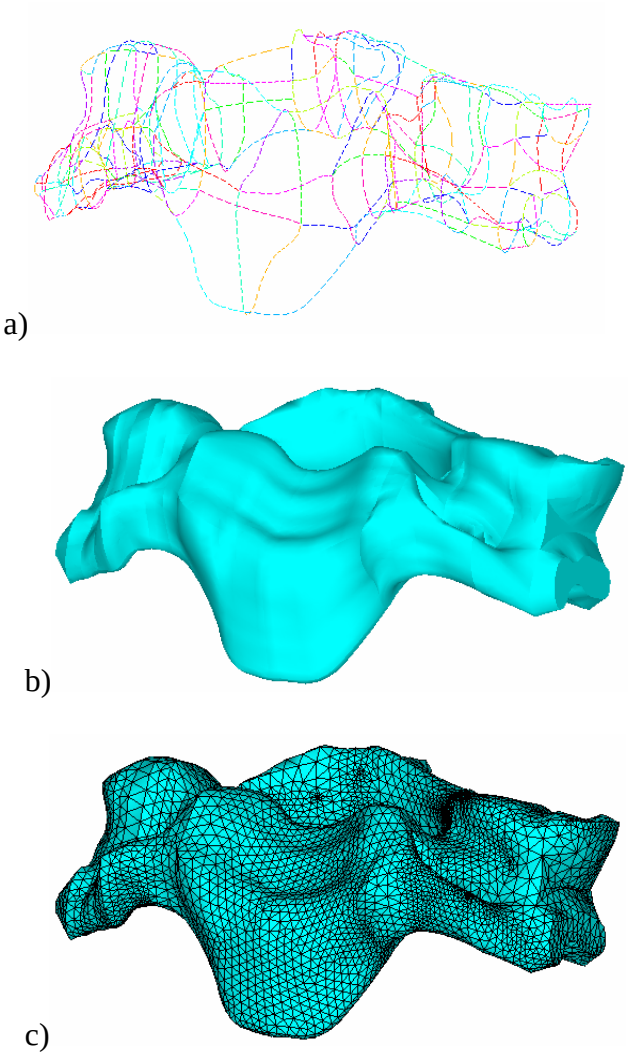

Figure 170: Illustration of the C3 model developed using the redefined methodology. a) wireframe model, b) solid model, c) finite element model.

8.2.7 Volume Modelling

Although previous redefined modelling approaches already represent some improvements over existing modelling techniques, the redefined modelling approaches still requires some manual work, which may take up to 1 day. Manual works included the creation of solid volumes from the wire-frame for meshing. The other much simpler methodology is called the three-dimensional volume based method. After the first part of the interactive tool mentioned earlier, the 3D reconstructed image was exported as an STL file. The STL file was imported into SURFACER (Structural Dynamics Research

Corporation, Ohio, USA) for surface refinement (make the model airtight) and export as IGES file for import into ANSYS as a solid volume (Figure 171).

a) b)

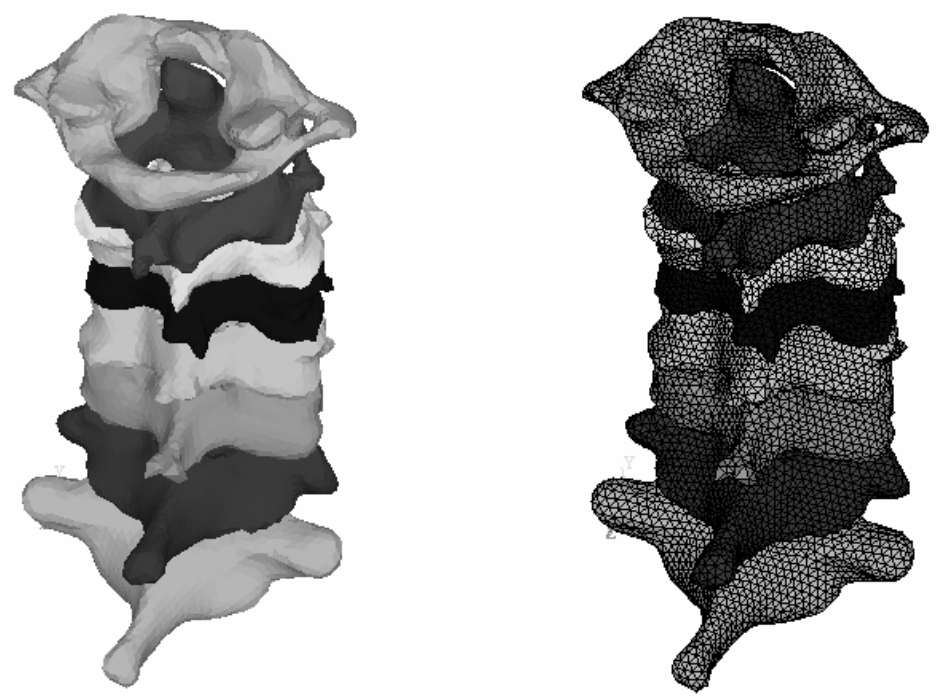

c) d)

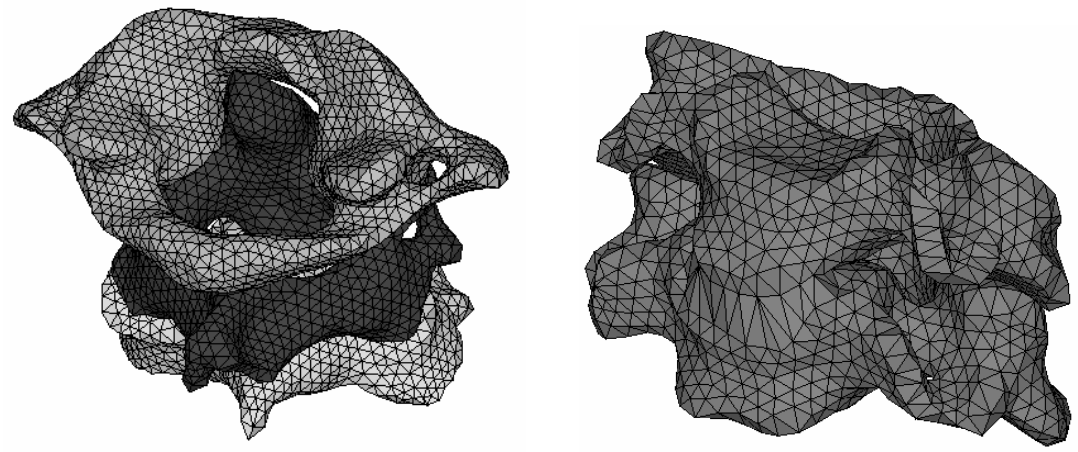

Figure 171: Solid and FE models created using the three-dimensional volume method. a) C1-T1 solid volume, b) C1-T1 FE mesh, c) C1-C3 FE mesh, d) C5-C6 FE mesh.

STL surface can also be converted to NURBS surfaces using the contour based method described earlier. In the last few years, some commercial programs were presented as solutions capable of doing the conversion semi-automatically, which only required

minimal user interference. Surgi-CAD by Integraph ISS, USA, Med-Link, by Dynamic Computer Resources, USA, and Mimic and MedCAD, by Materialise, Belgium are some of the examples. Unfortunately, the direct conversion of the CT data set of a human bone into NURBS solid model is not simple. Furthermore, none of these programs has been widely applied in the biomechanical engineering field due to complexity and cost. Effective methods for the conversion of CT data into CAD solid models still need to be developed (Sun and Lal, 2002).

8.3 Discussion

The author discussed the widely used modelling techniques reported in the literatures for the development of the human cervical spine model and proposed two new modelling approaches. These proposed approaches can help to reduce the development time and aid the creation of a patient specific model for the cervical spine instability analysis.

Although the proposed methods are efficient, there are some limitations. Cervical models constructed through the contour-based method and the volume-based methods contained only surface information. The internal details of the original image were lost during the three dimensional surface reconstruction. In the present study, the proposed model development techniques only consisted of hard tissues (bony vertebrae) modelling. This was due to the limitations of CT scan in capturing the soft tissues. To incorporate soft tissues into the present model, it is necessary to use MRI data. MRI is a non-invasive alternative that projects a 3-D image of the soft tissues together with bone. MRI has proved invaluable in visualizing pathology in soft tissue, especially in neurological, musculoskeletal and vascular diseases. However, segmenting and

modelling the soft tissues automatically require very complex algorithms and processing. Therefore, it is beyond the scope of this study. The other method is the modelling of soft tissues based on the quantitative and qualitative information reported in the literatures (similar to the techniques used in our earlier model development).

Chapter 9. Conclusions

It is hoped that the work presented in this thesis would be judged to have fulfilled the objectives and scopes of the project clearly and concisely whilst demonstrating that the intelligent use of the structural model (Finite Element Method) can be favourably employed in the biomechanical analysis of cervical spine structures under various conditions.

The major contributions and findings from this research are summarized below

- A comprehensive finite element model of the cervical spine incorporating all the important features was developed.
- Extensive validation of the intact model (single FSU (C5-C6), two FSU (C4-C6) and five FSU (C2-C7)) against experimental data.
- Incorporated statistical method of analysis into material sensitivity studies. The results showed the importance of soft tissue in maintaining the cervical spine physiological ROM. Among the soft tissues, disc annulus has the highest influence on the cervical spine biomechanics under all types of loading.
- Under unilateral and bilateral facetectomy, substantial increase in the ROM can be observed with unilateral or bilateral facet resection of greater than 50% under all loading modes. The increase in the ROM was accompanied by similar increases in the cortical bone and disc annulus stress.
- Percentage increase in the ROM after laminectomy at C5 compared well against experimental data. Most of the biomechanical changes after laminectomy occurred at the C4-C5 and C5-C6 segments, but some also occurred at C3-C4 and C6-C7 segments. Subsequent progressively facetectomy performed at C5 and C6 only

affected the inter-segmental responses at C5-C6 level. Increase in the ROM caused by laminectomy and facetectomy was accompanied by higher stress in the intervertebral disc and cortical bone, mainly at the C5 and C6 levels.

- Development of the research relevant equation regarding the minimum number of motion segments needed to perform laminectomy studies.
- A C2-C7 viscoelasticity model was successfully developed to investigate the cervical long-term post-surgical responses. Laminectomized model cause a higher percentage increase in the C2-C7 ROM in flexion as compared to the intact model at the end of the loading time. This showed that laminectomy, which requires the removal of spinous ligaments and ligamentum flavum, increase the load transfer through the intervertebral disc under flexion.
- The results indicated that the ROM for the intact model decreases with progressive disc degeneration under all direction of loading. Disc degeneration reduces the disc annulus stress and increases the cortical and cancellous bone stress. Disc degeneration also disrupts the normal function of the intervertebral disc and reduces the load sharing of the facets.
- Percentage increase in the C2-C7 ROM after laminectomy or/and facetectomy reduces with progressive disc degeneration. This is due to the increased cervical spine stiffness, which in turn reduces the function of the facets in providing stability.
- The author discussed the widely used modelling techniques reported in the literatures for the development of the human cervical spine model and proposed two new modelling approaches. These proposed approaches can help to reduce the development time and aid the creation of a patient specific model for the cervical spine instability analysis

Finally, it can be concluded that injuries, degeneration and various surgical treatments for the cervical and investigated in this study affect the biomechanical parameters of the cervical spine at either both the injury and adjacent levels or the injured levels only. The current results aim to provide a basic understanding of the cervical disorders and facilitated the development of cervical spine surgical treatment guidelines and definitions (An, 1998b; An and Simpson, 1994; Edwards et al., 2003).

9.1 Future Work

For any research, there are always opportunities for extensions and refinements of the methodology. The usefulness of the cervical studies reported herein can be greatly enhanced in the following areas:

- More in-depth material and geometrical characterisation
- Incorporate complex model idealization
    - Inclusion of bone microstructures
    - Neck muscles
- Advanced surgically altered models
    - Foraminectomy
    - Dynamic cervical plates like Aesculap ABC
- Complex injury simulations
    - Herniated disc model for discectomy studies
    - Viscoelastic model for the effect of neck movement speeds
    - Dynamic models for cervical spine burst fractures

References

Albert, T. J., & Vacarro, A. (1998). Postlaminectomy kyphosis. *Spine, 23*(24), 2738-2745.

Allen, B. L., Jr., Tencer, A. F., & Ferguson, R. L. (1987). The biomechanics of decompressive laminectomy. *Spine, 12*(8), 803-808.

An, H. S. (1998a). *Principles and techniques of spine surgery* (1st ed.). Baltimore: Williams & Wilkins.

An, H. S. (Ed.). (1998b). *Principles and techniques in spine surgery* (1st ed.). Baltimore: Williams & Wilkins.

An, H. S., & Simpson, J. M. (1994). *Surgery of the cervical spine*. London
Baltimore: Martin Dunitz ;
Distributed by Williams & Wilkins.

ANSYS 7.0 Documentation and User Manual. (2002). Ansys Inc.

Barnes, M. P., & Saunders, M. (1984). The effect of cervical mobility on the natural history of cervical spondylotic myelopathy. *J Neurol Neurosurg Psychiatry, 47*(1), 17-20.

Batzdorf, U., & Batzdorff, A. (1988). Analysis of cervical spine curvature in patients with cervical spondylosis. *Neurosurgery, 22*(5), 827-836.

Belytschko, T., Kulak, R. F., Schultz, A. B., & Galante, J. O. (1974). Finite element stress analysis of an intervertebral disc. *J Biomech, 7*(3), 277-285.

Belytschko, T., Schwer, L., & Privitzer, E. (1978). Theory and application of a three-dimensional model of the human spine. *Aviat Space Environ Med, 49*(1 Pt. 2), 158-165.

Best, B. A., Guilak, F., Setton, L. A., Zhu, W., Saed-Nejad, F., Ratcliffe, A., et al. (1994). Compressive mechanical properties of the human anulus fibrosus and their relationship to biochemical composition. *Spine, 19*(2), 212-221.

Bozic, K. J., Keyak, J. H., Skinner, H. B., Bueff, H. U., & Bradford, D. S. (1994). Three-dimensional finite element modeling of a cervical vertebra: an investigation of burst fracture mechanism. *J Spinal Disord, 7*(2), 102-110.

Bozkus, H., Karakas, A., Hanci, M., Uzan, M., Bozdag, E., & Sarioglu, A. C. (2001). Finite element model of the Jefferson fracture: comparison with a cadaver model. *Eur Spine J, 10*(3), 257-263.

Brolin, K., & von Holst, H. (2002). Cervical injuries in Sweden, a national survey of patient data from 1987 to 1999. *Inj Control Saf Promot, 9*(1), 40-52.

Brown, T. D., Pedersen, D. R., Gray, M. L., Brand, R. A., & Rubin, C. T. (1990). Toward an identification of mechanical parameters initiating periosteal remodeling: a combined experimental and analytic approach. *J Biomech, 23*(9), 893-905.

Butler, J. C., & Whitecloud, T. S. (1992). Postlaminectomy kyphosis. Causes and surgical management. *Orthop Clin North Am, 23*(3), 505-511.

Carter, D. R., & Hayes, W. C. (1977). The compressive behavior of bone as a two-phase porous structure. *J Bone Joint Surg Am, 59*(7), 954-962.

Chen, B. H., Natarajan, R. N., An, H. S., & Andersson, G. B. (2001). Comparison of biomechanical response to surgical procedures used for cervical radiculopathy: posterior keyhole foraminotomy versus anterior foraminotomy and discectomy versus anterior discectomy with fusion. *J Spinal Disord, 14*(1), 17-20.

Chua, H. C. (1999). *Three Dimensional Quantitative Study of Human Vertebrae - Asian Population.* Master Thesis, Nanyang Technological University.

Clark, C. R., Ducker, T. B., & Cervical Spine Research Society. Editorial Committee. (1998). *The cervical spine* (3rd ed.). Philadelphia: Lippincott-Raven.

Clausen, J. D., Goel, V. K., Traynelis, V. C., & Scifert, J. (1997). Uncinate processes and Luschka joints influence the biomechanics of the cervical spine: quantification using a finite element model of the C5-C6 segment. *J Orthop Res, 15*(3), 342-347.

Cline, H. E., & Lorensen, W. E. (1988). US4729098: System and method employing nonlinear interpolation for the display of surface structures contained within the interior region of a solid body. United States of America: General Electric Company, Schenectady, NY.

Cornish, B. L. (1968). Traumatic spondylolisthesis of the axis. *J Bone Joint Surg Br, 50*(1), 31-43.

Cramer, G. D., & Darby, S. A. (1995). *Basic and clinical anatomy of the spine, spinal cord, and ANS*. St. Louis: Mosby.

Cripton, P. A., Bruehlmann, S. B., Orr, T. E., Oxland, T. R., & Nolte, L. P. (2000). In vitro axial preload application during spine flexibility testing: towards reduced apparatus-related artefacts. *J Biomech, 33*(12), 1559-1568.

Cripton, P. A., Dumas, G. A., & Nolte, L. P. (2001). A minimally disruptive technique for measuring intervertebral disc pressure in vitro: application to the cervical spine. *J Biomech, 34*(4), 545-549.

Cusick, J. F., Pintar, F. A., & Yoganandan, N. (1995). Biomechanical alterations induced by multilevel cervical laminectomy. *Spine, 20*(22), 2392-2398; discussion 2398-2399.

Dietrich, M., Kedzior, K., & Zagrajek, T. (1991). A biomechanical model of the human spinal system. *Proc Inst Mech Eng [H], 205*(1), 19-26.

Dillin, W., & Simeone, F. A. (1998). *Posterior cervical spine surgery*. Philadelphia, PA: Lippincott-Raven.

Edwards, C. C., Riew, K. D., Anderson, P. A., Hilibrand, A. S., & Vaccaro, A. F. (2003). Cervical myelopathy. current diagnostic and treatment strategies. *Spine J, 3*(1), 68-81.

Edwards, W. T., Hayes, W. C., Posner, I., White, A. A., & Mann, R. W. (1987). Variation of lumbar spine stiffness with load. *J Biomech Eng, 109*(1), 35-42.

Effendi, B., Roy, D., Cornish, B., Dussault, R. G., & Laurin, C. A. (1981). Fractures of the ring of the axis. A classification based on the analysis of 131 cases. *J Bone Joint Surg Br, 63-B*(3), 319-327.

Eidelson, S. G. (2002). *Save Your Aching Back and Neck, A Patient's Guide*. New York: SYA Press.

Epstein, J. A. (1988). The surgical management of cervical spinal stenosis, spondylosis, and myeloradiculopathy by means of the posterior approach. *Spine, 13*(7), 864-869.

Epstein, N. (2002). Posterior approaches in the management of cervical spondylosis and ossification of the posterior longitudinal ligament. *Surg Neurol, 58*(3-4), 194-207; discussion 207-198.

Epstein, N. E. (2003). Laminectomy for cervical myelopathy. *Spinal Cord, 41*(6), 317-327.

Fagan, M. J., Julian, S., & Mohsen, A. M. (2002). Finite element analysis in spine research. *Proc Inst Mech Eng [H], 216*(5), 281-298.

FAROArm. (1997). *Caliper 3D Version 2.30*. Florida, USA: Faro Technologies, Inc.

Fielding, J. W., Cochran, G. B., Lawsing, J. F., & Hohl, M. (1974). Tears of the transverse ligament of the atlas. A clinical and biomechanical study. *J Bone Joint Surg Am, 56*(8), 1683-1691.

Ghosh, P. (1988). *The Biology of the intervertebral disc*. Boca Raton, FL: CRC Press.

Gilad, I., & Nissan, M. (1986). A study of vertebra and disc geometric relations of the human cervical and lumbar spine. *Spine, 11*(2), 154-157.

Gilbertson, L. G., Goel, V. K., Kong, W. Z., & Clausen, J. D. (1995). Finite element methods in spine biomechanics research. *Crit Rev Biomed Eng, 23*(5-6), 411-473.

Goel, V. K., Clark, C. R., Gallaes, K., & Liu, Y. K. (1988a). Moment-rotation relationships of the ligamentous occipito-atlanto-axial complex. *J Biomech, 21*(8), 673-680.

Goel, V. K., Clark, C. R., Harris, K. G., & Schulte, K. R. (1988b). Kinematics of the cervical spine: effects of multiple total laminectomy and facet wiring. *J Orthop Res, 6*(4), 611-619.

Goel, V. K., Clark, C. R., McGowan, D., & Goyal, S. (1984). An in-vitro study of the kinematics of the normal, injured and stabilized cervical spine. *J Biomech, 17*(5), 363-376.

Goel, V. K., & Clausen, J. D. (1998). Prediction of load sharing among spinal components of a C5-C6 motion segment using the finite element approach. *Spine, 23*(6), 684-691.

Goel, V. K., & Gilbertson, L. G. (1995). Applications of the finite element method to thoracolumbar spinal research--past, present, and future. *Spine, 20*(15), 1719-1727.

Goel, V. K., Monroe, B. T., Gilbertson, L. G., & Brinckmann, P. (1995). Interlaminar shear stresses and laminae separation in a disc. Finite element analysis of the L3-L4 motion segment subjected to axial compressive loads. *Spine, 20*(6), 689-698.

Graham, R. S., Oberlander, E. K., Stewart, J. E., & Griffiths, D. J. (2000). Validation and use of a finite element model of C-2 for determination of stress and fracture patterns of anterior odontoid loads. *J Neurosurg, 93*(1 Suppl), 117-125.

Hakim, N. S., & King, A. I. (1978). A computer-aided technique for the generation of a 3-D finite element model of a vertebra. *Comput Biol Med, 8*(3), 187-196.

Hakim, N. S., & King, A. I. (1979). A three dimensional finite element dynamic response analysis of a vertebra with experimental verification. *J Biomech, 12*(4), 277-292.

Halldin, P. H., Jakobsson, L., Brolin, K., Palmertz, C., Kleiven, S., & Holst, H. V. (2000). *Investigation of Conditions that Affect Neck Compression-Flexion Injuries Using Numerical Techniques.* Paper presented at the Proceedings 44th Stapp Car Crash Conference, Atlanta, USA.

Harris, J. H., Jr., Edeiken-Monroe, B., & Kopaniky, D. R. (1986). A practical classification of acute cervical spine injuries. *Orthop Clin North Am, 17*(1), 15-30.

Hattori, S., Oda, H., & Kawai, S. (1981). Cervical intradiscal pressure in movements and traction of the cervical spine. *Z Orthop, 119*, 568-569.

Ishida, Y., Suzuki, K., Ohmori, K., Kikata, Y., & Hattori, Y. (1989). Critical analysis of extensive cervical laminectomy. *Neurosurgery, 24*(2), 215-222.

Janevic, J., Ashton-Miller, J. A., & Schultz, A. B. (1991). Large compressive preloads decrease lumbar motion segment flexibility. *J Orthop Res, 9*(2), 228-236.

Kim, Y. E., Goel, V. K., Weinstein, J. N., & Lim, T. H. (1991). Effect of disc degeneration at one level on the adjacent level in axial mode. *Spine, 16*(3), 331-335.

Kleinberger, M. (1993). *Application of finite element techniques to the study of cervical spine mechanics.* Paper presented at the Proceedings of the 37th Stapp Car Crash Conference, Texas.

Kubo, S., Goel, V. K., Yang, S. J., & Tajima, N. (2003). Biomechanical evaluation of cervical double-door laminoplasty using hydroxyapatite spacer. *Spine, 28*(3), 227-234.

Kulak, R. F., Belytschko, T. B., & Schultz, A. B. (1976). Nonlinear behavior of the human intervertebral disc under axial load. *J Biomech, 9*(6), 377-386.

Kumaresan, S., Yoganandan, N., & Pintar, F. A. (1998). Finite element modeling approaches of human cervical spine facet joint capsule. *J Biomech, 31*(4), 371-376.

Kumaresan, S., Yoganandan, N., & Pintar, F. A. (1999a). Finite element analysis of the cervical spine: a material property sensitivity study. *Clin Biomech (Bristol, Avon), 14*(1), 41-53.

Kumaresan, S., Yoganandan, N., Pintar, F. A., & Maiman, D. J. (1999b). Finite element modeling of the cervical spine: role of intervertebral disc under axial and eccentric loads. *Med Eng Phys, 21*(10), 689-700.

Kumaresan, S., Yoganandan, N., Pintar, F. A., Maiman, D. J., & Goel, V. K. (2001). Contribution of disc degeneration to osteophyte formation in the cervical spine: a biomechanical investigation. *J Orthop Res, 19*(5), 977-984.

Kumaresan, S., Yoganandan, N., Pintar, F. A., Voo, L. M., Cusick, J. F., & Larson, S. J. (1997). Finite element modeling of cervical laminectomy with graded facetectomy. *J Spinal Disord, 10*(1), 40-46.

Kurowski, P., & Kubo, A. (1986). The relationship of degeneration of the intervertebral disc to mechanical loading conditions on lumbar vertebrae. *Spine, 11*(7), 726-731.

Lanyon, L. E., Hampson, W. G., Goodship, A. E., & Shah, J. S. (1975). Bone deformation recorded in vivo from strain gauges attached to the human tibial shaft. *Acta Orthop Scand, 46*(2), 256-268.

Lavaste, F., Skalli, W., Robin, S., Roy-Camille, R., & Mazel, C. (1992). Three-dimensional geometrical and mechanical modelling of the lumbar spine. *J Biomech, 25*(10), 1153-1164.

Law, M. D., Jr., Bernhardt, M., & White, A. A. (1995). Evaluation and management of cervical spondylotic myelopathy. *Instr Course Lect, 44*, 99-110.

Lee, M., Kelly, D. W., & Steven, G. P. (1995). A model of spine, ribcage and pelvic responses to a specific lumbar manipulative force in relaxed subjects. *J Biomech, 28*(11), 1403-1408.

Lestini, W. F., & Wiesel, S. W. (1989). The pathogenesis of cervical spondylosis. *Clin Orthop*(239), 69-93.

Lorensen, W. E., & Cline, H. E. (1987). *Marching Cubes: A High Resolution 3D Surface Construction Algorithm.* Paper presented at the Proceedings of SIGGRAPH.

Lu, Y. M., Hutton, W. C., & Gharpuray, V. M. (1996). Do bending, twisting, and diurnal fluid changes in the disc affect the propensity to prolapse? A viscoelastic finite element model. *Spine, 21*(22), 2570-2579.

Lu, Y. M., Hutton, W. C., & Gharpuray, V. M. (1998). The effect of fluid loss on the viscoelastic behavior of the lumbar intervertebral disc in compression. *J Biomech Eng, 120*(1), 48-54.

Maiman, D. J., Kumaresan, S., Yoganandan, N., & Pintar, F. A. (1999). Biomechanical effect of anterior cervical spine fusion on adjacent segments. *Biomed Mater Eng, 9*(1), 27-38.

Manson, R. D. (1991). *Statistics: an introduction*: Harcourt Brace Jovanovich.

Marchand, F., & Ahmed, A. M. (1990). Investigation of the laminate structure of lumbar disc anulus fibrosus. *Spine, 15*(5), 402-410.

Martini, F., & Ober, W. C. (2001). *Fundamentals of anatomy & physiology* (5th ed.). Upper Saddle River, N.J.: Prentice Hall.

Maurel, N., Lavaste, F., & Skalli, W. (1997). A three-dimensional parameterized finite element model of the lower cervical spine. Study of the influence of the posterior articular facets. *J Biomech, 30*(9), 921-931.

McNally, D. S., & Adams, M. A. (1992). Internal intervertebral disc mechanics as revealed by stress profilometry. *Spine, 17*(1), 66-73.

Mercer, S., & Bogduk, N. (1999). The ligaments and annulus fibrosus of human adult cervical intervertebral discs. *Spine, 24*(7), 619-626; discussion 627-618.

Mikawa, Y., Shikata, J., & Yamamuro, T. (1987). Spinal deformity and instability after multilevel cervical laminectomy. *Spine, 12*(1), 6-11.

Ministry.of.Health. (2003). *Health Facts Singapore 1998 - 2002*

Moroney, S. P., Schultz, A. B., Miller, J. A., & Andersson, G. B. (1988). Load-displacement properties of lower cervical spine motion segments. *J Biomech, 21*(9), 769-779.

Nachemson, A. (1960). Lumbar intradiscal pressure. Experimental studies on post-mortem material. *Acta Orthop Scand, Suppl 43*, 1-104.

Natarajan, R. N., Andersson, G. B., Patwardhan, A. G., & Andriacchi, T. P. (1999). Study on effect of graded facetectomy on change in lumbar motion segment torsional flexibility using three-dimensional continuum contact representation for facet joints. *J Biomech Eng, 121*(2), 215-221.

Natarajan, R. N., Ke, J. H., & Andersson, G. B. (1994). A model to study the disc degeneration process. *Spine, 19*(3), 259-265.

Ng, H. W., & Teo, E. C. (2001). Nonlinear finite-element analysis of the lower cervical spine (C4-C6) under axial loading. *J Spinal Disord, 14*(3), 201-210.

Nightingale, R. W., Winkelstein, B. A., Knaub, K. E., Richardson, W. J., Luck, J. F., & Myers, B. S. (2002). Comparative strengths and structural properties of the upper and lower cervical spine in flexion and extension. *J Biomech, 35*(6), 725-732.

Nissan, M., & Gilad, I. (1984). The cervical and lumbar vertebrae--an anthropometric model. *Eng Med, 13*(3), 111-114.

Nowinski, G. P., Visarius, H., Nolte, L. P., & Herkowitz, H. N. (1993). A biomechanical comparison of cervical laminaplasty and cervical laminectomy with progressive facetectomy. *Spine, 18*(14), 1995-2004.

Oliver, J., & Middleditch, A. (1991). *Functional anatomy of the spine*. Oxford ; Boston: Butterworth-Heinemann.

Orr, R. D., & Zdeblick, T. A. (1999). Cervical spondylotic myelopathy. Approaches to surgical treatment. *Clin Orthop*(359), 58-66.

Panjabi, M. (1979). Validation of mathematical models. *J Biomech, 12*(3), 238.

Panjabi, M., Dvorak, J., Duranceau, J., Yamamoto, I., Gerber, M., Rauschning, W., et al. (1988). Three-dimensional movements of the upper cervical spine. *Spine, 13*(7), 726-730.

Panjabi, M. M. (1973). Three-dimensional mathematical model of the human spine structure. *J Biomech, 6*(6), 671-680.

Panjabi, M. M. (1998). Cervical spine models for biomechanical research. *Spine, 23*(24), 2684-2700.

Panjabi, M. M. (2003). Clinical spinal instability and low back pain. *J Electromyogr Kinesiol, 13*(4), 371-379.

Panjabi, M. M., Crisco, J. J., Vasavada, A., Oda, T., Cholewicki, J., Nibu, K., et al. (2001). Mechanical properties of the human cervical spine as shown by three-dimensional load-displacement curves. *Spine, 26*(24), 2692-2700.

Panjabi, M. M., Duranceau, J., Goel, V., Oxland, T., & Takata, K. (1991). Cervical human vertebrae. Quantitative three-dimensional anatomy of the middle and lower regions. *Spine, 16*(8), 861-869.

Panjabi, M. M., Goel, V., Oxland, T., Takata, K., Duranceau, J., Krag, M., et al. (1992). Human lumbar vertebrae. Quantitative three-dimensional anatomy. *Spine, 17*(3), 299-306.

Panjabi, M. M., Krag, M. H., White, A. A., & Southwick, W. O. (1977). Effects of preload on load displacement curves of the lumbar spine. *Orthop Clin North Am, 8*(1), 181-192.

Panjabi, M. M., Oxland, T., Takata, K., Goel, V., Duranceau, J., & Krag, M. (1993). Articular facets of the human spine. Quantitative three-dimensional anatomy. *Spine, 18*(10), 1298-1310.

Panjabi, M. M., Summers, D. J., Pelker, R. R., Videman, T., Friedlaender, G. E., & Southwick, W. O. (1986). Three-dimensional load-displacement curves due to forces on the cervical spine. *J Orthop Res, 4*(2), 152-161.

Panjabi, M. M., White, A. A., & Johnson, R. M. (1975). Cervical spine mechanics as a function of transection of components. *J Biomech, 8*(5), 327-336.

Panjabi, M. M., White, A. A., Keller, D., Southwick, W. O., & Friedlaender, G. (1978). Stability of the cervical spine under tension. *J Biomech, 11*(4), 189-197.

Patwardhan, A. G., Havey, R. M., Carandang, G., Simonds, J., Voronov, L. I., Ghanayem, A. J., et al. (2003). Effect of compressive follower preload on the flexion-extension response of the human lumbar spine. *J Orthop Res, 21*(3), 540-546.

Patwardhan, A. G., Havey, R. M., Ghanayem, A. J., Diener, H., Meade, K. P., Dunlap, B., et al. (2000). Load-carrying capacity of the human cervical spine in compression is increased under a follower load. *Spine, 25*(12), 1548-1554.

Patwardhan, A. G., Havey, R. M., Meade, K. P., Lee, B., & Dunlap, B. (1999). A follower load increases the load-carrying capacity of the lumbar spine in compression. *Spine, 24*(10), 1003-1009.

Patwardhan, A. G., Meade, K. P., & Lee, B. (2001). A frontal plane model of the lumbar spine subjected to a follower load: implications for the role of muscles. *J Biomech Eng, 123*(3), 212-217.

Pelker, R. R., Duranceau, J. S., & Panjabi, M. M. (1991). Cervical spine stabilization. A three-dimensional, biomechanical evaluation of rotational stability, strength, and failure mechanisms. *Spine, 16*(2), 117-122.

Pintar, F. A., Schlick, M. B., Yoganandan, N., & Maiman, D. J. (1996). Instrumented artificial spinal cord for human cervical pressure measurement. *Biomed Mater Eng, 6*(3), 219-229.

Pintar, F. A., Yoganandan, N., Pesigan, M., Reinartz, J., Sances, A., Jr., & Cusick, J. F. (1995). Cervical vertebral strain measurements under axial and eccentric loading. *J Biomech Eng, 117*(4), 474-478.

Puttlitz, C. M., Goel, V. K., Clark, C. R., & Traynelis, V. C. (2000a). Pathomechanisms of failures of the odontoid. *Spine, 25*(22), 2868-2876.

Puttlitz, C. M., Goel, V. K., Clark, C. R., Traynelis, V. C., Scifert, J. L., & Grosland, N. M. (2000b). Biomechanical rationale for the pathology of rheumatoid arthritis in the craniovertebral junction. *Spine, 25*(13), 1607-1616.

Puttlitz, C. M., Goel, V. K., Traynelis, V. C., & Clark, C. R. (2001). A finite element investigation of upper cervical instrumentation. *Spine, 26*(22), 2449-2455.

Rao, A. A., & Dumas, G. A. (1991). Influence of material properties on the mechanical behaviour of the L5-S1 intervertebral disc in compression: a nonlinear finite element study. *J Biomed Eng, 13*(2), 139-151.

Raynor, R. B., Moskovich, R., Zidel, P., & Pugh, J. (1987). Alterations in primary and coupled neck motions after facetectomy. *Neurosurgery, 21*(5), 681-687.

Raynor, R. B., Pugh, J., & Shapiro, I. (1985). Cervical facetectomy and its effect on spine strength. *J Neurosurg, 63*(2), 278-282.

Richter, M., Wilke, H. J., Kluger, P., Claes, L., & Puhl, W. (1999). Biomechanical evaluation of a newly developed monocortical expansion screw for use in anterior internal fixation of the cervical spine. In vitro comparison with two established internal fixation systems. *Spine, 24*(3), 207-212.

Richter, M., Wilke, H. J., Kluger, P., Claes, L., & Puhl, W. (2000). Load-displacement properties of the normal and injured lower cervical spine in vitro. *Eur Spine J, 9*(2), 104-108.

Rohl, L., Larsen, E., Linde, F., Odgaard, A., & Jorgensen, J. (1991). Tensile and compressive properties of cancellous bone. *J Biomech, 24*(12), 1143-1149.

Rowland, L. P. (1992). Surgical treatment of cervical spondylotic myelopathy: time for a controlled trial. *Neurology, 42*(1), 5-13.

Saito, T., Yamamuro, T., Shikata, J., Oka, M., & Tsutsumi, S. (1991). Analysis and prevention of spinal column deformity following cervical laminectomy. I. Pathogenetic analysis of postlaminectomy deformities. *Spine, 16*(5), 494-502.

Sances, A., Jr., Myklebust, J. B., Maiman, D. J., Larson, S. J., Cusick, J. F., & Jodat, R. W. (1984). The biomechanics of spinal injuries. *Crit Rev Biomed Eng, 11*(1), 1-76.

Schmidt, M. H., Quinones-Hinojosa, A., & Rosenberg, W. S. (2002). Cervical myelopathy associated with degenerative spine disease and ossification of the posterior longitudinal ligament. *Semin Neurol, 22*(2), 143-148.

Schroeder, W., Martin, K. W., & Lorensen, B. (1998). *The visualization toolkit* (2nd ed.). Upper Saddle River, NJ: Prentice Hall PTR.

Schulte, K., Clark, C. R., & Goel, V. K. (1989). Kinematics of the cervical spine following discectomy and stabilization. *Spine, 14*(10), 1116-1121.

Schultz, A. B., & Galante, J. O. (1970). A mathematical model for the study of the mechanics of the human vertebral column. *J Biomech, 3*(4), 405-416.

Shea, M., Edwards, W. T., White, A. A., & Hayes, W. C. (1991). Variations of stiffness and strength along the human cervical spine. *J Biomech, 24*(2), 95-107.

Shirazi-Adl, A. (1992). Finite-element simulation of changes in the fluid content of human lumbar discs. Mechanical and clinical implications. *Spine, 17*(2), 206-212.

Shirazi-Adl, S. A., Shrivastava, S. C., & Ahmed, A. M. (1984). Stress analysis of the lumbar disc-body unit in compression. A three-dimensional nonlinear finite element study. *Spine, 9*(2), 120-134.

Singapore.Police.Force. (2002). *Road Accident Situation*

Skaggs, D. L., Weidenbaum, M., Iatridis, J. C., Ratcliffe, A., & Mow, V. C. (1994). Regional variation in tensile properties and biochemical composition of the human lumbar anulus fibrosus. *Spine, 19*(12), 1310-1319.

Sobotta, J., Putz, R., Pabst, R., & Taylor, A. N. (1997). *Sobotta atlas of human anatomy* (12th English , nomenclature in English / ed.). Baltimore: Williams & Wilkins.

Sun, W., & Lal, P. (2002). Recent development on computer aided tissue engineering--a review. *Comput Methods Programs Biomed, 67*(2), 85-103.

Takagi, H., Kawaguchi, Y., Kanamori, M., Abe, Y., & Kimura, T. (2002). T1-2 disc herniation following an en bloc cervical laminoplasty. *J Orthop Sci, 7*(4), 495-497.

Tan, S. B. (2002). *Notes in Biomechanics Lecture*. Singapore: Director of Orthopaedics Department, Singapore General Hospital.

Tan, S. H., Teo, E. C., & Chua, H. C. (2002). Quantitative three-dimensional anatomy of lumbar vertebrae in Singaporean Asians. *Eur Spine J, 11*(2), 152-158.

Tan, S. H., Teo, E. C., & Chua, H. C. (2004). Quantitative three-dimensional anatomy of cervical, thoracic and lumbar vertebrae of Chinese Singaporeans. *Eur Spine J, 13*(2), 137-146.

Teo, E. C., & Ng, H. W. (2001). First cervical vertebra (atlas) fracture mechanism studies using finite element method. *J Biomech, 34*(1), 13-21.

Teo, E. C., Paul, J. P., & Evans, J. H. (1994). Finite element stress analysis of a cadaver second cervical vertebra. *Med Biol Eng Comput, 32*(2), 236-238.

Ueno, K., & Liu, Y. K. (1987). A three-dimensional nonlinear finite element model of lumbar intervertebral joint in torsion. *J Biomech Eng, 109*(3), 200-209.

Voo, L. M., Kumaresan, S., Yoganandan, N., Pintar, F. A., & Cusick, J. F. (1997). Finite element analysis of cervical facetectomy. *Spine, 22*(9), 964-969.

Wang, J. L., Parnianpour, M., Shirazi-Adl, A., & Engin, A. E. (2000). Viscoelastic finite-element analysis of a lumbar motion segment in combined compression and sagittal flexion. Effect of loading rate. *Spine, 25*(3), 310-318.

Wang, J. L., Parnianpour, M., Shirazi-Adl, A., Engin, A. E., Li, S., & Patwardhan, A. (1997). Development and validation of a viscoelastic finite element model of an L2/L3 motion segment. *Theoretical and Applied Fracture Mechanics, 28*(1), 81-93.

Wen, N., Lavaste, F., Santin, J. J., & Lassau, J. P. (1993a). Three-dimensional biomechanical properties of the human cervical spine in vitro: I. Analysis of normal motion. *Eur Spine J, 2*, 2-11.

Wen, N., Lavaste, F., Santin, J. J., & Lassau, J. P. (1993b). Three-dimensional biomechanical properties of the human cervical spine in vitro: II. Analysis of instability after ligamentous injuries. *Eur Spine J, 2*, 12-15.

White, A. A., Johnson, R. M., Panjabi, M. M., & Southwick, W. O. (1975). Biomechanical analysis of clinical stability in the cervical spine. *Clin Orthop*(109), 85-96.

White, A. A., & Panjabi, M. M. (1990). *Clinical biomechanics of the spine* (2nd ed.). Philadelphia: Lippincott.

Whitecloud, T. S., & Dunsker, S. B. (1993). *Anterior cervical spine surgery*. New York: Raven Press.

Wilke, H. J., Wenger, K., & Claes, L. (1998). Testing criteria for spinal implants: recommendations for the standardization of in vitro stability testing of spinal implants. *Eur Spine J, 7*(2), 148-154.

Yoganandan, N., Kumaresan, S., & Pintar, F. A. (2000). Geometric and mechanical properties of human cervical spine ligaments. *J Biomech Eng, 122*(6), 623-629.

Yoganandan, N., Kumaresan, S., & Pintar, F. A. (2001). Biomechanics of the cervical spine Part 2. Cervical spine soft tissue responses and biomechanical modeling. *Clin Biomech (Bristol, Avon), 16*(1), 1-27.

Yoganandan, N., Kumaresan, S., Voo, L., & Pintar, F. A. (1996a). Finite element applications in human cervical spine modeling. *Spine, 21*(15), 1824-1834.

Yoganandan, N., Kumaresan, S. C., Voo, L., Pintar, F. A., & Larson, S. J. (1996b). Finite element modeling of the C4-C6 cervical spine unit. *Med Eng Phys, 18*(7), 569-574.

Yoganandan, N., Myklebust, J. B., Ray, G., & Sances, A., Jr. (1987). Mathematical and finite element analysis of spine injuries. *Crit Rev Biomed Eng, 15*(1), 29-93.

Young, W. F. (2000). Cervical spondylotic myelopathy: a common cause of spinal cord dysfunction in older persons. *Am Fam Physician, 62*(5), 1064-1070, 1073.

Yugue, I., Shiba, K., & Uezaki, N. (2003). [Static and dynamic modifications of the cervical spine after laminoplasty for cervical spondylotic myelopathy]. *Rev Chir Orthop Reparatrice Appar Mot, 89*(6), 487-495.

Zander, T., Rohlmann, A., Klockner, C., & Bergmann, G. (2003). Influence of graded facetectomy and laminectomy on spinal biomechanics. *Eur Spine J, 12*(4), 427-434.

Zdeblick, T. A., Abitbol, J. J., Kunz, D. N., McCabe, R. P., & Garfin, S. (1993). Cervical stability after sequential capsule resection. *Spine, 18*(14), 2005-2008.

Zdeblick, T. A., Zou, D., Warden, K. E., McCabe, R., Kunz, D., & Vanderby, R. (1992). Cervical stability after foraminotomy. A biomechanical in vitro analysis. *J Bone Joint Surg Am, 74*(1), 22-27.

Related Publications

1. Ng, H. W., Teo, E. C., & Zhang, Q. (2005). Influence of cervical disc degeneration after posterior surgical techniques in combined flexion-extension--a nonlinear analytical study. J Biomech Eng, 127(1), 186-192.

2. Ng, H. W., & Teo, E. C. (2005). Influence of preload magnitudes and orientation angles on the cervical biomechanics: a finite element study. J Spinal Disord Tech, 18(1), 72-79.

3. Ng, H. W., Teo, E. C., & Zhang, Q. (2004). Biomechanical effects of C2-C7 intersegmental stability due to laminectomy with unilateral and bilateral facetectomy. Spine, 29(16), 1737-1745.

4. NG H. W., Teo E. C. and Zhang QH (2004). Influence of Laminotomies and Laminectomies on Cervical Spine Biomechanics Under Combined Flexion-Extension. Journal of Applied Biomechanics, 20(3), 243-59.

5. Ng, H. W., Teo, E. C., & Zhang, Q. H. (2004). Prediction of inter-segment stability and osteophyte formation on the multi-segment C2-C7 after unilateral and bilateral facetectomy. Proc Inst Mech Eng [H], 218(3), 183-191.

6. Ng, H. W., Teo, E. C., & Lee, V. S. (2004). Statistical factorial analysis on the material property sensitivity of the mechanical responses of the C4-C6 under compression, anterior and posterior shear. J Biomech, 37(5), 771-777.

7. Ng, H. W., & Teo, E. C. (2004). Probabilistic design analysis of the influence of material property on the human cervical spine. J Spinal Disord Tech, 17(2), 123-133.

8. Ng, H. W., Teo, E. C., Lee, K. K., & Qiu, T. X. (2003). Finite element analysis of cervical spinal instability under physiologic loading. J Spinal Disord Tech, 16(1), 55-65.

9. Teo E. C. and Ng H. W. (2003). The Biomechanical Response of Lower Cervical Spine Under Axial, Flexion and Extension Loading using FE Method. Int J

Computer Applications in Technology (IJCAT) - Special Issue "Biomedical Engineering and IT", 20, 1-2:1-8.

10. Ng H. W. and Teo E. C. (2003). Finite Element Analysis of Cervical Stability after Ligamenteous Injuries. World Congress on Medical Physics and Biomedical Engineering, Sydney, Australia, 24-29 August.

11. Ng H. W., Lee V. S., Teo E. C., Seng K. Y., Neo L. D., Lee K. K., Qiu T. X., Yang K. (2002). Factorial analysis on the material sensitivity of the mechanical response of the C4-C6 FE model. International Congress on Biological and Medical Engineering, Singapore, 4-7 December.

Appendix A: FEM

A.1 Introduction to FEM

The finite element method (FEM) is a numerical method for solving problems of engineering and mathematical physics. FEM is useful for problems with complicated geometries (such as spine), loadings, and material properties where analytical solutions can not be obtained. The simulation steps involved discretizing the physical model into an equivalent system of smaller bodies or units (finite elements) interconnected at points common to two or more elements (nodes or nodal points) and/or boundary lines and/or surfaces. When the effects of loads and boundary conditions are considered, a set of linear or nonlinear algebraic equations is usually obtained. Solution of these equations gives the approximate behavior of the physical system. Because of the idealization and discretization, it is important to verify or validate that the response of the discrete model is realistic when the results are analyzed.

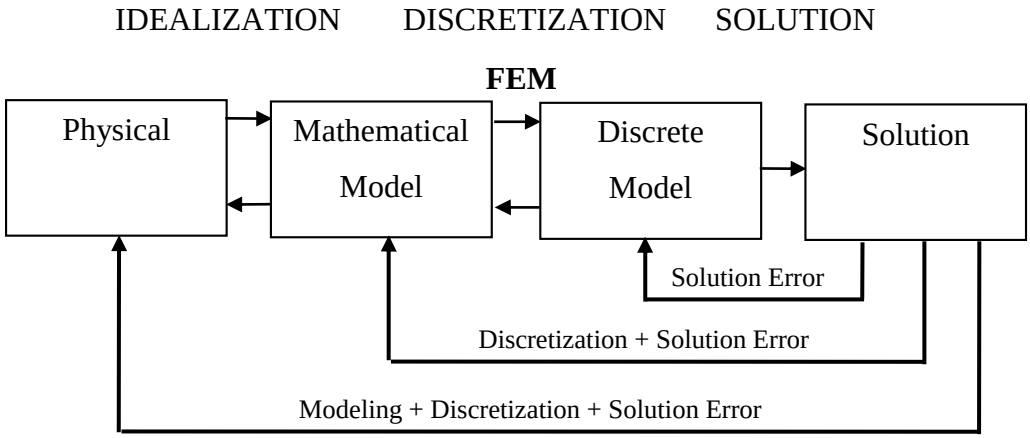

A simplified view of the finite element simulation process.

A.2 Mesh Sensitivity Studies

A.2.1 C4-C6 Axial Stiffness Mesh Sensitivity Studies

Five models were used to determine the optimum intervertebral mesh density for the analysis. The mesh was refined without altering the materials properties and geometry. However, the annulus fibers, anterior and posterior ligaments were not included in these analyses, as changes in the intervertebral disc will require very extensive re-modelling.

Results showed that the force decrease with increase in the mesh density under compression, anterior and posterior shear. Similar trend can be observed in the predicted stress obtained at various spinal components. Further increase in the mesh density from 768 to 1536 elements did not significantly alter the biomechanical responses. Generally, results showed that the model with 768 intervetebral mesh density was adequate for the present study. The other models with higher mesh density did not provide enough additional accuracy to offset the increase in computational time.

a) 96 Element or 1 Disc Layer

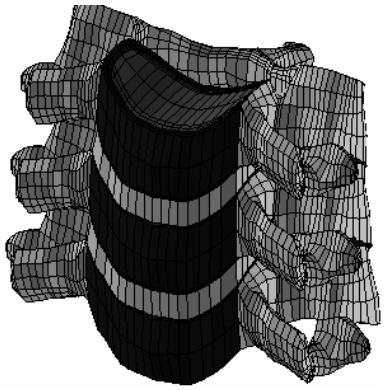

b) 192 Element or 2 Disc Layers

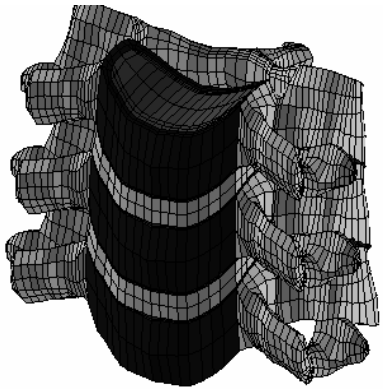

c) 384 Element or 4 Disc Layers

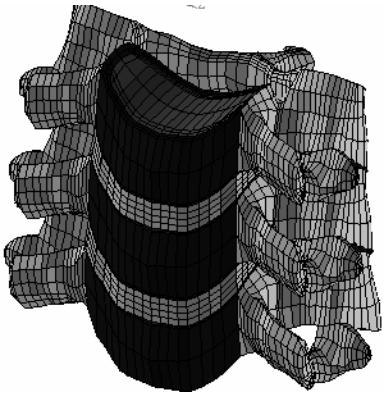

d) 768 Element or 8 Disc Layers

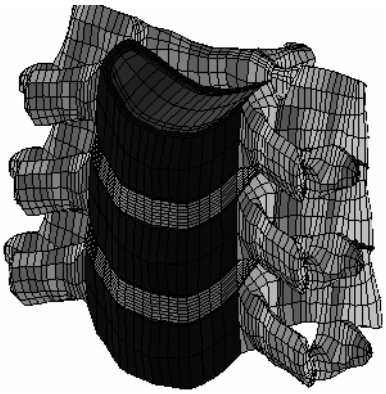

e) 1536 Element or 16 Disc Layers

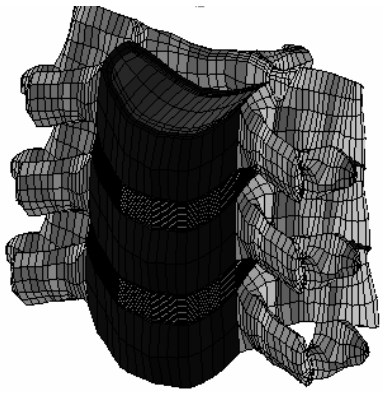

Influence of intervertebral mesh density under sagittal moments.

1mm Compression

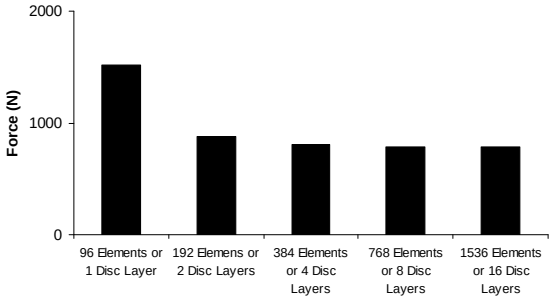

2mm Anterior Shear

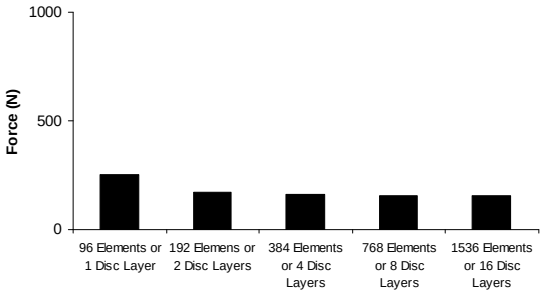

4mm Posterior Shear

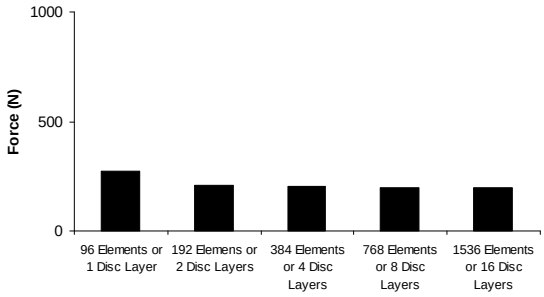

Predicted force-displacement responses for the five models with different intervertebral mesh density under compression, anterior and posterior shear.

1mm Compression

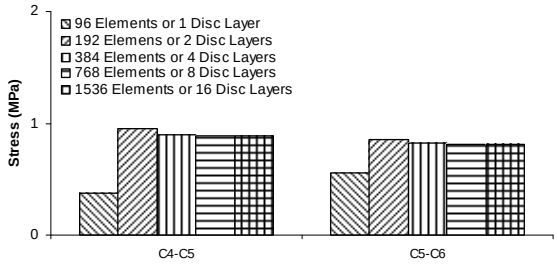

2mm Anterior Shear

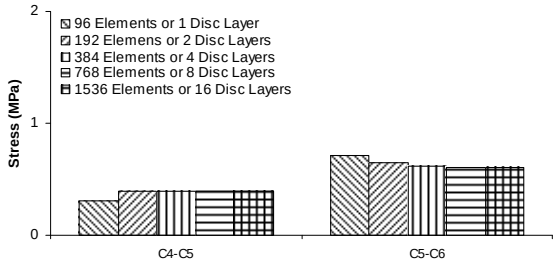

4mm Posterior Shear

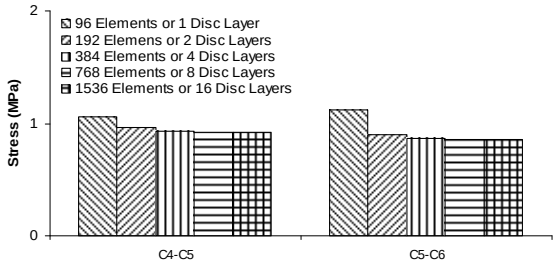

Predicted intervertebral disc stress for the five models with different intervertebral mesh density under compression, anterior and posterior shear.

1mm Compression

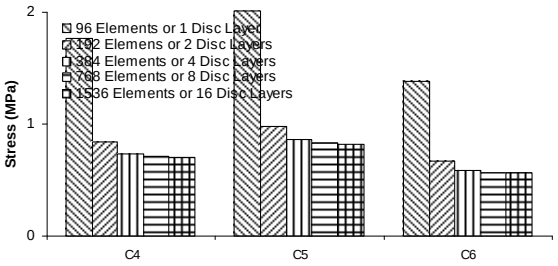

2mm Anterior Shear

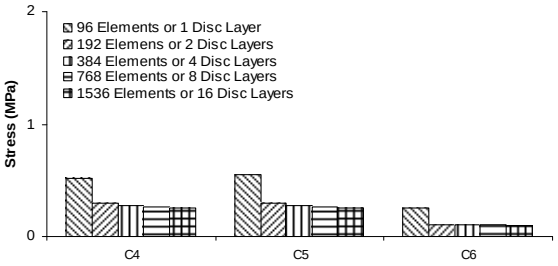

4mm Posterior Shear

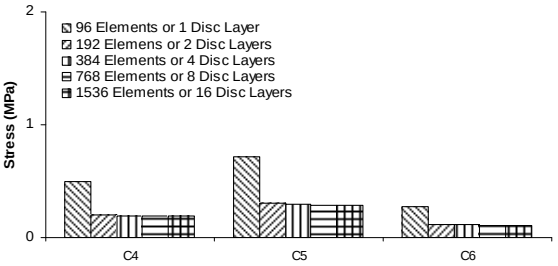

Predicted cancellous bone stress for the five models with different intervertebral mesh density under compression, anterior and posterior shear.

1mm Compression

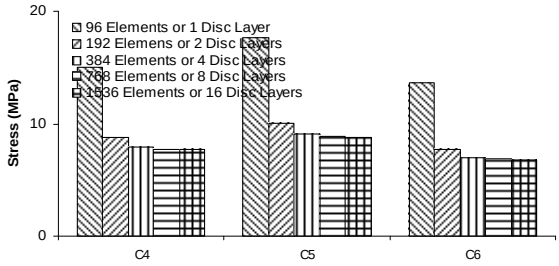

2mm Anterior Shear

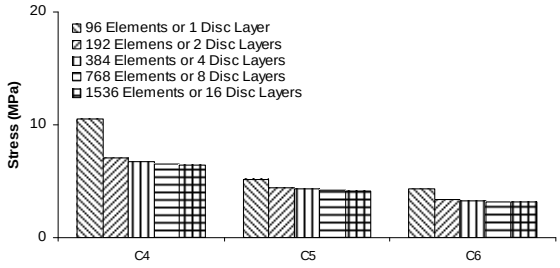

4mm Posterior Shear

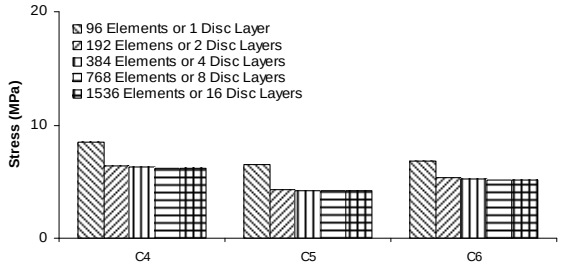

Predicted cortical bone stress for the five models with different intervertebral mesh density under compression, anterior and posterior shear.

1mm Compression

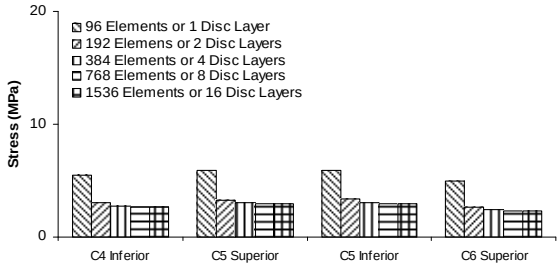

2mm Anterior Shear

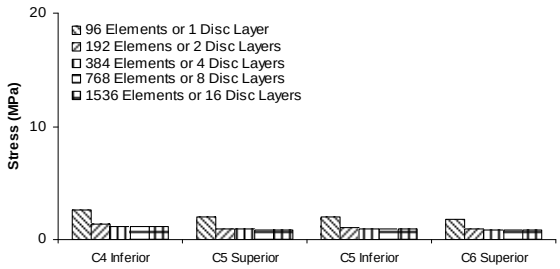

4mm Posterior Shear

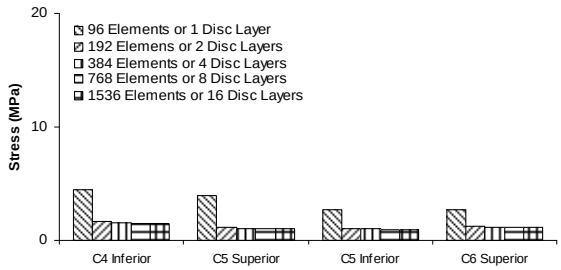

Predicted endplate stress for the five models with different intervertebral mesh density under compression, anterior and posterior shear.

A.2.2 C5-C6 Rotational Motions Mesh Sensitivity Studies

Similarly, five models of various mesh density were used to determine the effect of mesh sensitivity on the rotational motions under four type of loading modes (flexion, extension, lateral bending and axial rotation).

a) 96 Element or 1 Disc Layer

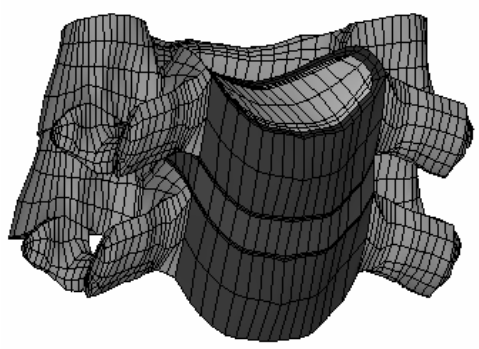

b) 192 Element or 2 Disc Layers

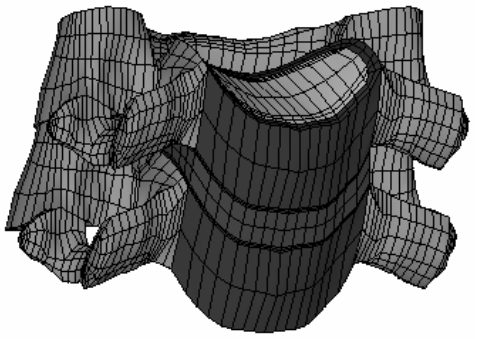

c) 384 Element or 4 Disc Layers

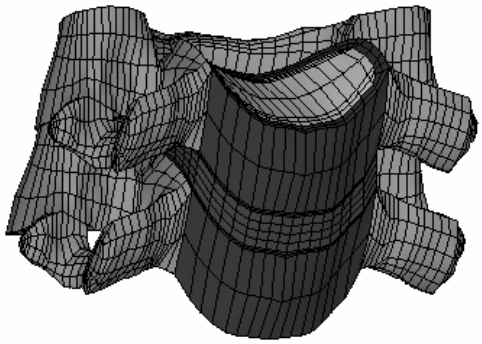

d) 768 Element or 8 Disc Layers

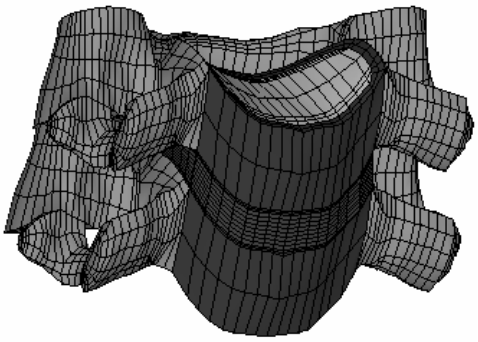

e) 1536 Element or 16 Disc Layers

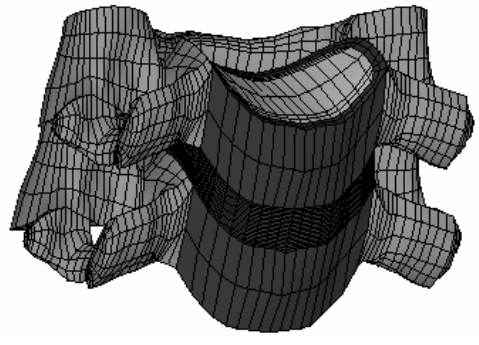

Influence of intervertebral mesh density under sagittal moments.

Flexion

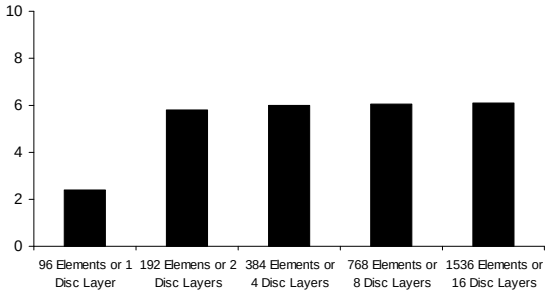

Extension

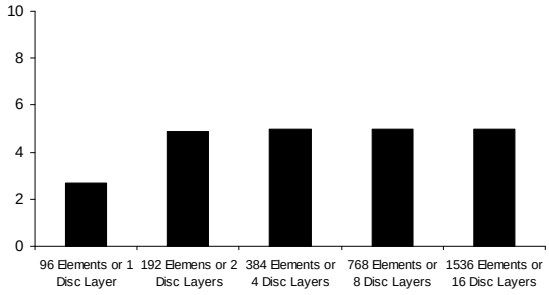

Lateral Bending

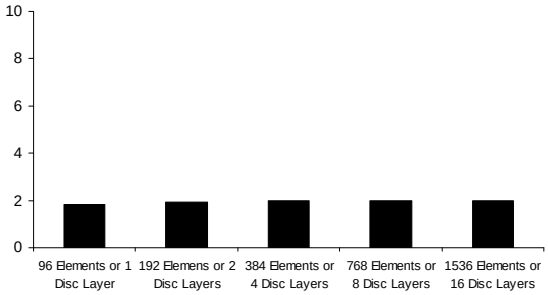

Axial Rotation

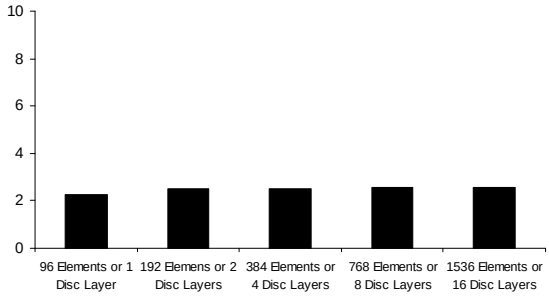

Influence of intervertebral mesh density on the ROM.

Flexion

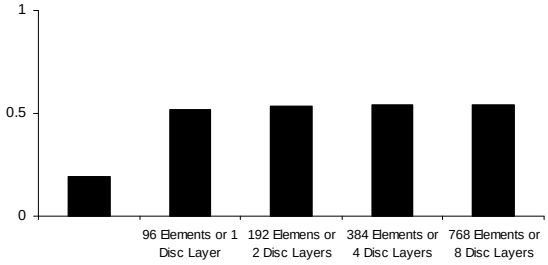

Extension

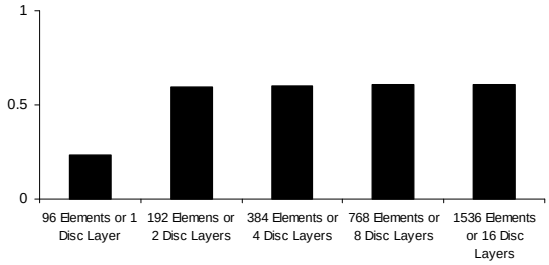

Lateral Bending

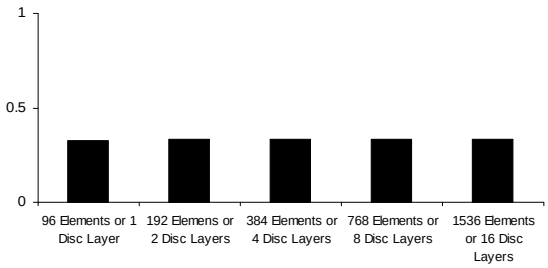

Axial Rotation

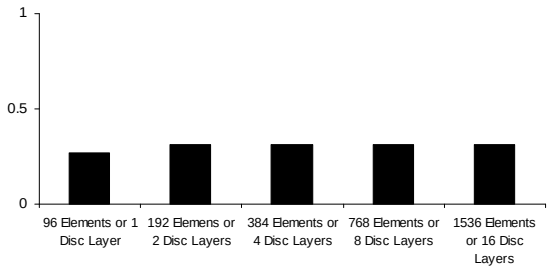

Influence of intervertebral mesh density on disc stress.

Flexion

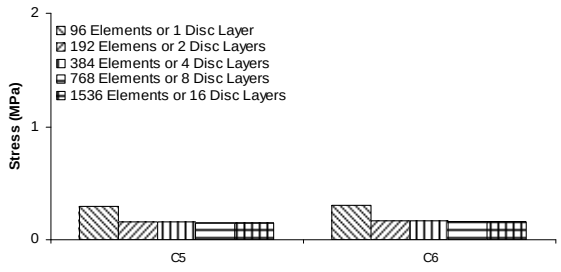

Extension

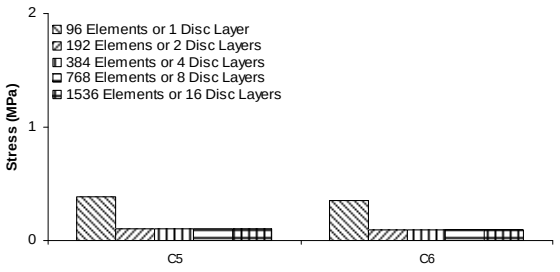

Lateral Bending

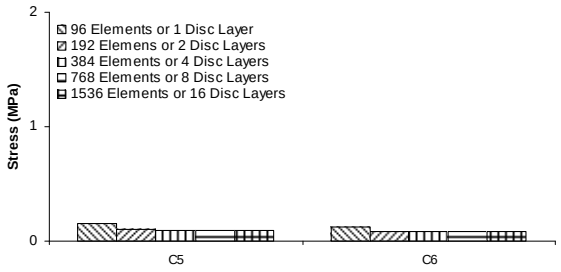

Axial Rotation

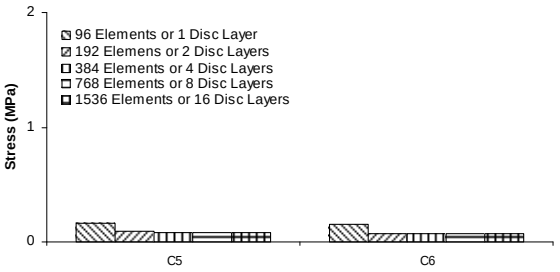

Influence of intervertebral mesh density on cancellous bone stress.

Flexion

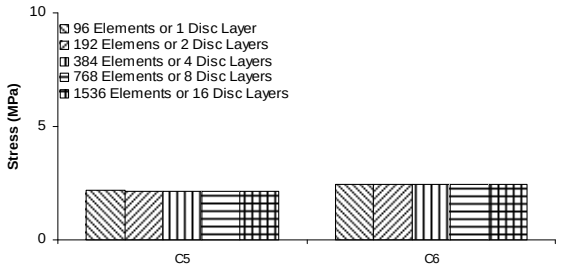

Extension

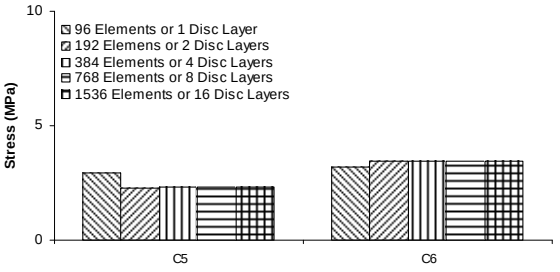

Lateral Bending

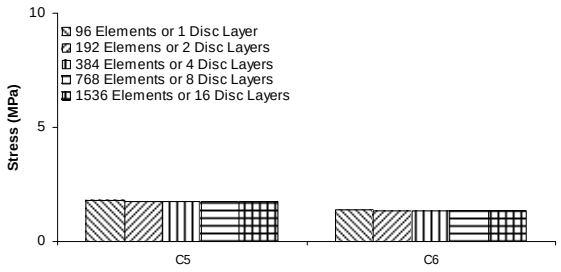

Axial Rotation

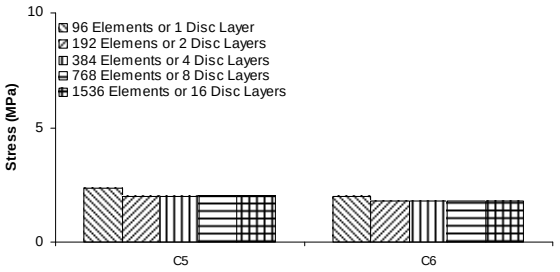

Influence of intervertebral mesh density on cortical bone stress.

Flexion

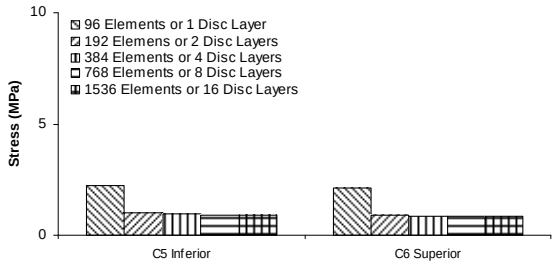

Extension

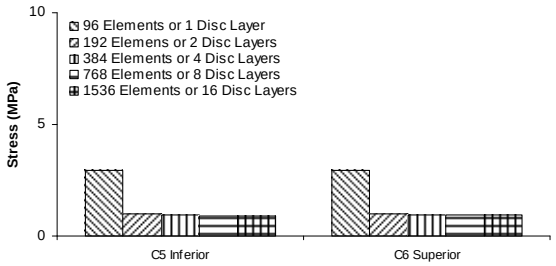

Lateral Bending

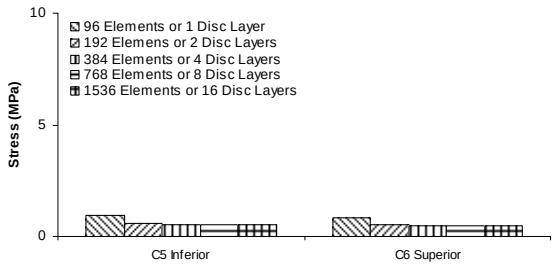

Axial Rotation

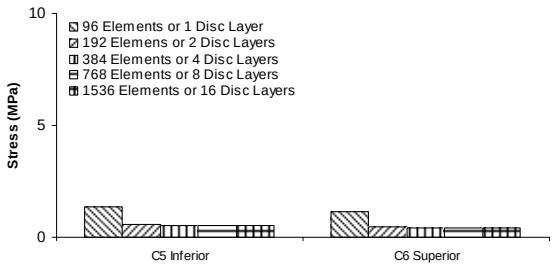

Influence of intervertebral mesh density on endplate stress.

A.3 Applying Pure Moments

It is well known that the FEA analysis depended on three main parameters; geometry, material and loading. In the current study, element type SOLID45 was used for the FE model, which supports only displacement degree of freedoms (UX, UY and UZ) and structural nonlinearity. This affects the direct application of pure moments to the FE model, because SOLID45 does not support rotational degree of freedoms (ROTX, ROTY and ROTZ). To simulate *in vitro* setup using pure moments accurately, it is important to understand the features available in the commercial FEA packages that allowed the application of pure moments to the cervical spinal model. In ANSYS, three methods are available to apply pure moments; distributed force constraint equation, rigid based constraint equation and rigid spider beam.

	Constraint Equation		Rigid Spider Beam
	Distributed Force (RBE3)	Rigid Based (CERIG)	
Master Node (1 node)	Dependent DOF	Independent DOF	Independent DOF
	Can only apply loads on master node	Can apply loads or constrain master node	Can apply loads or constrain master node
Slave Nodes	Independent DOF	Dependent DOF	Dependent DOF
Number of CEs Generated	1 ≤ CE ≥ 6	CE ≤ 1	-
Optional weight Factors	Supplied by array parameter	-	-
Example use	Distribute forces, moments, or mass	Describe a rigid region in model	Describe a rigid region in model

Difference among the three techniques used to apply pure moments.

Constraint equation provides many useful features in ANSYS, such as tying together dissimilar meshes, representing parts of the system not explicitly modelled, or distributing loads. Two automated methods of generating constraint equations are the RBE3 and CERIG. Constraint equation in ANSYS is linear, so they may **not be suitable for large-rotation analyses**. RIGID184 is a new element in version 7.0, which provides rigid spider beam capabilities**, is more suitable for large rotation problems**, as in the case of the cervical spinal instability studies after various surgical techniques.

In this section, three methods that allowed the application of pure moments to the cervical spinal models in ANSYS were investigated. In these series of linear and nonlinear analysis, the setup (loading and constraint) was similar to the *in vitro* condition by Moroney et al., 1988. The resulting ROM and stress were captured and compared. Using linear analysis, predicted ROM showed almost identical values under CERIG and rigid spider beam. The model with RBE3 showed different results. Under nonlinear analysis, the predicted ROM using RBE3 and rigid spider beam are very close. The intervertebral disc stress showed similar trends as seen in the prediction of the ROM. In this study, rigid spider beam was selected utilized in the current nonlinear analysis of the human cervical spine.

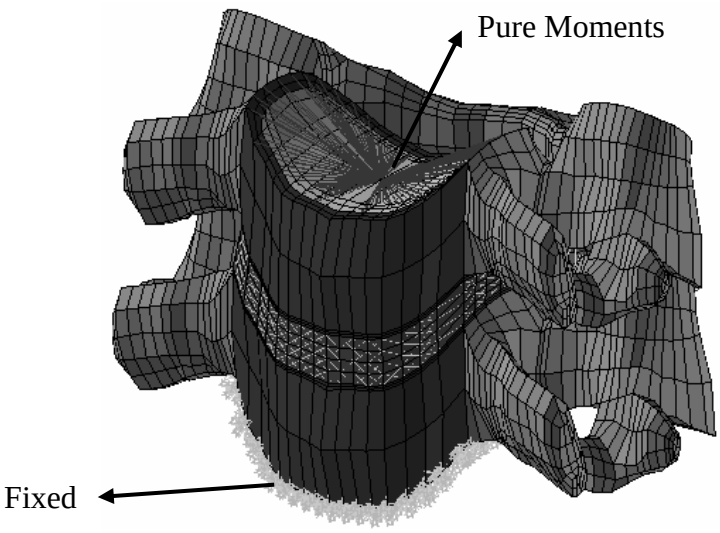

C5-C6 model showing the method of applying pure moments

Analysis Type		ROM (degree)			
		Constraint Equations		Rigid Spider Beam	Moroney et al., 1988
		Distributed Force (RBE3)	Rigid Based (CERIG)		
Linear	Flexion	6.71	6.66	6.66	5.55 (1.84)
	Extension	5.37	5.27	5.27	3.52 (1.94)
	Lateral Bending	1.76	1.13	1.13	4.71 (3.00)
	Axial Rotation	2.74	1.35	1.35	1.85 (0.67)
Non-Linear	Flexion	5.65	4.54	5.56	5.55 (1.84)
	Extension	4.60	3.48	4.41	3.52 (1.94)
	Lateral Bending	1.51	1.48	1.51	4.71 (3.00)
	Axial Rotation	2.01	1.95	2.02	1.85 (0.67)

Summary of the three techniques on the influences of C5-C6 ROM at final loading. () denotes standard deviation.

Analysis Type		Stress (MPa)		
		Constraint Equations		Rigid Spider Beam
		Distributed Force (RBE3)	Rigid Based (CERIG)	
Linear	Flexion	0.67	0.67	0.67
	Extension	0.60	0.60	0.60
	Lateral Bending	0.28	0.29	0.29
	Axial Rotation	0.36	0.35	0.35
Non-Linear	Flexion	0.58	0.47	0.57
	Extension	0.49	0.36	0.48

	Lateral Bending	0.24	0.23	0.24
	Axial Rotation	0.27	0.25	0.26

Summary of the three techniques on the influences of C5-C6 anterior disc stress.

Analysis Type		Stress (MPa)		
		Constraint Equations		Rigid Spider Beam
		Distributed Force (RBE3)	Rigid Based (CERIG)	
Linear	Flexion	0.55	0.55	0.55
	Extension	0.70	0.69	0.69
	Lateral Bending	0.45	0.45	0.45
	Axial Rotation	0.53	0.52	0.52
Non-Linear	Flexion	0.43	0.33	0.42
	Extension	0.59	0.49	0.57
	Lateral Bending	0.35	0.34	0.35
	Axial Rotation	0.33	0.31	0.33

Summary of the three techniques on the influences of C5-C6 posterior disc stress.

A.4 Validations Using Refined FE Model

Figures illustrated below showed the comparisons between the refined FE model and various *in vitro* data using the respective loading and boundary conditions.

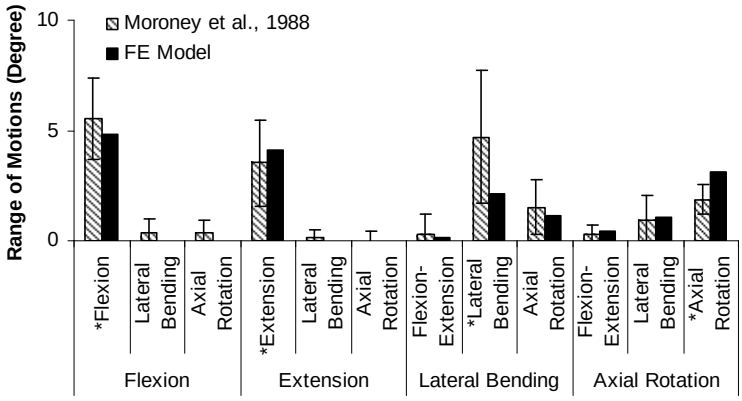

Comparisons against Moroney et al., 1988 using C5-C6 model.

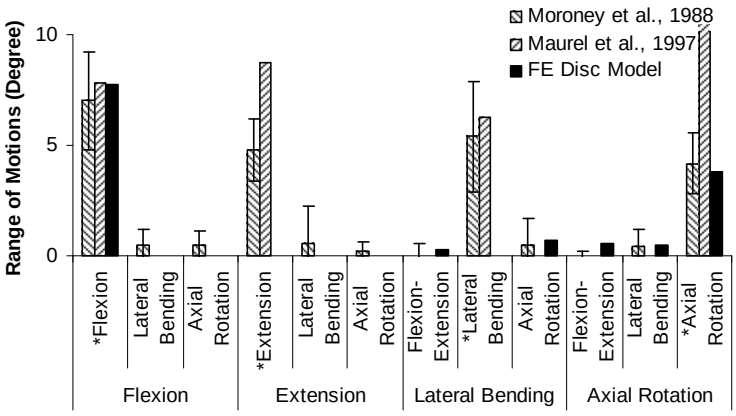

Comparisons against Moroney et al., 1988 and Maurel et al., 1997 using C5-C6 disc model.

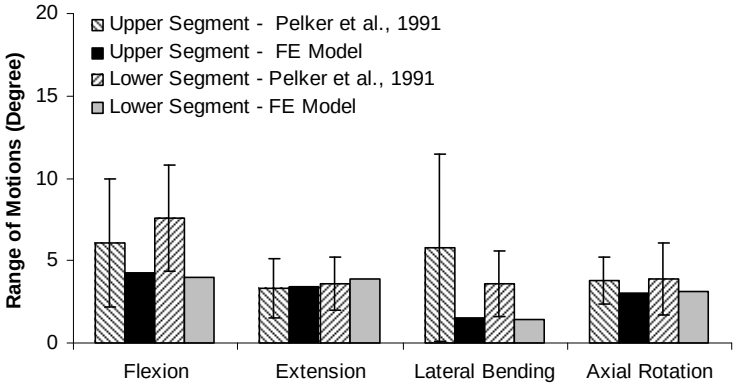

Comparisons against Pelker et al., 1991 using C4-C6 model.

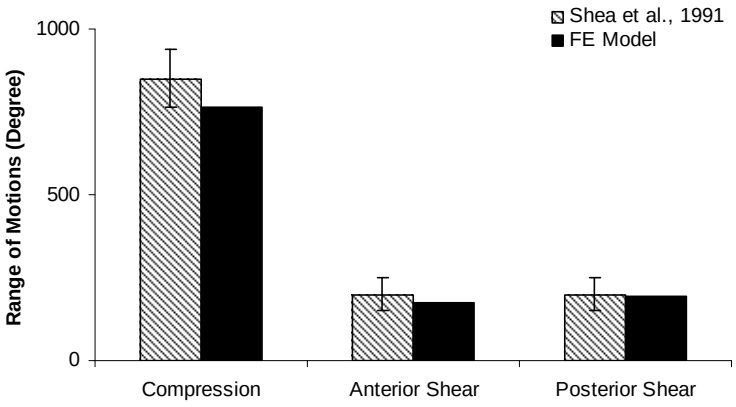

Comparison against Shea et al., 1991 using C4-C6 model.

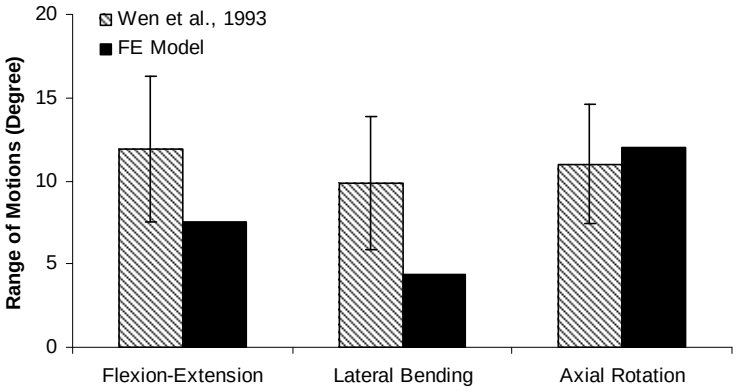

Comparisons against Wen et al., 1993 using C5-C6 model

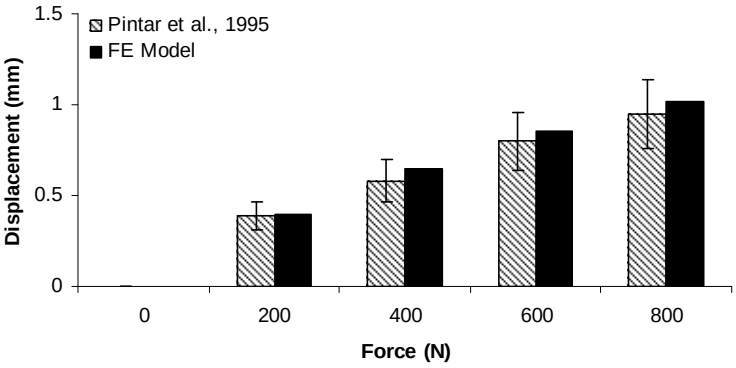

Comparisons against Pintar et al., 1995 using C4-C6 model.

.

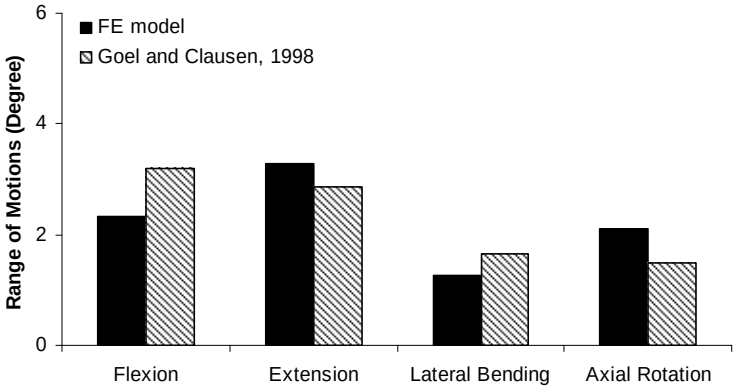

Comparisons against Goel and Clausen, 1998 using C5-C6 model.

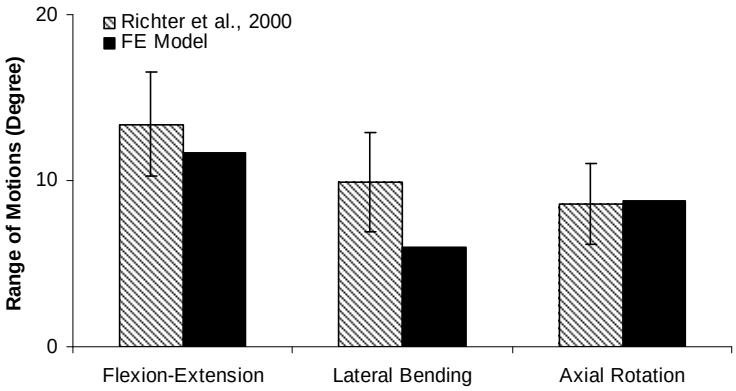

Comparisons against Richter et al., 2000 using C5-C6 model.

A.5 Additional Results for One/Two Level Laminotomies and Laminectomies

Inter-Segmental ROM	C2-C7 ROM
Left + Right Lateral Bending	

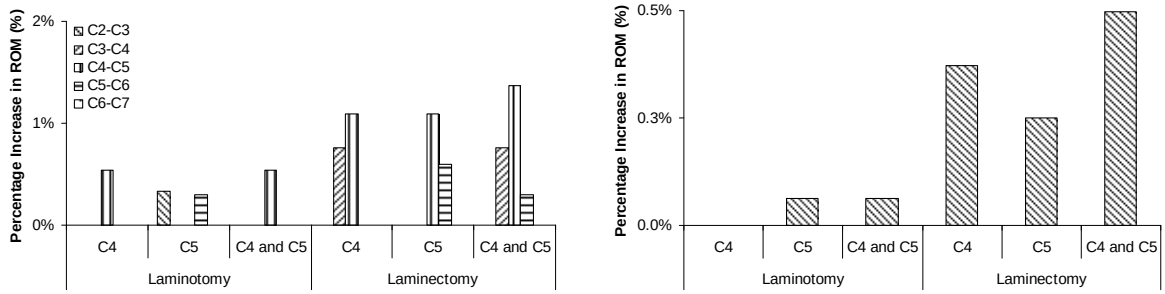

Left + Right Axial Rotation

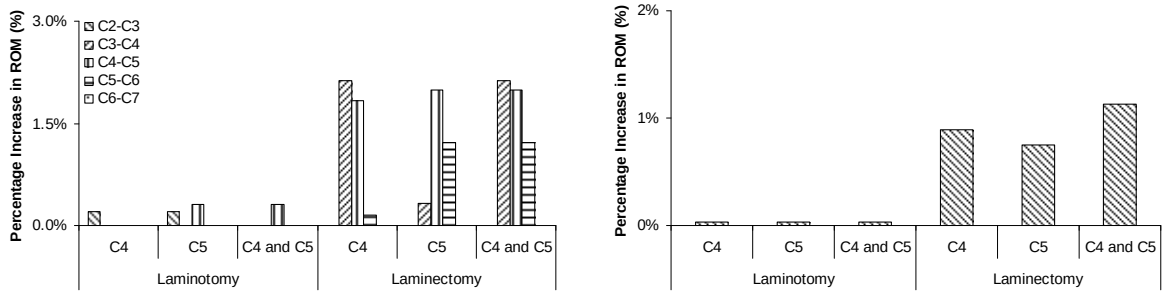

Percentage increase in the ROM after one or two level laminotomies and laminectomies.

Left + Right Lateral Bending

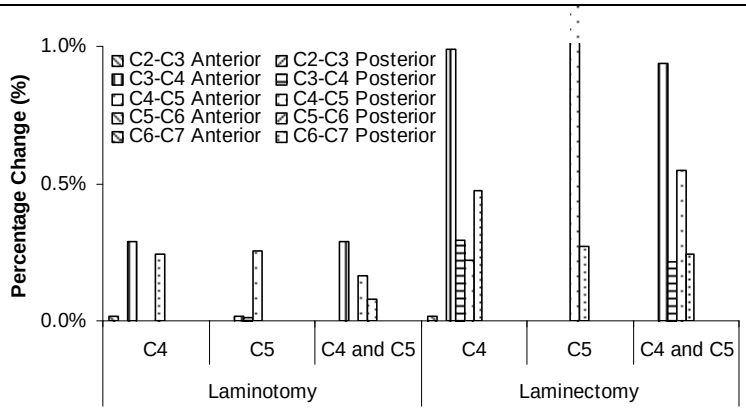

Left + Right Axial Rotation

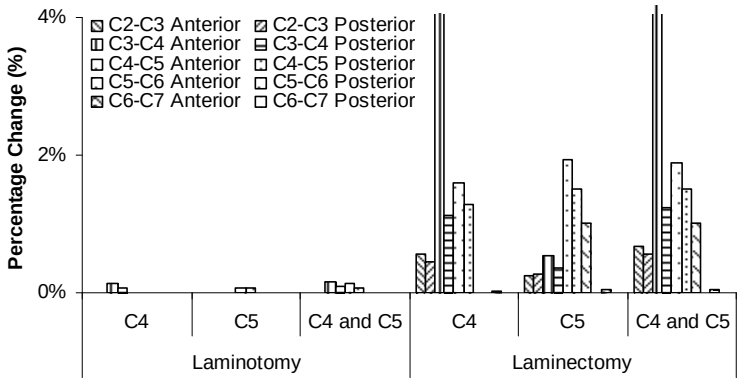

Percentage increase in the disc annulus stress after one or two level laminotomies and laminectomies.

Left + Right Lateral Bending

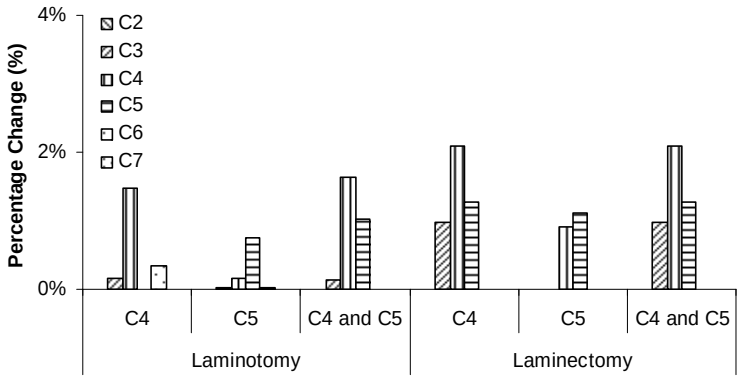

Left + Right Axial Rotation

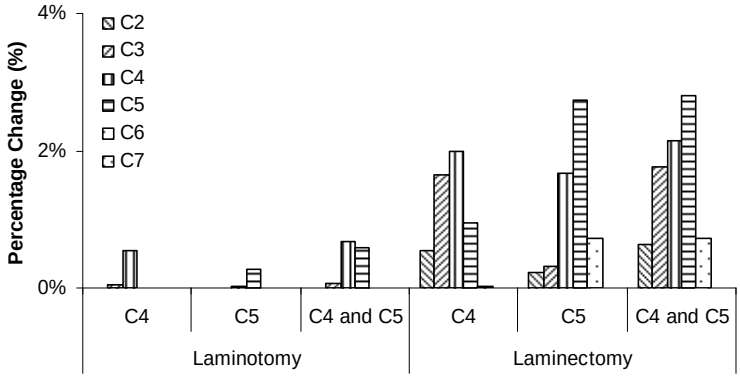

Percentage increase in the cortical bone stress after one or two level laminotomies and laminectomies.

Appendix B Programs

B.1 Conversion Program

```
MICROSOFT VISUAL BASIC VERSION 5.00
Object = "(Schulte et al.)#1.2#0"; "COMDLG32.OCX"
Begin VB.Form Form1
  Caption        =   "Ansys File Conversion Program by Hong Wan"

Private Sub Line_Click()

 Dim x
   Dim i
   Dim MyString As String
   Dim Firststring As String
   Dim Secondstring As String
   Dim Oneletter

   sSourceFile = CommonDialog3.FileName
   ConvertedName = CommonDialog4.FileName

   If ConvertedName <> "" Then
      Screen.MousePointer = vbHourglass
      Open sSourceFile For Input As #1 ' Open file.
      Open ConvertedName For Output As #2

      j = 0
      e = 0

      Do While Not EOF(1) ' Loop until end of file.

        e = e + 1
        Print #2, "/PREP7"

        Input #1, MyString ' Read data into one variable.

           i = 0

           For x = 1 To Len(MyString)
           Oneletter = Mid(MyString, x, 1)


      If Asc(Oneletter) = 9 Or Asc(Oneletter) = 32 Then
           Oneletter = ","

           i = i + 1

           If i = 1 Then
           Oneletter = ""
           Secondstring = ""
```

```
            End If

            If i = 2 Then
            Oneletter = ""
            Firststring = "," & Secondstring & ","
            Secondstring = ""

            End If

        End If

            DoEvents

               Secondstring = Secondstring & Oneletter

            If i = 3 Then

            Print #2, "LSTR" & Firststring & Secondstring
            lineconvert.Text = "LSTR" & Firststring & Secondstring

            j = j + 1
            Firststring = "," & Secondstring
            Secondstring = ""
            i = 2

            End If

        Next x

            lineno.Text = j
            lineerror.Text = e
            Firststring = ""
            Secondstring = ""


            DoEvents ' it is important to unlock the screen
         Loop
            Close #1 ' Close file.
            Close #2
            Screen.MousePointer = vbDefault
          Else
            MsgBox " Destination File Read Erorr.. "
          End If


End Sub

Private Sub PolyLines_Click()

 Dim x
```

```
Dim i
Dim pointno
Dim MyString As String
Dim Newstring As String
Dim Oneletter


sSourceFile = CommonDialog3.FileName
ConvertedName = CommonDialog4.FileName


If ConvertedName <> "" Then
   Screen.MousePointer = vbHourglass
   Open sSourceFile For Input As #1 ' Open file.
   Open ConvertedName For Output As #2

   j = 0
   e = 0

   Do While Not EOF(1) ' Loop until end of file.


     Input #1, MyString ' Read data into one variable.

     i = 0

   For x = 1 To Len(MyString)
   Oneletter = Mid(MyString, x, 1)
   If Asc(Oneletter) = 9 Or Asc(Oneletter) = 32 Then
        i = i + 1

    End If

  Next x

 pointno = i - 1

 Print #2, "FLST,3," & pointno & ",3"
 lineconvert.Text = "FLST,3," & pointno & ",3"

     i = 0

        For x = 1 To Len(MyString)
        Oneletter = Mid(MyString, x, 1)

  If Asc(Oneletter) = 9 Or Asc(Oneletter) = 32 Then

        i = i + 1
      If i = 1 Or i = pointno + 1 Then
        Newstring = ""
        lineerror.Text = j
```

```
        Else
          Oneletter = ""
          Print #2, "FITEM , 3," & Newstring
          lineconvert.Text = "FITEM , 3," & Newstring
          Newstring = ""
          i = 1
          End If


    End If

          DoEvents
            Newstring = Newstring & Oneletter
    Next x


          Print #2, "BSPLIN , , P51X"
          lineconvert.Text = "BSPLIN , , P51X"
          j = j + 1
          lineno.Text = j
          Newstring = ""


          DoEvents ' it is important to unlock the screen
     Loop
          Close #1 ' Close file.
          Close #2
          Screen.MousePointer = vbDefault
        Else
          MsgBox " Destination File Read Erorr.. "
        End If

End Sub

Private Sub outputfile1_Click()
  CommonDialog2.ShowSave
  outputname1.Text = CommonDialog2.FileName

End Sub

Private Sub outputfile2_Click()
  CommonDialog4.ShowSave
  outputname2.Text = CommonDialog4.FileName
End Sub

Private Sub Points_Click()

    Dim x
    Dim i
    Dim MyString As String
    Dim Newstring As String
```

```
Dim Oneletter

sSourceFile = CommonDialog1.FileName
ConvertedName = CommonDialog2.FileName

If ConvertedName <> "" Then
   Screen.MousePointer = vbHourglass
   Open sSourceFile For Input As #1 ' Open file.
   Open ConvertedName For Output As #2

   j = 0

   Do While Not EOF(1) ' Loop until end of file.
      Input #1, MyString ' Read data into one variable.

      i = 0

      For x = 1 To Len(MyString)
         Oneletter = Mid(MyString, x, 1)

   If Asc(Oneletter) = 9 Or Asc(Oneletter) = 32 Then
            Oneletter = ","

         i = i + 1

         If i = 3 Then
         Oneletter = ""
         Print #2, "k,x," & Newstring
         pointconvert.Text = "k,x," & Newstring
         Newstring = ""
         i = 0
         j = j + 1
         End If

   End If

         DoEvents
            Newstring = Newstring & Oneletter
         Next x

         Print #2, "k,x," & Newstring
         pointconvert.Text = "k,x," & Newstring
         j = j + 1
         pointno.Text = j
         Newstring = ""

         DoEvents ' it is important to unlock the screen
    Loop

         Close #1 ' Close file.
         Close #2
```

```
            Screen.MousePointer = vbDefault
        Else
            MsgBox " Destination File Read Erorr.. "
        End If

End Sub

Private Sub PolyLines2_Click()

 Dim x
   Dim i
   Dim spline1 As Integer
   Dim spline2 As Integer
   Dim MyString As String
   Dim Newstring As String
   Dim Oneletter

   sSourceFile = CommonDialog3.FileName
   ConvertedName = CommonDialog4.FileName

   If ConvertedName <> "" Then
      Screen.MousePointer = vbHourglass
      Open sSourceFile For Input As #1 ' Open file.
      Open ConvertedName For Output As #2

      j = 0
      e = 0
      k = 0

      Do While Not EOF(1) ' Loop until end of file.
        Input #1, MyString ' Read data into one variable.

        i = 0

      For x = 1 To Len(MyString)
      Oneletter = Mid(MyString, x, 1)
      If Asc(Oneletter) = 9 Or Asc(Oneletter) = 32 Then
           i = i + 1

       End If

      Next x

      spline1 = i - 1

      i = -1
      Counter = 1

   If spline1 > 4 Then

      For x = 1 To Len(MyString)
```

```
Oneletter = Mid(MyString, x, 1)

If Asc(Oneletter) = 9 Or Asc(Oneletter) = 32 Then

   i = i + 1

   If i = 0 And Counter = 1 Then

   If spline1 > 200 Then
   spline2 = 200
   spline1 = spline1 - 200
   Else
   spline2 = spline1
   End If

   Newstring = ""
   lineerror.Text = j
   Print #2, "FLST,3," & spline2 & ",3"
   lineconvert.Text = "FLST,3," & spline2 & ",3"

   ElseIf i = 1 And Counter > 1 Then

   If spline1 > 200 Then
   spline2 = 200
   spline1 = spline1 - 200
   Else
   spline2 = spline1
   End If

   Print #2, "FLST,3," & spline2 & ",3"
   lineconvert.Text = "FLST,3," & spline2 & ",3"

   Oneletter = ""
   Print #2, "FITEM , 3," & Newstring
   lineconvert.Text = "FITEM , 3," & Newstring
   Newstring = ""


   Else
      Oneletter = ""
      Print #2, "FITEM , 3," & Newstring
      lineconvert.Text = "FITEM , 3," & Newstring
      Newstring = ""

   End If

End If

If i = 200 Then
      Print #2, "BSPLIN , , P51X"
      lineconvert.Text = "BSPLIN , , P51X"
```

```
            Counter = Counter + 1
            Newstring = ""
            i = 0
            j = j + 1
            lineno.Text = j

        End If

            DoEvents
               Newstring = Newstring & Oneletter

        Next x

            Print #2, "BSPLIN , , P51X"
            lineconvert.Text = "BSPLIN , , P51X"
            Counter = Counter + 1
            j = j + 1
            lineno.Text = j
            Newstring = ""
Else
k = k + 1
disline.Text = k

End If

            DoEvents ' it is important to unlock the screen
       Loop
            Close #1 ' Close file.
            Close #2
            Screen.MousePointer = vbDefault
          Else
            MsgBox " Destination File Read Erorr.. "
          End If

End Sub
```